

Thiolactone based coupling agents for the synthesis of poly(amide/urethane)s

Von der Fakultät für Mathematik, Informatik und Naturwissenschaften der
RWTH Aachen University zur Erlangung des akademischen Grades
eines Doktors der Naturwissenschaften genehmigte Dissertation

vorgelegt von

M.Sc. RWTH

Stefan Mommer,

aus Eupen, Belgien

Berichter: Universitätsprofessor Dr. rer. nat. Martin Möller
 Universitätsprofessor Dr. rer. nat. Andrij Pich

Tag der mündlichen Prüfung: 02.05.17

Diese Dissertation ist auf den Internetseiten der
Universitätsbibliothek online verfügbar.

I hereby declare that I have created this work completely on my own and used no other sources or tools than the ones listed, and that I have marked any citations accordingly.

Hiermit versichere ich, dass ich die vorliegende Arbeit selbständig verfasst und keine anderen als die angegebenen Quellen und Hilfsmittel benutzt sowie Zitate kenntlich gemacht habe.

Aachen, May 2017
Stefan Mommer

Contents

Abstract	v
Überblick	vii
Acknowledgements	ix
Publications	xi
1 Introduction & Motivation	1
2 The Art of Coupling	9
2.1 Macromolecular Design through Coupling Agents	9
2.2 Coupling via Cycloaddition Reaction	21
3 The Role of Thiols in Polymer Chemistry	35
3.1 Reactions of Thiols and Thiol Derivatives	36
3.2 Homocysteine Thiolactone as Functional Key Feature	52

4	A Novel Ethylene Carbonate Thiolactone Coupler	73
4.1	Introduction	73
4.2	Results & Discussion	76
4.3	Conclusion	81
4.4	Experimental Data	82
5	Tailored Thiol-functional Polyamides via a Bis(thiolactone)	93
5.1	Introduction	93
5.2	Results & Discussion	95
5.3	Conclusion	107
5.4	Experimental Data	108
6	An Epoxy Thiolactone on Stage	121
	Part I	121
6.1	Introduction	121
6.2	Results & Discussion	124
6.3	Conclusion	140
6.4	Experimental Data	141
	Part II	155
6.5	Introduction	155
6.6	Results & Discussion	157

6.7	Conclusion	170
6.8	Experimental Data	171
7	Summary	185
A	Additional Information	189
A.1	Ethylene Carbonate Thiolactone Coupler	189
A.2	Bis(Thiolactone) Coupler	194
A.3	Epoxy Thiolactone Coupler	200

Abstract

In this thesis, three different coupling agents are synthesized, which consist each of two cycles: (i) ethylene carbonate - thiolactone, (ii) bis(thiolactone) and (iii) epoxy - thiolactone. The syntheses of each are optimized to give high yields and pure products. Each coupling agent is thoroughly investigated concerning the orthogonal reactivity of its cycles. For the ethylene carbonate thiolactone coupling agent, a one-pot procedure is established where four different building blocks are incorporated into one molecule. Every intermediate in this reaction sequence is isolated and fully characterized. The bis(thiolactone) coupler is again investigated regarding its chemoselectivity towards amines at different temperatures. Then, the bis(thiolactone) is reacted as an AA-type monomer with diamines as BB-type comonomers in a step-growth polymerization. Using two comonomers in different ratios for the polyaddition, thermal properties of the resulting polymers are adjusted. The obtained polymers, which carry thiol groups in the side chain, are functionalized via a simple Michael addition to different substrates. The Michael addition with acrylate functional PEG building blocks gives access to water-soluble polymeric amphiphiles. Regarding the last coupling agent, the reactivity of the cycles is explored towards mono- and dialkylamines. In a one-pot procedure, a four component reaction is carried out using the coupler and three other building blocks. Upon amidation of the thiolactone at low temperatures, an

epoxy thiol intermediate is prepared, which undergoes a base-catalyzed thiol-epoxy polyaddition in situ. This polyaddition is put to sound investigations regarding the used catalyst, the catalyst loading, concentration of the monomer, the solvent polarity and the formation of cyclic oligomers. The reaction conditions are optimized to obtain high number average molecular weights and low dispersities. Finally, the use of this coupler for the synthesis of bulk hydrogels is demonstrated. In a second part, this epoxy thiolactone is used for the synthesis of polyelectrolytes. The provided substrates are amino acids and derivatives of such. Upon polyaddition, pH-responsive polyelectrolytes and -ampholytes are obtained. Using two oppositely charged polyelectrolytes, polyelectrolyte complex nanoparticles are synthesized via macromolecular salt formation in solution. The particles are analyzed regarding their size and morphology.

Überblick

In der vorliegenden Arbeit werden drei unterschiedliche Kopplungsreagenzien synthetisiert, die jeweils aus zwei verschiedenen Cyclen bestehen: (i) Ethylencarbonat - Thiolacton, (ii) Bis(thiolacton) und (iii) Epoxy - Thiolacton. Die Synthesen dieser Koppler sind optimiert worden um möglichst hohe Ausbeuten und reine Produkte zu erhalten. Jedes Kopplungsreagenz ist bezüglich der orthogonalen Reaktivität seiner Cyclen gründlich untersucht worden. Für den Ethylencarbonat Thiolacton Koppler ist eine Eintopfprozedur etabliert worden, in der vier verschiedene Bausteine in ein einziges Molekül integriert werden. Dabei wird jedes Intermediat in dieser Reaktionsabfolge einzeln isoliert und vollständig charakterisiert. Der Bis(thiolacton) Koppler wird ebenfalls auf seine Chemoselektivität gegenüber Aminen bei unterschiedlichen Temperaturen untersucht. Dann, wird das Bis(thiolacton) als AA-artiges Monomer mit entsprechenden Diaminen als BB-artige Comonomere in einer Polymerisation mit Stufenwachstum umgesetzt. Unter Nutzung zweier Diamine in verschiedenen Verhältnissen für die Polyaddition werden so die thermischen Eigenschaften der entstehenden Polymere angepasst. Die erhaltenen Polymere, welche nun Thiolgruppen in den Seitenketten tragen, werden über eine simple Michael-Addition mit unterschiedlichen Substraten modifiziert. Dabei schafft die Michael-Addition mit Acrylat-funktionalisierten PEG Bausteinen den Zugang zu

wasserlöslichen polymeren Amphiphilen. Beim letzten Koppler wird die Reaktivität der Cyclen gegenüber Mono- und Dialkylaminen untersucht. In einer Eintopfreaktion wird somit eine Vierkomponentenreaktion unter Nutzung des Kopplers und drei anderer Reagenzien durchgeführt. Wird lediglich die Amidierung des Thiolactons durchgeführt, entsteht somit bei niedrigen Temperaturen ein Epoxythiol-Intermediat, welches seinerseits eine Basen-katalysierte Thiol-Epoxy Polyaddition in situ durchläuft. Diese Polyaddition wird bezüglich des verwendeten Katalysators, der Katalysatormenge, der Monomerkonzentration, Lösungsmittelpolarität und der Bildung von cyclischen Oligomeren solider Untersuchungen unterzogen. Die Reaktionsbedingungen werden optimiert um Polymere mit möglichst hohen zahlengemittelten Molekulargewichten und möglichst niedrigen Polydispersitäten zu erhalten. Mit Hilfe dieses Kopplers werden schlussendlich Hydrogele hergestellt. In einem zweiten Teil wird das Epoxy-Thiolacton Monomer zur Herstellung von Polyelektrolyten genutzt. Zu den vorgesehenen Substraten gehören Aminosäuren und Derivate solcher. Nach jener Polyaddition werden pH-responsive Polyelektrolyte und Polyampholyte erhalten. Unter Verwendung von zwei Polyelektrolyten mit entgegengesetzter Ladung lassen sich schließlich Polyelektrolytkomplexe-Nanopartikel über makromolekulare Salzbildung in Lösung synthetisieren. Diese Partikel werden dann entsprechend ihrer Größe und Morphologie untersucht.

Acknowledgements

The present work was carried out at the DWI - Leibniz Institute for Interactive Materials and the Institute of Technical and Macromolecular Chemistry from January 2013 to September 2016 under the supervision of Prof. Martin Möller. I want to thank Prof. Martin Möller for offering me to be a part of his research group and related to this, the interesting topic, friendly and inspiring discussions. Further, I want to thank him for his steady support for both my work and the continuing education I received throughout my time at the institute as well as the given freedom in terms of organization of my work. I am very grateful for having had Dr. Helmut Keul as my subgroup leader, I enjoyed working with him both as a professional as well as an individual. During my work at the institute he continuously was a source of knowledge, inspiration and also criticism in the most positive way. During my time, he gave me scientifically and also humanly a lot of input to take along. Next, I want to thank Gent Kapiti, my lab partner for all the fruitful scientific but also off-topic discussions. Also I want to thank all of my fellow colleagues in the Keul group and in the DWI in general, which I have partially known for years back from my studies in Aachen and others I got to know later on. I think I do not exaggerate when I say that we had great times not only at work but above all in private as friends. Special thanks go to Rainer Haas, who helped me a lot during my thesis with all technical problems, like he probably always did. His capacities

and his knowledge and experience about analytical devices and issues are way beyond his kind and are of invaluable importance for the whole institute. During my PhD thesis I had the chance to be part of the Interreg Research Consortium "BioMiMedics". I would like to thank all members for the interesting meetings, symposia and workshops we had.

Besonderer Dank gilt schlussendlich meinen Eltern. Sie haben mir nicht nur ein Studium hier an der RWTH Aachen ermöglicht, sondern mich während des Studiums und weit darüber hinaus immer wieder unterstützt.

Publications

Parts of this thesis are published, submitted to be published and presented at conferences.

Articles

1. Mommer, S; Lamberts, K; Keul, H; Möller, M, A novel multifunctional coupler: the concept of coupling and proof of principle. *Chemical Communications*, **2013**, 49(32), 3288-3290. *see Chapter 4*
2. Mommer, S; Keul, H; Möller, M, Tailored thiol-functional polyamides: Synthesis and functionalization. *Macromolecular Rapid Communications*, **2014**, 35, 1986-1993. *see Chapter 5*
3. Mommer, S.; Truong, K.-N.; Keul, H.; Möller, M, An epoxy thiolactone on stage: four component reactions, synthesis of poly(thioether urethane)s and the respective hydrogels. *Polymer Chemistry*, **2016**, 7, 2291-2298. *see Chapter 6*
4. Mommer, S; Keul, H; Möller, M, One-Pot Synthesis of Amino Acid-Based Polyelectrolytes and Nanoparticle Synthesis. *Biomacromolecules*, **2017**, 18(1), 159-168. *see Chapter 6*

Posters and Talks

1. *Tailored thiol-functional polyamides: Synthesis and Characterization*, Mommer, S; Keul, H; Möller, M, *Frontiers of Polymer Science*, **2015**, Riva del Garda (Italy).

2. *Thiolactone chemistry - Paving the way to functional polymers*, Mommer, S; Keul, H; Möller, M, Scientific Advisory Board Meeting of the DWI - Leibniz Institute of Interactive Materials, **2015**, Aachen (Germany).
3. *Thiolactone chemistry - Paving the way to functional polymers*, Mommer, S; Keul, H; Möller, M, 252nd ACS National Meeting & Exposition - Chemistry of the People, by the People and for the People, **2016**, Philadelphia, Pennsylvania (USA).

Chapter 1

Introduction & Motivation

Organic chemistry has been a major field in the chemical sciences. Although the field of organic chemistry is less than 200 years old, today's databases contain more than 40 million different chemical compounds.¹ Organic chemistry lives and pays itself by a mere non-imaginable amount of compounds which can be created by chemical means. Whatever molecule a chemist can think of, he can try to connect corresponding atoms or molecules together to get the desired structure using a manifold number of techniques, catalysts and reaction set-ups. This turns the number of possible organic compounds to infinite. Compared to systems found in nature it therefore is indeed much broader regarding the amount of building blocks, and thus its diversity (Figure 1.1).

However, if we look at nature based systems, they are generally of immense complexity. In contrast to pure organic chemistry, nature is based on defined classes of substances (amino acids, saccharides, fatty acids, etc.), which although very rich in number are somewhere limited in the variety of types.² With this limited number of compounds at hand, nature

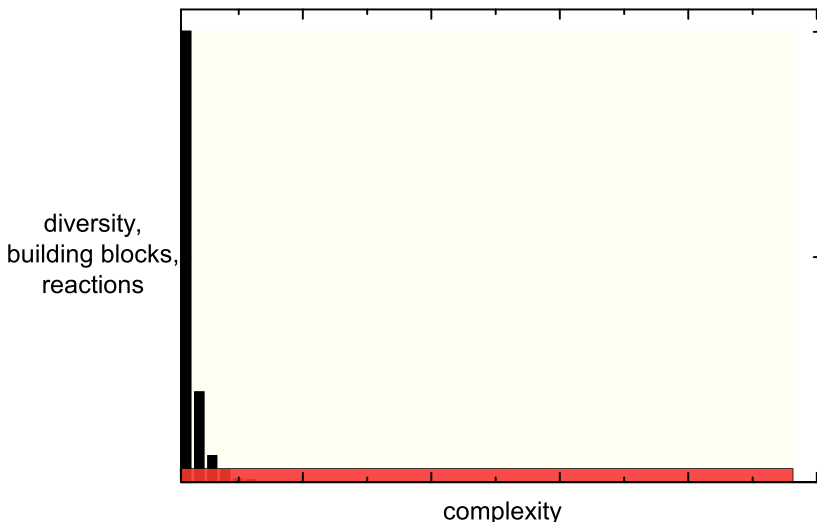


Figure 1.1: Diversity and number of building blocks in relation to the complexity of the created systems and architectures, distinguishing organic chemistry (black bars) from nature (red bar).

is able to build up peptides from amino acids, proteins and enzymes from peptides up to complex molecular machines arising from tertiary and quaternary structures of the corresponding peptide building blocks.³ These highly complex materials cover a broad variety of systems and functions. Just to name a few examples there are (i) cells being able to grow, interact and reproduce, (ii) permeable barriers like the phospholipid layer of cell membranes, (iii) systems which are able to store and release energy on demand (e.g. transformation of adenosine tri- to -diphosphate) and use it in shape of (iv) kinetic energy to translate in a specific direction (myosin or kinesin).^{4,5} All these systems are part of and ultimately lead to life. Today's materials scientist often authorize themselves to use techniques of nature related systems or try to mimic such. In this consent, nature has been a continuous source of inspiration regarding the development of concepts and systems in polymer chemistry or material sciences. In order to get small steps closer to complex systems it is inevitable to make use of not

only covalent bonds between atoms and molecules but also of a broad range of non-covalent interactions like hydrogen-bonding, electrostatic interactions, π -interactions, the hydrophobic effect and many more. However, as we focus on the preparation of macromolecular architectures and polymers the question arises of how new structures bearing new properties are to be generated. To create new structures, covalent linkages between molecules and building blocks are of large interest, since complex structures also require advanced connection chemistries (Figure 1.2). To

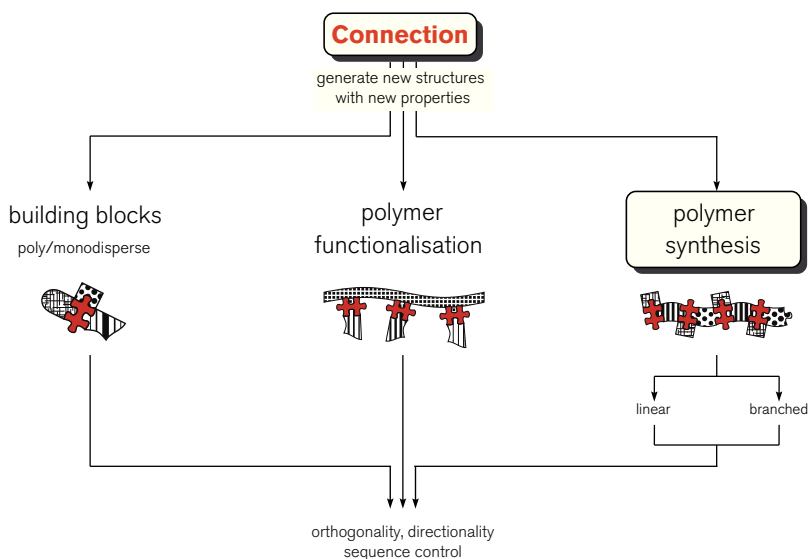


Figure 1.2: Complex structures need advanced connection chemistries. Therefore, three major synthetic pathways are disclosed: Connection of building blocks, polymer functionalization and polymer synthesis.

do so, the connection of molecules should run under very simple and efficient conditions. This for example excludes methodologies like the Merrifield solid phase synthesis for the controlled linkage of amino acids and short peptides, since protection chemistry shall be avoided. Instead and without doubt, there is a need for simple but efficient ligations or click-like reaction strategies. Nature helps itself with template chemistry, lock-and-

key principle etc.^{6,7} As synthetic polymer chemist, we don't have these methods at hand. Therefore we are more dependent on methods, which guarantee chemical selectivity and orthogonality as well as sequence control or directionality of the reaction. Connecting molecules of whatsoever nature (bioactive compounds, peptides, low-molecular weight or polymeric residues) to biohybrids has gained more and more attention in the last two decades.⁸

The connection of molecules can generally be accomplished in three different manners. (i) Several building blocks (poly- or monodisperse) are linked to one molecule, combining the properties of each and showing synergistic effects. (ii) An existing eventually commercially available reactive polymer is functionalized via post-polymerization modification. (iii) Monomers are connected to chains in a linear or branched fashion to build up polymers. Alternatively, cross-linked gels or networks are prepared therefrom. The requirements for such reactions and advanced connections have to be clearly defined (Figure 1.3).

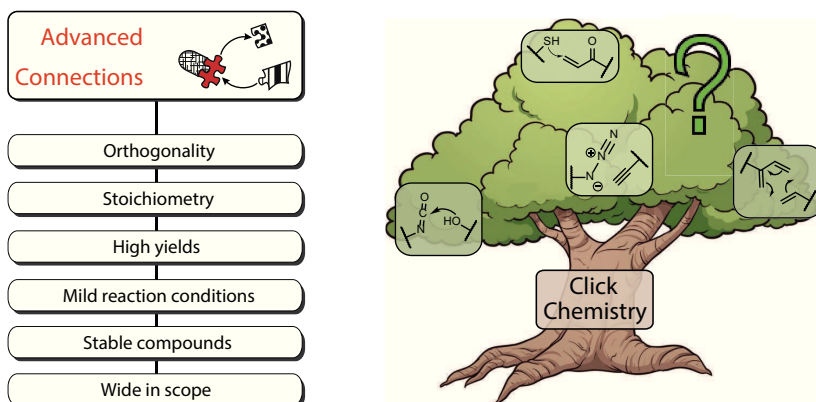


Figure 1.3: General requirements for efficient reactions providing advanced connections between multiple molecules.

First, such reactions should be orthogonal, which is expressed by a complete chemo- and regioselectivity. The process should always follow

a single reaction trajectory. Secondly, the reaction should proceed with stoichiometric amounts of reagents. Working with an excess of one reagent always entails an extensive work-up. For low-molecular weight products this is mainly restricted to recrystallization processes or purification through flash column chromatography. If working with polymeric residues, a reaction with an excess of one reagent is only tolerable, if the excess reagent is easily separated from the product polymer by evaporation or if the latter is isolated by precipitation, since chromatographic methods are restricted. Given that the reaction is fully orthogonal and stoichiometric, it should result in a high yield of pure product. As a consequence of these requirements, neither side- nor by-products are produced. A clean product should be obtained ideally using mild reaction conditions. The compounds should be insensitive to air or water, and the reaction should be easy to handle in small as well as in large scale. The reaction product should be stable if either stored on the lab bench or operated in an physiological environment. Finally, the reaction itself should be wide in scope. Whatever polymer backbone, compound or reagent is present, the reaction should proceed evenly good. All these headwords fit in to one term which was introduced for the first time by Sharpless, namely the term "click" chemistry.^{9,10} Meanwhile a broad portfolio of click-like procedures have been elaborated and transformed from simple organic reactions to the field of polymer chemistry and material sciences. These reactions reach from addition reactions (alcohol-isocyanate, thiol-acrylate) to Diels-Alder ligations or 1,3-dipolar cycloadditions and many more. It was in our group, where we tried to add or invent new ways to connect molecules in a click-like manner to grow this tree of click chemistries. To do so, a line-up of different linker molecules was developed, where the orthogonality of the different reaction sites enables a selective conversion of each functional group. Through this strategy, a new field was disclosed and many new polymeric materials were synthesized, the field of couplers and coupling chemistry.

Motivation

The work which has been done in the last years was mainly related to the synthesis of carbonate couplers and their use as monomers or coupling agents in polymer chemistry. While these coupling agents show by all means unique reactivity and good tendency for step-growth polymerizations, the functionality of the resulting materials has been mostly restricted to oxygen-based cycles and the alcohols resulting from their ring-opening. The motivation of this thesis is to open a new door towards functional diversity of the reactive coupling molecules by using an entirely new, but structurally versatile element: thiolactones. With the thiolactone as new key feature for coupling agents and its inherent multifaceted reactivity, three novel powerful coupling molecules are created. With the thiolactone, and the derived thiol group therefrom, a vast bandwidth of thiol-X reactions becomes available. Thanks to its orthogonal nature and "click"-like reactivity, opportunities and strategies towards functional materials enter a new dimension.

Scope of the thesis

In **Chapter 2** first an overview of couplers known in the literature is presented. The scope of applications for polymeric materials is demonstrated, whether it be in terms of synthetic possibilities or in final applications as functional materials. In the second part, cycloaddition reaction as highly used alternative ligation technique is discussed. The most prominent reactions are presented by way of example applications in polymer science.

Chapter 3 covers the role of thiols in polymer chemistry. The first part highlights the huge plurality of thiol-X reactions in combination with

recently published works in macromolecular chemistry. The second part deals with the thiolactone unit as key feature for the novel couplers and polymers. Its origin, first experimental studies and finally its use in state-of-the-art polymer and material sciences is demonstrated.

The first coupler/monomer, which has been synthesized, consists of a thiolactone and a ethylene carbonate linked by an O-methyl urethane spacer. In **Chapter 4**, its use as a straight coupler, linking four low-molecular weight building blocks together is shown. Later on, a one pot procedure to connect four different building blocks is established.

Chapter 5 deals with the second coupler/monomer, which is composed of two thiolactone rings with different substitution pattern and linked by an amide bond. This coupler is again studied in model reactions and as monomer for step-growth reaction to form polyamides.

Chapter 6 brings the last coupling molecule into focus, which combines a thiolactone unit with an oxirane via an O-methyl urethane spacer. The first part of this chapter deals with the synthesis of this coupler and its use in model reactions. Next, a step-growth polyaddition which proceeds via the thiol-epoxy addition is explored; different parameters are varied. Finally, the coupler's capacity to form hydrogels is demonstrated via two different reaction approaches. In part two of this chapter, the coupler is reacted with different α -amino acids and derivatives to prepare polymers with charged side groups. Various polyelectrolytes and polyamphiphiles are synthesized and investigated regarding their pH-responsive behavior. By combination of two oppositely charged polyelectrolytes, nanoparticles are prepared via polyelectrolyte complexation.

References

- (1) Vollhardt, K. P. C.; Schore, N. E., *Organische Chemie*, 5th; Wiley-VCH Verlag GmbH & Co. KGaA: 2011.
- (2) Lehn, J.-M. *Resonance* **1996**, *1*, 39–53.
- (3) Voet, D.; Voet, J. G.; Pratt, C. W., *Lehrbuch der Biochemie*, 2nd; Wiley-VCH Verlag GmbH & Co. KGaA: 2010.
- (4) Ballardini, R.; Balzani, V.; Credi, A.; Gandolfi, M. T.; Venturi, M. *Accounts of Chemical Research* **2001**, *34*, 445–455.
- (5) Bu, Z.; Callaway, D. J. In *Protein Structure and Diseases*, Donev, R., Ed.; Advances in Protein Chemistry and Structural Biology, Vol. 83; Academic Press: 2011, pp 163–221.
- (6) Fischer, E. In; Springer Berlin Heidelberg: Berlin, Heidelberg, 1909; Chapter Einfluss der Konfiguration auf die Wirkung der Enzyme. I, pp 836–844.
- (7) Koshland, D. E. *Angewandte Chemie* **1994**, *106*, 2468–2472.
- (8) *Chemistry of Bioconjugates: Synthesis, Characterization, and Biomedical Applications*; Narain, R., Ed.; John Wiley & Sons, Inc.: 2014.
- (9) Kolb, H. C.; Finn, M. G.; Sharpless, K. B. *Angewandte Chemie International Edition* **2001**, *40*, 2004–2021.
- (10) Barner-Kowollik, C.; DuPrez, F. E.; Espeel, P.; Hawker, C. J.; Junkers, T.; Schlaad, H.; VanCamp, W. *Angewandte Chemie International Edition* **2011**, *50*, 60–62.

Chapter 2

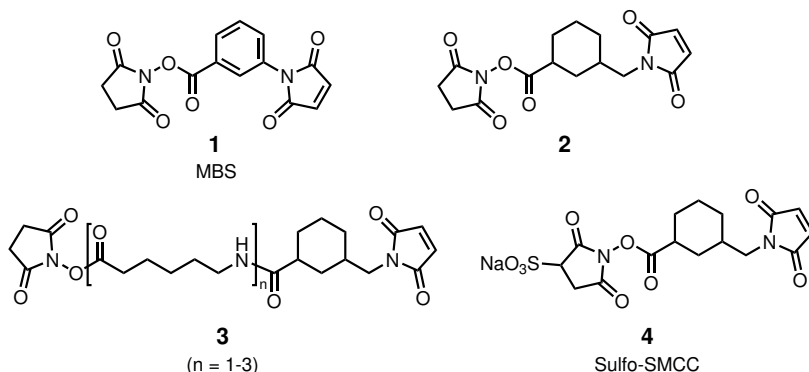
The Art of Coupling

2.1 Macromolecular Design through Coupling Agents

In the following sections, the use and development of coupling agents in different disciplines of chemistry and biochemistry will be discussed. Throughout history and with growing number of publications in this field, it becomes evident, that linking building blocks to each other puts the use of coupling agents in the focal point of scientific interest. This interest extends beyond various interdisciplinary fields of polymer and material sciences.

2.1.1 Bioconjugation Chemistry

The term coupling agent is firstly used in the field of bioconjugation chemistry.¹⁻³ Here, Kitagawa et al. use a heterobifunctional *meta*-maleimidobenzoyl N-hydroxysuccinimide ester (MBS) to couple β -D-galactosidase to insulin in neutral, aqueous solution (Scheme 2.1). The



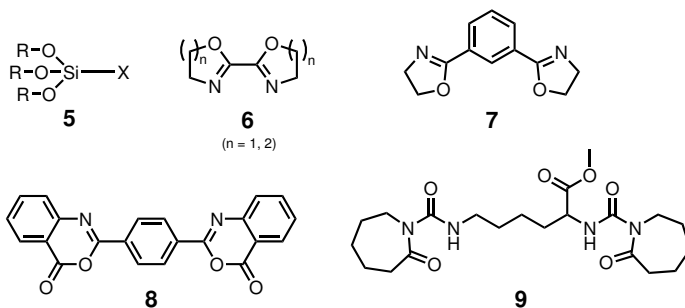
Scheme 2.1: Heterobifunctional coupling agents based on a succinimide active ester and a maleimide moiety.

reactivity of **1** relies on an active succinimide ester which is replaced in a substitution reaction by an amino acid; and the maleimide group which is able to react with a cysteine thiol moiety to form a thioether.⁴ Compound **2**, a derivative of **1**, connects the reactive sites via a cyclohexylmethyl spacer being more stable at physiological pH.⁵ The concept is later on picked up and improved by Bienarz et al. in synthesizing derivative **3**.⁶⁻⁹ Hereby, the end-to-end distance of each reactive site counted in atoms is increased from 9 (compound **2**) to 16, 23 and 30 (corresponding to $n = 1, 2$ or 3). With increasing length of the coupling molecule, the steric hindrance of the reaction environment is reduced and the prepared protein conjugates show enhanced activities. The synthetic protocol for coupler **3** is later improved by Reddy et al.¹⁰ Additionally, coupling agent **4** is introduced (also known as sulfo-SMCC), where a sulfonate group is installed at the succin-

imide ring to maximize its water solubility for protein conjugations.¹¹

2.1.2 Silanes and Other Step-growth Processes

Not only at academic research, but also in industry the use of coupling agents plays a vital role. In silane chemistry, coupling agents have found broad application. Here, they depict compounds like organofunctional silane **5** which consist of several siloxane residues and a reactive group bound to the silicon (Scheme 2.2). The reactive silicon ester groups are able to bind to inorganic materials (glass, metals, silica stones). The remaining reactive group introduces an organic residue (epoxy-/amino groups, hydrophobic/hydrophilic residues) to enhance the material's adhesion properties, mechanical strength of composite materials or simply as resin or surface modification.¹²⁻¹⁴ Beside what we describe as coupling agents has been used in industry as chain extenders for step-growth polymerizations (polycondensations or polyadditions). Compared to free radical polymerization, polymers obtained by step-growth mechanisms such as polyamides, polyesters and polyurethanes are quite limited in their molecular weight and the mechanical properties. To either increase the molecular weights of such polymers, adjust their flexibility and mechanical properties or both, chain extenders are reacted with the reactive end groups of the polymers. However, such chain extenders were mainly restricted to homobifunctional molecules, since there was neither a need nor an interest in orthogonality of the different reaction sites. Therefore, bisoxazolines like compound **6** were synthesized. Next to amines, alcohols and thiols, these are able to react with carboxylic acids, too, giving amide and ester bonds at elevated temperatures (about 200 °C).¹⁵⁻¹⁷ In later studies, the bisoxazolines are refined by introducing a phenylene residue or other aromatic spacers (**7**).¹⁸⁻²⁰ A more recent example shows the use of such bisoxazolines as AA-type monomers for polyaddition. Converting **7** with a selection of aliphatic dicarboxylic acids gives rise to poly(ester amide)s



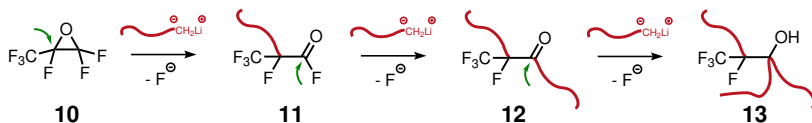
Scheme 2.2: Silane coupling agent and homobifunctional coupling agents based on heterocycles used as chain extenders for polycondensates.

up to a number average molecular weight (M_n) of $M_n = 25000$ g/mol.²¹ Meanwhile, Inata et al. have used benzoxazinones **8** to extend polyesters. Benzoxazinones are converted with hydroxyl groups to form new ester bonds.^{22,23} Very recently, to chain-extend polyurethanes without using toxic diisocyanates, a lysine-based bis(acyl lactam) **9** has been developed. Upon reaction with alcohols, the lactam groups are cleaved off and new carbamates are delivered. This way, biocompatible polyurethanes are synthesized reacting **9** with poly(ϵ -caprolactone) (PCL), polytetrahydrofuran (PTHF) or poly(ethylene glycol) (PEG). Molecular weights up to 65000 g/mol are obtained. Replacing the carboxylic methylester by a biotinyl residue gives polyurethanes (PU) having a number average molecular weight of $M_n = 3500$ g/mol.²⁴

2.1.3 Synthesis of Star Polymers

Hillmyer et al. have developed a multifunctional coupler for the combination of three polymer chains (Scheme 2.3). Hexafluoropropylene oxide **10** (HFPO) is able to connect three propagating Lithium activated polymer chains. The first carbanion is opening the oxirane ring. Upon formation of

a carbonyl fluoride, one fluoride anion is split off giving macromolecule **11**. Succeeding active polymer chains add to the carbonyl group. First another fluoride is cleaved off delivering **12**, and lastly the carbonyl is transformed into an alcohol resulting in a three-arm star polymer **13**. 90% of the polymer chains are connected to three arm star polymers, a small amount of two-chain coupling product is, however, inevitable and reflects as a slight shoulder in the SEC traces.²⁵

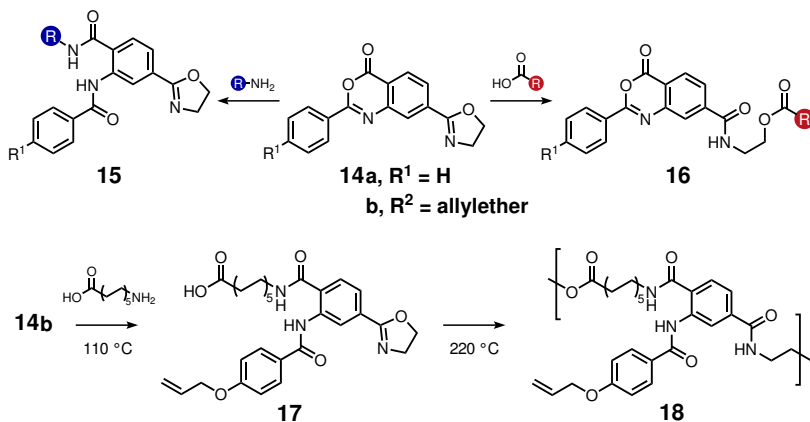


Scheme 2.3: Hexafluoropropylene oxide coupling agent, coupling three active polymer chains of the same type.

2.1.4 Heterocyclic Coupling Agents

Altogether, there has been a continuous effort for the development of novel methods to couple building blocks in the most efficient way. Yet, the main disadvantage of these coupling agents is, that they mostly consist of two reactive sites of the same functionality and thus are of homobifunctional nature. This makes orthogonal reaction strategies or their use as AA'-type monomers for step-growth polymerization impossible. Besides and for some, there are by-products such as succinimides, lactams or fluoride anions. Based on these findings, Böhme et al. have developed a series of heterobi- and -trifunctional couplers based on a benzoxazinone and an oxazoline. An example for a trifunctional coupling agent is given in Scheme 2.4. Coupler **14a** is used to combine aliphatic carboxylic acids and aliphatic alcohols or amines.²⁶ The benzoxazinone group is the more reactive one and reacts at temperatures above 110 °C in toluene at reflux to give amide **15**. At this temperature, neither the oxazoline,

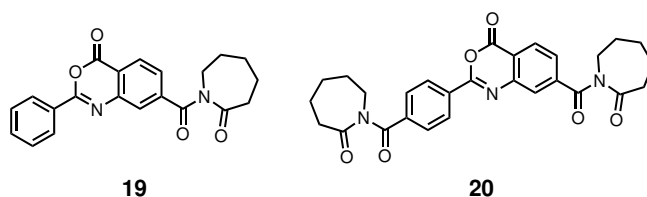
nor the allyl group in case of trifunctional derivative **14b** is touched by the nucleophile. Heating to temperatures above 200 °C in presence of an amine, both cycles start to react. Still, the reaction of amines with



Scheme 2.4: Heterobi- and -trifunctional coupling agents, based on benzoxazinones and oxazolines, showing the selective conversion of each reactive cycle and the preparation of poly(ester amides).

the benzoxazinone is much faster than its concurrent reaction with the oxazoline. Using a carboxylic acid instead to functionalize the coupling agent gives rise to selective conversion of **14** to the ester amide **16**. Model reactions have been carried out using different amines, alcohols and acids. Later, **14b** is used to prepare allyloxy-functional poly(ester amide)s. This is achieved by selective transformation of the benzoxazinone of **14b** with 11-aminoundecanoic acid to give **17**. Upon heating the reaction mixture to 220 °C in the melt, poly(ester amide) **18** is obtained, exhibiting a glass transition temperature of $T_g = 78.8$ °C.²⁷ Moreover, the present allyloxy groups in the side chain allow functionalization via post-polymerization modification. Beside the use of **14** as AA'-type monomer, it is also employed as chain extender for polyamide 6 and 12.²⁸ Furthermore, segmented block copolymers are obtained, when polyamide 12 and acid-functional poly(propylene oxide) (PPO) or poly(buylene terephthalate)

is employed.^{29,30} Other examples for multifunctional coupling agents in the Böhme group are compounds **19** and **20** consisting of a benzoxazinone and either one or two acyl lactam groups (Scheme 2.5). Here the selective conversion distinguishes between amino- and alcohol-functional building blocks. Alcohols are converted at 195 °C by substituting the lactam group(s). At temperatures about 210 °C, the benzoxazinone is opened by amines under formation of an amide bond. A broad range of model reactions is carried out with these compounds, and multifunctional polyamides are synthesized.^{31–33}

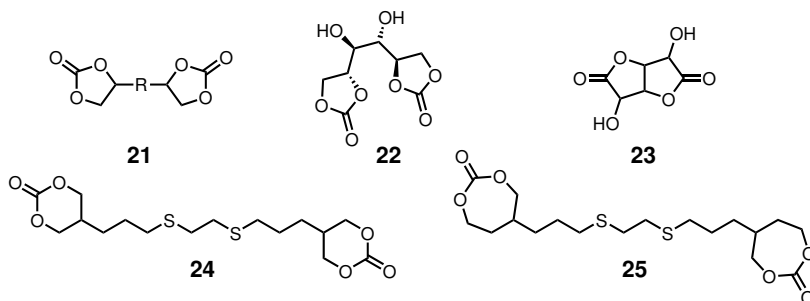


Scheme 2.5: Coupling agents based on acyl lactams and benzoxazinones.

2.1.5 Cyclic Carbonate based Coupling Agents

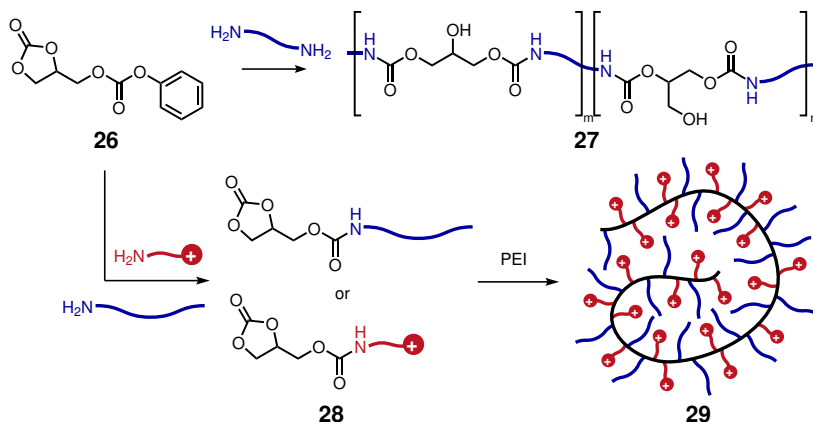
Next to the reviewed literature about coupling agents, our group has done extensive research in the field of coupling chemistry in the last decade. The motivation to develop new coupling agents originally arose from step-growth polymerizations. Polyesters, PU or PA (synthesized by step-growth polymerizations) have entered our daily life and are nowadays indispensable. However, the synthesis of such is mostly associated with the use of diisocyanates or acid chlorides which usually exhibit high toxicities. This hurdle has driven many scientists to look for alternatives, which resulted in the design of a broad variety of new bicyclic monomers. For the synthesis of hydroxy-functional polyurethanes and polyesters, our group recently wrote a mini-review.³⁴ However, major findings of bicyclic coupling agents

and their use in polymer synthesis and functionalization will be briefly discussed. At an early stage, the development of novel bicyclic monomers for step-growth polymerizations was tied to homobifunctional AA-type coupling agents with focus on renewable resources (Scheme 2.6). Endo



Scheme 2.6: Biscarbonate and bislactone couplers for the synthesis of hydroxy-functional PU/PA.

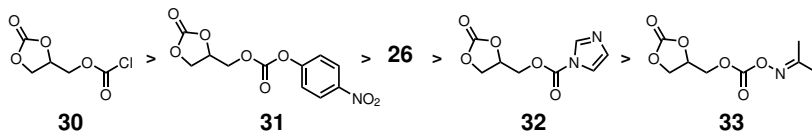
et al. have firstly introduced a 5-membered biscarbonate **21**. Later 6- and 7-membered biscarbonates **24** and **25** are investigated for polycondensation, too.^{35–41} By converting a diamine with the biscarbonates, both cycles are opened. With the formation of each amide bond, a new reactive side group - a hydroxyl group - is released. No by-products are produced during the reaction and the reagents themselves are insensitive to hydrolysis by residual water which makes anhydrous conditions superfluous. According to Höcker et al, hydroxy-functional polyurethanes are also obtained by reacting diamines with D-mannitol dicarbonate **22**. Furthermore, with compound **23** the authors firstly introduce a saccharic bislactone for the synthesis of poly(hydroxy amide)s. The free hydroxyl groups of **23** do not interfere with the polyaddition reaction.^{42,43} With the need for isocyanate-free polyurethanes also the first heterobifunctional coupler is synthesized (Scheme 2.7).⁴⁴ Compound **26** is composed of an ethylene carbonate fused to an O-methyl phenyl carbonate. The phenyl carbonate is the more reactive site and undergoes substitution by a nucleophilic amine at temperatures around 25 °C. The ethylene carbonate is less susceptible to



Scheme 2.7: Carbonate coupler **26** as monomer for hydroxy-functional PU and building block for multifunctional polymers.

aminolysis and starts reacting at temperatures around 50-70 °C. However, as for the preparation of hydroxy-functional polyurethanes the orthogonality is not exploited and thus upon reaction of **26** with diamines at elevated temperatures poly(hydroxy urethane)s **27** are formed by step-growth reaction. Upon addition of the amine to the carbonate and subsequent cleavage of one of the α -oxygens, two different isomeric alcohol groups are generated. Hence, the backbone of the polymer is equipped with hydroxymethyl and hydroxyl groups. The hydroxyl isomer is favored over the hydroxymethyl one. This is due to intramolecular hydrogen bonding as of whom a 5-membered cycle for the hydroxyl isomer is more stable than a 6-membered one for the hydroxymethyl isomer. Regarding the nucleophilic diamine, an increased number of methylene groups lowers the glass transition temperature of the amorphous material. A prosperous concept for coupling agents like **26** is also the modification of existing polymers or activated surfaces. Therefore, **26** is reacted with an amine which is functionalized with the property-introducing residue. Upon full conversion of this amidation, a functionalized carbonate coupler **28** is obtained. As shown in the example the carbonate coupler is functionalized with aliphatic

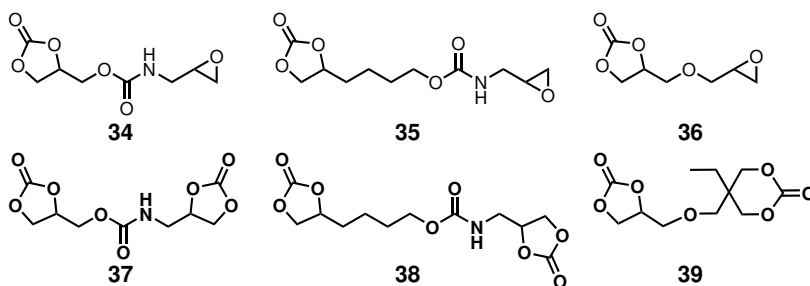
hydrophobic amines and cationic groups, respectively. These functionalized couplers are then coupled to an existing poly(ethylene imine) via ring-opening of the ethylene carbonate at higher temperatures to give the functionalized polymer **29**. The resulting polymer is used as coating for negatively charged surfaces, but has also demonstrated anti-bacterial effects.^{45–49} With the same technique, poly(dimethyl siloxane) has been equipped with quaternary ammonium groups at the α - and ω -endings.⁵⁰ Beside the carbonate coupler **26** a variety of derivatives have been synthesized with different leaving groups. A tendency of reactivity is clearly observed among the activated carbonates (Scheme 2.8).⁵¹ Further coupling reagents have been synthesized, which are based on substituted ethylene carbonate and chloroformate/phenylcarbonate groups linked by spacers of varying chain length; they will not be further discussed.⁵² Al-



Scheme 2.8: Alternative carbonate couplers with different carbonate bound leaving groups.

though the aforementioned strategy serves as an efficient tool to couple building blocks together, there is still an issue of purification, since the cleaved leaving groups always have to be removed to get a pure coupling product. Therefore, various heterobifunctional couplers have been designed, which rely on two cycles of different nature. In addition, these cycles are linked by different spacers to each other (Scheme 2.9). The reactivity of each will be briefly discussed. Coupling agents **34–36** have the well-investigated ethylene carbonate combined with an oxirane ring. Epoxides are able to react with primary or secondary amines and even with tertiary amines delivering cationic ammonium containing compounds. Anyhow, the reaction rate of the ring-opening diminishes with raising degree of substitution of the amine. Since the ethylene carbonate is only able

to react with primary amines, the combination of primary/secondary or primary/tertiary amines should be 100% selective. The ratio of consumed ethylene carbonate to oxirane has been tested using a sole amine in stoichiometric amounts to one equivalent of the coupler. At room temperature in dimethylsulfoxide (DMSO), **34** reacts in a ratio of 0.55:0.45. Coupler **35** shows at the same conditions a conversion ratio of 0.10:0.90 (oxirane ring is much more reactive towards amines at room temperature). Compound **36** which belongs to the class of ethers gives a conversion ratio of 0.45:0.31 after 4 days at room temperature (remaining 0.24 not converted **36**).⁵² As a heterobifunctional coupler, only **35** is a valuable representa-



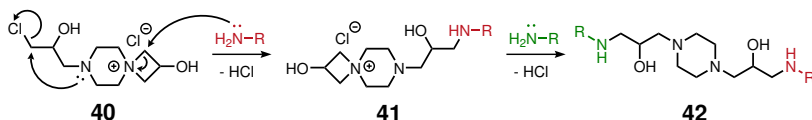
Scheme 2.9: Biscyclic heterobifunctional couplers linked by different spacers.

tive. As anticipated for the reaction of secondary or tertiary amines with the oxirane, full orthogonality is observed. Coupling agents **37** and **38** consist of two 5-membered ethylene carbonates, yet are connected by different spacers. After all, the electronic effect of the substituting spacer was not strong enough to induce any selectivity of one reactive site over the other.⁵² The final coupling agent synthesized in our group is the bis-carbonate **39**, which fuses a 5- and a 6-membered carbonate via an ether bridge. In contrast to the 5-membered carbonate, the 6-membered carbonate is more reactive towards amines and is readily opened at room temperature. Consequently, the chemical selectivity for the orthogonal junction of amines is given.⁵³ Alternatively, derivatives of **39** have been used to build up hydroxy-functional polyurethanes in an AA-type polyaddi-

tion.^{54,55}

2.1.6 Piperazine-based Azetidinium Coupler

As a last example for a bisfunctional coupling agent, azetidinium coupler **40** should be mentioned (Scheme 2.10). Synthesized from piperazine and two equivalents (eq) of epichlorhydrin at ambient temperature in water, **40** acts as a water-borne and water-soluble coupling agent. Withal the water as a highly polar solvent stabilizes the azetidinium group, which is selectively addressed using functional amines to give molecule **41**. It is exceptional, that only the azetidinium group is consumed during this reaction. Its high reactivity towards amines is mainly driven by the ring strain of the four-membered azocycle. The chlorhydrine remains fully intact and is not able to undergo a nucleophilic substitution under these reaction conditions. However, the water as solvent stabilizes the azetidinium in such a way, that upon elimination of the chlorine in 1-position the spirocyclic azetidinium is favorably reformed. At this stage, the functional coupler **41** is able to react with another amino species to obtain the fully functionalized adduct **42**. The coupling process is carried out at temper-



Scheme 2.10: Heterobifunctional azetidinium coupler based on piperazine and epichlorhydrin and its reactivity towards functional amines.

atures of 90 °C or at reflux in water without catalyst. Using this coupler, polyamines or amino-telechelic PTHF are functionalized to give azetidinium grafted polymers. The azetidinium grafts are still reactive towards amines and are converted in a second step. In doing so, aliphatic amines are coupled to the azetidinium grafted polymers.^{56,57} If the azetidinium

modified polyamines are only partially converted with aliphatic amines, polymers with anti-microbial properties are obtained (carrying cationic and aliphatic groups in the side chain). Similar properties have been explored for azetidinium-functional PTHF.^{58,59}

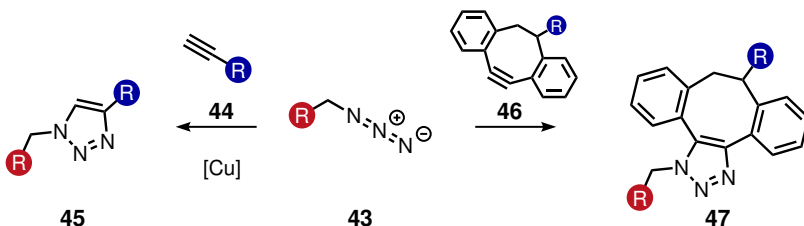
2.2 Coupling via Cycloaddition Reaction

As a very efficient tool and alternative to classic coupling chemistry, cycloaddition reactions have flooded applied concepts in polymer and material sciences and with this the corresponding publications and reports which have been released. One of the most famous and first discovered cycloaddition reactions is the Diels-Alder reaction, which has been described by Otto Diels and Kurt Alder in 1928. With this cycloaddition, they introduced a very efficient reaction to create carbon-carbon bonds in a simple and click-like manner.⁶⁰ At first the [4+2] cycloaddition is demonstrated using an electron-rich diene (e.g. furan or derivatives) and an electron-poor dienophile (vinyl ketones, etc.) to build up cyclic alkene adducts.⁶¹ Later, retro-Diels-Alder reactions and hetero-Diels-Alder reactions are discovered. The former describes a Diels-Alder (DA) reaction with thermal reversibility. The latter extends the common carbon-based Diels-Alder reagents by heteroatom-based dienophiles and dienes.^{62,63} Besides, other cycloadditions have emerged very rapidly; for instance the copper mediated azide-alkyne 1,3-dipolar cycloaddition to just name the most famous among them.⁶⁴ Because of their single reaction trajectory and orthogonal and reversible nature, cycloaddition reactions have become a very prominent coupling or ligation technique (not only in the field of organic chemistry but more and more in macromolecular design). In the following section, several cycloadditions in the field of polymer synthesis are presented. However for a deeper and broader overview of the published works, we refer explicitly to the well-investigated review by M.

A. Tasdelen.⁶⁵

2.2.1 1,3-Dipolar Alkyne-azide Cycloaddition

The first discussed and most prominent cycloaddition reaction used in macromolecular chemistry is the copper-mediated azide-alkyne 1,3-dipolar cycloaddition (CuAAC) of an azide **43** and a terminal alkyne **44** to give a triazole adduct **45** (Scheme 2.11).^{64,66,67} Although alkynes are usually not very effective 1,3-dipole acceptors, the copper(I) as catalyst is able to bind to the terminal alkyne. This massively increases the reaction rate and makes these type of cycloadditions readily accessible. Instead of copper(I), often copper(II) in combination with a reducing agent such as sodium ascorbate is used. The reducing agent produces copper(I) in situ.⁶⁸ In a polymeric framework, this reaction has been uti-



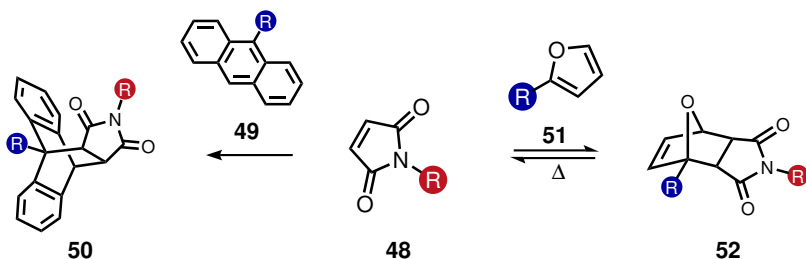
Scheme 2.11: Reaction of azides with alkynes via the copper-catalyzed 1,3-dipolar azide-alkyne cycloaddition or the strain-promoted azide-alkyne cycloaddition.

lized for different target polymers. Either ω -azide-functional polymers are added via CuAAC to polymer chains producing block copolymers or amphiphiles^{69,70} or low-molecular weight building blocks or peptides are coupled to the macromolecule giving biohybrid materials.^{71–73} In another approach, macromolecules bearing both, an azide and an alkyne group at the α - and ω -endings are coupled in a step-growth manner. Through this addition process, polymers are generated whose molecular weights are

increased by some multiple single chain molecular weights.⁷⁴ As an alternative, the CuAAC is used to functionalize existing polymers. These are synthesized with monomers having azide or alkyne groups in the side chain. In a subsequent reaction step, the complementary building block (alkyne or azide) is conjugated to the polymer backbone to deliver functionalized polymers or grafts.⁷⁵ Since the use of copper(I) compounds has been evaluated to be toxic for *in vivo* reactions and cells, the need for a copper-free ligation is especially given, when biomaterials are in the focus of research. An alternative strategy comprises the use of strained cycles, which are able to undergo [2+3] cycloaddition without using a copper catalyst. A cyclooctyne moiety **46** represents such a strained cycle, which is able to react in a copper-free strain-promoted azide-alkyne cycloaddition (spAAC) to give adduct **47** (Scheme 2.11).⁷⁶ As an example, Bertozzi et al. use this spAAC to modify biomolecules *in vitro* and in living cells without encountering any signs of toxicity.⁷⁷

2.2.2 Retro-Diels-Alder Reaction

The well known [4+2] Diels-Alder reaction between dienophiles and dienes finds its entry in the polymer science mainly in the shape of electron poor maleimides **48** and dienophiles like anthracene derivatives (**49**) and substituted furans (**51**) (Scheme 2.12). The DA ligation with anthracene **49** gives a bicyclooctane-based compound **50**. The reaction is carried out in toluene at reflux without a catalyst. This methodology has been used for various functionalizations and ligations; functionalizing polyamides or polymethacrylates with pendant anthracene units^{78,79} or in a grafting to approach of PEG to anthracene-functional polystyrene (PS)⁸⁰ to give just a few examples. The concept of Diels-Alder ligation has been extended by the use of substituted furan **51**, which is now able to form an oxabicycloheptane species **52** in a reversible way.⁸¹ The DA ligation itself is feasible at temperatures ranging from 25 °C up to 120 °C. Above 120 °C,



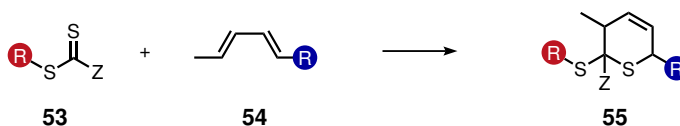
Scheme 2.12: Reaction of functional maleimides with anthracenes in an irreversible process and the reversible DA reaction of **48** using furan derivatives.

the thermally induced retroDA reaction occurs and furan **51** is removed to give maleimide **48** again. The retroDA ligation opens up quite new possibilities regarding the design of functional materials. For the functionalization of PS with pendant maleimide groups or the step-growth polymerization of bismaleimides and difurans the retroDA ligations has been used by Gandini et al. and others.^{82–85} Besides, the thermal reversibility of this reaction gives rise to dendrimers or cross-linked elastomers, which are now both thermally degradable and responsive.^{86,87} Furthermore, the reversible retroDA ligation is used to protect maleimides, which are highly reactive to thiols or other nucleophiles. In combination with the anthracene chemistry, the maleimides are first protected by DA ligation with a furan derivative. Subsequently and at higher temperatures, the furan adduct is removed and replaced by an anthracene moiety in one-pot to give block copolymers.^{88,89} Further applications and developments in retroDA materials chemistry have been profoundly pointed and reviewed.^{90,91}

2.2.3 Hetero-Diels-Alder Reactions

With the continuous development of the regular DA ligation and its extension to heteroDA reactions, DA reactions are of central importance in organic chemistry and natural product syntheses.^{61,92} Meanwhile, het-

eroDA ligations of imines, nitriloxides and many more^{64,93–95} have only found limited attention in polymer sciences.^{96,97} More recently, the group of Barner-Kowollik introduced a heteroDA technique taking benefit from dithioesters. Thioaldehydes and dithioesters of type **53** are well known to be very reactive heterodienophiles if equipped with electron-withdrawing groups (Scheme 2.13).^{98–100} Additionally, dithioesters are end groups for polymers prepared by reversible addition-fragmentation chain transfer polymerization (RAFT).¹⁰¹ Following a literature procedure with trifluoroacetic acid (TFA) as catalyst, dithioester **53** (with electron-withdrawing group Z) and functional diene **54** are converted to dihydrothiopyran adduct **55**. Via this metal-free strategy, PS - synthesized with a benzyl 2-pyridinecarbodithioate RAFT agent - is coupled to a hexadienol-initiated PCL. This reaction proceeds smoothly and fully selective at T = 50 °C to give a PS-*block*-PCL copolymer.¹⁰² With cyclopentadiene as end group, this heteroDA ligation is adopted to aqueous conditions, ambient temperature and even without a catalyst.^{103,104} Further achievements beside the synthesis of block copolymers are the preparation of graft copolymers, the functionalization of carbon nanotubes or surface patterning applications via thioaldehydes.^{105–107}

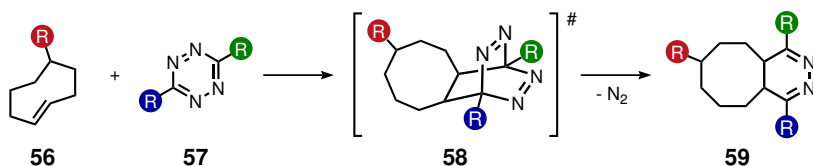


Scheme 2.13: HeteroDA reaction of classic RAFT agents like model dithioester **53** with a dienophile to give a dihydrothiopyran adduct.

2.2.4 Azo-based Diels-Alder Ligations

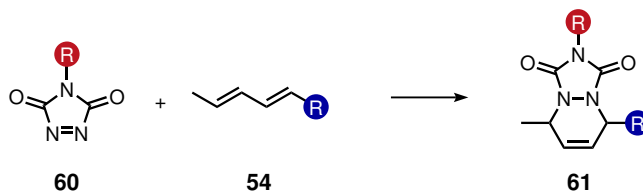
Looking at the frontier orbital theory of DA reagents, normal DA reactions proceed via the highest occupied molecular orbital (HOMO) of the electron-rich diene and the lowest unoccupied molecular orbital (LUMO)

of the electron-poor dienophile. In contrast to this standard behaving DA reactions, DA ligations involving azo-based heterocycles often follow an inverse electron demand mechanism. Here, the LUMO of the diene, which is an electron-poor molecule now, reacts with the HOMO of the electron-rich dienophile. Thus, this DA ligation is also called inverse electron demand DA reaction (DA_{inv}).¹⁰⁸ 1,2,4,5-Tetrazines – firstly studied by Carboni et al. – are of unique electronic structure being able to react with various dienophiles.^{109–111} Although the reaction with selected (cyclo)alkenes is possible, the DA ligation with *trans*-cyclooctene (**56**) is of significantly higher rate due to its specific spatial conformation and ring strain.^{112,113} Hence, if the DA_{inv} reaction is undertaken using 3,6-functional tetrazines **57** and *trans*-cyclooctene **56** modified in C5-position, a transition state is reached giving DA adduct **58** (Scheme 2.14). Upon elimination of molecular nitrogen, dihydro-pyridazine **59** is generated which makes this process irreversible.¹⁰⁸ In polymer chemistry, this click-like approach has received broad attention due to its orthogonality and fast reaction rate. Although the synthesis of tetrazines requires the use of toxic hydrazine, the DA_{inv} – using the former – is favored for biochemical conjugations. This is mainly ascribed to the reaction's metal-free conditions and wide applicability regarding the solvent choice (organic solvents, water, cell media). In this consent, Fox et al. have conjugated a thioredoxin protein of 11.7 kDa to a bis(2-pyridyl)tetrazine.¹¹⁴ Other authors have pursued this DA strategy for cell imaging via tetrazine fluorophores,^{115–117} the conjugation of quantum dots,¹¹⁸ the synthesis of meter-long fibres through interfacial polymerization of telechelic polymers¹¹⁹ or protein-polymer conjugates.¹²⁰ Alterna-



Scheme 2.14: Inverse electron demand Diels-Alder reaction of functional 1,2,4,5-tetrazines with *trans*-cyclooctene.

tively to cyclooctenes, Du Prez et al. have successfully used other ring-strained cycloalkenes like norbornenes for the DA_{inv} ligation with tetrazine-functional polymers to obtain block copolymers.¹²¹ Very recently, another DA_{inv} click-like ligation was introduced to macromolecular chemistry by the same group (Scheme 2.15). Therein, they use triazolinediones (**60**) for the ligation of different polymers. The former are known to be reactive dienophiles and are transformed with the corresponding diene **54** into the final product **61**.⁹³ In a layer-by-layer approach using triazolinedione



Scheme 2.15: Reaction of triazolinediones with random hexadienyl-equipped residues.

chemistry, multiple (up to 58) thin organic films were deposited on a surface.¹²² Besides, this system has impressively shown to which precise extend it is applicable in microcontact printing.¹²³ The synthesis of such triazolinediones, their use as clickable moieties and for polymer synthesis have been thoroughly reviewed.¹²⁴

References

- (1) Hermanson, G. T. In *Bioconjugate Techniques (Second Edition)*, Hermanson, G. T., Ed., Second Edition; Academic Press: New York, 2008; Chapter 4, pp 234–275.
- (2) Hermanson, G. T. In *Bioconjugate Techniques (Second Edition)*, Hermanson, G. T., Ed., Second Edition; Academic Press: New York, 2008; Chapter 5, pp 276–335.
- (3) Hermanson, G. T. In *Bioconjugate Techniques (Second Edition)*, Hermanson, G. T., Ed., Second Edition; Academic Press: New York, 2008; Chapter 6, pp 336–345.

- (4) Kitagawa, T.; Aikawa, T. *Journal of Biochemistry* **1976**, *79*, 233–236.
- (5) Yoshitake, S.; Yamada, Y.; Ishikawa, E.; Masseyeff, R. *European Journal of Biochemistry* **1979**, *101*, 395–399.
- (6) Bieniarz, C.; Welch, C.; Barnes, G. Heterobifunctional coupling agents., 4994385, 1991.
- (7) Bieniarz, C.; Welch, C.; Barnes, G. Heterobifunctional maleimido containing coupling agents., 5053520, 1991.
- (8) Bieniarz, C.; Welch, C.; Barnes, G.; Schlesinger, C. Covalent attachment of antibodies and antigens to solid phases using extended length heterobifunctional coupling agents., 5002883, 1991.
- (9) Bieniarz, C.; Husain, M.; Barnes, G.; King, C. A.; Welch, C. J. *Bioconjugate Chemistry* **1996**, *7*, 88–95.
- (10) Reddy, R. E.; Chen, Y.-Y.; Johnson, D. D.; Beligere, G. S.; Rege, S. D.; Pan, Y.; Thottathil, J. K. *Bioconjugate Chemistry* **2005**, *16*, 1323–1328.
- (11) Farooqui, F.; Reddy, P. Efficient synthesis of protein-oligonucleotide conjugates., 6942972, 2005.
- (12) Serman, S.; Marsden, J. G. *Industrial & Engineering Chemistry* **1966**, *58*, 33–37.
- (13) Rykowski, J. J. Silane coupling agents., 4197537, 1979.
- (14) Plueddemann, E. P., *Silane Coupling Agents*, 2nd; Springer US: 1991.
- (15) Douhi, A.; Fradet, A. *Journal of Polymer Science Part A: Polymer Chemistry* **1995**, *33*, 691–699.
- (16) Chalamet, Y.; Taha, M. *Journal of Polymer Science Part A: Polymer Chemistry* **1997**, *35*, 3697–3705.
- (17) Torres, N.; Robin, J. J.; Boutevin, B. *Journal of Applied Polymer Science* **2001**, *79*, 1816–1824.
- (18) Loontjens, T.; Pauwels, K.; Derks, F.; Neilen, M.; Sham, C. k.; Serné, M. *Journal of Applied Polymer Science* **1997**, *65*, 1813–1819.
- (19) Wörner, C.; Müller, P.; Mülhaupt, R. *Journal of Applied Polymer Science* **1997**, *66*, 633–642.
- (20) Nery, L.; Lefebvre, H.; Fradet, A. *Macromolecular Chemistry and Physics* **2004**, *205*, 448–455.
- (21) Luston, J.; Kronek, J.; Markus, O.; Janigová, I.; Böhme, F. *Polymers for Advanced Technologies* **2007**, *18*, 165–172.
- (22) Inata, H.; Matsumura, S. *Journal of Applied Polymer Science* **1986**, *32*, 4581–4594.

- (23) Inata, H.; Matsumura, S. *Journal of Applied Polymer Science* **1987**, *34*, 2609–2617.
- (24) Yin, J.; Wildeman, J.; Loontjens, T. *Journal of Polymer Science Part A: Polymer Chemistry* **2015**, *53*, 2036–2049.
- (25) Switek, K. A.; Bates, F. S.; Hillmyer, M. A. *Macromolecules* **2004**, *37*, 6355–6361.
- (26) Jakisch, L.; Komber, H.; Häussler, L.; Böhme, F. *Macromolecular Symposia* **2000**, *149*, 237–244.
- (27) Jakisch, L.; Komber, H.; Böhme, F. *Journal of Polymer Science Part A: Polymer Chemistry* **2003**, *41*, 655–667.
- (28) Jakisch, L.; Komber, H.; Wursche, R.; Böhme, F. *Journal of Applied Polymer Science* **2004**, *94*, 2170–2177.
- (29) Dung, B. T.; Jakisch, L.; Komber, H.; Häussler, L.; Voit, B.; Nghia, N. D.; Böhme, F. *Macromolecular Chemistry and Physics* **2006**, *207*, 1953–1964.
- (30) Böhme, F.; Jakisch, L.; Komber, H.; Wursche, R. *Polymer Degradation and Stability* **2007**, *92*, 2270–2277.
- (31) Jakisch, L.; Komber, H.; Böhme, F. *Macromolecular Materials and Engineering* **2007**, *292*, 557–570.
- (32) Zhang, H.; Jakisch, L.; Komber, H.; Voit, B.; Böhme, F. *Tetrahedron* **2013**, *69*, 3656–3663.
- (33) Zhang, H.; Jakisch, L.; Komber, H.; Häussler, L.; Voit, B.; Böhme, F. *Polymer* **2015**, *79*, 232–242.
- (34) Hahn, C.; Keul, H.; Möller, M. *Polymer International* **2012**, *61*, 1048–1060.
- (35) Kihara, N.; Endo, T. *Journal of Polymer Science Part A: Polymer Chemistry* **1993**, *31*, 2765–2773.
- (36) Kihara, N.; Kushida, Y.; Endo, T. *Journal of Polymer Science Part A: Polymer Chemistry* **1996**, *34*, 2173–2179.
- (37) Tomita, H.; Sanda, F.; Endo, T. *Journal of Polymer Science Part A: Polymer Chemistry* **2001**, *39*, 851–859.
- (38) Tomita, H.; Sanda, F.; Endo, T. *Journal of Polymer Science Part A: Polymer Chemistry* **2001**, *39*, 162–168.
- (39) Tomita, H.; Sanda, F.; Endo, T. *Journal of Polymer Science Part A: Polymer Chemistry* **2001**, *39*, 4091–4100.
- (40) Tomita, H.; Sanda, F.; Endo, T. *Journal of Polymer Science Part A: Polymer Chemistry* **2001**, *39*, 860–867.
- (41) Tomita, H.; Sanda, F.; Endo, T. *Journal of Polymer Science Part A: Polymer Chemistry* **2001**, *39*, 3678–3685.

- (42) Prömpers, G.; Keul, H.; Höcker, H. *Designed Monomers and Polymers* **2005**, *8*, 547–569.
- (43) Prömpers, G.; Keul, H.; Höcker, H. *Green Chemistry* **2006**, *8*, 467–478.
- (44) Ubaghs, L.; Fricke, N.; Keul, H.; Höcker, H. *Macromolecular Rapid Communications* **2004**, *25*, 517–521.
- (45) Pasquier, N.; Keul, H.; Möller, M. *Designed Monomers and Polymers* **2005**, *8*, 679–703.
- (46) Pasquier, N.; Keul, H.; Heine, E.; Möller, M. *Biomacromolecules* **2007**, *8*, 2874–2882.
- (47) Pasquier, N.; Keul, H.; Heine, E.; Möller, M.; Angelov, B.; Linser, S.; Willumeit, R. *Macromolecular Bioscience* **2008**, *8*, 903–915.
- (48) He, Y.; Keul, H.; Möller, M. *European Polymer Journal* **2011**, *47*, 1607–1620.
- (49) He, Y.; Heine, E.; Keusgen, N.; Keul, H.; Möller, M. *Biomacromolecules* **2012**, *13*, 612–623.
- (50) Novi, C.; Mourran, A.; Keul, H.; Möller, M. *Macromolecular Chemistry and Physics* **2006**, *207*, 273–286.
- (51) Fricke, N.; Keul, H.; Möller, M. *Macromolecular Chemistry and Physics* **2009**, *210*, 242–255.
- (52) He, Y.; Goel, V.; Keul, H.; Möller, M. *Macromolecular Chemistry and Physics* **2010**, *211*, 2366–2381.
- (53) He, Y.; Keul, H.; Möller, M. *Reactive and Functional Polymers* **2011**, *71*, 175–186.
- (54) Anders, T.; Keul, H.; Möller, M. *Designed Monomers and Polymers* **2011**, *14*, 593–608.
- (55) Anders, T.; Keul, H.; Möller, M. *e-Polymers* **2013**, *11*, 832–850.
- (56) Chattopadhyay, S.; Keul, H.; Möller, M. *Green Chemistry* **2013**, *15*, 3135–3139.
- (57) Chattopadhyay, S.; Keul, H.; Möller, M. *Macromolecules* **2013**, *46*, 638–646.
- (58) Chattopadhyay, S.; Heine, E. T.; Keul, H.; Möller, M. *Macromolecular Bioscience* **2014**, *14*, 1116–1124.
- (59) Chattopadhyay, S.; Heine, E.; Keul, H.; Möller, M. *Polymers* **2014**, *6*, 1618.
- (60) Diels, O.; Alder, K. *Justus Liebigs Annalen der Chemie* **1928**, *460*, Diels1928, 98–122.
- (61) Nicolaou, K. C.; Snyder, S. A.; Montagnon, T.; Vassilikogiannakis, G. *Angewandte Chemie International Edition* **2002**, *41*, 1668–1698.

- (62) Diels, O.; Alder, K. *Berichte der deutschen chemischen Gesellschaft (A and B Series)* **1929**, *62*, 2337–2372.
- (63) Gresham, T. L.; Steadman, T. R. *Journal of the American Chemical Society* **1949**, *71*, 737–738.
- (64) Huisgen, R. *Angewandte Chemie International Edition* **1963**, *2*, 565–598.
- (65) Tasdelen, M. A. *Polym. Chem.* **2011**, *2*, 2133–2145.
- (66) Huisgen, R. *Angewandte Chemie International Edition in English* **1963**, *2*, 633–645.
- (67) Lutz, J.-F. *Angewandte Chemie International Edition* **2007**, *46*, 1018–1025.
- (68) Rostovtsev, V. V.; Green, L. G.; Fokin, V. V.; Sharpless, K. B. *Angewandte Chemie* **2002**, *114*, 2708–2711.
- (69) Cosemans, I.; Vandenbergh, J.; D'Olieslaeger, L.; Ethirajan, A.; Lutsen, L.; Vanderzande, D.; Junkers, T. *European Polymer Journal* **2014**, *55*, 114–122.
- (70) Lopez, G.; Guerre, M.; Schmidt, J.; Talmon, Y.; Ladmiral, V.; Habas, J.-P.; Ameduri, B. *Polym. Chem.* **2016**, *7*, 402–409.
- (71) Tsarevsky, N. V.; Sumerlin, B. S.; Matyjaszewski, K. *Macromolecules* **2005**, *38*, 3558–3561.
- (72) Lutz, J.-F.; Schlaad, H. *Polymer* **2008**, *49*, 817–824.
- (73) Lutz, J.-F.; Zarafshani, Z. *Advanced Drug Delivery Reviews* **2008**, *60*, Design and Development Strategies of Polymer Materials for Drug and Gene Delivery Applications, 958–970.
- (74) Johnson, J. A.; Finn, M. G.; Koberstein, J. T.; Turro, N. J. *Macromolecular Rapid Communications* **2008**, *29*, 1052–1072.
- (75) Royes, J.; Rebolé, J.; Custardoy, L.; Gimeno, N.; Oriol, L.; Tejedor, R. M.; Pinol, M. *Journal of Polymer Science Part A: Polymer Chemistry* **2012**, *50*, 1579–1590.
- (76) Lutz, J.-F. *Angewandte Chemie International Edition* **2008**, *47*, 2182–2184.
- (77) Agard, N. J.; Prescher, J. A.; Bertozzi, C. R. *Journal of the American Chemical Society* **2004**, *126*, 15046–15047.
- (78) Rabjohns, M. A.; Hodge, P.; Lovell, P. A. *Polymer* **1997**, *38*, 3395–3407.
- (79) Kim, T.-D.; Luo, J.; Tian, Y.; Ka, J.-W.; Tucker, N. M.; Haller, M.; Kang, J.-W.; Jen, A. K.-Y. *Macromolecules* **2006**, *39*, 1676–1680.
- (80) Gacal, B.; Durmaz, H.; Tasdelen, M. A.; Hizal, G.; Tunca, U.; Yagci, Y.; Demirel, A. L. *Macromolecules* **2006**, *39*, 5330–5336.
- (81) Ripoll, J. L.; Rouessac, A.; Rouessac, F. *Tetrahedron* **1978**, *34*, 19–40.

- (82) Diakoumakos, C. D.; Mikroyannidis, J. A. *Journal of Polymer Science Part A: Polymer Chemistry* **1992**, *30*, 2559–2567.
- (83) Laita, H.; Boufi, S.; Gandini, A. *European Polymer Journal* **1997**, *33*, 1203–1211.
- (84) Goussé, C.; Gandini, A.; Hodge, P. *Macromolecules* **1998**, *31*, 314–321.
- (85) Goussé, C.; Gandini, A. *Polymer International* **1999**, *48*, 723–731.
- (86) McElhanon, J. R.; Wheeler, D. R. *Organic Letters* **2001**, *3*, 2681–2683.
- (87) Gheneim, R.; Perez-Berumen, C.; Gandini, A. *Macromolecules* **2002**, *35*, 7246–7253.
- (88) Durmaz, H.; Colakoglu, B.; Tunca, U.; Hizal, G. *Journal of Polymer Science Part A: Polymer Chemistry* **2006**, *44*, 1667–1675.
- (89) Alkayal, N.; Hadjichristidis, N. *Polym. Chem.* **2015**, *6*, 4921–4926.
- (90) Sanyal, A. *Macromolecular Chemistry and Physics* **2010**, *211*, 1417–1425.
- (91) Gandini, A. *Progress in Polymer Science* **2013**, *38*, Topical Issue on Polymer Chemistry, 1–29.
- (92) Corey, E. J. *Angewandte Chemie International Edition* **2002**, *41*, 1650–1667.
- (93) Waldmann, H. *Synthesis* **1994**, *1994*, 535–551.
- (94) Jorgensen, K. A. *Angewandte Chemie International Edition* **2000**, *39*, 3558–3588.
- (95) Bodnar, B. S.; Miller, M. J. *Angewandte Chemie International Edition* **2011**, *50*, 5630–5647.
- (96) Vretik, L.; Ritter, H. *Macromolecules* **2003**, *36*, 6340–6345.
- (97) Singh, I.; Zarafshani, Z.; Lutz, J.-F.; Heaney, F. *Macromolecules* **2009**, *42*, 5411–5413.
- (98) Vedejs, E.; Eberlein, T. H.; Varie, D. L. *Journal of the American Chemical Society* **1982**, *104*, 1445–1447.
- (99) Vedejs, E.; Eberlein, T. H.; Mazur, D. J.; McClure, C. K.; Perry, D. A.; Ruggeri, R.; Schwartz, E.; Stults, J. S.; Varie, D. L. *The Journal of Organic Chemistry* **1986**, *51*, 1556–1562.
- (100) Dentel, H.; Gulea, M. *Phosphorus, Sulfur, and Silicon and the Related Elements* **2013**, *188*, 349–355.
- (101) Keddie, D. J.; Moad, G.; Rizzardo, E.; Thang, S. H. *Macromolecules* **2012**, *45*, 5321–5342.
- (102) Sinnwell, S.; Inglis, A. J.; Davis, T. P.; Stenzel, M. H.; Barner-Kowollik, C. *Chemical Communications* **2008**, 2052–2054.

- (103) Inglis, A.; Sinnwell, S.; Stenzel, M.; Barner-Kowollik, C. *Angewandte Chemie International Edition* **2009**, *48*, 2411–2414.
- (104) Glassner, M.; Delaître, G.; Kaupp, M.; Blinco, J. P.; Barner-Kowollik, C. *Journal of the American Chemical Society* **2012**, *134*, 7274–7277.
- (105) Bousquet, A.; Barner-Kowollik, C.; Stenzel, M. H. *Journal of Polymer Science Part A: Polymer Chemistry* **2010**, *48*, 1773–1781.
- (106) Zydziak, N.; Preuss, C. M.; Winkler, V.; Bruns, M.; Hübner, C.; Barner-Kowollik, C. *Macromolecular Rapid Communications* **2013**, *34*, 672–680.
- (107) Glassner, M.; Oehlschlaeger, K. K.; Welle, A.; Bruns, M.; Barner-Kowollik, C. *Chemical Communications* **2013**, *49*, 633–635.
- (108) Eicher, T.; Hauptmann, S., *The Chemistry of Heterocycles, 2nd, Completely Revised, and Enlarged Edition*; John Wiley & Sons, Inc.: 2003.
- (109) Carboni, R. A.; Jr., R. V. L. *Journal of the American Chemical Society* **1959**, *81*, 4342–4346.
- (110) Boger, D. L. *Chemical Reviews* **1986**, *86*, 781–793.
- (111) Wiley, P. F. In *Chemistry of Heterocyclic Compounds*; John Wiley & Sons, Inc.: 2008; Chapter 5, pp 179–249.
- (112) Thalhammer, F.; Wallfaher, U.; Sauer, J. *Tetrahedron Letters* **1990**, *31*, 6851–6854.
- (113) Knall, A.-C.; Slugovc, C. *Chem. Soc. Rev.* **2013**, *42*, 5131–5142.
- (114) Blackman, M. L.; Royzen, M.; Fox, J. M. *Journal of the American Chemical Society* **2008**, *130*, 13518–13519.
- (115) Devaraj, N. K.; Weissleder, R.; Hilderbrand, S. A. *Bioconjugate Chemistry* **2008**, *19*, 2297–2299.
- (116) Devaraj, N.; Upadhyay, R.; Haun, J.; Hilderbrand, S.; Weissleder, R. *Angewandte Chemie International Edition* **2009**, *48*, 7013–7016.
- (117) Murrey, H. E.; Judkins, J. C.; am Ende, C. W.; Ballard, T. E.; Fang, Y.; Riccardi, K.; Di, L.; Guilmette, E. R.; Schwartz, J. W.; Fox, J. M.; Johnson, D. S. *Journal of the American Chemical Society* **2015**, *137*, 11461–11475.
- (118) Han, H.-S.; Devaraj, N. K.; Lee, J.; Hilderbrand, S. A.; Weissleder, R.; Bawendi, M. G. *Journal of the American Chemical Society* **2010**, *132*, 7838–7839.
- (119) Liu, S.; Zhang, H.; Remy, R. A.; Deng, F.; Mackay, M. E.; Fox, J. M.; Jia, X. *Advanced Materials* **2015**, *27*, 2783–2790.
- (120) Lorenzo, M. M.; Decker, C. G.; Kahveci, M. U.; Paluck, S. J.; Maynard, H. D. *Macromolecules* **2016**, *49*, 30–37.

- (121) Hansell, C. F.; Espeel, P.; Stamenović, M. M.; Barker, I. A.; Dove, A. P.; Prez, F. E. D.; O'Reilly, R. K. *Journal of the American Chemical Society* **2011**, *133*, 13828–13831.
- (122) Vonhören, B.; Roling, O.; Bruycker, K. D.; Calvo, R.; Prez, F. E. D.; Ravoo, B. J. *ACS Macro Letters* **2015**, *4*, 331–334.
- (123) Roling, O.; Bruycker, K. D.; Vonhören, B.; Stricker, L.; Körsgen, M.; Arlinghaus, H. F.; Ravoo, B. J.; Prez, F. E. D. *Angewandte Chemie International Edition* **2015**, *54*, 13126–13129.
- (124) De Bruycker, K.; Billiet, S.; Houck, H. A.; Chattopadhyay, S.; Winne, J. M.; Du Prez, F. E. *Chemical Reviews* **2016**, *116*, 3919–3974.

Chapter 3

The Role of Thiols in Polymer Chemistry

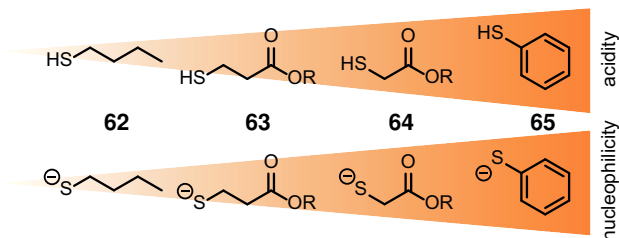
The word thiol is the portmanteau or blended word of thio-alcohol. Thiols are thus the representative sulfur analogue to alcohols. However, in contrast to oxygen related compounds, thiols differ a lot in their reactivity and properties. The main aspect of these differences are attributed to the physico-chemical nature of the S-H bond. Compared to the O-H bond (459 kJ/mol, 96 pm distance), the S-H bond is not only weaker (363 kJ/mol) but also the distance between the sulfur and the hydrogen atom is larger (134 pm).¹ Further, the sulfur itself is less electronegative than its oxygen counterpart. As a result, the phenomenon of hydrogen bonding is only very weakly experienced with thiol compounds. The fact, that the S-H bond is weaker, increases the acidity of thiol compounds. Hence, in dissolved state the thiols tend to dissociate easier and provide H^+ cations.² Due to the lower electronegativity and its higher atomic number and radius, the softer sulfur is more polarizable and the electron cloud

is delocalized and equally distributed resulting in a well stabilized thiolate anion.³ As a consequence, thiolates are also good nucleophiles and exhibit a broad portfolio of chemical reactions.^{4–7} In the following sections, a compilation of thiol reactions will be presented to give an overview of their chemical diversity. The reactions will be referenced to macromolecular chemistry, in which they play a crucial role in state-of-the-art coupling and click chemistry. Finally, the thiol chemistry will be brought together with the thiolactone chemistry, as the thiolactone motif is the key part of the novel couplers presented throughout this thesis.

3.1 Reactions of Thiols and Thiol Derivatives

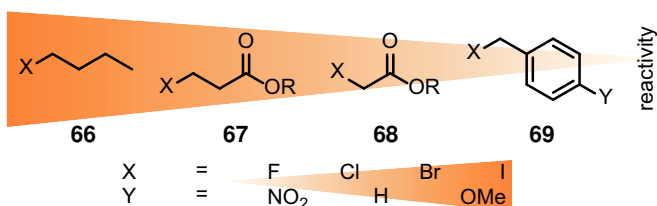
In the circular figure, a compilation of 17 different reaction strategies employing thiols as reactive component is portrayed (Figure 3.1). This high number of orthogonal reactions shows at the same time, that not only over the last century, moreover very recently the reaction toolbox of thiol-X chemistry has continuously been developed and extended. Additionally, it points out that the need for such simple, efficient and competitive reactions in the scientific community is still highly up-to-date and in existence.

But before we look at single reactions, thiols can get involved in, one should cast a glance on the reactivity trend of thiols (Scheme 3.1). As already mentioned, thiols are of higher acidity than alcohols. With the increasing capacity to withdraw electrons from the sulfur atom, the acidity raises from **62** to **65**. As an example, butanethiol **62** has a $\text{p}K_{\text{a}} = 10$, whereas **65** has a lower $\text{p}K_{\text{a}} = 6$.⁸ The nucleophilicity shows exactly the same behaviour. Looking at **62–65** in their thiolate form, the aromatic thiol exhibits the highest nucleophilicity, as the anion is stabilized the most.^{9,10} Regardless of these general trends, the influence of the reactant, solvent polarity or catalyst should not be neglected for each synthetic route, when



Scheme 3.1: Series of thiol compounds showing the trends of acidity and nucleophilicity.

donating residues generally favor thiolysis.⁹ With the use of dihaloalkanes and dithiols it has been possible to prepare aliphatic polythioether for the first time in a polycondensation process.¹⁴ Later on, in polymer chemistry this technique was mostly used for end group modification of polymers (in α - or ω -position) or to prepare telechelic dithioethers.^{15,16} As example, atom transfer radical polymerization (ATRP) based glycopolymers were synthesized with help of thiol-bromo chemistry.¹⁷ In an alternative approach, dendrimers and hyperbranched polymers are prepared via a thiol-bromo coupling.^{18,19} The thiol-arylhalide substitution has already been in-



Scheme 3.2: Reactivity of a series of alkylhalides.

tensively investigated and known for quite a time.⁹ However, the *para*-substitution of pentafluorobenzol residues got first into the focus when porphyrine chemistry emerged. The synthesis of porphyrine derivatives and their use as catalysts has raised the question for alternative coupling approaches.²⁰ The answer is the thiolate conjugation in *para*-position of pentafluorobenzol-functional porphyrines. Because of their unique elec-

tronic structure – ascribed to the electron-withdrawing fluoro-substituents – the substitution in *para*-position becomes mostly favorable and proceeds smoothly in polar solvents like dimethylformamid (DMF) in a basic environment at room temperature.^{21–23} Quickly, this concept found entrance to polymer chemistry, too. In 2009, Becer et al. have prepared glycopolymers by S-glycosylation of pentafluorostyrene copolymers.²⁴ Furthermore, the thiol-*para*fluoro route has been used for post-polymerization modification of (multiarm star) polymers and films.^{25–28}

Switching to addition reactions, thiols are also able to react with isocyanates and isothiocyanates. Upon reaction of a thiol with an isocyanate or an isothiocyanate at benign temperatures with a base as catalyst (often Et₃N is used), a carbamothioate or a carbamodithioate is produced, respectively.²⁹ Compared to the reaction with isocyanates, the addition to isothiocyanates is slightly slower. However, in contrast to the former, carbamodithioates are reversibly formed and can be re-transformed into the reactants. This makes them an interesting conjugation species in biochemistry.^{30–33} In polymer chemistry, the isothiocyanate addition has been less applied than the concurrent isocyanate addition. Yet, comparisons between analogous materials show, that polymers based on dithiourethanes exhibit lower glass transition temperatures (T_g) and are generally softer and more flexible than their thiourethane counterparts.³⁴ Besides, thiol-isocyanate strategies have been used for the end-functionalization of polymers,^{35,36} modification of polymer beads and surfaces^{37,38} and the synthesis of linear polymers, networks and nanocarriers.^{39–42}

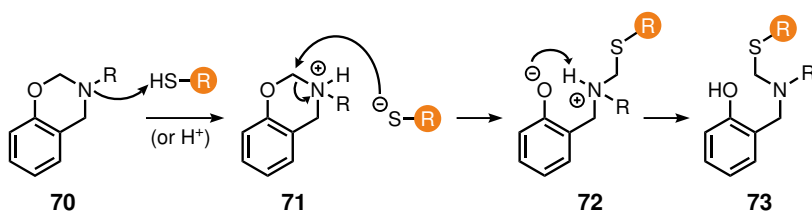
Similar to alcohols and amines, thiols are able to open oxirane rings, too. While amines are nucleophilic enough to add to oxiranes without a catalyst, thiols need activation by a base, with whom it is possible to fully convert epoxides to β -hydroxy thioethers. The thiol-epoxy addition has frequently been a tool for the ligation of enzymes and proteins via the cys-

teine using a homobifunctional epoxy linker.⁴³ Not less important is the concept of thiol-epoxy reactions in industrial adhesion chemistry. Here, many two-component adhesives and resins comprise epoxides and thiol components to build up networks during the curing process at ambient temperature.⁴⁴ Beside the importance of epoxides as monomers in anionic and cationic polymerizations, the interest in the polyaddition of epoxides has been noticeably increased. Either bisepoxides in combination with bithiols or solely AB-type epoxy thiols are used in a polyaddition process to obtain polythioethers with pendant hydroxyl groups.^{45–47} Another example shows the end group modification of RAFT prepared homopolymers by lysis of the RAFT initiator followed by thiol-epoxy addition of the ω -thiol to functional epoxides.⁴⁸ Meanwhile, Khan et al. furnished poly(methyl methacrylate)s (PMMA) with oxiranes as side-groups. Upon thiol modification, diverse functionalities become available.^{49,50} Another synthetic strategy demonstrates elegantly, how AB₂-type monomers consisting of one thiol and two oxirane rings are self-condensated at mild conditions to afford hyperbranched hydroxy-functional polymers.⁵¹

Being less famous than the thiol-epoxide reaction, the nucleophilic addition of thiols to aziridines has attracted far less attention. Aziridines, are like their oxygen analogues, 3-membered rings, which due to the ring strain, are of strong electrophilicity. Thus, a broad range of thiols can be added to the aziridine ring to deliver a thioether and a free amine group in one step.^{52–55} However, in macromolecular chemistry the thiol-aziridine reaction has found very confined application. Aziridine-containing polymers have recently been modified by alcohol-functional moieties,⁵⁶ the thiol-aziridine reaction has only been studied in the case of polymer beads with thiol groups on the surface and the functionalization with tosylaziridine of such.³⁷

Benzoxazine resins have profoundly been studied in the last years.⁵⁷ To just name a few advantages to commonly used epoxy- or phenolic resins,

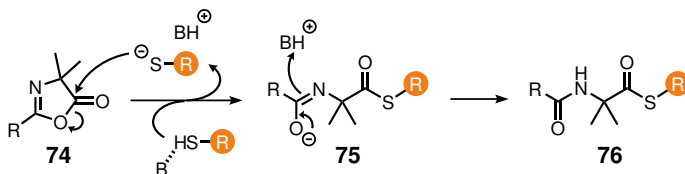
polybenzoxazines have good high-temperature properties, low water absorption, near-zero volumetric change and no by-products upon curing.⁵⁸ The catalytic opening of lateral benzoxazine rings by thiols (COLBERT) was firstly established by Gorodisher et al. The finding, that thiols are able to react with benz[1,3]oxazines at ambient temperature has disclosed new opportunities to synthesize benzoxazine-containing polymers at very mild reaction conditions (Scheme 3.3). Hereby, the nitrogen atom in 1-position of compound **70** is partly protonated by either the thiol or through acid catalysis under formation of a thiolate and an ammonium species **71**. Next, the thiolate induces ring-opening by nucleophilic attack at the adjacent C2 carbon and the CH₂-O bond is broken to generate species **72**. Finally, the hydrogen of the cationic ammonium is transferred to the newly formed phenolate group to afford product **73**.⁵⁹ This synthetic route is picked up by Yagci et al. and others, who use either benzoxazine derivatives to functionalize polystyrene end groups or thiols to functionalize polybenzoxazines as well as for the synthesis of gels or self-healing materials.^{60–65}



Scheme 3.3: Proposed mechanism of the COLBERT process.

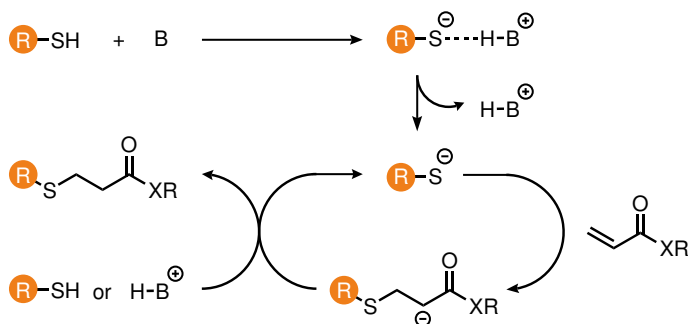
The next heterocyclic thiol ligation, which is rather a niche reaction in the field of thiol chemistry, is the base-catalyzed ring-opening of azlactones by thiols (Scheme 3.4). Upon addition of a thiolate to the carbonyl group of an azlactone **74**, the ester group is transformed into a thioester group. After complete dissociation of the C-O ester bond, intermediate **75** is formed. The negatively charged oxygen forms a new carbonyl group and the N=C

double bond is transformed into an amide by proton transfer from the base to give product thioester **76**.⁶⁶ In polymer chemistry, there is yet only one contemporary work referring specifically to this thiol-azlactone reaction. The group around Padma Gopalan makes use of this ligation; polycarbonate or silicon surfaces are first coated with a terpolymer equipped with azlactones in the side chain. The installment of a peptide is thus achieved via the thiol-azlactone reaction of a cysteine with the coated surface.⁶⁷



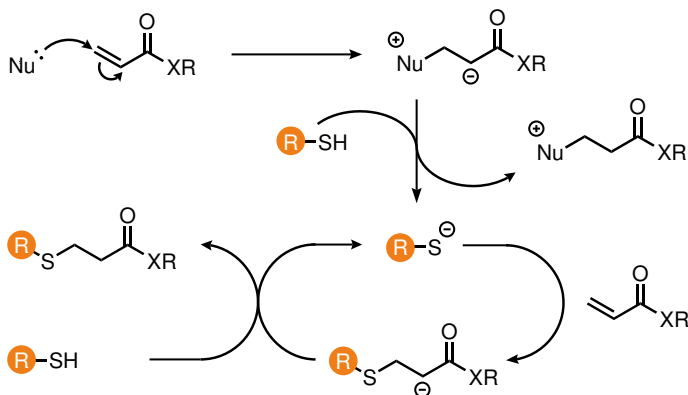
Scheme 3.4: Base-catalyzed azlactone ring-opening using thiols.

After this side trip to rather exotic reactions of thiols with heterocycles, one should not forget the most prominent thiol reaction, namely the thio-ene Michael-type addition. The first report on the thio-Michael (S-C) addition goes back to the year 1964 and is authored by Allen and Humphlett. In their report, they describe the syntheses of a variety of thio-Michael adducts.⁶⁸ This disclosure has facilitated synthetic strategies in organic chemistry and not long since has entered the field of macromolecular chemistry. Beside the carbo- and the aza-Michael addition, the thio-Michael addition has again specific merits to benefit from. Again as in all precedented reactions, thiolates are very soft nucleophiles, their acidity favors easy deprotonation by only catalytic amounts of base.⁶⁹ The mechanisms by which the thio-Michael addition is catalyzed has been studied well. The reaction either runs in a base- or a nucleophile-catalyzed fashion. At the base-catalyzed mechanism, the thiol species is firstly deprotonated to give a thiolate (Scheme 3.5). This active thiolate performs now the Michael addition to the acrylate or acrylamide to generate a thioether with a carbanion in α -position to the carbonyl group. Pro-



Scheme 3.5: Base-catalyzed Michael-type thiol-ene addition of a thiol to an acryl species (X = O, NH).

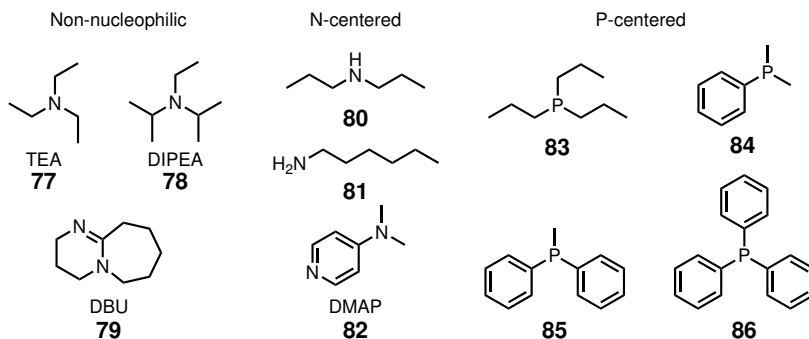
ton abstraction by the carbanion finally delivers the desired product. The nucleophile-catalyzed mechanism works different (Scheme 3.6). Here, the nucleophile actively participates in the initiation reaction by addition to the C=C double bond and formation of a zwitterionic species. This zwitterionic species is transformed into a cationic one via deprotonation of the thiol. Now, the active thiolate is able to react with the double bond to give the Michael adduct in the same way as for the base-catalyzed mechanism. Whether the reaction follows the one or the other mechanism, depends solely on the employed catalyst.^{8,70,71} Scheme 3.7 gives a selection of different nitrogen and phosphor-based thiol-ene catalysts. Among them are the more sterically hindered and hence non-nucleophilic bases and N- and P-centered nucleophilic bases. The former comprise bases such as triethylamine **77** (TEA), diisopropylethylamine **78** (DIPEA) and cyclic bases such as 1,8-diazabicyclo[5.4.0]undec-7-ene **79** (DBU). The N-centered nucleophilic bases include alkyl amines like **80**, **81** or dimethylaminopyridine (**82**, DMAP). Within the amino-functional bases, the following trend is observed, when hexyl acrylate is reacted with hexanethiol using 0.057 mol% of the catalyst: **79** \gg **81** $>$ **80** $>$ **77** (**78** and **82** not being investigated).⁷² Among the P-centered nucleophiles are alkylphosphine **83** and arylphosphines such as mono-, di-, and triphenylphosphines



Scheme 3.6: Nucleophile-catalyzed Michael-type thiol-ene addition of a thiol to an acryl species (X = O, NH).

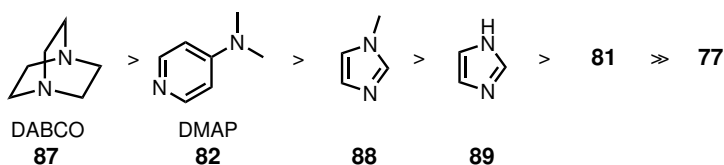
84-86. Although phosphine bases are generally weaker bases than the corresponding amines, they are able to catalyze the thiol-ene reaction up to high conversions using a lower catalyst loading. Again hexyl acrylate and hexanethiol are reacted using different catalysts, this time setting a catalyst concentration of 0.0005 mol%. The trend of the reaction rates follows the order: **83** > **84** > **79** (using the same concentration) \gg **85** \gg **86**.⁷² It must be said, that in general nucleophilic bases tend to favor the nucleophile-catalyzed pathway. However, often a hybrid of both mechanisms is observed.^{8,72-74} Additionally to the exceptional rate of the thiol-ene reaction with **83**, phosphines are able to catalyze the Michael addition of methyl methacrylates, which are rather problematic to bring to full conversion with conventional catalysts like **77**. However, there is a twist when it comes to the choice of the solvent. Catalysts, which act via the nucleophile-based mechanism are more sensitive to proton sources. In some cases, protic solvents may thus lead to a total inhibition of the reaction.⁷⁵

With progressing research on the thiol-ene Michael reaction and deployable substrates, new Michael acceptors have been explored. Vinylsul-



Scheme 3.7: Selection of bases catalyzing the thiol-ene Michael addition. Bases are separated in non-nucleophilic, N-centered and P-centered bases.

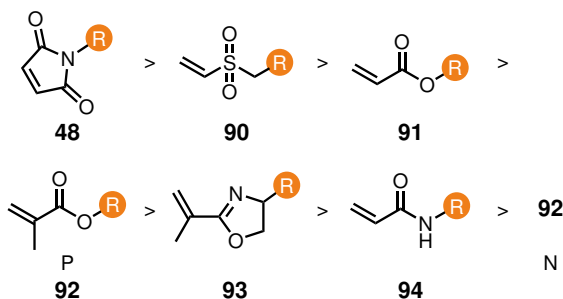
ones readily react with thiols to deliver β -thiosulfonyl compounds. The reaction takes place at very mild conditions, with slightly basic pH values and in water or buffer solutions in an physiological environment. Furthermore, the Michael adduct is resistant to hydrolysis at neutral pH. This makes the thiol-vinylsulfone ligation a predestined coupling reaction for proteins, enzymes or other.⁶ The reactivity of vinylsulfones towards thiols with a series of catalysts has been investigated by Bowman et al. Their results affirm the catalytic activity of heterocyclic azo-catalysts being 1,4-diazabicyclo[2.2.2]octane (**87**, DABCO) the catalyst with the highest activity, followed by **82** over imidazoles **88** and **89**. All azo-heterocyclic catalysts are still more active than amines **81** and **77** which is attributed to the nucleophile-based pathway of the reaction (Scheme 3.8).^{76,77} Further,



Scheme 3.8: Catalytic activity of heterocyclic azo-catalysts for the thiol-vinylsulfone Michael addition.

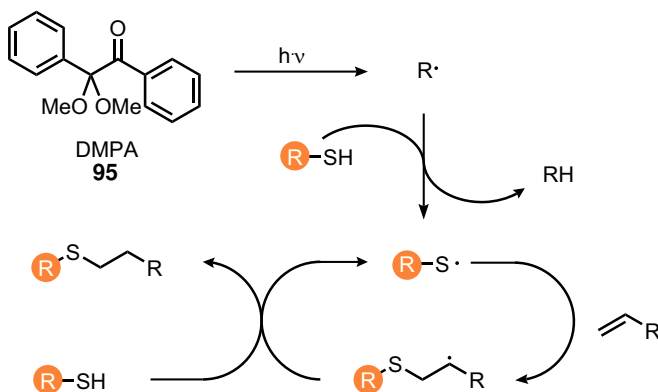
it has been examined, that for the reaction of thiols in presence of hexyl acrylate and vinylsulfone in equimolar amounts using one of the above mentioned catalysts, the thiol-vinylsulfone addition is strongly preferred leaving the acrylate basically untouched.⁷⁵ Meanwhile in polymer chemistry, this technique has been applied for the synthesis of gels by converting tri- or tetrathiols with corresponding di- or trivinylsulfones.^{76,78,79} Another example shows the preparation of micellar solutions through aggregation of amphiphilic block copolymers with vinylsulfone groups at the outer shell and their coupling to peptides.⁸⁰ Besides, polymers with pendant vinylsulfone groups, dendritic structures or shape-memory materials have been synthesized.^{81–83}

One of the most reactive Michael acceptors ever since the elaboration of thio-Michael reactants is the maleimide group. Maleimides are 5-membered cyclic imides hosting a double bond in α -position to the carbonyl group and equipped with N-centered functional residues. Maleimides are good electrophiles and highly reactive towards thiols, due to (i) the electron-withdrawing effect of the two carbonyl groups and (ii) the release of the ring strain upon saturation of the double bond. Thus, they serve as excellent Michael acceptors for the thiol-ene reaction. The thiol-maleimide addition – well known as ligation technique in biochemistry^{43,84–88} – does not require a catalyst and proceeds again at very mild conditions even in water or aqueous buffer solutions.⁸⁹ In polar solvents with high dielectric constants like DMSO or DMF, the reaction is considered as self-catalyzed or solvent-promoted.^{74,90} Thioether adducts exhibit a lifetime of weeks to several month, as studies on the long-term stability have shown.⁹¹ In polymer synthesis, the thiol-maleimide reaction has been employed to connect biomolecules like glutathione or bovine serum albumin (BSA) to maleimide-functional polymers.^{92,93} In another work, DA furan-protected maleimide acrylates are polymerized. Next, deprotection of the maleimide groups via retroDA reaction at elevated temperatures prior to thiol-maleimide addition affords functionalized polymers.⁹⁴ Finally,



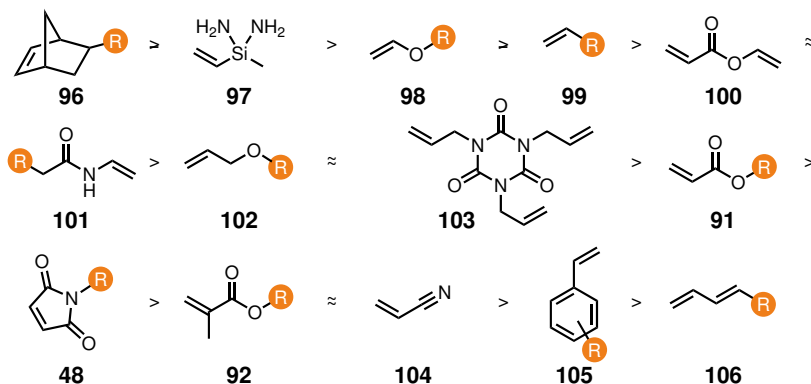
Scheme 3.9: Overall reactivity of Michael acceptors towards thiols. N and P depict either azo- or phospho-based catalysis.

if we discuss the Michael addition as one single reaction type of thiols towards Michael acceptors, a tendency of reactivity becomes apparent. As a general trend one can state, that with increasing strength of the electron-withdrawing group, the electron deficiency at the double bond and therefore the Michael acceptor character increases. Out of experimental results the series of Michael acceptors **48**, **90** to **94** is classified in terms of their reactivity towards thiols (Scheme 3.9).⁸⁹



Scheme 3.10: Radical thiol-ene addition of thiols to alkenes using – exemplary – the photoinitiator DMPA (**95**).

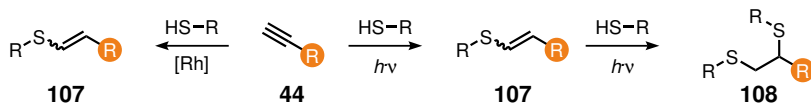
Side by side with the thiol-ene Michael addition the radical thiol-ene reaction enlarges not only the variety of substrates susceptible to thiols, but also the range of applications and synthetic methods.^{74,95} The history of thiol-ene chemistry has been well documented,⁹⁶ however a few characteristics about the reaction should be mentioned. The radical thiol-ene reaction proceeds similar to the thiol-ene Michael addition at very mild reaction conditions. Unlike the latter though, the radical thiol-ene reaction follows a radical mechanism and is initiated by a photoinitiator (in the most common cases, Scheme 3.10). Upon the irradiation with UV light, photoinitiator **95** decomposes and generates radicals; for illustration purposes 2,2-dimethoxy-2-phenylacetophenone (DMPA) is depicted. One of these radicals reacts now with the functional thiol by hydrogen abstraction to give an active thiyl species. The radical thiyl is added to the C=C double bond in an *anti*-Markovnikov orientation and forms a thioether with a carbon-centered radical. In the second step, the carbon radical abstracts a proton from a thiol to generate the product thioether and a new thiyl radical. Termination reactions occur as simple radical-radical recombinations.^{74,97,98} Although the thiol-ene radical polymerization is nearly unlimited when it comes to the choice of substrate (as long a C=C bond is present), a group of functional alkenes prevails of which the reactivity towards thiols are presented below (Scheme 3.11). Norbornene **96** exhibits the highest reaction rate. This is probably due to the high ring strain of the bicyclo-based structure. In general, the reactivity of electrophilic enes decreases with decreasing electron density at the C=C double bond. This trend is reflected in the whole series of electrophiles. Consequently, the reactivity of C=C double bonds decreases from silane **97**, to vinyl ether **98** and alkene **99**. Unsaturated esters and amides are again less, but equally reactive (**100-101**). Allyl ether **102** shows the same electrophilicity as triallyl isocyanurate **103**, both representing popular cross-linking motifs. In opposition to the corresponding thio-Michael addition, acrylates and maleimides (**91** and **48**) are of quite low reactivity for the thiol-ene radical addition. Lower reactivities are only observed by methacrylate **92**,



Scheme 3.11: Overall reactivity of alkenes towards thiols for the radical thiol-ene addition.

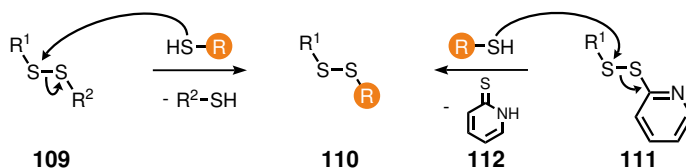
acrylonitrile **104** and substituted styrenes or conjugated dienes (**105-106**). The low reactivities of the latter (**92,104-106**) are caused by the inherent stabilization of the radical, resulting in a low hydrogen abstraction rate of the thiyl-addition products.⁹⁹⁻¹⁰¹ The thiol-ene radical polymerization has been mostly used to prepare networks and functional gels.¹⁰²⁻¹⁰⁵ In a recent publication of our group, statistical and block copolymers are synthesized from allyl glycidyl ether (AGE) and *tert*-butyl glycidyl ether (tBGE) or ethoxy ethyl glycidyl ether (EEGE). Using photoinitiator **95** and a dithiol in oil-in-water (o/w) emulsions, nanogels are obtained. Upon deprotection of either the tBGE or the EEGE fractions in the gels, nanogels with phase-segregated hydrophobic and hydrophilic domains are generated.¹⁰⁶ As alkynes are electrophilic compounds too, they are able to react with thiols in a similar reaction mechanism. The difference in thiol-yne radical addition is, that two equivalents of thiols can be linked to the alkyne **44**. Firstly, **44** is transformed into a vinyl thioether **107** prior to the second addition to afford dithioether **108** (Scheme 3.12).¹⁰⁷ To selectively achieve a monothiolation of alkyne **44**, Tang et al. have recently implemented first a Rhodium(I)-catalyzed procedure and later on a catalyst-free protocol into polymer chemistry. With the aforementioned systems, they are able

to synthesize regioselective monosubstituted vinyl thioether polymers at mild conditions.^{108,109} Further applications are partly similar to the thiol-ene chemistry and have been recently documented.¹¹⁰



Scheme 3.12: Reaction of alkynes to mono- and dithioethers via radical-mediated thiol-yne reaction and selective Rhodium-catalyzed addition.

In addition to its nucleophilic reactions, thiols are also sensitive to oxidation and can be oxidized to disulfides. In biology, this equilibrium between the oxidized and the reduced form (thiols or disulfides) plays a vital role for a variety of functions in proteins, enzymes and other.¹¹¹ The main building block for thiols in nature is based on the amino acid cysteine. Two cysteine thiol groups can be oxidized to a cystine group containing a disulfide bond. The disulfide bond is of crucial importance for the stability of proteins and has significant impact on the protein folding and its ultimate function. Yet, it is not only a structural motif but a key feature for the modulation of protein activity, too.^{112,113} The oxidation of thiols to disulfides is a redox process and proceeds in a physiological environment, either in air, at slightly basic pH or by an oxidant (e.g. aqueous H_2O_2).^{114,115} In macromolecular science, the polymerization of dithiols via oxidation has been investigated by Marvel and Olsen and others.^{116,117} A broad palette of polydisulfides has been synthesized and studied ever since.¹¹⁸ Recent publications show further the importance of disulfides in prodrugs¹¹⁹ or in a green dithiol polymerization to give redox-sensitive degradable polydisulfides.¹²⁰ Rather than via a radical redox process, in biology the disulfide formation mostly follows a $\text{S}_\text{N}2$ mechanism through an enzyme-mediated thiol-disulfide interchange (**109** \rightarrow **110**, Scheme 3.13). Moreover, the disulfide bond is cleaved by reducing agents like 1,4-dithio-D-threitol (DTT) or tris(2-carboxyethyl)phosphine (TCEP).⁶ As biochemical thiol-disulfide



Scheme 3.13: Thiol-disulfide exchange reaction as found in nature and the chemical approach via pyridyl disulfides.

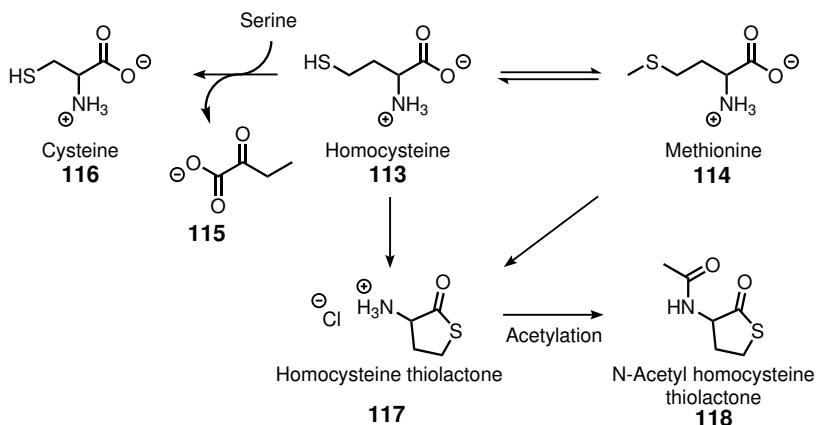
exchanges are often enzyme-catalyzed systems, the need for an alternative approach in chemical synthesis has led to the exploration of pyridyl disulfides (**111**) as thiol-disulfide exchange reagents.¹²¹ If pyridyl disulfide **111** is converted at mild temperatures with a functional thiol, the non-symmetrical disulfide **110** is delivered. The main driving force for this orthogonal reaction is the irreversible formation of 2-thiopyridone **112**. Compound **112** is a stable by-product and thus not susceptible to thiols. Also in polymer science, the pyridyl disulfide chemistry has been used. As an example, pyridyl disulfide-functional monomers are utilized to prepare polymers with pyridyl disulfide units in the backbone. Upon functionalisation of such or a grafting-from strategy, detachable disulfide-linked side-chains are introduced.^{122,123} An alternative to the pyridyl disulfide chemistry is provided by the thiol-thiosulfonate exchange reaction. In the same way, the thiol reacts here with the covalent sulfur in α -thiosulfonate to give a mixed disulfide.^{124,125} This strategy has been picked up by Theato et al. They functionalize the ω -site of RAFT prepared polymers via thiol-thiosulfonate chemistry.¹²⁶ The final thiol reaction is enabled by its reactivity towards metal particles and surfaces. As a thiolate anion is a very soft Lewis-base, it shows strong tendency to bind to metals like Mercury, Nickel or Silver.⁹ However the most prominent example of a metal-thiol linkage is the thiol-Gold ligation.⁶ Although the thiol-Au bond itself is yet not fully understood, it is said that the thiol-Gold linkage can be seen as a $\text{R-S-Au}^{(I)}$ connection with the strength of a covalent bond.^{127,128} In combination with the synthesis of spherical or rod-shaped Gold nanoparti-

cles, the thiol stabilization has found diverse applications comprising polymer grafting approaches,^{129–134} surface modifications,¹³⁵ studies on self-assembly^{136,137} and many more.¹³⁸

3.2 Homocysteine Thiolactone as Functional Key Feature

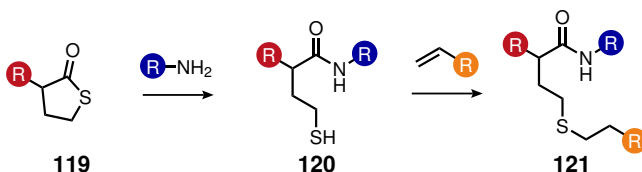
Homocysteine is a homologue of the amino acid cysteine. It has a thiol group in γ -position to the carbonyl, whereas the cysteine's thiol group is located in β -position. Further, it shows structural similarity to methionine, which instead of a free thiol carries a methylthioether group. Homocysteine is neither involved in DNA-coding nor is it part of naturally occurring proteins. However, homocysteine (**113**) takes part in few biochemical processes (Scheme 3.14).¹³⁹ It is transformed via methylation into the amino acid methionine (**114**) or reversely synthesized therefrom via removal of the terminal methyl-group of **114**.¹⁴⁰ In biochemistry, **113** is further involved in the transformation of Serine into Cysteine. Firstly, a condensate of both (cystathionine) is generated (not shown). Upon elimination of α -ketobutyrate **115**, the amino acid cysteine (**116**) is formed.¹⁴¹ Another reaction is the ring-closure of the homocysteine under elimination of water. In this case, homocysteine thiolactone (**117**) is formed.¹⁴² This happens by a methionyl-tRNA synthetase of **113** if the methylation and the cystathionine γ -lyase are inhibited.¹⁴³

Moreover, it is possible to obtain **117** via cyclization of **113** or **114** using acid catalysis.^{144–146} The amino group of HCTL **117** has a pK_a of 6.67, which is lower compared to the free homocysteine ($\text{pK}_a = 8.87$). The decrease in pK_a is attributed to the thioester being of electron-withdrawing nature.¹⁴⁷ If the free amine group of **117** is protected through acylation, N-acetyl homocysteine thiolactone (**118**) is obtained. The reactivity of thi-



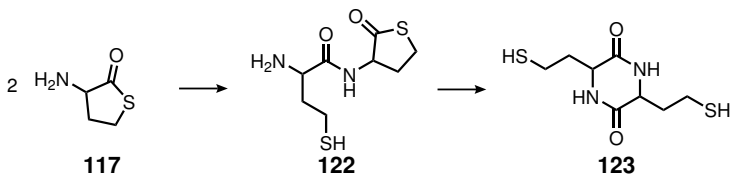
Scheme 3.14: Metabolism and chemical transformations of homocysteine.

olactones (**117**) towards amines is known for quite a while.¹⁴⁸ Considering a general thiolactone with a functional residue in α -position (**119**), the following reactivity is observed (Scheme 3.15): In an aminolysis, the thiolactone ring is opened under formation of an amide; simultaneously a free thiol is liberated. This process occurs at benign reaction conditions even in a physiological environment. However, using such pH-neutral conditions the γ -thiolactones react only with primary amines and not with higher substituted amines, thiols or alcohols. The latter convert **119** only at strongly basic conditions. Further and in contrast to lactones, nucleophiles only add to the carbonyl group (C=O); alkylations inducing acyl-sulfur cleavage are not observed. In general, thiolactones are more susceptible to ring-opening than corresponding lactones or lactams.^{146,149} This is due to the fact, that (i) thioesters are active esters and (ii) the five-membered cycle endures a strained ring conformation. In a second step, the generated thiol **120** is transformed by one of the manifold thiol-X reactions to give a product species **121** (Section 3.1).¹⁴⁶ The whole two-step process (**119** \rightarrow **121**) can be carried out in one-pot and is often referred to as one-pot double modification.



Scheme 3.15: Reaction of a thiolactone derivative with a functional amine and subsequent thiol-X reaction.

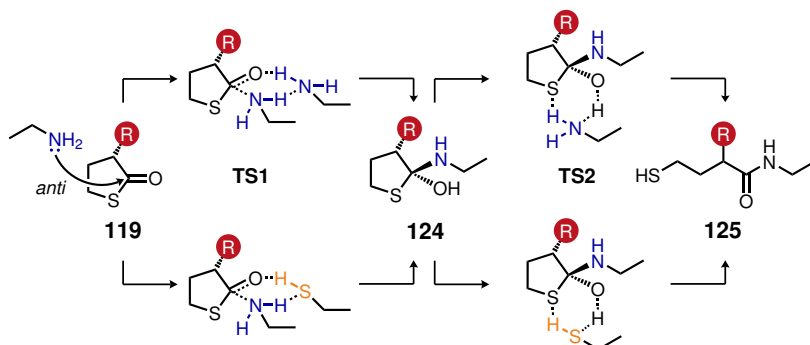
In biochemistry, early experiments have demonstrated, that enzymes or proteins are easily thiolated by amidation of **118**.^{150–155} The need for the N-acetyl protection group arises from the fact, that **117** in its neutral amino-form undergoes amidation with itself. A specific reaction set-up has shown, that upon condensation of two HCTL molecules the dimer **122** is formed (Scheme 3.16). This dimer undergoes an intramolecular rearrangement to build a diketopiperazine product (**123**). A possible polymerization step by oxidation of the thiols would lead to polydisulfides.¹⁴⁹ In the unprotected form, the amine-group of HCTL is further able to react with electrophiles like acid chlorides^{156,157} or in a condensation with aldehydes.^{147,158,159} The hydrolysis of the thiolactone ring has been well investigated. Presented pH profiles indicate, that for pH = 6 - 7, a “water-catalyzed” hydrolysis slowly takes place. At pH values higher than 7, a base- or OH⁻-catalyzed hydrolysis engages exhibiting growing rate constants with raise of the pH (up to 28 times faster than the “water-catalyzed” hydrolysis).^{160–162}



Scheme 3.16: Auto-amidation of the neutral thiolactone forming a diketopiperazine.

Further, the mechanism of the aminolysis has been described to involve several intra- as well as intermolecular proton transfers. The analysis of the aminolysis is later deepened by computational calculations of the amino-induced thiolactone ring-opening. Generally, two different mechanisms are postulated: an amine-assisted and a thiol-assisted one (Scheme 3.17). Within the stepwise mechanism, addition of ethylamine to a substituted thiolactone **119**, *anti* to the R group is favored. As soon as the attacking amine approaches, a transition state (**TS1**) occurs where an ethylamine is forming a bond to the carbonyl. At the amine-assisted route, another amine is functioning as a proton donor for the oxygen of the carbonyl. At the thiol-assisted mechanism, the assisting proton source is represented by a thiol of the product species. After this six-membered ring transition state, carbinolamine **124** of tetrahedral geometry is obtained. In the second step, the assisting species again promotes a six-membered transition state (**TS2**). The proton source – whether it be an amine or a thiol – transfers a proton from the alcohol to the thioester. This results in the cleavage of the thioester giving the final product **125**. It has to be noted, that the amine-assisted path is preferred at high amine concentration. However, the impact of the thiol assistance is not to be neglected and becomes apparent at low amine concentrations, and thus, higher product/thiol concentrations.^{163,164}

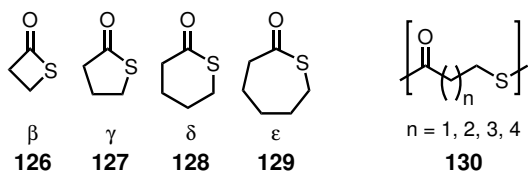
It is quite remarkable, that although (i) thiolactones have been used extensively in organic synthesis and biochemistry¹⁶⁵ and (ii) their oxygen analogues (lactones) are well known to undergo ring-opening polymerization¹⁶⁶ the use of thiolactones as monomers for polymerization has been very limited (Scheme 3.18). For example, β -thiolactone **126** and α, α -disubstituted derivatives of **126** are polymerized at elevated temperatures with traces of water.^{167–169} Just in 2016, Suzuki et al. polymerized thiolactone **126** furnished with a BOC-protected amine group in α -position (derived from N-BOC-cysteine) to afford poly(thioester)s. These polymers are either reacted in a ω -thiol-X reaction or upon deprotection



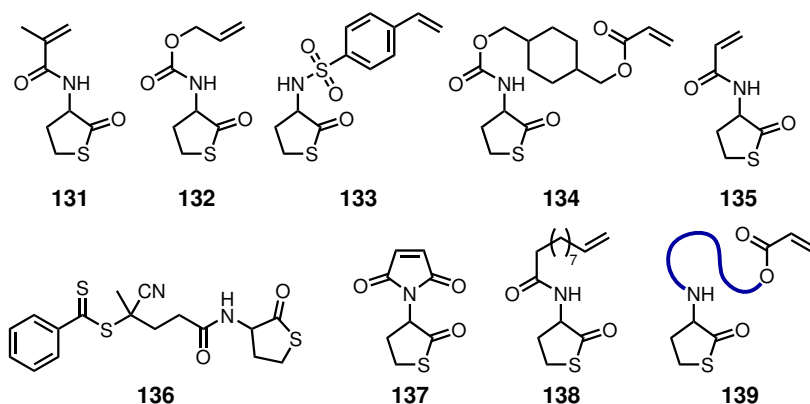
Scheme 3.17: Stepwise mechanism of the nucleophilic addition of ethylamine via the amine-assisted and the thiol-assisted path.

of the amines, S-to-N acyl migration is observed delivering polyamides with thiol side-groups.¹⁷⁰ Overberger et al. have managed to polymerize δ - and ϵ -thiolactones (**128** and **129**), both with a basic initiator (KO^tBu) at temperatures about 155 °C for periods up to 40 h.¹⁷¹ Besides these harsh anionic conditions, efforts have been made to polymerize **129** using $\text{BF}_3 \cdot \text{OEt}_2$ in a cationic ROP or by organocatalytic means.^{172,173} However, the five-membered cyclic γ -thiolactone **127** has proven to be inert under conditions used by Overberger et al.¹⁷⁴ In 2000, a report on the ROP of mixtures of oxiranes and **127** has shown that both of these substrates are polymerized in an alternating way generating poly(ester sulfide)s.¹⁷⁵ In 2005, further attempts to polymerize **127** in a cationic ROP have been unsuccessful. Surprisingly, the desired poly(thioester) **130** is prepared by polymerization of the corresponding γ -thionobutyrolactone in bulk at 100 °C using $\text{Sc}(\text{OTf})_3$ as catalyst via cationic ROP.¹⁷⁶

Apart from thiolactone **127**, derivatives **117** and **118** have attracted much more attention in polymer synthesis. The orthogonal nature and unique reactivity of α -substituted **127** has been introduced as key element in monomers, polymers or initiators (Scheme 3.19).



Scheme 3.18: Thiolactones and poly(thioester) obtained through ring-opening polymerization.



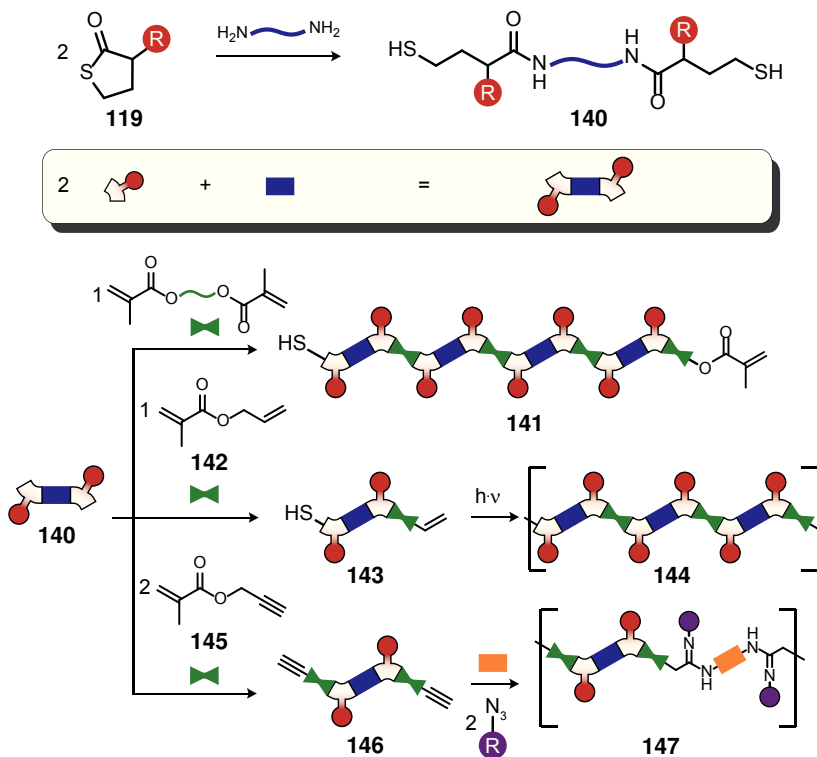
Scheme 3.19: Thiolactone **117** as a key element in macromolecular design of functional polymers.

Firstly, it has been used in association with polymerized liposomes. In the mentioned work, Kitano et al. couple HTCL **117** to methacryloyl chloride. With this functional monomer **131** and potassium peroxydisulfate (KPS) as initiator at hand, statistical polymers with liposome-like structure are prepared via radical polymerization. Upon acidification, the HCTL units are hydrolyzed and the subsequent volume change induces a release of the fluorophore Eosyn Y from the polymeric liposomes to the bulk phase.¹⁷⁷ After this very interesting report, nearly 21 years nothing has been reported regarding the implementation of **117** to proper polymer chemistry. Just in 2011, the group around Filip Du Prez focussed on the homocysteine thiolactone as building block for the design of macromolec-

ular structures. As a first concept, they have prepared the allyl thiolactone monomer **132**. Upon reaction with an amine, the thiolactone ring opens and a thiol is generated. With the use of DMPA as photocatalyst, a radical thiol-ene polymerization is initiated which results in the formation of thioether urethane polymers (TEU) of number average molecular weights up to $M_n = 22,000$ g/mol.¹⁷⁸ Similar to Kitano's approach, Du Prez et al. synthesized a thiolactone-functional styrene monomer (**133**) for RAFT copolymerization. Polymerizing this monomer with styrene up to molar percentages of 20, statistical thiolactone-functional PS is obtained. In a one-pot double modification of the thiolactone using an amine and a maleimide, properties of the polymer are further adjusted.¹⁷⁹ Compound **134** consists of a thiolactone and an acrylate bridged by a cyclohexyl spacer. Again, ring-opening of the thiolactone by amines prior to thiol-ene Michael addition gives rise to polyurethanes with defined side functionalities.¹⁸⁰ By synthesis of the thiolactone-functional chain transfer agent **136** (CTA), it is further shown that – using the RAFT process – polymers are prepared with α -thiolactone- and ω -benzodithioate-functional ends. After aminolysis of the dithioate and the thiolactone, cyclic polymers are produced via disulfide formation between the α - and ω -reaction sites.¹⁸¹ The group of Michael J. Monteiro use a CTA which is quite similar to **136**. With this CTA, poly(NIPAAm-*block*-PS) is synthesized in water/oil emulsion to obtain latex particles. These latex particles are assembled to nanorods and nanoworms prior to functionalization of the peripheral thiolactones.¹⁸² Another strategy is to use the acrylamide-analogue **135** of Kitano's methacrylamide **131** in defined portions with N-isopropylacrylamide (NIPAAm) for copolymerization. This way, thermoresponsive poly(NIPAAm) is created, which has been functionalized via double modification of the thiolactone, cross-linked by nucleophilic thiolysis of dichloromethane, or immobilized on amino-functional silica gel for chromatographic purposes.^{183–186} The same monomer (**135**) is used to build up sequence-defined oligomers (up to tetramers) by sequential cycles of (i) amidation of the thiolactone / (ii) thiol-ene addi-

tion to the acrylamide.¹⁸⁷ Polythiolactones with **135** as comonomer have also been used for the preparation of redox-responsive layers for the reversible release of functional molecules. Firstly, the amine-driven ring-opening of thiolactones leads to thiols. Next, the polythiol is partially bound to Gold-coated surfaces via thiol-Gold interaction; remaining thiols are transformed with small thiol-containing compounds into redox-responsive disulfide moieties.¹⁸⁸ Another thiolactone-functional monomer is the maleimido-thiolactone **137**. With controlled radical polymerization techniques like the RAFT process, polythiols and thiolactone-containing polymers are synthesized. Homopolymers of this monomer reach a number average molecular weight of $M_n = 1500$ g/mol. If copolymers of **137** with styrene or NIPAM are prepared, thiolactone contents up to 50% with respective molecular weights of $M_n = 6900 - 8900$ g/mol are obtained.¹⁸⁹ Compound **138** is synthesized from undec-10-enoic acid chloride and **117**. The former is derived from an unsaturated fatty acid, the latter – as already mentioned – from an amino acid, both being available from renewable sources. With **138** and the aminolysis/thiol-ene cascade reaction, block like functional polymers are obtained.¹⁹⁰ In extending this concept to polymeric building blocks, polymers of the structure of **139** have been synthesized, equipped with a thiolactone at one end and an acrylate at the other end. The macromolecular connection of **139** (**bold blue line**) depicts a poly(isobornyl acrylate) spacer. With this high-molecular weight building block and different functional amines, the amidation of the α -thiolactone prior to thiol-ene Michael addition gives rise to multisegmented block-polymers with defined side functionalities.¹⁹¹ Finally, recent works have shown, that the thiolactone ring serves as an efficient tool to functionalize existing polymers, too.^{192,193} As a decent piece of sugar chemistry, it has been demonstrated that thiolactone **117** (in its neutral form) is successfully used for the modification of chitosan. By furnishing the glycans with thiolactone units, the modified chitosan shows strong mucoadhesive properties. By installment of **118** to the chitosan, glycans are prepared which are able to cross-link at air through disulfide formation.^{194,195}

While the aforementioned examples show the incorporation of the thiolactone as key feature either in the side chain, at α - or ω -ends of the polymers created by controlled radical polymerization processes or simply by reaction of amines with the thiolactone, there are only few works which consider the use of these thiolactones as building blocks for the backbone of polymers. Within these few publications different strategies to involve thiolactone moieties in multicomponent reactions have prevailed (Scheme 3.20).

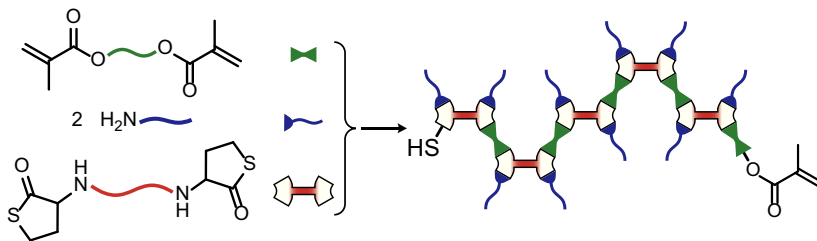


Scheme 3.20: Random thiolactone **119** as reagent for multicomponent reactions.

The first step in the one-pot reaction is mostly confined to the ring-opening of a functional thiolactone **119**. The ring-opening is achieved by using a

functional diamine and delivers a bis(thiol) **140**. If a bis(methacrylate) is present, intermediate **140** is subsequently converted to polymer **141** in an AA/BB-fashioned polyaddition.¹⁹⁶ If instead the allyl methacrylate **142** is added in stoichiometric amounts, allyl thiol **143** is generated. This reactive AB-type monomer is able to undergo radical thiol-ene polymerization under the irradiation of light and leads to polymer **144**.^{197,198} A more complex reaction set-up demonstrates the combination of two multicomponent reactions. Again, **119** is submitted to the appropriate conditions (aminolysis/thiol-ene addition) with a functional diamine and this time 2 eq propargyl methacrylate **145**. Full conversion of all reactants delivers bis(propargyl) **146**. Now a second multicomponent reaction – the alkyne-azide-amine coupling¹⁹⁹ – is used to create polymers comprising amidine groups (**147**). The main feature of this special reaction sequence is that beside the diamine, compound **119** and **145** the way for two further completely different building blocks is paved. In taking a functional azide and another diamine, a polymer consisting five different building blocks is accessible.²⁰⁰ By use of this same strategy dendritic polymers have been synthesized.²⁰¹ As the combination of more than one multicomponent reaction has proven to be very useful for the synthesis of functional polymers, another example is depicted (Scheme 3.21). Through the Passerini three component reaction firstly a bis(methacrylate) is prepared (not shown). This intermediate product is subsequently transformed in a three component reaction with a bis(thiolactone) and an amine. First, the amine opens the thiolactone ring. After the release of the thiol group, thiol-ene Michael addition proceeds to deliver the product polymer.²⁰²

When we finally look how the thiolactone is operated in all the presented polymers and literature procedures it is left to say, that the thiolactone poses a very interesting and useful building block as key feature for macromolecular architectures. Whether it be used in the polymer backbone, as side functionality or at peripheral ends, the thiolactone serves as a reliable tool for the functionalization of polymers, the introduction of new function-



Scheme 3.21: Reaction of a bis(thiolactone) in a multicomponent cascade.

alities and with this the alteration of polymer properties or the combination of building blocks in an orthogonal manner.

References

- (1) Cottrell, T. L., *The Strengths of Chemical Bonds*, 2nd; Academic Press/Butterworths: 1958.
- (2) Crampton, M. R. In *The Thiol Group (1974)*; John Wiley & Sons, Ltd.: 1974, pp 379–415.
- (3) Csizmadia, I. G. In *The Thiol Group (1974)*; John Wiley & Sons, Ltd.: 1974, pp 1–109.
- (4) Knight, A. R. In *The Thiol Group (1974)*; John Wiley & Sons, Ltd.: 1974, pp 455–479.
- (5) Koval, I. V. *Russian Journal of Organic Chemistry* **2007**, *43*, 319–346.
- (6) Hermanson, G. T. In *Bioconjugate Techniques (Second Edition)*, Hermanson, G. T., Ed., Second Edition; Academic Press: New York, 2008; Chapter 2, pp 169–212.
- (7) Stenzel, M. H. *ACS Macro Letters* **2012**, *2*, 14–18.
- (8) Nair, D. P.; Podgórski, M.; Chatani, S.; Gong, T.; Xi, W.; Fenoli, C. R.; Bowman, C. N. *Chemistry of Materials* **2014**, *26*, 724–744.
- (9) Peach, M. E. In *The Thiol Group (1974)*; John Wiley & Sons, Ltd.: 1974, pp 721–784.
- (10) Hoyle, C. E.; Lowe, A. B.; Bowman, C. N. *Chemical Society Reviews* **2010**, *39*, 1355–1387.
- (11) Miller, J., *Aromatic Nucleophilic Substitution*; Elsevier Applied Science: 1968.

- (12) Sohda, T.; Mizuno, K.; Tawada, H.; Sugiyama, Y.; Fujita, T.; Kawamatsu, Y. *Cemical & Pharmaceutical Bulletin* **1982**, *30*, 3563–3573.
- (13) Khurana, J. M.; Sahoo, P. K. *Synthetic Communications* **1992**, *22*, 1691–1702.
- (14) Sadykhov, Z. A.; Gambarova, S. A. *Chem. Abstr.* **1972**, *77*, 61415.
- (15) Segui, F.; Qiu, X.-P.; Winnik, F. M. *Journal of Polymer Science Part A: Polymer Chemistry* **2008**, *46*, 314–326.
- (16) Xu, J.; Tao, L.; Boyer, C.; Lowe, A. B.; Davis, T. P. *Macromolecules* **2010**, *43*, 20–24.
- (17) Zhang, Q.; Anastasaki, A.; Li, G.-Z.; Haddleton, A. J.; Wilson, P.; Haddleton, D. M. *Polymer Chemistry* **2014**, *5*, 3876–3883.
- (18) Rosen, B. M.; Lligadas, G.; Hahn, C.; Percec, V. *Journal of Polymer Science Part A: Polymer Chemistry* **2009**, *47*, 3931–3939.
- (19) Han, J.; Zhao, B.; Tang, A.; Gao, Y.; Gao, C. *Polym. Chem.* **2012**, *3*, 1918–1925.
- (20) Smith, K.; Kadish, K.; Guillard, R., *Handbook of Porphyrin Science: with Applications to Chemistry, Physics, Materials Science, Engineering, Biology and Medicine (volume 3)*; Handbook of Porphyrin Science Bd. 14; World Scientific: 2012.
- (21) Battioni, P.; Brigaud, O.; Desvaux, H.; Mansuy, D.; Traylor, T. G. *Tetrahedron Letters* **1991**, *32*, 2893–2896.
- (22) Shaw, S. J.; Elgie, K. J.; Edwards, C.; Boyle, R. W. *Tetrahedron Letters* **1999**, *40*, 1595–1596.
- (23) Samaroo, D.; Vinodu, M.; Chen, X.; Drain, C. M. *Journal of Combinatorial Chemistry* **2007**, *9*, 998–1011.
- (24) Becer, C. R.; Babiuch, K.; Pilz, D.; Hornig, S.; Heinze, T.; Gottschaldt, M.; Schubert, U. S. *Macromolecules* **2009**, *42*, 2387–2394.
- (25) Riedel, M.; Stadermann, J.; Komber, H.; Simon, F.; Voit, B. *European Polymer Journal* **2011**, *47*, 675–684.
- (26) De Leon, A. S.; Campo, A. d.; Labrugere, C.; Fernandez-Garcia, M.; Munoz-Bonilla, A.; Rodriguez-Hernandez, J. *Polym. Chem.* **2013**, *4*, 4024–4032.
- (27) Noy, J.-M.; Koldevitz, M.; Roth, P. J. *Polymer Chemistry* **2015**, *6*, 436–447.
- (28) Cakir, N.; Tunca, U.; Hizal, G.; Durmaz, H. *Macromolecular Chemistry and Physics* **2016**, *217*, 636–645.
- (29) Dyer, E.; Glenn, J. F. *Journal of the American Chemical Society* **1957**, *79*, 366–369.
- (30) Drobnica, L.; Podhradsky, D.; Gemeiner, P. *Collect. Czech. Chem. Commun.* **1975**, *40*, 3688–3697.
- (31) Drobnica, L.; Gemeiner, P. *Collect* **1975**, *40*, 3346–3356.

- (32) Wilderspin, A. F.; Green, N. M. *Analytical Biochemistry* **1983**, *132*, 449–455.
- (33) Conaway, C. C.; Krzeminski, J.; Amin, S.; Chung, F.-L. *Chemical Research in Toxicology* **2001**, *14*, 1170–1176.
- (34) Li, Q.; Zhou, H.; Wicks, D. A.; Hoyle, C. E.; Magers, D. H.; McAlexander, H. R. *Macromolecules* **2009**, *42*, 1824–1833.
- (35) Li, H.; Yu, B.; Matsushima, H.; Hoyle, C. E.; Lowe, A. B. *Macromolecules* **2009**, *42*, 6537–6542.
- (36) Gody, G.; Rossner, C.; Moraes, J.; Vana, P.; Maschmeyer, T.; Perrier, S. *Journal of the American Chemical Society* **2012**, *134*, 12596–12603.
- (37) Gokmen, M. T.; Brassinne, J.; Prasath, R. A.; Du Prez, F. E. *Chemical Communications* **2011**, *47*, 4652–4654.
- (38) Hensarling, R. M.; Rahane, S. B.; LeBlanc, A. P.; Sparks, B. J.; White, E. M.; Locklin, J.; Patton, D. L. *Polymer Chemistry* **2011**, *2*, 88–90.
- (39) Hastings, G. W.; Johnston, D. *British Polymer Journal* **1971**, *3*, 83–85.
- (40) Shin, J.; Matsushima, H.; Chan, J. W.; Hoyle, C. E. *Macromolecules* **2009**, *42*, 3294–3301.
- (41) Shin, J.; Matsushima, H.; Comer, C. M.; Bowman, C. N.; Hoyle, C. E. *Chemistry of Materials* **2010**, *22*, 2616–2625.
- (42) Kuypers, S.; Pramanik, S. K.; D'Olieslaeger, L.; Reekmans, G.; Peters, M.; D'Haen, J.; Vanderezande, D.; Junkers, T.; Adriaensens, P.; Ethirajan, A. *Chemical Communications* **2015**, *51*, 15858–15861.
- (43) Hermanson, G. T. In *Bioconjugate Techniques (Second Edition)*, Hermanson, G. T., Ed., Second Edition; Academic Press: New York, 2008; Chapter 4, pp 234–275.
- (44) *Chemistry and Technology of Epoxy Resins*, 1st; Ellis, B., Ed.; Springer-Science + Business Media, B.V.: 1993.
- (45) Brandle, A.; Khan, A. *Polymer Chemistry* **2012**, *3*, 3224–3227.
- (46) Binder, S.; Gadwal, I.; Biemann, A.; Khan, A. *Journal of Polymer Science Part A: Polymer Chemistry* **2014**, *52*, 2040–2046.
- (47) Chen, J.; Yu, C.; Shi, Z.; Yu, S.; Lu, Z.; Jiang, W.; Zhang, M.; He, W.; Zhou, Y.; Yan, D. *Angewandte Chemie International Edition* **2015**, *54*, 3621–3625.
- (48) Harvison, M. A.; Davis, T. P.; Lowe, A. B. *Polymer Chemistry* **2011**, *2*, 1347–1354.
- (49) Gadwal, I.; Rao, J.; Baettig, J.; Khan, A. *Macromolecules* **2013**, *47*, 35–40.
- (50) Gadwal, I.; Stuparu, M. C.; Khan, A. *Polymer Chemistry* **2015**, *6*, 1393–1404.
- (51) Gadwal, I.; Binder, S.; Stuparu, M. C.; Khan, A. *Macromolecules* **2014**, *47*, 5070–5080.

- (52) Maligres, P. E.; See, M. M.; Askin, D.; Reide, P. J. *Tetrahedron Letters* **1997**, *38*, 5253–5256.
- (53) Hu, X. E. *Tetrahedron* **2004**, *60*, 2701–2743.
- (54) Lu, P. *Tetrahedron* **2010**, *66*, 2549–2560.
- (55) Rasheed, O. K.; Bailey, P. D.; Lawrence, A.; Quayle, P.; Raftery, J. *European Journal of Organic Chemistry* **2015**, *32*, 6988–6993.
- (56) Jang, H.-J.; Lee, J. T.; Yoon, H. J. *Polym. Chem.* **2015**, *6*, 3387–3391.
- (57) Ghosh, N.; Kiskan, B.; Yagci, Y. *Progress in Polymer Science* **2007**, *32*, 1344–1391.
- (58) Nair, C. *Progress in Polymer Science* **2004**, *29*, 401–498.
- (59) Gorodisher, I.; DeVoe, R. J.; Webb, R. J. In *Handbook of Benzoxazine Resins*, Ishida, H., Agag, T., Eds.; Elsevier: Amsterdam, 2011, pp 211–234.
- (60) Beyazkılıç, Z.; Kahveci, M. U.; Aydoğan, B.; Kiskan, B.; Yagci, Y. *Journal of Polymer Science Part A: Polymer Chemistry* **2012**, *50*, 4029–4036.
- (61) Kawaguchi, A. W.; Sudo, A.; Endo, T. *ACS Macro Letters* **2013**, *2*, 1–4.
- (62) Musa, A.; Kiskan, B.; Yagci, Y. *Polymer* **2014**, *55*, 5550–5556.
- (63) Semerci, E.; Kiskan, B.; Yagci, Y. *European Polymer Journal* **2015**, *69*, 636–641.
- (64) Bektas, S.; Kiskan, B.; Orakdogan, N.; Yagci, Y. *Polymer* **2015**, *75*, 44–50.
- (65) Arslan, M.; Kiskan, B.; Yagci, Y. *Macromolecules* **2015**, *48*, 1329–1334.
- (66) Mukerjee, A. K.; Kumar, P. *Heterocycles* **1981**, *16*, 1995–2034.
- (67) Schmitt, S. K.; Trebatoski, D. J.; Krutty, J. D.; Xie, A. W.; Rollins, B.; Murphy, W. L.; Gopalan, P. *Biomacromolecules* **2016**, *17*, 1040–1047.
- (68) Allen, C. F. H.; Humphlett, W. J. *Canadian Journal of Chemistry* **1966**, *44*, 2315–2321.
- (69) Mather, B. D.; Viswanathan, K.; Miller, K. M.; Long, T. E. *Progress in Polymer Science* **2006**, *31*, 487–531.
- (70) Lowe, A. B.; Harvison, M. A. *Australian Journal of Chemistry* **2010**, *63*, 1251–1266.
- (71) Li, G.-Z.; Randev, R. K.; Soeriyadi, A. H.; Rees, G.; Boyer, C.; Tong, Z.; Davis, T. P.; Becer, C. R.; Haddleton, D. M. *Polymer Chemistry* **2010**, *1*, 1196–1204.
- (72) Chan, J. W.; Hoyle, C. E.; Lowe, A. B.; Bowman, M. *Macromolecules* **2010**, *43*, 6381–6388.
- (73) Chan, J. W.; Wei, H.; Zhou, H.; Hoyle, C. E. *European Polymer Journal* **2009**, *45*, 2717–2725.
- (74) Lowe, A. B. *Polymer Chemistry* **2010**, *1*, 17–36.

- (75) Chatani, S.; Nair, D. P.; Bowman, C. N. *Polymer Chemistry* **2013**, *4*, 1048–1055.
- (76) Xi, W.; Wang, C.; Kloxin, C. J.; Bowman, C. N. *ACS Macro Letters* **2012**, *1*, 811–814.
- (77) Wang, C.; Qi, C. *Tetrahedron* **2013**, *69*, 5348–5354.
- (78) Podgórski, M.; Chatani, S.; Bowman, C. N. *Macromolecular Rapid Communications* **2014**, *35*, 1497–1502.
- (79) Podgórski, M.; Becka, E.; Chatani, S.; Claudino, M.; Bowman, C. N. *Polym. Chem.* **2015**, *6*, 2234–2240.
- (80) Bae, J. W.; Lee, E.; Park, K. M.; Park, K. D. *Macromolecules* **2009**, *42*, 3437–3442.
- (81) Zhou, J.; Chen, P.; Deng, C.; Meng, F.; Cheng, R.; Zhong, Z. *Macromolecules* **2013**, *46*, 6723–6730.
- (82) Chatani, S.; Podgórski, M.; Wang, C.; Bowman, C. N. *Macromolecules* **2014**, *47*, 4894–4900.
- (83) Chatani, S.; Wang, C.; Podgórski, M.; Bowman, C. N. *Macromolecules* **2014**, *47*, 4949–4954.
- (84) Ghosh, S. S.; Kao, P. M.; McCue, A. W.; Chappelle, H. L. *Bioconjugate Chemistry* **1990**, *1*, 71–76.
- (85) Hermanson, G. T. In *Bioconjugate Techniques (Second Edition)*, Hermanson, G. T., Ed., Second Edition; Academic Press: New York, 2008; Chapter 5, pp 276–335.
- (86) Hermanson, G. T. In *Bioconjugate Techniques (Second Edition)*, Hermanson, G. T., Ed., Second Edition; Academic Press: New York, 2008; Chapter 6, pp 336–345.
- (87) Sanchez, A.; Pedrosa, E.; Grandas, A. *Chemical Communications* **2013**, *49*, 309–311.
- (88) Han, J.; Sun, L.; Chu, Y.; Li, Z.; Huang, D.; Zhu, X.; Qian, H.; Huang, W. *Journal of Medicinal Chemistry* **2013**, *56*, 9955–9968.
- (89) Nguyen, L.-T. T.; Gokmen, M. T.; Du Prez, F. E. *Polymer Chemistry* **2013**, *4*, 5527–5536.
- (90) Northrop, B. H.; Frayne, S. H.; Choudhary, U. *Polym. Chem.* **2015**, *6*, 3415–3430.
- (91) Fontaine, S. D.; Reid, R.; Robinson, L.; Ashley, G. W.; Santi, D. V. *Bioconjugate Chemistry* **2014**, *26*, 145–152.
- (92) Mantovani, G.; Lecolley, F.; Tao, L.; Haddleton, D. M.; Clerx, J.; Cornelissen, J. J. L. M.; Velonia, K. *Journal of the American Chemical Society* **2005**, *127*, 2966–2973.
- (93) Ji, S.; Zhu, Z.; Hoye, T. R.; Macosko, C. W. *Macromolecular Chemistry and Physics* **2009**, *210*, 823–831.

- (94) Dispinar, T.; Sanyal, R.; Sanyal, A. *Journal of Polymer Science Part A: Polymer Chemistry* **2007**, *45*, 4545–4551.
- (95) Lowe, A. B. *Polymer Chemistry* **2014**, *5*, 4820–4870.
- (96) Cramer, N. B.; Bowman, C. N. In *Thiol-X Chemistries in Polymer and Materials Science*; The Royal Society of Chemistry: 2013; Chapter 1, pp 1–27.
- (97) Kade, M. J.; Burke, D. J.; Hawker, C. J. *Journal of Polymer Science Part A: Polymer Chemistry* **2010**, *48*, 743–750.
- (98) Derboven, P.; D'hooge, D. R.; Stamenović, M. M.; Espeel, P.; Marin, G. B.; Du Prez, F. E.; Reyniers, M.-F. *Macromolecules* **2013**, *46*, 1732–1742.
- (99) Cramer, N. B.; Bowman, C. N. *Journal of Polymer Science Part A: Polymer Chemistry* **2001**, *39*, 3311–3319.
- (100) Hoyle, C. E.; Lee, T. Y.; Roper, T. *Journal of Polymer Science Part A: Polymer Chemistry* **2004**, *42*, 5301–5338.
- (101) Northrop, B. H.; Coffey, R. N. *Journal of the American Chemical Society* **2012**, *134*, 13804–13817.
- (102) Cramer, N. B.; Reddy, S. K.; O'Brien, A. K.; Bowman, C. N. *Macromolecules* **2003**, *36*, 7964–7969.
- (103) Rydholm, A. E.; Reddy, S. K.; Anseth, K. S.; Bowman, C. N. *Polymer* **2007**, *48*, 4589–4600.
- (104) Killops, K. L.; Campos, L. M.; Hawker, C. J. *Journal of the American Chemical Society* **2008**, *130*, 5062–5064.
- (105) Hoyle, C.; Bowman, C. *Angewandte Chemie* **2010**, *122*, 1584–1617.
- (106) Schulte, B.; Walther, A.; Keul, H.; Möller, M. *Macromolecules* **2014**, *47*, 1633–1645.
- (107) Lowe, A. B.; Chan, J. W. In *Functional Polymers by Post-Polymerization Modification*; Wiley-VCH Verlag GmbH & Co. KGaA: 2012, pp 87–118.
- (108) Liu, J.; Lam, J. W. Y.; Jim, C. K. W.; Ng, J. C. Y.; Shi, J.; Su, H.; Yeung, K. F.; Hong, Y.; Faisal, M.; Yu, Y.; Wong, K. S.; Tang, B. Z. *Macromolecules* **2011**, *44*, 68–79.
- (109) Yao, B.; Mei, J.; Li, J.; Wang, J.; Wu, H.; Sun, J. Z.; Qin, A.; Tang, B. Z. *Macromolecules* **2014**, *47*, 1325–1333.
- (110) Lowe, A. B. *Polymer* **2014**, *55*, 5517–5549.
- (111) Zhang, L.; Chou, C. P.; Moo-Young, M. *Biotechnology Advances* **2011**, *29*, 923–929.
- (112) Sevier, C. S.; Kaiser, C. A. *Molecular Cell Biology* **2002**, *3*, 836–847.
- (113) Hogg, P. J. *Trends in Biochemical Sciences* **2003**, *28*, 210–214.

- (114) Luo, D.; Smith, S. W.; Anderson, B. D. *Journal of Pharmaceutical Sciences* **2005**, *94*, 304–316.
- (115) Witt, D. *Synthesis* **2008**, *2008*, 2491–2509.
- (116) Marvel, C. S.; Olson, L. E. *Journal of the American Chemical Society* **1957**, *79*, 3089–3091.
- (117) Goethals, E. J.; Sillis, C. *Die Makromolekulare Chemie* **1968**, *119*, 249–251.
- (118) Bang, E.-K.; Lista, M.; Sforazzini, G.; Sakai, N.; Matile, S. *Chem. Sci.* **2012**, *3*, 1752–1763.
- (119) Caldarelli, S. A.; Hamel, M.; Duckert, J.-F.; Ouattara, M.; Calas, M.; Maynadier, M.; Wein, S.; Périgaud, C.; Pellet, A.; Vial, H. J.; Peyrottes, S. *Journal of Medicinal Chemistry* **2012**, *55*, 4619–4628.
- (120) Rosenthal, E. Q.; Puskas, J. E.; Wesdemiotis, C. *Biomacromolecules* **2011**, *13*, 154–164.
- (121) King, T. P.; Li, Y.; Kochoumian, L. *Biochemistry* **1978**, *17*, 1499–1506.
- (122) Wong, L.; Boyer, C.; Jia, Z.; Zareie, H. M.; Davis, T. P.; Bulmus, V. *Biomacromolecules* **2008**, *9*, 1934–1944.
- (123) Engler, A. C.; Chan, J. M. W.; Fukushima, K.; Coady, D. J.; Yang, Y. Y.; Hedrick, J. L. *ACS Macro Letters* **2013**, *2*, 332–336.
- (124) Gilman, H.; Smith, L. E.; Parker, H. H. *Journal of the American Chemical Society* **1925**, *47*, 851–860.
- (125) Parsons, T. F.; Buckman, J. D.; Pearson, D. E.; Field, L. *The Journal of Organic Chemistry* **1965**, *30*, 1923–1926.
- (126) Roth, P. J.; Kessler, D.; Zentel, R.; Theato, P. *Journal of Polymer Science Part A: Polymer Chemistry* **2009**, *47*, 3118–3130.
- (127) Hakkinen, H. *Nat Chem* **2012**, *4*, 443–455.
- (128) Xue, Y.; Li, X.; Li, H.; Zhang, W. *Nat Commun* **2014**, *5*, DOI: 10.1038/ncomms5348.
- (129) Shan, J.; Nuopponen, M.; Jiang, H.; Viitala, T.; Kauppinen, E.; Kontturi, K.; Tenhu, H. *Macromolecules* **2005**, *38*, 2918–2926.
- (130) Zubarev, E. R.; Xu, J.; Sayyad, A.; Gibson, J. D. *Journal of the American Chemical Society* **2006**, *128*, 15098–15099.
- (131) Zubarev, E. R.; Xu, J.; Sayyad, A.; Gibson, J. D. *Journal of the American Chemical Society* **2006**, *128*, 4958–4959.
- (132) Boyer, C.; Whittaker, M. R.; Luzon, M.; Davis, T. P. *Macromolecules* **2009**, *42*, 6917–6926.

- (133) Wang, G.; Liu, C.; Pan, M.; Huang, J. *Journal of Polymer Science Part A: Polymer Chemistry* **2009**, *47*, 1308–1316.
- (134) D'Souza-Mathew, M.; Cayre, O. J.; Hunter, T. N.; Biggs, S. R. *Journal of Colloid and Interface Science* **2013**, *407*, 187–195.
- (135) Chiu, J. J.; Kim, B. J.; Kramer, E. J.; Pine, D. J. *Journal of the American Chemical Society* **2005**, *127*, 5036–5037.
- (136) Nie; Fava, D.; Rubinstein, M.; Kumacheva, E. *Journal of the American Chemical Society* **2008**, *130*, 3683–3689.
- (137) Soliman, M. G.; Pelaz, B.; Parak, W. J.; del Pino, P. *Chemistry of Materials* **2015**, *27*, 990–997.
- (138) Daniel, M.-C.; Astruc, D. *Chemical Reviews* **2004**, *104*, 293–346.
- (139) Bolander-Gouaille, C., *Focus on Homocysteine*; Springer Paris: 2001.
- (140) Finkelstein, J. D.; Martin, J. J. *Journal of Biological Chemistry* **1984**, *259*, 9508–9513.
- (141) Mudd, S. H.; Skovby, F.; Levy, H. L.; Pettigrew, K. D.; Wilcken, B.; Pyeritz, R. E.; Andria, G.; Boers, G. H. J.; Bromberg, I. L.; Cerone, R.; Fowler, B.; Gröbe, H.; Schmidt, H.; Schweitzer, L. *American Journal of Human Genetics* **1985**, *37*, 1–31.
- (142) Riegel, B.; DuVigneaud, V. *Journal of Biological Chemistry* **1935**, *112*, 149–154.
- (143) Jakubowski, H.; Goldman, E. *FEBS Letters* **1993**, *317*, 237–240.
- (144) Baernstein, H. D. *The Journal of Biological Chemistry* **1934**, *106*, 451–456.
- (145) Jakubowski, H. *The Journal of Nutrition* **2000**, *130*, 3775–3815.
- (146) Espeel, P.; Goethals, F.; Du Prez, F. E. In *Thiol-X Chemistries in Polymer and Materials Science*; The Royal Society of Chemistry: 2013; Chapter 9, pp 195–216.
- (147) Jakubowski, H. *Chem. Eur. J.* **2006**, *12*, 8039–9043.
- (148) DuVigneaud, V.; Patterson, W. I.; Hunt, M. *Journal of Biological Chemistry* **1938**.
- (149) Linkova, M. G.; Kuleshova, N. D.; Knunyants, I. L. *Russian Chemical Reviews* **1964**, *33*, 493.
- (150) Benesch, R.; Benesch, R. E. *Journal of the American Chemical Society* **1956**, *78*, 1597–1599.
- (151) Benesch, R.; Benesch, R. E. *Proc. Natl. Acad. Sci* **1958**, *44*, 848–853.
- (152) Abadi, D. M.; Wilcox, P. E. *Journal of Biological Chemistry* **1960**, *235*, 396–404.
- (153) Klotz, I. M.; Elfbaum, S. G. *Biochimica et Biophysica Acta (BBA) - General Subjects* **1964**, *86*, 100–105.
- (154) McCully, K. S. *Annals of Clinical and Laboratory Science* **1993**, *23*, 477–493.

- (155) Hermanson, G. T. In *Bioconjugate Techniques (Second Edition)*, Hermanson, G. T., Ed., Second Edition; Academic Press: New York, 2008; Chapter 1, pp 3–168.
- (156) Leanza, W. J.; Chupak, L. S.; Tolman, R. L.; Marburg, S. *Bioconjugate Chemistry* **1992**, *3*, 514–518.
- (157) Kunzmann, M. H.; Staub, I.; Böttcher, T.; Sieber, S. A. *Biochemistry* **2011**, *50*, 910–916.
- (158) Grigg, R.; Sarker, M. A. B. *Tetrahedron* **2006**, *62*, 10332–10343.
- (159) Jakubowski, H. *Cell. Mol. Life Sci.* **2004**, *61*, 470–478.
- (160) Schjånberg, E. *Berichte der deutschen chemischen Gesellschaft (A and B Series)* **1942**, *75*, 468–482.
- (161) Duerre, J. A.; Miller, C. H. *Analytical Biochemistry* **1966**, *17*, 310–315.
- (162) Garel, J.; Tawfik, D. S. *Chemistry - A European Journal* **2006**, *12*, 4144–4152.
- (163) Yang, W.; Drueckhammer, D. G. *Organic Letters* **2000**, *2*, 4133–4136.
- (164) Desmet, G. B.; D'hooge, D. R.; Sabbe, M. K.; Marin, G. B.; Du Prez, F. E.; Espeel, P.; Reyniers, M.-F. *The Journal of Organic Chemistry* **2015**, *80*, 8520–8529.
- (165) Paryzek, Z.; Skiera, I. *Organic Preparations and Procedures International* **2007**, *39*, 203–296.
- (166) Labet, M.; Thielemans, W. *Chemical Society Reviews* **2009**, *38*, 3484–3504.
- (167) I.L. Knunyants, M. G. L.; Kuleshova, N. D. *Chem. Abstr.* **1964**, *61*, 2966.
- (168) Fles, D.; Tomasić, V. *Journal of Polymer Science Part B: Polymer Letters* **1968**, *6*, 809–813.
- (169) Vasil'eva, T. P.; Bystrova, V. M.; Kil'disheva, O. V.; Knunyants, I. L. *Bulletin of the Academy of Sciences of the USSR, Division of chemical science* **1986**, *35*, 1176–1180.
- (170) Suzuki, M.; Makimura, K.; Matsuoka, S.-i. *Biomacromolecules* **2016**, *17*, 1135–1141.
- (171) Overberger, C. G.; Weise, J. *Journal of Polymer Science Part B: Polymer Letters* **1964**, *2*, 329–331.
- (172) Sanda, F.; Jirakanjana, D.; Hitomi, M.; Endo, T. *J. Polym. Sci. A Polym. Chem.* **2000**, *38*, 4057–4061.
- (173) Bannin, T. J.; Kiesewetter, M. K. *Macromolecules* **2015**, *48*, 5481–5486.
- (174) Overberger, C. G.; Weise, J. K. *Journal of the American Chemical Society* **1968**, *90*, 3533–3537.
- (175) Nishikubo, T.; Kameyama, A.; Kawakami, S. *Macromolecules* **1998**, *31*, 4746–4752.
- (176) Kikuchi, H.; Tsubokawa, N.; Endo, T. *Chemistry Letters* **2005**, *34*, 376–377.

- (177) Kitano, H.; Wolf, H.; Ise, N. *Macromolecules* **1990**, *23*, 1958–1961.
- (178) Espeel, P.; Goethals, F.; Du Prez, F. E. *Journal of the American Chemical Society* **2011**, *133*, 1678–1681.
- (179) Espeel, P.; Goethals, F.; Stamenović, M. M.; Petton, L.; Du Prez, F. E. *Polymer Chemistry* **2012**, *3*, 1007–1015.
- (180) Espeel, P.; Goethals, F.; Driessen, F.; Nguyen, L.-T. T.; Du Prez, F. E. *Polymer Chemistry* **2013**, *4*, 2449–2456.
- (181) Stamenović, M. M.; Espeel, P.; Baba, E.; Yamamoto, T.; Tezuka, Y.; Du Prez, F. E. *Polymer Chemistry* **2013**, *4*, 184–193.
- (182) Jia, Z.; Bobrin, V. A.; Truong, N. P.; Gillard, M.; Monteiro, M. J. *Journal of the American Chemical Society* **2014**, *136*, 5824–5827.
- (183) Reinicke, S.; Espeel, P.; Stamenović, M. M.; Du Prez, F. E. *ACS Macro Letters* **2013**, *2*, 539–543.
- (184) Reinicke, S.; Espeel, P.; Stamenović, M. M.; Du Prez, F. E. *Polymer Chemistry* **2014**, *5*, 5461–5470.
- (185) Chen, Y.; Espeel, P.; Reinicke, S.; Du Prez, F. E.; Stenzel, M. H. *Macromolecular Rapid Communications* **2014**, *35*, 1128–1134.
- (186) Satti, A. J.; Espeel, P.; Martens, S.; Hoeylandt, T. V.; Prez, F. E. D.; Lynen, F. *Journal of Chromatography A* **2015**, *1426*, 126–132.
- (187) Espeel, P.; Carrette, L. L. G.; Bury, K.; Capenberghs, S.; Martins, J. C.; Prez, F. D.; Madder, A. *Angewandte Chemie International Edition* **2013**, *52*, 13261–13264.
- (188) Belbekhouche, S.; Reinicke, S.; Espeel, P.; Prez, F. E. D.; Eloy, P.; Dupont-Gillain, C.; Jonas, A. M.; Demoustier-Champagne, S.; Glinel, K. *ACS Applied Materials & Interfaces* **2014**, *6*, 22457–22466.
- (189) Rudolph, T.; Espeel, P.; Du Prez, F. E.; Schacher, F. H. *Polymer Chemistry* **2015**, *6*, 4240–4251.
- (190) Goethals, F.; Martens, S.; Espeel, P.; van den Berg, O.; Du Prez, F. E. *Macromolecules* **2013**, *47*, 61–69.
- (191) Driessen, F.; Du Prez, F. E.; Espeel, P. *ACS Macro Letters* **2015**, *4*, 616–619.
- (192) Zhao, Y.; Yang, B.; Zhang, Y.; Wang, S.; Fu, C.; Wei, Y.; Tao, L. *Polymer Chemistry* **2014**, *5*, 6656–6661.
- (193) Driessen, F.; Martens, S.; Meyer, B. D.; Du Prez, F. E.; Espeel, P. *Macromolecular Rapid Communications* **2016**, DOI: 10.1002/marc.201600150.
- (194) Juntapram, K.; Praphairaksit, N.; Siraleartmukul, K.; Muangsin, N. *Carbohydrate Polymers* **2012**, *87*, 2399–2408.

- (195) Ferris, C.; Casas, M.; Lucero, M. J.; de Paz, M.; Jiménez-Castellanos, M. *Carbohydrate Polymers* **2014**, *111*, 125–132.
- (196) Zhang, Z.; You, Y.-Z.; Wu, D.-C.; Hong, C.-Y. *Polymer* **2014**, *64*, 221–226.
- (197) Yan, J.-J.; Wang, D.; Wu, D.-C.; You, Y.-Z. *Chemical Communications* **2013**, *49*, 6057–6059.
- (198) Yu, L.; Wang, L.-H.; Hu, Z.-T.; You, Y.-Z.; Wu, D.-C.; Hong, C.-Y. *Polymer Chemistry* **2015**, *6*, 1527–1532.
- (199) Bae, I.; Han, H.; Chang, S. *Journal of the American Chemical Society* **2005**, *127*, 2038–2039.
- (200) Zhang, Z.; You, Y.-Z.; Wu, D.-C.; Hong, C.-Y. *Macromolecules* **2015**, *48*, 3414–3421.
- (201) Zhang, Z.; Tan, Z.-B.; Hong, C.-Y.; Wu, D.-C.; You, Y.-Z. *Polym. Chem.* **2016**, *7*, 1468–1474.
- (202) Yang, L.; Zhang, Z.; Cheng, B.; You, Y.; Wu, D.; Hong, C. *Science China Chemistry* **2015**, *58*, 1734–1740.

Chapter 4

A Novel Ethylene Carbonate Thiolactone Coupler

4.1 Introduction

Multifunctional polymers are mainly prepared by chain growth reaction. Atom transfer radical polymerization for example is tolerant to many functional groups within the monomer yielding polymers with various functionalities along the polymer chain.¹ By post-polymerization modification the range of functional side groups and grafts can be increased especially by using “click” reactions: (i) the azide-alkyne Huisgen 1,3-dipolar cycloaddition,^{2,3} (ii) Diels-Alder,⁴ and (iii) thiol-click⁵ as well as transformations of activated ester⁶ and carbonate side groups⁷ with amines. These reactions permit, by sequential or simultaneous modifications, control of the

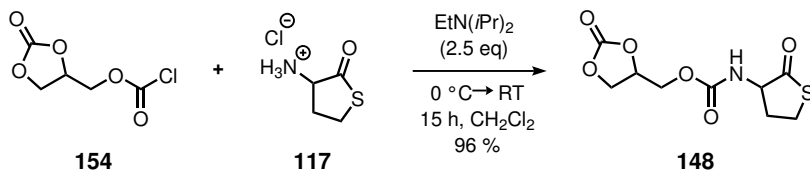
number and spatial location of the functional groups.⁸ It is more difficult to obtain linear polymers with functional side groups by step growth polymerization, since the use of trifunctional monomers leads to branched, highly branched or cross-linked polymers. Linear polycondensates with functional side groups, however, are obtained using AA-type bicyclic monomers. Polyurethanes with hydroxyl side groups for example are obtained by reaction of AA-type monomers with two cyclic carbonate groups with diamines.⁹ These monomers are also used as coupling agents to prepare multifunctional monodisperse or polydisperse molecules.^{10–12} This chapter presents a new concept of a multifunctional coupler with two reactive cycles which enables the combination of four building blocks within one molecule. The multifunctional coupler **148** we report, is based on an ethylene carbonate ring and a thiolactone ring linked by an O-methyl urethane spacer. A particular reaction concept was established (Scheme 4.1): the thiolactone ring reacts first at room temperature selectively with an amine building block (A) under ring-opening, formation of an amide bond and release of a thioethyl group. Then, the free thiol group is addressed by a Michael-type addition with a second building block (B) bearing an acrylate group. Conversion of the ethylene carbonate ring at elevated temperatures (60–80 °C) with the third building block (C) bearing an amine group leads, upon ring-opening, to a urethane and a hydroxyl group. The thioether formation by Michael-type addition and reaction of the ethylene carbonate with amines may be exchanged (these reactions proceed in any sequence). Subsequently, reaction of the hydroxyl group with a building block (D) bearing an acyl halide group (or alternatively an isocyanate group) furnishes the fully functionalized molecule. Beside the fact that only mild reaction conditions are required, all transformations of the coupler (except for the acylation) are addition reactions, thus no side products are formed during the reaction.

This chapter describes a facile one-step synthesis of a novel multifunctional coupler. Then, a concise synthetic route to the fully functionalized

coupler (with all four model compounds) is explored. The intermediates were isolated and fully characterized by ^1H , ^{13}C NMR spectroscopy, mass spectrometry and FTIR spectroscopy. Finally the coupler was telescoped in a cascade reaction to again obtain the fully functionalized product.

4.2 Results & Discussion

A diastereomeric mixture of the multifunctional coupler was obtained by reacting equimolar amounts of racemic glycerol carbonate chloroformate **154** and DL-homocysteine thiolactone hydrochloride **117** in CH_2Cl_2 at $0\text{ }^\circ\text{C}$ in the presence of ethyl-diisopropylamine as an acid scavenger (Scheme 4.2). Upon warming to room temperature, a precipitate oc-



Scheme 4.2: One-step synthesis of the multifunctional coupler from glycerol carbonate chloroformate and homocysteine thiolactone hydrochloride.

curred which was assumed to be ethyl-diisopropylamine hydrochloride. Therefore, it was initially included into the work-up. Later by filtration it was investigated separately and turned out to be a mixture of remaining ethyl-diisopropylamine hydrochloride and the *RR/SS* diastereomer. The partially precipitated but pure *RR/SS* diastereomer **148** was obtained washing this mixture with CH_2Cl_2 and 1 M $\text{HCl}_{(\text{aq})}$ to give crystals of pure *RR/SS* diastereomers. The remaining organic solution was concentrated and subjected to flash column chromatography to accumulate (*RS/SR*)-**148** diastereomers as the major component. ^{13}C NMR spectra were recorded of pure (*RR/SS*)-**148** and a mixture of diastereomers

with (*RS/SR*)-**148** being the major component to trace subtle differences (Figure 4.1). Different chemical shifts are observed for signals 4 and 1. The *RR/SS* diastereomers show the urethane carbon 4 at $\delta = 155.51$ ppm, whereas the same signal for the *RS/SR* diastereomers appears at $\delta = 155.47$ ppm. The methylene carbon 1 of the *RR/SS* diastereomers is found at $\delta = 63.63$ ppm. For the *RS/SR* diastereomers this signal is shifted to $\delta = 63.71$ ppm. Since the spectra of the *RS/SR* diastereomers is not entirely pure, a small peak of the *RR/SS* diastereomer is observed, which allows the distinction of both mixtures of diastereomers.

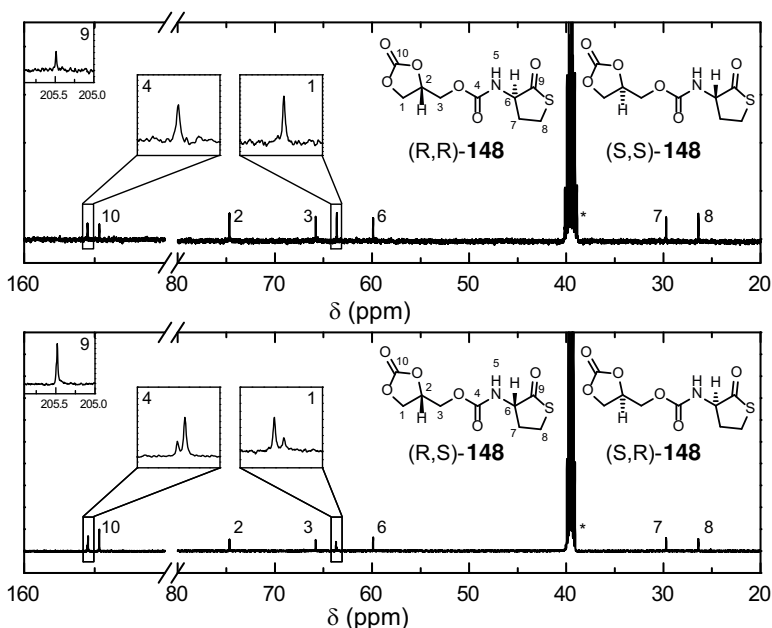


Figure 4.1: Comparison of the ¹³C NMR spectra of (*RR/SS*)-**148** (top) and the enriched *RS/SR* diastereomeric mixture (bottom).

Single crystal X-ray diffraction experiments confirmed the general structure of (*RR/SS*)-**148** with respect to its configuration and protonation state. The asymmetric unit consists of one homochiral molecule, whereas the

other enantiomer is generated by a crystallographic inversion centre resulting in a 1/1 *RR/SS* ratio. The two molecules are connected by hydrogen bonds formed between the NH-group and the carbonate oxygen building a centrosymmetric dimeric structure (Figure 4.2). Information on data collection and refinement of the crystal structure are given at section A.1.1 (CCDC 919540).

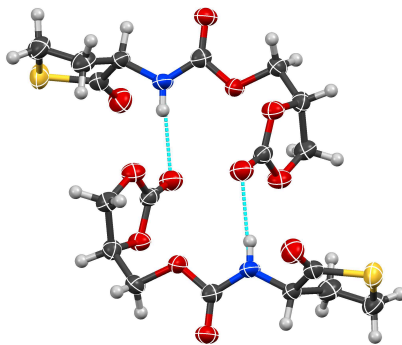


Figure 4.2: Displacement ellipsoid plot of two asymmetric units of the *RR/SS* diastereomer forming a dimer (drawn at 80% probability, color code: C - black, H - white, O - red, N - blue, S - yellow).

The mixture of diastereomers dissolved in THF, whereas pure (*RR/SS*)-**148** only dissolved in DMF or DMSO. We assume that the poor solubility of (*RR/SS*)-**148** is caused by the hydrogen bonding and thus it can only be broken at higher temperature or using aprotic dipolar solvents. Most characteristic signals of the ^1H NMR spectrum of the coupler are those related to the ring protons especially signals of protons 2 and 6 at the stereocenters. Conversion of the rings is monitored by the disappearance/shift of these signals (Figure 4.3). Equimolar amounts of coupler **148** and hexylamine (HA) as building block A were reacted in THF at room temperature for 24 h. Under these conditions the thiolactone ring is converted highly selective, while the ethylene carbonate ring remains intact. With increasing solvent polarity, for example by using DMF, the selectivity decreases: beside the thiolactone ring, 11% of the ethylene

carbonate ring is converted leaving the same amount of thiolactone ring intact. Purification by flash column chromatography delivered thiol **149** in 63% yield. As the thiolactone ring is opened during the reaction, proton **6** of the stereocenter as well as protons **5**, **7** and **8** are shifted to higher field. The newly formed amide proton appears at 7.85 ppm (★, Figure 4.3). To

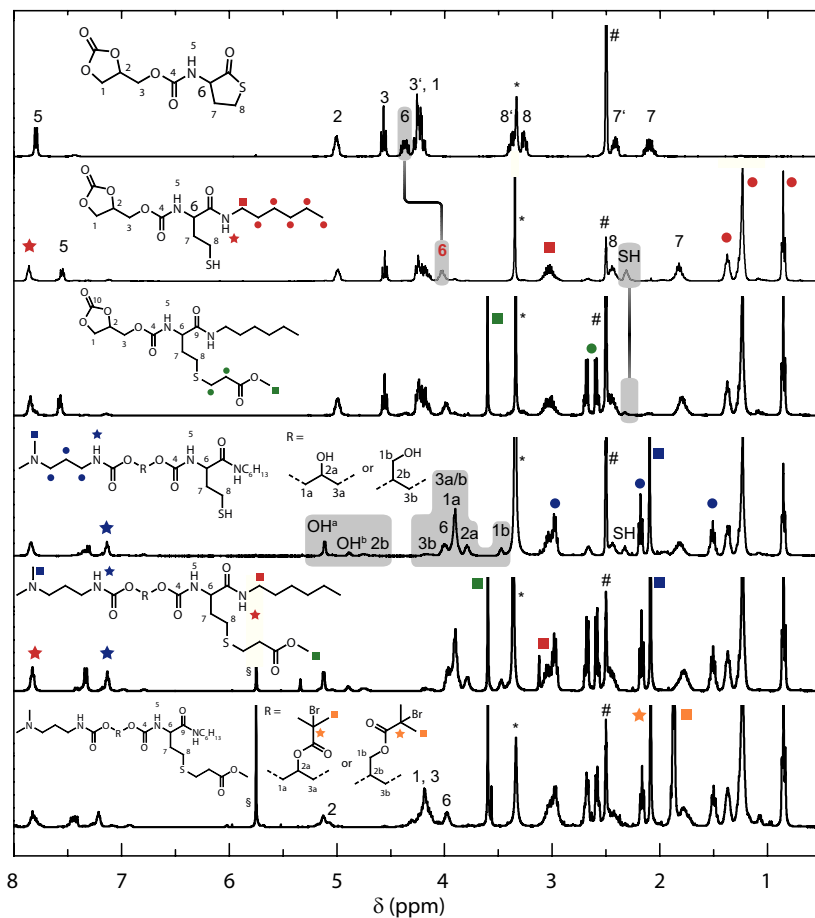


Figure 4.3: Comparison of the ^1H NMR spectra of the multifunctional coupler (**148**), the thiol (**149**), thioether **150**, thiol-alcohol **151**, thioether alcohol **152** and the fully functionalized coupler **153**. Residual solvent peaks: * H_2O , # DMSO , § CH_2Cl_2 .

introduce building block B, methyl acrylate was reacted with thiol **149** in THF at room temperature to yield the Michael adduct **150** in 51% yield after purification. Successful conversion of methyl acrylate was proven by ^1H NMR spectroscopy: first the protons attached to the sp^2 hybridized carbon atoms disappeared and characteristic signals of an ethylidene group appeared at $\delta = 2.68$ and 2.60 ppm (●), whereas the signals of the thiol proton vanish. The methyl ester group (■) is detected at $\delta = 3.61$ ppm as a sharp singlet (Figure 4.3). Alternatively, the ethylene carbonate ring of compound **149** was first converted by reaction with equimolar amounts of 3-(dimethylamino)-1-propylamine (building block C) at 70 °C. Purification by flash column chromatography delivered thiol-alcohol **151a/b** in 61% yield. Regarding the ^1H NMR spectrum, the dimethylamino group (■) is found at $\delta = 2.09$ ppm; the newly formed urethane proton shows a broad triplet at $\delta = 7.14$ ppm (★). Signals 1, 2 and 3 related to the glycerol unit in compound **149** split up due to the formation of two isomers **151a/b** (82:18) (asymmetrically substituted ethylene carbonates in most cases give both isomers when reacted with amines).¹³ The OH group of isomer **151a** is identified as a doublet at $\delta = 5.12$ ppm, whereas the OH group of isomer **151b** shows a doublet of doublets at $\delta = 4.89$ ppm (Figure 4.3). A more detailed analysis regarding the proton splitting of glycerol isomers and ^1H NMR spectra are given at section A.1.3. Depending on which building block was introduced first (B or C), compound **152a/b** was obtained from the corresponding precursor **150** or **151a/b** using the reaction conditions described in the experimental part. The ^1H NMR data of compound **152a/b** revealed an exact combination of the spectra of the acrylate group of **150** and compound **151a/b** (Figure 4.3). By reacting compound **152a/b** with α -bromoisobutyryl bromide (building block D), a potential initiation site for the atom transfer radical polymerization of methyl methacrylate was linked to the hydroxyl groups of the starting material. The reaction was performed in CH_2Cl_2 solution at 60 °C to give the corresponding acylated product **153** in 17% yield after purification. In the ^1H NMR spectrum of compound **153a/b** the protons 1 and 3 are shifted to lower field. Me-

thine proton 2 shifts to lower field, too. The appearance of the singlet at $\delta = 1.93$ ppm represents both methyl groups of the α -bromoisobutyryl residue (■, Figure 4.3). Finally, all four reaction steps were carried out in a one-pot reaction. Therefore, the coupler was stirred first with hexylamine at ambient temperature, then with 3-(dimethylamino)-1-propylamine at 70 °C. This two-step reaction sequence was followed by the addition of 5.0 eq of methyl acrylate to afford alcohol **152a/b**. After the solvent was evaporated, the residue was dissolved in CH_2Cl_2 . α -Bromoisobutyryl bromide (1.2 eq) was added and the reaction mixture was stirred at 60 °C for 20 h. After an alkaline work-up the crude product was purified by flash column chromatography to give the fully functionalized molecules **153a/b** in 38% yield (average yield for each step: 79%).

4.3 Conclusion

In this work, a facile one-step synthesis of a novel multifunctional coupler based on homocysteine thiolactone and glycerol carbonate chloroformate is presented. Two diastereomers were obtained. The crystal structure of the *RR/SS* diastereomer was determined. The coupler was successfully reacted with two amines. Michael-type addition of the thiol released by the ring-opening of the thiolactone gave the corresponding thioether. The alcohol groups released by ring-opening of the ethylene carbonate were addressed using an acyl halide. All reactions proceeded highly selectively and under mild reaction conditions without side products. The coupler shows good potential for the preparation of polymers with complex structures, such as miktoarm star polymers.¹⁴ For purification fractional precipitation or dialysis will be used.

4.4 Experimental Data

4.4.1 Materials

D,L-homocysteine thiolactone hydrochloride (HCTL·HCl, 99%, ABCR), glycerol carbonate chloroformate, N,N-diisopropylethylamine (DIPEA, 99%, ABCR), hexylamine (99%, Sigma Aldrich), methyl acrylate (MA, 99%, Sigma Aldrich), triethylamine ($\geq 99\%$, Sigma Aldrich), 3-(dimethylamino)-1-propylamine (99%, Acros Organics), α -bromoisobutryl bromide (98%, Sigma Aldrich) were used without further purification. Unless otherwise indicated, all solvents were purchased from commercial sources and were used without further purification. All reactions were performed under an Argon atmosphere, unless otherwise noted. Argon (Linde) was passed over molecular sieves (4 Å) and finely dispersed potassium on aluminum oxide before use.

4.4.2 Measurements

^1H and ^{13}C NMR spectra were recorded on a Bruker DPX-400 FT NMR spectrometer (400 MHz and 100 MHz, respectively) and are reported as follows: chemical shift δ (ppm) (multiplicity, coupling constant J (Hz), number of protons, assignment). Dimethylsulfoxide (DMSO, $\delta_{\text{H}} = 2.50$ ppm, $\delta_{\text{C}} = 39.5$ ppm) was used as an internal standard. Chemical shifts are reported in ppm to the nearest 0.01 ppm for ^1H and the nearest 0.1 ppm for ^{13}C .

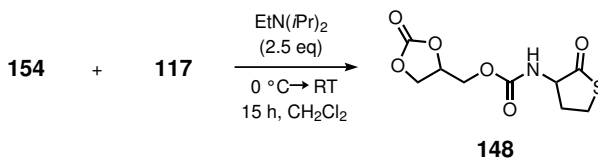
Infrared spectra were carried out on a ThermoNicolet FT-IR Nexus spectrometer and are recorded between KBr disks or using an ATR unit (ThermoNicolet, Smart SplitPEA). Transmission maxima are reported in wavenumbers (cm^{-1}) and only selected intensities are reported.

Mass spectra were recorded on a Finnigan SSQ 7000 spectrometer and

HRMS spectra on a Thermo Scientific LTQ Orbitrap XL spectrometer. Differential scanning calorimetry (DSC) analysis was performed on a Netzsch DSC 204 'Phoenix' (Netzsch, Selb, Germany) under nitrogen atmosphere using a scan rate of 10 K·min⁻¹. For mp the inflexion point was selected.

4.4.3 Syntheses

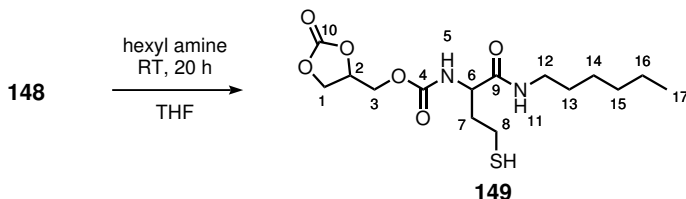
Synthesis of Coupler 148



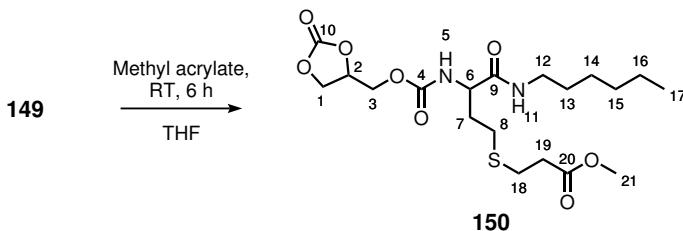
To a stirred suspension of DL-homocysteine thiolactone hydrochloride **117** (5.00 g, 32.5 mmol) and glycerol carbonate chloroformate **154** (5.876 g, 32.5 mmol) in CH₂Cl₂ (40 mL) at 0 °C was added slowly (8 mL/h) ethyl-diisopropylamine (14 mL, 81.4 mmol). The reaction mixture was allowed to warm slowly to room temperature and stirred at room temperature for 15 h. The organic layer was washed with 1 M HCl_(aq) (2 x 20 mL). Then, the aqueous layer was extracted with CH₂Cl₂ (5 x 15 mL). The combined organic layers were dried (MgSO₄), the solvent was evaporated under reduced pressure to give the crude product. Purification by flash column chromatography on silica gel with EtOAc-DCM (3:1) as eluent, gave the urethane **148** (6.411 g, 76%) as a colorless oil. Mp 162.8 °C; ¹H NMR (400 MHz, DMSO) δ 7.80 (d, *J* = 8.6 Hz, 1H, H5), 5.14 - 4.90 (m, 1H, H2), 4.57 (td, *J* = 8.6, 2.6 Hz, 1H, H3), 4.43 - 4.32 (m, 1H, H6), 4.31 - 4.17 (m, 3H, H1 and H3), 3.45 - 3.36 (m, 1H, H8), 3.26 (dd, *J* = 10.6, 6.8 Hz, 1H, H8), 2.46 - 2.37 (m, 1H, H7), 2.18 - 2.03 (m, 1H, H7). ¹³C NMR (101 MHz, DMSO) δ 205.5 (C9), 155.5 (C4), 154.7 (C10), 74.7 (C2), 65.8 (C3),

63.6 (C1), 59.9 (C6), 29.7 (C7), 26.4 (C8). IR (KBr) 3297 (NH), 3077, 2926, 1777 (O₂C=O), 1732 (CONH), 1720, 1690 (COS), 1556, 1407, 1298, 1273, 1252, 1193, 1176, 1070, 920, 850, 773. HRMS (ESI) m/z for C₉H₁₁NO₆S (M + H)⁺ 262.0370, (M + Na)⁺ 284.0188.

Synthesis of Thiol 149

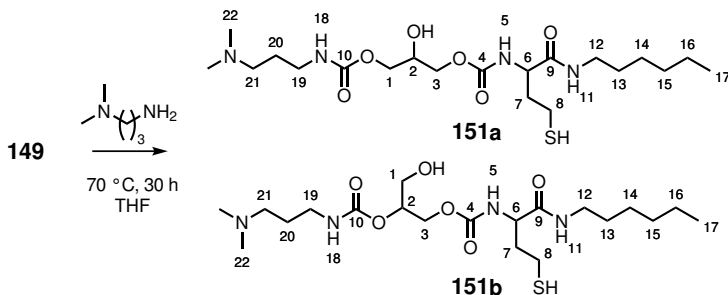


Hexylamine (630 μ L, 4.8 mmol) was added to a stirred solution of **148** (1.246 g, 4.8 mmol) in DMF (14 mL) at room temperature. The reaction mixture was stirred at room temperature for 20 h. Then, the solvent was evaporated under reduced pressure to give the crude product. Purification by flash column chromatography on silica gel with EtOAc-CH₂Cl₂-MeOH (9:1:0.1) as eluent gave thiol **149** (1.095 g, 63%) as a colorless oil. ¹H NMR (400 MHz, DMSO) δ 7.92 (br. t, J = 5.4 Hz, 1H, H11), 7.61 (dd, J = 7.9, 5.3 Hz, 1H, H5), 5.11 - 5.02 (m, 1H, H2), 4.62 (t, J = 8.5 Hz, 1H, H3), 4.37 - 4.18 (m, 3H, H3 and H1), 4.14 - 4.03 (m, 1H, H6), 3.19 - 2.97 (m, 2H, H12), 2.55 - 2.43 (m, 2H, H8), 2.38 (td, J = 7.8, 3.6 Hz, 1H, SH), 1.99 - 1.78 (m, 2H, H7), 1.49 - 1.38 (m, 2H, H13), 1.38 - 1.26 (m, 6H, H14-16), 0.92 (t, J = 6.8 Hz, 3H, H17). ¹³C NMR (101 MHz, DMSO) δ 170.9 (C9), 155.5 (C4), 154.7 (C10), 74.8 (C2), 65.8 (C3), 63.4 (C1), 53.7 (C6), 38.5 (C12), 36.3 (C7), 30.9 (C14), 29.0 (C13), 26.0 (C15), 22.1 (C16), 20.5 (C8), 13.9 (C17). IR (KBr) 3308, 3083 (NH), 2956, 2930, 2858, 2563 (SH), 1794 (O₂C=O), 1723 (OCONH), 1657 (CONH), 1536, 1443, 1393, 1244, 1173, 1100, 1057, 772, 716, 661. HRMS (ESI) m/z for C₁₅H₂₆N₂O₆S (M + H)⁺ 363.1575, (M + Na)⁺ 385.1395.

Synthesis of Thioether **150**

Methyl acrylate (2.9 mL, 32.0 mmol) and Et_3N (10 μL , 0.064 mmol) were added to a stirred solution of **149** (2.317 g, 6.4 mmol) in THF (12 mL) at room temperature. The reaction mixture was stirred at room temperature for 6 h. Then, the solvent was evaporated under reduced pressure to give the crude product. Purification by flash column chromatography on silica gel with $\text{EtOAc-CH}_2\text{Cl}_2\text{-MeOH}$ (9:1:0.1) as eluent gave thioether **150** (1.462 g, 51%) as a colorless oil. ^1H NMR (400 MHz, DMSO) δ 7.85 (br. t, $J = 5.4$ Hz, 1H, H11), 7.58 (dd, $J = 7.8, 4.9$ Hz, 1H, H5), 5.06 - 4.92 (m, 1H, H2), 4.56 (t, $J = 8.5$ Hz, 1H, H3), 4.30 - 4.12 (m, 3H, H3 and H1), 4.06 - 3.94 (m, 1H, H6), 3.61 (s, 3H, H21), 3.14 - 2.94 (m, 2H, H12), 2.75 - 2.63 (m, 2H, H19), 2.63 - 2.55 (m, 2H, H18), 2.51 - 2.39 (m, 2H, H8), 1.90 - 1.70 (m, 2H, H7), 1.46 - 1.31 (m, 2H, H13), 1.31 - 1.17 (m, 6H, H14-16), 0.86 (t, $J = 6.8$ Hz, 3H, H17). ^{13}C NMR (101 MHz, DMSO) δ 171.9 (C20), 170.9 (C9), 155.5 (C4), 154.7 (C10), 74.7 (C2), 65.8 (C3), 63.3 (C1), 54.0 (C6), 51.4 (C21), 38.4 (C12), 34.1 (C18), 32.1 (C7), 30.9 (C14), 28.9 (C13), 27.4 (C8), 26.0 (C19), 25.9 (C15), 22.0 (C16), 13.9 (C17). IR (KBr) 3319, 2955, 2930, 2858, 1797 ($\text{O}_2\text{C=O}$), 1731 (OCOO and OCONH), 1659 (CONH), 1535, 1439, 1362, 1246, 1172, 1096, 1056, 772, 716. HRMS (ESI) m/z for $\text{C}_{19}\text{H}_{32}\text{N}_2\text{O}_8\text{S}$ ($\text{M} + \text{H}$) $^+$ 449.1921, ($\text{M} + \text{Na}$) $^+$ 471.1739.

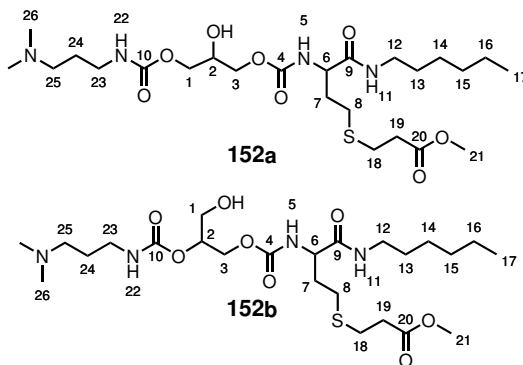
Synthesis of Thiol-Alcohol 151



3-(Dimethylamino)-propylamine (450 μL , 3.6 mmol) was added to a stirred solution of **149** (1.301 g, 3.6 mmol) in THF (11 mL) at 70 $^{\circ}\text{C}$. The reaction mixture was stirred at 70 $^{\circ}\text{C}$ for 30 h. Then, the solvent was evaporated under reduced pressure to give the crude product, which contained an 82:18 mixture of isomeric alcohols **151a** and **151b** (by ^1H NMR spectroscopy). Purification by flash column chromatography on aluminum oxide with CH_2Cl_2 -MeOH (9:1) as eluent gave a 82:18 mixture (by ^1H NMR spectroscopy) of alcohols **151a** and **151b** (1.016 g, 61%) as a colorless oil. ^1H NMR (400 MHz, DMSO) δ 7.85 (s, 1H, H11), 7.45 - 7.27 (m, 1H, H5), 7.14 (br. t, $J = 4.8$ Hz, 1H, H18), 5.12 (d, $J = 4.9$ Hz, 0.82H, OH^a), 4.89 (dd, $J = 10.8, 5.0$ Hz, 0.18H, OH^b), 4.76 (br. s, 0.18H, $\text{H}2^b$), 4.26 - 4.07, 3.99 - 3.83 (m, 0.36H, $\text{H}3^b$), 4.06 - 3.95 (m, 1H, H6), 3.99 - 3.83 (m, 3.28H, $\text{H}1^a$ and $\text{H}3^a$), 3.86 - 3.71 (m, 0.82H, $\text{H}2^a$), 3.53 - 3.44 (m, 0.32H, $\text{H}1^b$), 3.13 - 2.90 (m, 4H, H12 and H19), 2.53 - 2.38 (m, 2H, H8), 2.33 (t, $J = 7.1$ Hz, 1H, SH), 2.18 (t, $J = 7.1$ Hz, 2H, H21), 2.10 (s, 6H, H22), 1.91 - 1.73 (m, 2H, H7), 1.59 - 1.45 (m, 2H, H20), 1.45 - 1.32 (m, 2H, H13), 1.32 - 1.14 (m, 6H, H14-16), 0.86 (t, $J = 6.2$ Hz, 3H, H17). ^{13}C NMR (101 MHz, DMSO) δ 171.1 (C9), 156.2 (C4), 156.0 (C10), 72.3 (C2b), 67.0 (C2a), 65.4 (C1a), 65.1 (C3a), 63.8 (C3b), 60.0 (C1b), 56.6 (C21), 53.7 (C6), 45.1 (C22), 38.6 (C19 and C12), 36.4 (C7), 31.0 (C14), 29.0 (C13), 27.4 (C20), 26.0 (C15), 22.1 (C16), 20.6 (C8), 13.96 (C17). IR (ATR) 3313 (NH), 3079, 2953, 2932, 2859, 2821, 2779, 2559 (SH), 1705 (OCONH),

1660 (CONH), 1538, 1464, 1252, 1145, 1051, 776. HRMS (ESI) m/z for $C_{20}H_{40}N_4O_6S$ ($M + H$)⁺ 465.2727.

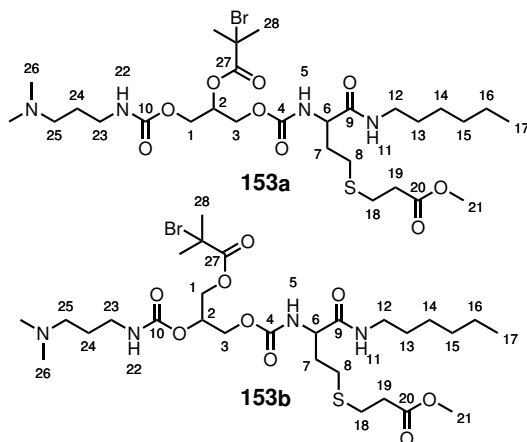
Synthesis of Alcohol 152



3-(Dimethylamino)-propylamine (535 μL , 4.2 mmol) was added to a stirred solution of **151** (1.902 g, 4.2 mmol) in THF (12 mL) at 70 $^{\circ}\text{C}$. The reaction mixture was stirred at 70 $^{\circ}\text{C}$ for 20 h. Then, the solvent was evaporated under reduced pressure to give the crude product, which contained an 80:20 mixture of isomeric alcohols **152a** and **152b** (by ^1H NMR spectroscopy). Purification by flash column chromatography on aluminum oxide with CH_2Cl_2 -MeOH (9:1) as eluent gave a 80:20 mixture (by ^1H NMR spectroscopy) of alcohols **152a** and **152b** (0.765 g, 37%) as a colorless oil. ^1H NMR (400 MHz, DMSO) δ 7.83 (br. t, $J = 4.7$ Hz, 1H, H11), 7.34 (d, $J = 8.0$ Hz, 1H, H5), 7.14 (t, $J = 5.4$ Hz, 1H, H22), 5.11 (d, $J = 5.0$ Hz, 0.80H, OH^a), 4.89 (dd, $J = 11.2, 5.8$ Hz, 0.20H, OH^b), 4.75 (br. s, 0.18H, H2^b), 4.23 - 4.09, 3.98 - 3.84 (m, 0.40H, H3^b), 4.03 - 3.84 (m, 1H, H6), 3.98 - 3.84 (m, 3.20H, H1^a and H3^a), 3.84 - 3.73 (m, 0.80H, H2^a), 3.60 (s, 3H, H21), 3.48 (br. s, 0.40H, H1^b), 3.13 - 2.90 (m, 4H, H12 and H23), 2.75 - 2.64 (m, 2H, H19), 2.63 - 2.54 (m, 2H, H18), 2.51 - 2.38 (m, 2H, H8), 2.17 (t, $J = 7.1$ Hz, 2H, H25), 2.09 (s, 6H, H26), 1.90 - 1.66 (m, 2H, H7), 1.57 -

1.45 (m, 2H, H₂₄), 1.44 - 1.32 (m, 2H, H₁₃), 1.32 - 1.14 (m, 6H, H₁₄₋₁₆), 0.86 (t, $J = 6.7$ Hz, 3H, H₁₇). ¹³C NMR (101 MHz, DMSO) δ 171.9 (C₂₀), 171.1 (C₉), 156.1 (C₄), 155.9 (C₁₀), 72.2 (C_{2b}), 66.9 (C_{2a}), 65.3 (C_{1a}), 64.9 (C_{3a}), 63.5 (C_{3b}), 60.3 (C_{1b}), 56.5 (C₂₅), 53.9 (C₆), 51.4 (C₂₁), 45.1 (C₂₆), 38.6 (C₂₃), 38.4 (C₁₂), 34.1 (C₁₈), 32.2 (C₈), 30.9 (C₁₄), 28.9 (C₁₃), 27.4 (C₂₄ and C₇), 26.0 (C₁₉ and C₁₅), 22.0 (C₁₆), 13.9 (C₁₇). IR (KBr) 3319 (NH), 3072, 2953, 2932, 2859, 2821, 2780, 1720 (OCONH and OCOO), 1661 (CONH), 1537, 1462, 1439, 1359, 1249, 1145, 1050, 980, 829, 777, 661. HRMS (ESI) m/z for C₂₄H₄₆N₄O₈S (M + H)⁺ 551.3095.

Synthesis of the Fully Functionalized Coupler 153



α -Bromoisobutyryl bromide (140 μ L, 1.1 mmol) was added to a stirred solution of **152** (0.511 g, 0.9 mmol) in CH₂Cl₂ (5 mL) at room temperature. The reaction mixture was stirred at 60 °C for 20 h. Then, saturated NaCl_(aq) (5 mL) was added. The layers were separated, and the organic layer was washed with saturated NaCl_(aq) (5 mL). The aqueous layers were extracted with CH₂Cl₂ (5 x 5 mL). The combined organic layers were

dried (MgSO_4) and evaporated under reduced pressure to give the crude product. Purification by flash column chromatography on aluminum oxide with CH_2Cl_2 -MeOH (9.8:0.2) as eluent gave the fully functionalized coupler **153** (0.294 g, 17%) as a light brown oil. ^1H NMR (400 MHz, DMSO) δ 7.94 - 7.81 (m, 1H, H11), 7.57 - 7.45 (m, 1H, H5), 7.28 (br. t, J = 5.1 Hz, 1H, H22), 5.30 - 5.08 (m, 1H, H2), 4.45 - 4.09 (m, 4H, H1 and H3), 4.09 - 3.94 (m, 1H, H6), 3.66 (s, 3H, H21), 3.19 - 2.96 (m, 4H, H12 and H23), 2.82 - 2.70 (m, 2H, H19), 2.70 - 2.60 (m, 2H, H18), 2.56 - 2.43 (m, 2H, H8), 2.23 (t, J = 7.1 Hz, 2H, H25), 2.15 (s, 6H, H26), 1.93 (s, J = 5.5 Hz, 6H, H28), 1.90 - 1.74 (m, 2H, H7), 1.66 - 1.50 (m, 2H, H24), 1.43 (s, 2H, H13), 1.38 - 1.22 (m, 6H, H14-16), 0.92 (t, J = 6.7 Hz, 3H, H17). ^{13}C NMR (101 MHz, DMSO) δ 171.9 (C20), 171.0 (C9), 170.4 (C27), 155.7 (C4), 155.5 (C10), 71.9 (C2a), 69.2 (C2b), 62.2 (C1), 61.8 (C3), 56.9 (C28), 56.4 (C25), 54.0 (C6), 51.4 (C21), 44.9 (C26), 39.5 (C23 and C12), 34.1 (C18), 32.1 (C7), 31.0 (C14), 30.2 (C29), 29.0 (C13), 27.5 (C8), 27.1 (C24), 26.0 (C19 and C15), 22.1 (C16), 13.9 (C17). IR (KBr) 3292 (NH), 2955, 2858, 2678, 2511, 2471, 1725 (CONH), 1662 (CONH), 1530, 1462, 1439, 1359, 1245, 1166, 1058, 980, 949, 814, 775, 726, 651. HRMS (ESI) m/z for $\text{C}_{28}\text{H}_{51}\text{BrN}_4\text{O}_9\text{S}$ ($\text{M} + \text{H}$) $^+$ 701.2602, ($\text{M} + \text{H} - \text{HBr}$) $^+$ 619.3359.

One-pot procedure: Hexylamine (379 μL , 2.9 mmol) was added to a stirred solution of the coupler **148** (0.801 mg, 2.9 mmol) in DMF (10 mL) at room temperature. The reaction mixture was stirred at room temperature for 24 h. Then, 3-(Dimethylamino)-propylamine (362 μL , 2.9 mmol) was added and the reaction mixture was stirred at 70 $^\circ\text{C}$ for 24 h. Next, methyl acrylate (1.3 mL, 14.4 mmol) and Et_3N (4 μL , 0.029 mmol) were added and the reaction mixture was stirred at room temperature for 24 h. The solvent and excess of methyl acrylate were evaporated under reduced pressure to give the crude alcohol (**152**), which contained an 82:18 mixture of isomeric alcohols **152a** and **152b** (by ^1H NMR spectroscopy). Finally, α -bromoisobutyryl bromide (0.76 mL, 3.7 mmol) was added to a

stirred solution of **152** in CH_2Cl_2 (10 mL) at 60 °C. The reaction mixture was stirred for 24 h at 60 °C. Then, 1 M $\text{NaOH}_{(aq)}$ (20 mL) was added and the solution stirred for 10 minutes. The layers were separated. The organic layer was washed with 1 M $\text{NaOH}_{(aq)}$ (2 x 20 mL). The aqueous layer was extracted with CH_2Cl_2 (3 x 10 mL). All combined organic layers were dried (MgSO_4) and evaporated under reduced pressure to give the crude product. Purification by flash column chromatography on aluminum oxide with CH_2Cl_2 -MeOH (10:0 → 9.8:0.2) as eluent gave the fully functionalized coupler **153** (772 mg, 38%) as a light brown oil.

References

- (1) Coessens, V.; Pintauer, T.; Matyjaszewski, K. *Progress in Polymer Science* **2001**, *26*, 337–377.
- (2) Kolb, H. C.; Finn, M. G.; Sharpless, K. B. *Angewandte Chemie International Edition* **2001**, *40*, 2004–2021.
- (3) Nebhani, L.; Barner-Kowollik, C. *Adv. Mater.* **2009**, *21*, 3442–3468.
- (4) Arumugam, S.; Popik, V. V. *Journal of the American Chemical Society* **2011**, *133*, 15730–15736.
- (5) Hoyle, C. E.; Bowman, C. N. *Angewandte Chemie International Edition* **2010**, *49*, 1540–1573.
- (6) Kessler, D.; Nilles, K.; Theato, P. *J. Mater. Chem.* **2009**, *19*, 8184–8189.
- (7) Adelman, R.; Mennicken, M.; Popescu, D.; Heine, E.; Keul, H.; Möller, M. *European Polymer Journal* **2009**, *45*, 3093–3107.
- (8) Christman, K. L.; Schopf, E.; Broyer, R. M.; Li, R. C.; Chen, Y.; Maynard, H. D. *Journal of the American Chemical Society* **2009**, *131*, 521–527.
- (9) Hahn, C.; Keul, H.; Möller, M. *Polymer International* **2012**, *61*, 1048–1060.
- (10) He, Y.; Heine, E.; Keusgen, N.; Keul, H.; Möller, M. *Biomacromolecules* **2012**, *13*, 612–623.
- (11) He, Y.; Keul, H.; Möller, M. *European Polymer Journal* **2011**, *47*, 1607–1620.
- (12) He, Y.; Keul, H.; Möller, M. *Reactive and Functional Polymers* **2011**, *71*, 175–186.

-
- (13) Rahane, S. B.; Hensarling, R. M.; Sparks, B. J.; Stafford, C. M.; Patton, D. L. *J. Mater. Chem.* **2012**, *22*, 932–943.
- (14) Hadjichristidis, N.; Pitsikalis, M.; Pispas, S.; Iatrou, H. *Chemical Reviews* **2001**, *101*, 3747–3792.

Chapter 5

Tailored Thiol-functional Polyamides via a Bis(thiolactone)

5.1 Introduction

Therapeutic treatment of infected, inflamed or cancer tissue in the human body using low-molecular weight drug agents experiences a continuous shift towards the development of macromolecular drug delivery systems. Efficient drug targeting by defined release mechanisms of either covalently bound drugs or polymer/drug blends is one of the key challenges. Straightforward drug delivery to the target organ leads to a reduction of drug doses and thus adverse effects are circumvented.^{1,2} Prerequisites for polymer therapeutics are water solubility, nontoxicity and either biodegradability or elimination from the organism after delivery of the

active compound. Polyamides fulfil most of these criteria, they are non-toxic, biodegradable by enzymes like papain, pepsin^{3,4} and trypsin⁵ and additionally offer tunable mechanical properties.^{6–8} However, the majority of synthetic strategies to obtain polyamides involve peptide coupling reagents^{9,10} or acyl chlorides;^{8,11–13} thus, toxic contaminants cannot be excluded from the synthetic procedure. In addition polyamides prepared by conventional polycondensation are restricted to either linear (in case of AA- and BB-type monomers) or cross-linked architectures (in case of tri- or multifunctional monomers), since the reaction does not allow a distinction between the reactive groups within the monomer. Several efforts have been made to introduce functionalities into polyamides: Alcohol-functional polyamides are obtained by polymerization and subsequent deprotection of dicarboxylic esters (bearing acetal protection groups) and diamines.¹⁴ Polyamides with pendant carboxylic acids are synthesized by polyaddition of cyclic bis(anhydrides) and diamines.¹⁵ Diamines equipped with alkyne side groups serve (after polycondensation) as an efficient anchor for thiol-alkyne click chemistry or azide-alkyne cycloaddition.¹³ Another approach encompasses the use of multicomponent reactions like the Passerini reaction or the Ugi four component reaction. Functional building blocks are integrated directly in the side chain during the polymerization process.^{16–18} Besides, recent advances in ruthenium catalysis show good potential for the formation of polyamides starting from diamines and diols.¹⁹ Concentrating on bio-based and bio-compatible building blocks, we introduce a new AA-type monomer containing two thiolactone rings. One thiolactone is readily available from itaconic acid, which is known to be a common platform chemical²⁰ based on renewable resources. The second thiolactone is introduced as homocysteine thiolactone whose reactivity towards amines has been investigated thoroughly in recent publications by our group^{21,22} and others.^{23–33} Both thiolactone rings linked by an amide group result in a bicyclic AA-type monomer, which is expected to react with diamines by ring-opening to form a polyamide with thiol groups in the side chains. In this chapter, the synthesis route to this AA-type monomer, the

bis(thiolactone), and its reaction with (di)amines is presented. Isolated intermediates are fully characterized by ^1H -, ^{13}C NMR, IR spectroscopy and mass spectrometry. Some examples of multifunctional polymers, their characterization by ^1H NMR, SEC and DSC are given. Furthermore, two hydrophobic polyamides are functionalized via Michael addition to obtain functionalized water-soluble polyamides.

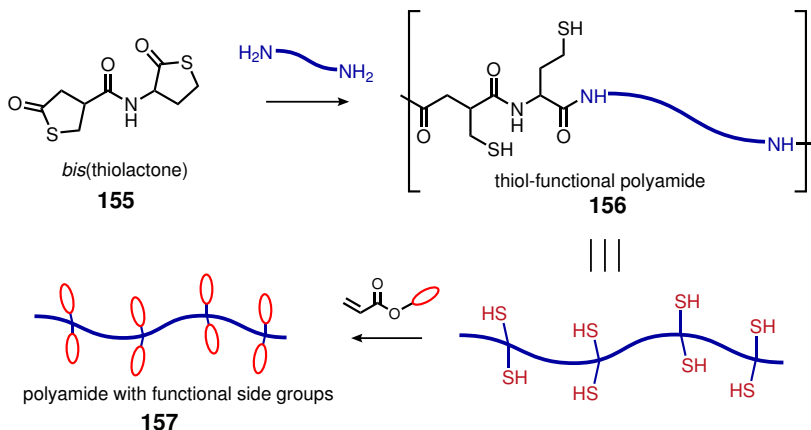
5.2 Results & Discussion

Regarding our synthetic strategy, bis(thiolactone) **155** (an AA-type monomer) is expected to react with diamines (BB-type comonomers) of different constitution. Both thiolactone rings undergo ring-opening by nucleophilic addition of amines forming an amide and simultaneously releasing a thiomethyl and a thioethyl side group. In contrast to a common polycondensation, no condensation products (H_2O or HCl) are generated upon ring-opening of the cycles. Depending on the chosen diamine, different properties are accessible for product **156**. Mixing two different diamines as comonomers, thiol-functional polyamides with statistical incorporation of both diamines are obtained. Finally, these free thiol groups are converted with functional acrylate building blocks via Michael addition to polyamide **157** with functional side groups (Scheme 5.1).

5.2.1 Synthesis of the Bis(thiolactone)

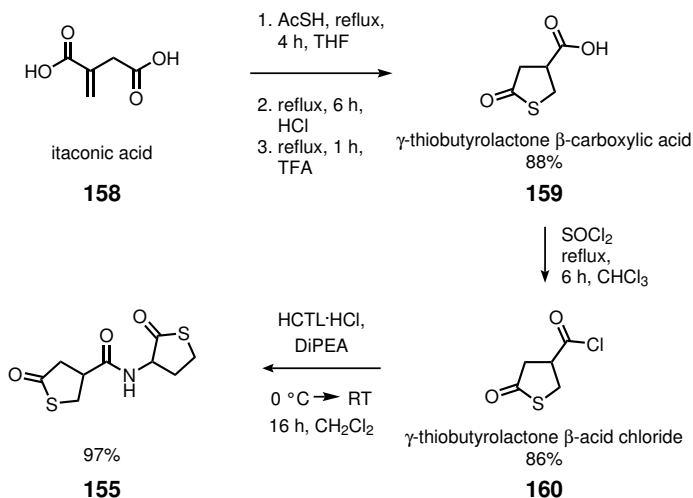
The synthesis of bis(thiolactone) **155** is based on itaconic acid and DL-homocysteine thiolactone hydrochloride (Scheme 5.2).

Starting with itaconic acid and thioacetic acid at reflux for 4 h in THF a Michael adduct of the thioacetic acid to the double bond of **158** is formed.



Scheme 5.1: Concept for the preparation of thiol-functional polyamides with subsequent modification of the pendant thiol groups to obtain a polyamide with functionalized side groups.

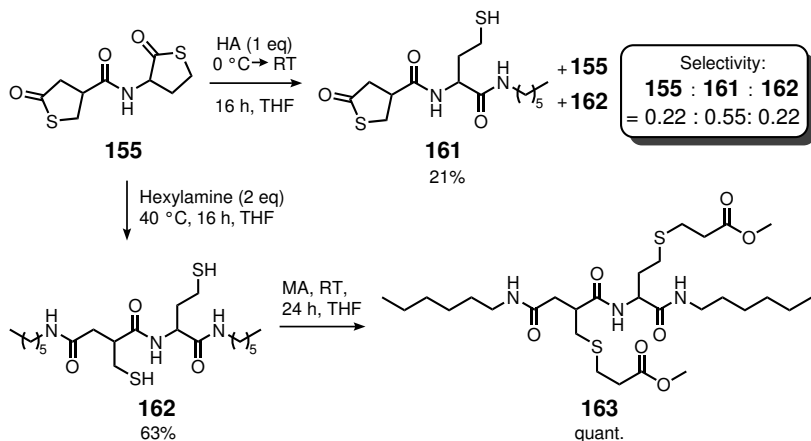
Without further purification, this intermediate is refluxed for 6 h in 6 M $\text{HCl}_{(aq)}$ and 1 h in TFA. This reaction step drives the thioacetate to undergo hydrolysis followed by cyclization to give the acid **159**. The procedure is inspired by the synthetic protocol of Gabiras et al.³⁴ Pursuing these steps in one-pot, the first thiolactone building block – γ -butyrolactone- β -carboxylic acid **159** – was obtained in 88% yield after recrystallization in chloroform. Subsequently, the reaction of **159** with thionyl chloride transformed the carboxylic acid into the acid chloride **160** (86% yield after vacuum distillation). Finally, **117** (HCTL-HCl) – the second thiolactone building block – was connected by amidation with the previously prepared acid chloride **160** to give bis(thiolactone) **155** in 97% yield after purification by flash column chromatography.



Scheme 5.2: Synthesis route for the preparation of bis(thiolactone) **155**.

5.2.2 Model Reactions

To evaluate the reactivity of both cycles of bis(thiolactone) **155**, model reactions with hexylamine were carried out (Scheme 5.3). Reaction of one equivalent of hexylamine and bis(thiolactone) **155** resulted in a mixture of non-converted bis(thiolactone) **155**, monosubstituted and disubstituted products (**161** and **162**). In detail, 55% of the charged amount of hexylamine reacted only with the homocysteine thiolactone ring to deliver **161**. 45% reacted with both cycles converting **155** into bis(thiol) **162**. Consequently, 22.5% of **155** remained untouched. This rather low regioselectivity was not sufficient for the selective conversion of only one thiolactone ring. Hence, bis(thiolactone) **155** was prospectively considered as AA-type monomer rather than as AA¹-type monomer with different reactivity of the rings. Reacting **155** with two equivalents of hexylamine gave bis(thiol) **162** in 100% conversion. However, after purification by flash column chromatography the isolated yield of bis(thiol) **162** decreased to



Scheme 5.3: Conversion of bis(thiolactone) **155** with hexylamine and subsequent Michael addition with methyl acrylate.

63% due to strong interaction with the stationary phase. The final step involved the transformation of **162** into the corresponding Michael adduct **163** using excess of methyl acrylate. No purification was necessary; thus, bis(thioether) **163** was isolated in quantitative yield (quant.). The ^1H NMR spectra of compounds **155**, **162** and **163** are shown in Figure 5.1.

For bis(thiolactone) **155**, the amide proton 6 is found at $\delta = 8.51$ ppm. The adjacent methine proton 7 appears as multiplet at $\delta = 4.64$ ppm. In contrast, the methine proton 3 of the second cycle is assigned to the multiplet at higher field ($\delta = 3.38 - 3.24$ ppm) overlapping with protons 2 and 9. Methylene protons 4, adjacent to methine proton 3 appear as a multiplet at $\delta = 2.83 - 2.63$ ppm. The protons of methylene group 8 show two multiplets at $\delta = 2.50 - 2.39$ ppm and $\delta = 2.16 - 2.00$ ppm demonstrating the rigidity of the ring. ^{13}C NMR, COSY and HSQC spectra give further proof of the structure (Section A.2.1). The ring-opening of the thiolactones is monitored by the disappearance of the signal for the methine protons 3 and 7 of bis(thiolactone) **155**. As both thiolactone rings are opened, both methine protons are shifted to higher field, proton 7 to $\delta = 4.34 - 4.21$ and

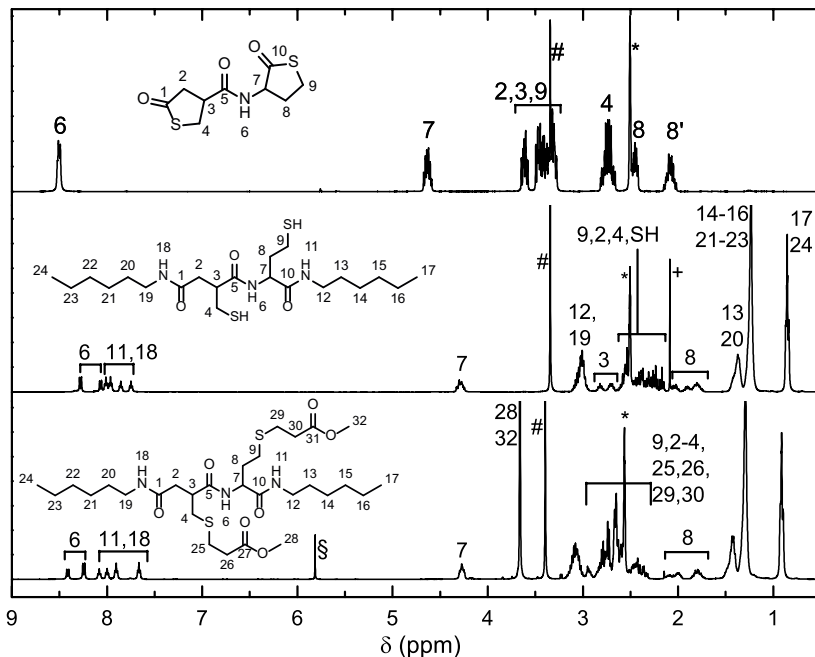


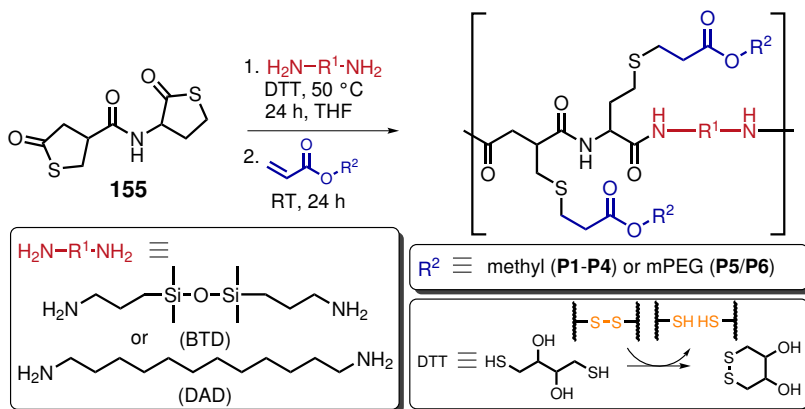
Figure 5.1: ¹H NMR spectra of bis(thiolactone) **155** and the corresponding products resulting from the model reactions with hexylamine and methyl acrylate to deliver **162** and **163**, respectively. Residual solvent peaks: * DMSO, + Acetone, # H₂O, § CH₂Cl₂.

proton **3** to $\delta = 2.88 - 2.65$ ppm splitting up in two multiplets. The amide protons show some remarkable signals. Every amide proton is split in two peaks of the same multiplicity. This is expected to result from possible hydrogen bonding of the different diastereomers, so that two main rigid conformations occur. Consequently, amide **6** shows two doublets, whereas the freshly formed amides **11** and **18** show each two triplets in the region of $\delta = 8.04 - 7.70$ ppm. The adjacent methylene groups appear as a multiplet at $\delta = 3.13 - 2.91$ ppm. It should also be mentioned, that methylene protons **8** split up in three multiplets ($\delta = 2.09 - 1.72$ ppm), possibly driven by the same two conformations (one does split up; the other does not). After Michael addition to obtain **163**, it is observed that (i) the

thiol protons (for **162**: $\delta = 2.32 - 2.12$ ppm) vanish, (ii) methylene protons 25, 26, 29 and 30 are overlapping with signals of protons 9 and 2 - 4 ($\delta = 2.83 - 2.59$ ppm) and (iii) the shift and intensity of the amide protons changes ($\delta = 8.51 - 7.55$ ppm), all signals being better resolved.

5.2.3 Polymer Synthesis

As a consequence of the non-regioselectivity of bis(thiolactone) **155** (as revealed by the model reactions), either one diamine or two different diamines in a specific ratio were employed for polyaddition. This way, from two diamines AA, BB-type polycondensates with a statistical comonomer distribution in the main chain were obtained. In the present section, monomer **155** was reacted with two diamines of different chain flexibility leading to polyamides with different thermal properties: Bis(aminopropyl)tetramethyldisiloxane (BTD) embodies properties of poly(dimethylsiloxane), which is known to result in rubber elastic materials exhibiting low T_g . In contrast, 1,12-diaminododecane (DAD) was selected as an aliphatic comonomers which is able to form semicrystalline materials. For the synthesis of thiol-functional polyamides, bis(thiolactone) **155** was reacted with equimolar amounts of a diamine mixture comprising two diamines in different ratios. Dithiothreitol was added to prevent cross-linking of the resulting thiol polymers. Successively, the thiols were converted with methyl acrylate to give the functionalized polyamide (Scheme 5.4). The diamines were used in different ratios of BTD to DAD: 1:0 (**P1**), 0.5:0.5 (**P2**), 0.25:0.75 (**P3**) and 0:1 (**P4**). For purification, the polymers were precipitated two times in ice-chilled water. The proposed microstructure was confirmed by ^1H NMR spectroscopy as shown exemplary for **P1** (Figure 5.2). All amide protons (6, 11 and 18) appear in the expected region ($\delta = 8.42 - 7.51$ ppm). The signal of methine proton 7 is shifted upon ring-opening to $\delta = 4.19$ ppm. The broad multiplet at $\delta = 3.17 - 2.81$ ppm is assigned to methylene protons 12 and 17 adjacent to



Scheme 5.4: Preparation of polyamides using bis(thiolactone) **155** and different diamines (BTD and DAD). DTT was used to prevent cross-linking of **P1-P4**. Post-polymerization modification of a thiol-functional polyamide **P1** using acrylate-functional mPEG to give the water-soluble polymers **P5** and **P6**.

the amide groups. The four methyl groups of the tetramethylsiloxane (a) are located at $\delta = 0.00$ ppm. Methylene groups c resulting from Michael addition to methyl acrylate are overlapping with signals from protons 2 - 4 at $\delta = 2.83 - 2.17$ ppm. For polymers **P2**, **P3** and **P4** similar results

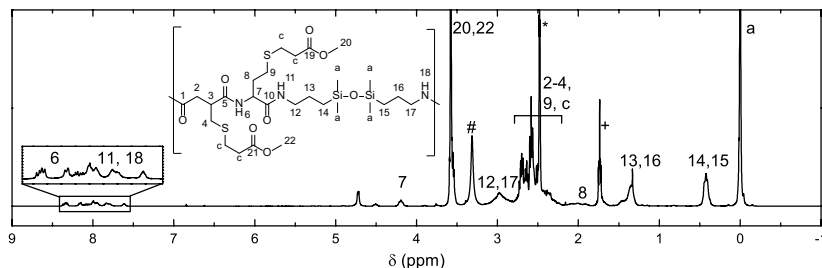


Figure 5.2: ^1H NMR spectrum of polymer **P1** prepared from bis(thiolactone) **155** and BTD. Residual solvent peaks: * DMSO, # H_2O , + THF.

were obtained (Section A.2). SEC was performed to determine M_n and the dispersity index (M_w/M_n or Đ). The lowest number average molecular

weight is obtained for polymer **P1**, which is presumably caused by the low reactivity of BTB. Hence, the number average molecular weight increases with the DAD content (**P1** to **P4**). The dispersity indices (M_w/M_n) for **P1**-**P3** are around two as expected for a step-growth reaction (Table 5.1). **P4** reaches a dispersity value of $M_w/M_n = 3.58$. This is attributed to adventitious disulfide bond formation. All SEC traces show maxima for specific oligomers (Figure A.14).

Table 5.1: Experimental data of the prepared polyamides.

No.	Composition BTB:DAD	$M_{n,SEC}$ [g/mol]	M_w/M_n	Yield [%]	T_g [°C]
P1	100:0	980	1.83	quant.	-50
P2	50:50	1300	2.11	quant.	-48/60
P3	25:75	1300	2.08	quant.	33
P4	0:100	2400	3.58	99%	92

All polymers were analysed by differential scanning calorimetry (DSC) (Figure 5.3). Thermal effects occurred only in the first heating; in the second heating cycle no transition was observed due to deficient relaxation times.

Polymer **P1** shows a glass transition of about $T_g = -50$ °C. Increasing the content of DAD to 50%, two glass transitions are observed: T_{g1} at -48 °C and T_{g2} at 60 °C. It is assumed, that due to different reactivity of the diamines a polymer with a blocky structure is obtained, thus two thermal transitions are observed. In contrast, for polymer **P3** the amount of BTB is low resulting in a statistical incorporation. Hence, only one glass transition is observed at $T_g = 33$ °C. Using 100% of DAD (**P4**) a glass transition at $T_g = 92$ °C is found. Another side effect observed for **P3** and **P4** is the overshooting of the glass transition at the high heating rate of 10 K·min⁻¹. This is reflected in a slight peak instead of a neat glass transition. Furthermore, the lack of crystalline domains in **P4** was validated by X-ray diffraction (Figure 5.4). Only minor crystalline signals are detected for the

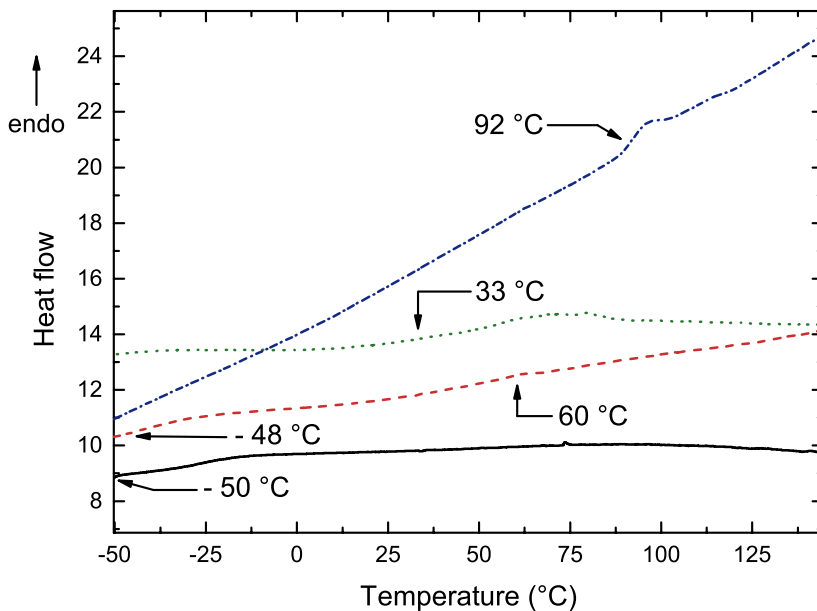


Figure 5.3: DSC first heating curve for polyamides with different ratios of BTD:DAD showing **P1** (1:0, solid), **P2** (0.5:0.5, dash), **P3** (0.25:0.75, dot) and **P4** (0:1, dash dot).

chain direction (c) for hydrogen bonding with interplanar distances of $d = 18 \text{ \AA}$ and $d = 4.25 \text{ \AA}$, respectively. Nevertheless, amorphous regions dominate the corresponding diffraction pattern. The two big diffusion halos (a) superimpose with crystalline signals. To sum up, only low crystallinity is observed, although the actual degree of crystallinity could not be calculated due to the dominating amorphous content and the corresponding signals. The thermal behaviour of **P4** was also observed under the microscope equipped with a heating plate. A heating rate of $3 \text{ K}\cdot\text{min}^{-1}$ was applied. Amorphous domains disappear over a large temperature range, which is explained by the high dispersity of the polymer making a sharp thermal transition impossible. As the polymer is cooled down, no crystallization is observed, which is consistent with our obtained data, since second heating curves show no further thermal transitions (Figure A.15).

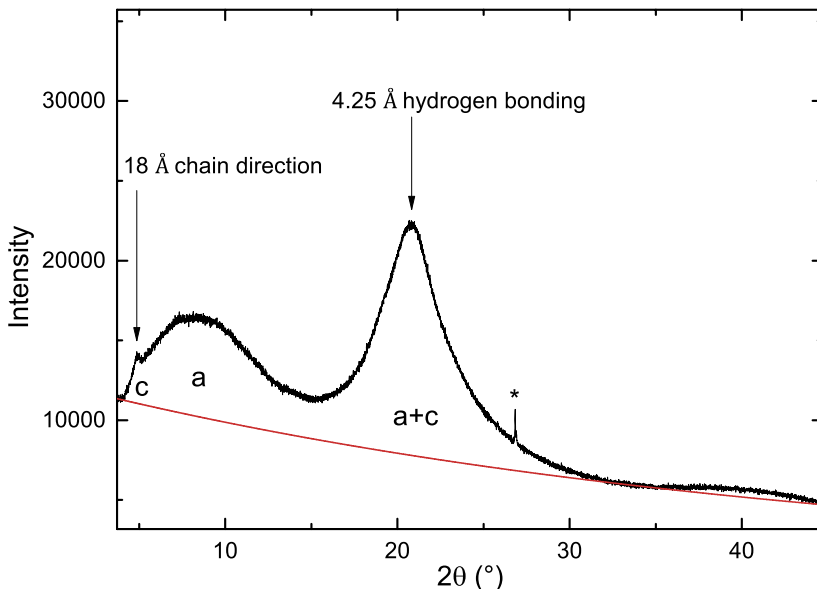


Figure 5.4: X-ray diffraction pattern of polymer **P4** (BTD:DAD, 0:1) with baseline (red). Only minor crystalline peaks are observed (c). Two big diffusion halos (a) dominate the diffraction pattern and superimpose with the remaining crystalline signals. Therefore, only low crystallinity is estimated (crystallinity could not be calculated due to the high amorphous content of the polymer). * marks an artifact peak caused by the detector.

5.2.4 Post-Polymerization Modification

Post-polymerization modification of the thiol groups formed during ring-opening poses an essential advantage since properties of the main chain, mainly dominated by the BB-type comonomer, are independently combined with new properties arising from the side chains. To demonstrate the versatility of this strategy, first the water-insoluble polyamide **P1** is synthesized. Next, this thiol-functional precursor is converted with an mPEG acrylate by Michael addition (Scheme 5.4). Two different acrylate-functional PEG building blocks were used. **164a** was a commercially available PEG methyl ether acrylate and its degree of polymerization was

about $n \cong 10$ ($M_n = 480$ g/mol). An acrylate-terminated PEG of higher molecular weight was synthesized in heating a commercially available PEG monomethyl ether with acryloyl chloride. Upon esterification an acrylate-functional PEG with a $M_n = 1700$ g/mol and average repeating units of $n \cong 45$ was obtained (**164b**, Section 5.4) To guarantee a good sep-

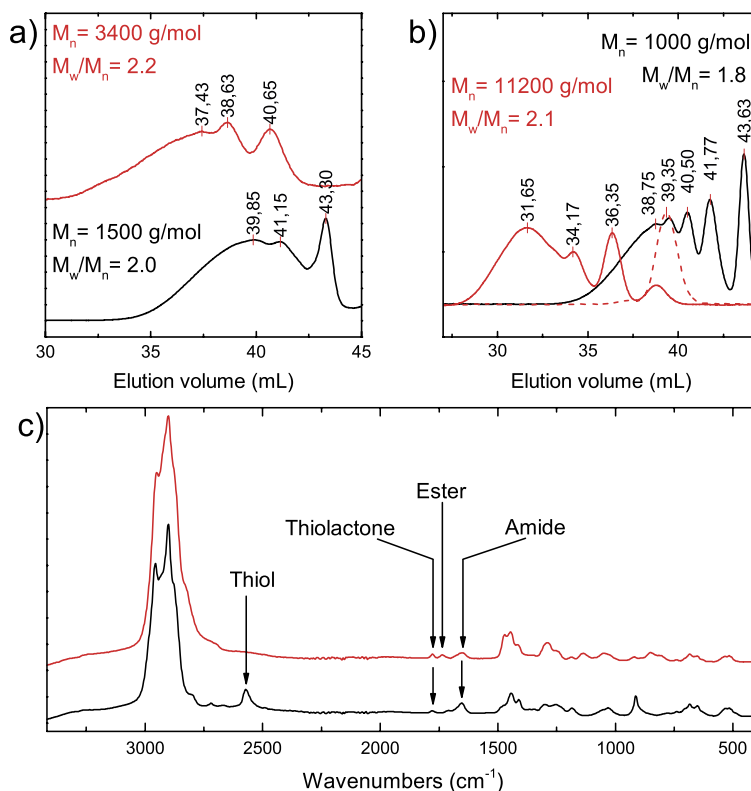


Figure 5.5: a) SEC elugrams of the thiol-functional precursor (black line) and product **P5** (red line). b) Overlapping elugrams showing the thiol-functional polymer precursor (black line), the acrylate-functional PEG with a $M_n = 1700$ g/mol (dashed red line) and the final product **P6** (solid red line). c) Raman spectra of the starting thiol-functional polymer (black line) and product **P5** (red line) obtained by post-polymerization modification.

aration of the final product from non-reacted mPEG acrylate, one equiv-

alent of the mPEG acrylate per thiol group was used. Consequently, to prevent the mPEG acrylate of being consumed by DTT, the amount of DTT in the polycondensation step was reduced, too. After the two-step reaction sequence, the product is fully soluble in water, which indicates that the transformation of the thiol groups was successful. Thus, the thermal properties of polyamides are combined with water solubility of PEG to give the final product **P5** (^1H NMR see Figure A.13). As shown by the SEC traces (Figure 5.5a), after the polyaddition of bis(thiolactone) **155** and BTD the elution maximum of the resulting polymer is at $V_E = 39.85$ mL, with oligomer peaks at $V_E = 41.15$ and 43.30 mL (total $M_n = 1500$ g/mol and $M_w/M_n = 2.0$). After attachment of **164a** forming the corresponding Michael adduct **P5**, the elution maximum shifts to $V_E = 37.43$ mL, showing oligomer peaks at $V_E = 38.83$ and 40.65 mL. Successful Michael addition to mPEG acrylate **164a** also reflects in an increase of the number average molecular weight to $M_n = 3400$ g/mol. Meanwhile, the dispersity index increases only slightly to $M_w/M_n = 2.2$, which is probably caused by the newly formed amphiphilic polymer and hence a different hydrodynamic radius of **P5** in solution. Another proof for the effective linking of the mPEG side chains is acquired by Raman spectroscopy (Figure 5.5c). For the thiol-functional polymer a broad absorption band at 2570 cm^{-1} appears. This absorption band vanishes after conversion of the thiol groups. After introduction of the mPEG side chains, a small absorption band for the ester group is detected at 1736 cm^{-1} . To achieve higher molecular weights using the thiol-functional polyamides, side chains of higher molecular weight are introduced (**164b**, Figure 5.5b). Again, a polyamide precursor is firstly prepared ($V_{E,max} = 38.75$ mL). Upon addition of the acrylate-functional PEG **164b** ($V_{E,max} = 39.35$ mL, $M_n = 1700$ g/mol), the elution maximum of the thiol-functional polyamide shifts to lower elution volumes with $V_E = 31.65$ mL and oligomer peaks at $V_E = 34.17$ and 36.35 mL. The number average molecular weight increases to $M_n = 11200$ g/mol with a dispersity value of $M_w/M_n = 2.1$.

5.3 Conclusion

In this chapter, a high-yielding synthesis of a bis(thiolactone) **155** was described. The reactivity of this bis(thiolactone) towards amines was examined showing that the bis(thiolactone) was not able to undergo regioselective ring-opening of the thiolactone rings under specific reaction conditions. Reacting the bis(thiolactone) with two equivalents of amine (at 50 °C), both cycles were opened. The conversion of thiol groups (obtained during polyaddition) with methyl acrylate was successful. Then, the bis(thiolactone) was used as AA-type monomer in a step-growth polymerization. As BB-comonomer, 1,12-diaminododecane (DAD) and 1,3-bis(aminopropyl)tetramethyldisiloxane (BTD) were employed. Four different polymers were prepared with different contents of two diamines: BTD:DAD (**P1**, 1:0; **P2**, 0.5:0.5; **P3**, 0.25:0.75 and **P4**, 0:1). For all polymers (**P1-P4**), the microstructure was confirmed by ¹H NMR spectroscopy and the number average molecular weight was $980 < M_n < 2400$ g/mol. Dispersity values were in agreement with those anticipated for step-growth polymerizations ($1.8 < M_w/M_n < 3.6$). Thermal analysis via DSC revealed glass transitions ranging from $(-50\text{ °C} < T_g < 92\text{ °C})$. The capability of the thiol-functional polymers for stoichiometric post-polymerization modification by Michael addition with mPEG acrylate was demonstrated. Using PEG acrylate monomethyl ether **164a** and **164b**, hydrophobic polyamides with hydrophilic PEG side chains were prepared (**P5** and **P6**). The amphiphilic polyamide was completely soluble in water, which shows the potential for the modification of polyamides. In the future, other BB-type comonomers will be tested and modification of technical polyamides will be pursued.

5.4 Experimental Data

5.4.1 Materials

Itaconic acid (99%, Alfa Aesar), thioacetic acid (96%, Sigma Aldrich), concentrated HCl (p.A, Th. Geyer Chemsolute), trifluoroacetic acid (TFA, 99%, Sigma Aldrich), thionyl chloride (99.7%, Acros Organics), DL-homocysteine thiolactone hydrochloride (99%, ABCR), N,N-diisopropylethylamine (99%, ABCR), hexyl amine (99%, Sigma Aldrich), methyl acrylate (99%, Sigma Aldrich), DL-dithiothreitol ($\geq 99\%$, Sigma Aldrich), 1,3-bis(aminopropyl)tetramethyldisiloxane (97%, ABCR), 1,12-diaminododecane ($>98\%$, Alfa Aesar), poly(ethylene glycol) methyl ether acrylate ($M_n = 480$, Sigma Aldrich), acryloyl chloride (for Synthesis, Merck), poly(ethylene glycol methyl ether ($M_n = 2000$, Sigma Aldrich; by GPC in DMF $M_n = 1700$ g/mol was determined) were used without further purification. Tetrahydrofuran was dried on an MBraun MB SPS Compact solvent purification system. Unless otherwise indicated, all solvents were purchased from commercial sources and were used without further purification. All reactions were performed under an atmosphere of argon, unless otherwise noted. Argon (Linde) was passed over molecular sieves (4 Å) and finely dispersed potassium on aluminum oxide before use.

5.4.2 Measurements

^1H and ^{13}C NMR spectra were recorded on a Bruker DPX-400 FT NMR spectrometer (400 MHz and 100 MHz, respectively) and are reported as follows: chemical shift δ (ppm) (multiplicity, coupling constant J (Hz), number of protons, assignment). Dimethylsulfoxide (DMSO, $\delta_H = 2.50$ ppm, $\delta_C = 39.5$ ppm) or chloroform (CDCl_3 , $\delta_H = 7.26$ ppm, $\delta_C = 77.0$ ppm) were used as an internal standard. Chemical shifts are reported in ppm to

the nearest 0.01 ppm for ^1H and the nearest 0.1 ppm for ^{13}C .

Molecular weights (M_n and M_w) and dispersity values (M_w/M_n) were determined by size exclusion chromatography (SEC). SEC analyses were carried out with dimethylformamid (DMF) as eluent. SEC with DMF (HPLC grade, VWR) as eluent was performed using an Agilent 1100 system equipped with a dual RI-/Visco detector (ETA-2020, WGE). The eluent contained $1 \text{ g}\cdot\text{L}^{-1}$ LiBr ($\geq 99\%$, Sigma Aldrich). The sample solvent contained traces of distilled water as internal standard. One pre-column (8x50 mm) and four PSS GRAM gel columns (8x300 mm) were applied at a flow rate of $1.0 \text{ mL}\cdot\text{min}^{-1}$ at $40 \text{ }^\circ\text{C}$. The diameter of the gel particles measured $10 \text{ }\mu\text{m}$, the nominal pore widths were 30, 10^2 , 10^3 and 3000 \AA . Calibration was achieved using narrowly distributed poly(ethylene glycol) standards (PSS Std. Mainz). Results were evaluated using the PSS WinGPC UniChrom software (Version 8.1).

Raman spectroscopy was carried out on a Bruker FT-Raman-Spectrometer RFS 100/S with a Nd:YAG laser. The power of the laser was 200 mV at 1064 nm with a spectral resolution of 4 cm^{-1} . For each spectrum 500 scans were recorded. Raman intensity maxima are reported in wavenumbers (cm^{-1}).

Differential scanning calorimetry (DSC) analysis was performed on a PerkinElmer DSC 8000 (PerkinElmer LAS, Rodgau, Germany) under nitrogen atmosphere using a scan rate of $10 \text{ K}\cdot\text{min}^{-1}$. For T_g the inflexion point was selected.

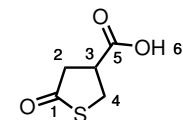
Infrared spectra were carried out on a ThermoNicolet FT-IR Nexus spectrometer and are recorded between KBr disks or using an ATR unit (ThermoNicolet, Smart SplitPEA). Transmission maxima are reported in wavenumbers (cm^{-1}) and only selected intensities are reported.

ESI mass spectra were recorded on a Finnigan SSQ 7000 spectrometer and HRMS spectra on a Thermo Scientific LTQ Orbitrap XL spectrometer. NALDI-TOF mass spectrometry was performed on a Bruker ultrafleXtreme equipped with a 337 nm smartbeam laser in the reflective mode. THF solutions of sodium trifluoroacetate ($2 \text{ }\mu\text{L}$ of $10 \text{ mg}\cdot\text{mL}^{-1}$), and analyte (20

μL of $10 \text{ mg}\cdot\text{mL}^{-1}$) were mixed and $2 \mu\text{L}$ thereof were applied on the sample plate. Laser shots (6000) with 24% up to 60% laser power were collected. The laser repetition rate was 1000 Hz.

5.4.3 Syntheses

Synthesis of γ -Thiobutyrolactone β -Carboxylic Acid (**159**)



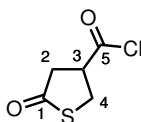
γ -thiobutyrolactone
 β -carboxylic acid

159

γ -thiobutyrolactone β -carboxylic acid **159** was prepared according to the literature; however, without purification of the intermediates.³⁴ Thioacetic acid (3.3 mL, 46.1 mmol) was added to a stirred solution of itaconic acid **158** (3.00 g, 23.1 mmol) in dry THF (11.5 mL, 2 M) at room temperature. The reaction mixture was heated at reflux for 4 h. Then, the solvent and excess of thioacetic acid were evaporated under reduced pressure to give the crude substituted succinic acid as a light yellow solid. ^1H NMR (400 MHz, DMSO) δ 12.44 (s, 2H, OH), 3.15 (dd, $J = 13.6, 6.2$ Hz, 1H, CH_2S), 3.06 (dd, $J = 13.6, 6.6$ Hz, 1H, CH_2S), 2.90 - 2.80 (m, 1H, CHCO_2H), 2.56 - 2.47 (dd, $J = 16.7, 8.2$ Hz, 1H, $\text{CH}_2\text{CO}_2\text{H}$), 2.40 (dd, $J = 16.9, 5.4$ Hz, 1H, $\text{CH}_2\text{CO}_2\text{H}$), 2.33 (s, 3H, CH_3). The crude product was dissolved in 6 M $\text{HCl}_{(aq)}$ (20 mL, 1.2 M). The reaction mixture was heated at reflux for 15 h. Then, the solvent was evaporated under reduced pressure, TFA (20 mL, 1.2 M) was added. The reaction mixture was heated at reflux for 1.5 h. Next, the solvent was evaporated under reduced pressure to give the crude product. Purification by recrystallization in CHCl_3 gave the

carboxylic acid **159** (2.967 g, 88%) as a white solid. ^1H NMR (400 MHz, DMSO) δ 12.87 (br. s, 1H, H6), 3.65 (dd, $J = 11.2$, 6.7 Hz, 1H, H4), 3.58 (dd, $J = 11.2$, 6.2 Hz, 1H, H4), 3.49 - 3.38 (m, 1H, H3), 2.85 - 2.67 (m, 2H, H2). IR (KBr) 3443, 3143 (OH), 1728 (COOH), 1664 (COS), 1400, 1214, 1176, 1113, 849, 656. HRMS (ESI) m/z for $\text{C}_5\text{H}_6\text{O}_3\text{S}$ ($M + \text{H}$) $^+$ 147.0108. The spectroscopic data are consistent with those reported in the literature.³⁴

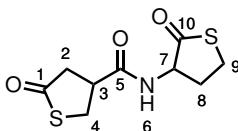
Synthesis of γ -Thiobutyrolactone β -Acid Chloride (**160**)



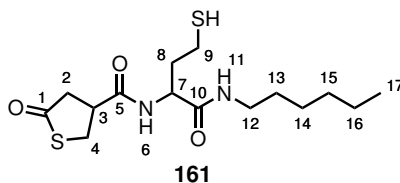
γ -thiobutyrolactone
 β -acid chloride

160

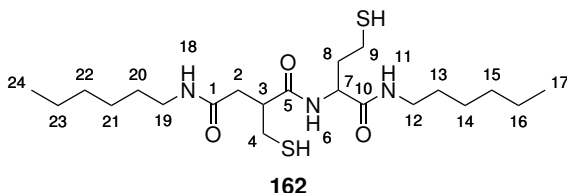
Thionyl chloride (17.7 mL, 0.244 mol) was added to a stirred solution of **159** (17.8 g, 0.122 mol) in CHCl_3 (120 mL, 1 M) at room temperature. The reaction mixture was heated at reflux for 6 h. Then, the solvent and excess of thionyl chloride were evaporated under reduced pressure to give the crude product. Purification by vacuum distillation ($1 \cdot 10^{-3}$ mbar, 85 °C) gave the acid chloride **160** (17.3 g, 86%) as a yellow oil. ^1H NMR (400 MHz, CDCl_3) δ 3.89 - 3.78 (m, 1H, H3), 3.75 - 3.69 (m, 2H, H4), 3.00 (dd, $J = 17.1$, 8.5 Hz, 1H, H2), 2.90 (dd, $J = 17.1$, 7.4 Hz, 1H, H2). ^{13}C NMR (101 MHz, CDCl_3) δ 202.5 (C1), 172.8 (C5), 53.4 (C3), 43.3 (C2), 33.7 (C4). IR (KBr) 3390, 2988, 2928, 1786 (COCl), 1705 (COS), 1445, 1411, 1070, 1006, 934, 879, 861, 779, 721, 627.

Synthesis of Bis(thiolactone) **155****155**

Ethyl diisopropylamine (2.60 mL, 15.2 mmol) was added slowly (1.3 mL/h) to a stirred suspension of HCTL (933 mg, 6.08 mmol) and acid chloride **160** (1.00 g, 6.08 mmol) in dry CH_2Cl_2 (12 mL, 0.5 M) at 0 °C. The reaction mixture was allowed to warm slowly to room temperature and stirred at room temperature for 16 h. The organic layer was washed with 1 M $\text{HCl}_{(aq)}$ (2 x 10 mL). Then, the aqueous layer was extracted with CH_2Cl_2 (6 x 10 mL). The combined organic extracts were dried (MgSO_4) and the solvent was partially evaporated under reduced pressure. Purification by flash column chromatography on silica gel using CH_2Cl_2 as eluent gave bis(thiolactone) **155** (1.44 g, 97%) as a slightly yellow solid. ^1H NMR (400 MHz, DMSO) δ 8.60 - 8.39 (m, 1H, H6), 4.72 - 4.55 (m, 1H, H7), 3.67 - 3.55 (m, 1H, H2), 3.51 - 3.24 (m, 4H, H2, H3 and H9), 2.83 - 2.64 (m, 2H, H4), 2.50 - 2.39 (m, 1H, H8), 2.17 - 1.99 (m, 1H, H8). ^{13}C NMR (101 MHz, DMSO) δ 206.6, 206.5 (C1), 205.2 (C10), 170.9 (C5), 58.4, 58.3 (C7), 43.7, 43.5 (C4), 43.0 (C3), 35.10, 34.9 (C2), 30.1 (C8), 26.80 (C9). IR (KBr) 3454, 3305 (NH), 1705 (COS), 1650 (CONH 1), 1543 (CONH 2), 1275, 1224, 1069, 1021, 929, 651. HRMS (NALDI) m/z for $\text{C}_9\text{H}_{11}\text{NO}_3\text{S}_2$ ($\text{M} + \text{Na}$)⁺ 268.048.

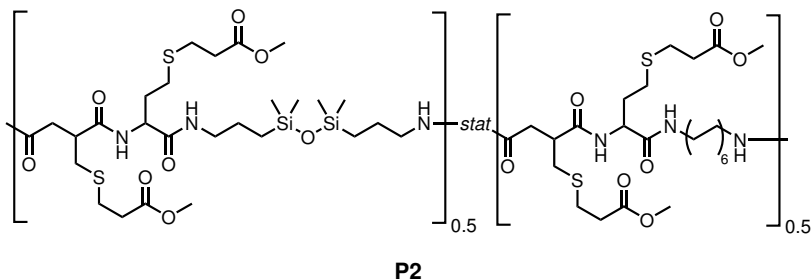
Synthesis of Thiol **161**

Hexyl amine (162 μL , 1.23 mmol) was added to a stirred solution of **155** (301 mg, 1.23 mmol) in dry THF (10 mL, 0.125 M) at room temperature. The reaction mixture was stirred at room temperature for 24 h. Then, the solvent was evaporated under reduced pressure to give the crude product. Purification by flash column chromatography on silica gel with CH_2Cl_2 -EtOAc-MeOH (9:1:0.1) as eluent gave thiol **161** (90.1 mg, 21%) as a white solid. R_F (9:1:0.1 CH_2Cl_2 -EtOAc-MeOH) 0.32. ^1H NMR (400 MHz, DMSO) δ 8.31 (dd, $J = 13.3, 8.2$ Hz, 1H, H6), 7.96 (dd, $J = 11.3, 5.6$ Hz, 1H, H11), 4.39 - 4.28 (m, 1H, H7), 3.68 - 3.54 (m, 1H, H2), 3.52 - 3.24 (m, 2H, H3), 3.14 - 2.93 (m, 2H, H12), 2.85 - 2.61 (m, 2H, H4), 2.47 - 2.34 (m, 2H, H9), 1.96 - 1.72 (m, 2H, H8), 1.37 (m, 2H, H13), 1.22 (s, 6H, H14-16), 0.86 (t, $J = 6.69$ Hz, 3H, H17). ^{13}C NMR (101 MHz, DMSO) δ 206.8, 206.7 (C1), 170.6, 170.5 (C5, C10), 51.8, 51.7 (C7), 43.8 (C4), 42.8 (C3), 38.4 (C12), 36.7 (C8), 34.9 (C2), 30.9 (C14), 28.9 (C13), 25.9 (C15), 22.0 (C16), 20.4 (C9), 13.9 (C17). IR (KBr) 3292 (NH A), 3081 (NH B), 2955, 2930, 2857, 2559 (SH), 1705 (COS), 1637 (CONH 1), 1548 (CONH 2), 1442, 1228, 1065, 682. HRMS (NALDI) m/z for $\text{C}_{15}\text{H}_{26}\text{N}_2\text{O}_3\text{S}_2$ ($\text{M} + \text{Na}$) $^+$ 369.172.

Synthesis of Bis(thiol) **162**

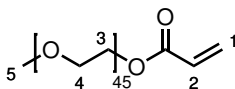
Hexyl amine (444 μL , 3.36 mmol) was added to a stirred solution of **155** (413 mg, 1.68 mmol) in dry THF (12 mL, 0.14 M) at room temperature. The reaction mixture was stirred at room temperature for 18 h. Then, the solvent was evaporated under reduced pressure to give the crude product. Purification by flash column chromatography on silica gel with CH_2Cl_2 -EtOAc-MeOH (9:1:0.1) as eluent gave bis(thiol) **162** (473 mg, 63%) as a white solid. R_F (9:1:0.1 CH_2Cl_2 -EtOAc-MeOH) 0.11. ^1H NMR (400 MHz, DMSO) δ 8.28, 8.07 (d, 1H, H6), 8.01, 7.86 (t, 1H, H11), 7.96, 7.75 (t, 1H, H18), 4.34 - 4.21 (m, 1H, H7), 3.15 - 2.91 (m, 4H, H12 and H19), 2.88 - 2.76, 2.75 - 2.65 (m, 1H, H3), 2.63 - 2.13 (m, 8H, H2, H4, H9 and both SH), 2.08 - 1.69 (m, 2H, H8), 1.40 (m, 4H, H13 and H20), 1.23 (s, 12H, H14-16 and H21-23), 0.86 (t, 6H, H17 and H24). ^{13}C NMR (101 MHz, DMSO) δ 173.2, 172.7 (C5), 170.9, 170.7, 170.6, 170.0 (C10 and C18), 51.7, 51.3 (C7), 45.4 (C3), 38.5 (C12 and C19), 37.0 (C2), 36.0, 35.2 (C8), 31.0, 30.9 (C14 and C21), 29.0, 28.9 (C13 and C20), 26.1, 26.0, 25.9 (C15, C22 and C4), 22.0 (C16 and C23), 20.8, 20.5 (C9), 13.8 (C17 and C24). IR (KBr) 3284 (NH A), 3083 (NH B), 2957, 2929, 2871, 2858, 2561 (SH), 1637 (CONH 1), 1556 (CONH 2), 1378, 1303, 1249, 1227, 724, 689. HRMS (NALDI) m/z for $\text{C}_{21}\text{H}_{41}\text{N}_3\text{O}_3\text{S}_2$ ($\text{M} + \text{Na}$) $^+$ 470.233.

Typical Procedure for the Polycondensation of Bis(thiolactone) **155** with Selected Diamines: Synthesis of **P2**



1,3-Bis(aminopropyl)tetramethyldisiloxane (231 μL , 0.834 mmol), 1,12-diaminododecane (167 mg, 0.834 mmol) and dithiothreitol (515 mg, 3.34 mmol) were added to a stirred solution of **155** (403 mg, 1.67 mmol) in dry THF (10 mL, 0.167 M) at room temperature. The reaction mixture was stirred at 50 $^{\circ}\text{C}$ for 24 h. Then, methyl acrylate (3.02 mL, 33.4 mmol) was added and the reaction mixture was stirred at room temperature for 18 h. Next, the solvent and excess of methyl acrylate were evaporated under reduced pressure to give the crude product. Purification by precipitation from THF in H_2O (2 x 200 mL, 0 $^{\circ}\text{C}$) gave polyamide **P2** (780 mg, quant.) as a dark yellow oil. $M_n = 1300$ g/mol, $M_w/M_n = 2.1$. Polyamides **P1**, **P3** and **P4** were synthesized according to this procedure (Table 5.2).

Synthesis of Acrylate-functional PEG (164b)



164b

Acryloyl chloride (4.91 mL, 60.7 mmol) was added to a stirred solution of poly(ethylene glycol) methyl ether ($M_n = 1700$ g/mol, 2.02 g, 1.01 mmol)

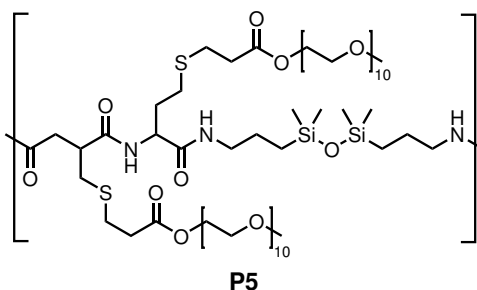
Table 5.2: Polyaddition of bis(thiolactone) **155** using different compositions of the selected diamines.

No.	bis(thiolactone) 155 g (mmol)	BTD mL (mmol)	DAD g (mmol)	t^a [h]
P1	0.414 (1.69)	0.468 (1.69)	-	24
P2	0.409 (1.67)	0.231 (0.834)	0.167 (0.834)	24
P3	0.343 (1.40)	0.097 (0.350)	0.210 (1.05)	18
P4	0.406 (1.66)	-	0.332 (1.66)	18

^a Reaction time of the polyaddition step. The subsequent Michael addition was always carried out overnight (14 - 24 h).

in dry CH_2Cl_2 (20 mL, 0.05 M) at room temperature. The reaction mixture was stirred and heated at reflux for 24 h. Then, the solvent was partially evaporated under reduced pressure. Purification by precipitation in cold Et_2O (200 mL) gave the acrylate-functional PEG **164b** (1.85 g, 89%) as a white solid. $M_n = 1700$ g/mol, $M_w/M_n = 1.0$. $^1\text{H NMR}$ (400 MHz, CHCl_3) δ 6.36 (dd, $J = 17.3, 1.5$ Hz, 1H, H1^{trans}), 6.09 (dd, $J = 17.3, 10.5$ Hz, 1H, H2), 5.77 (dd, $J = 10.5, 1.5$ Hz, 1H, H1^{cis}), 4.38 - 4.02 (m, 2H, 3^E), 3.58 (s, backbone, H3 and H4), 3.31 (s, 3H, H5).

Typical Procedure for the Preparation of PEG-functional Polyamides: Synthesis of P5



1,3-Bis(aminopropyl)tetramethyldisiloxane (400 μL , 1.44 mmol) and dithiothreitol (40.5 mg, 0.262 mmol) were added to a stirred solution of **155** (322 mg, 1.31 mmol) in dry THF (8.6 mL, 0.167 M) at room temperature. The reaction mixture was stirred at 50 °C for 18 h. Then, mPEG acrylate **164a** ($M_n = 480$ g/mol, 1.260 g, 2.62 mmol) was added and the reaction mixture was stirred at room temperature for 24 h. Next, the solvent was evaporated under reduced pressure to give the crude product. The residue was dissolved in water (15 mL), filtered and extracted with CH_2Cl_2 (2 x 5 mL). Lyophilization of the aqueous layer gave polyamide **P5** (955 mg, 49%) as a yellow oil. $M_n = 3400$ g/mol, $M_w/M_n = 2.2$. The synthesis of **P6** was conducted in an analogue manner. Yet, the purification of **P6** was achieved via dialysis using Spectra/Por dialysis membranes (Spectrumlabs.com, RC, MWCO = 2000 Da) in water (3 L) prior to lyophilization. NMR spectra see section A.2.

References

- (1) El-Aneed, A. *Journal of Controlled Release* **2004**, *94*, 1–14.
- (2) Haag, R.; Kratz, F. *Angewandte Chemie International Edition* **2006**, *45*, 1198–1215.
- (3) Bechaouch, S.; Coutin, B.; Sekiguchi, H. *Macromolecular Chemistry and Physics* **1996**, *197*, 1661–1668.
- (4) Bechaouch, S.; Gachard, I.; Coutin, B.; Sekiguchi, H. *Polymer Bulletin* **1997**, *38*, 365–370.
- (5) Negoro, S. In *Biopolymers Online*; Wiley-VCH Verlag GmbH & Co. KGaA: 2005.
- (6) Woodward, A. E.; Crissman, J. M.; Sauer, J. A. *Journal of Polymer Science* **1960**, *44*, 23–34.
- (7) Lin, J.; Sherrington, D. C. In *Polymer Synthesis; Advances in Polymer Science*, Vol. 111; Springer Berlin Heidelberg: 1994; Chapter 5, pp 177–219.
- (8) Fan, Y.; Kobayashi, M.; Kise, H. *Polymer Journal* **2000**, *32*, 817–822.
- (9) Hsiao, S.-H.; Chang, Y.-M. *Journal of Polymer Science Part A: Polymer Chemistry* **2004**, *42*, 4056–4062.

- (10) Okamura, A.; Hirai, T.; Tanihara, M.; Yamaoka, T. *Polymer* **2002**, *43*, 3549–3554.
- (11) Chern, Y.-T.; Chung, W.-H. *Journal of Polymer Science Part A: Polymer Chemistry* **1996**, *34*, 117–124.
- (12) Thiem, J.; Bachmann, F. *Die Makromolekulare Chemie* **1993**, *194*, 1035–1057.
- (13) Billiet, L.; Hillewaere, X. K. D.; Du Prez, F. E. *European Polymer Journal* **2012**, *48*, 2085–2096.
- (14) Chiellini, E. M. O.; Bizzarri, R.; Bonaguidi, P.; Talamelli, P.; Solaro, R. *Journal of Macromolecular Science, Part A* **1999**, *36*, 901–915.
- (15) Hamada, T.; Takayama, T.; Kudo, K. *Chemistry Letters* **2010**, *39*, 1106–1107.
- (16) Wang, Y.-Z.; Deng, X.-X.; Li, L.; Li, Z.-L.; Du, F.-S.; Li, Z.-C. *Polymer Chemistry* **2013**, *4*, 444–448.
- (17) Kakuchi, R. *Angewandte Chemie International Edition* **2014**, *53*, 46–48.
- (18) Sehlinger, A.; Dannecker, P.-K.; Kreye, O.; Meier, M. A. R. *Macromolecules* **2014**, *47*, 2774–2783.
- (19) Malineni, J.; Merkens, C.; Keul, H.; Möller, M. *Catalysis Communications* **2013**, *40*, 80–83.
- (20) Medway, A. M.; Sperry, J. *Green Chemistry* **2014**, *16*, 2084–2101.
- (21) Keul, H.; Mommer, S.; Möller, M. *European Polymer Journal* **2013**, *49*, 853–864.
- (22) Mommer, S.; Lamberts, K.; Keul, H.; Möller, M. *Chemical Communications* **2013**, *49*, 3288–3290.
- (23) Hansell, C. F.; Espeel, P.; Stamenović, M. M.; Barker, I. A.; Dove, A. P.; Prez, F. E. D.; O'Reilly, R. K. *Journal of the American Chemical Society* **2011**, *133*, 13828–13831.
- (24) Espeel, P.; Goethals, F.; Stamenović, M. M.; Petton, L.; Du Prez, F. E. *Polymer Chemistry* **2012**, *3*, 1007–1015.
- (25) Reinicke, S.; Espeel, P.; Stamenović, M. M.; Du Prez, F. E. *ACS Macro Letters* **2013**, *2*, 539–543.
- (26) Espeel, P.; Carrette, L. L. G.; Bury, K.; Capenberghs, S.; Martins, J. C.; Prez, F. D.; Madder, A. *Angewandte Chemie International Edition* **2013**, *52*, 13261–13264.
- (27) Espeel, P.; Goethals, F.; Driessen, F.; Nguyen, L.-T. T.; Du Prez, F. E. *Polymer Chemistry* **2013**, *4*, 2449–2456.
- (28) Goethals, F.; Martens, S.; Espeel, P.; van den Berg, O.; Du Prez, F. E. *Macromolecules* **2013**, *47*, 61–69.
- (29) Stamenović, M. M.; Espeel, P.; Baba, E.; Yamamoto, T.; Tezuka, Y.; Du Prez, F. E. *Polymer Chemistry* **2013**, *4*, 184–193.

- (30) Chen, Y.; Espeel, P.; Reinicke, S.; Du Prez, F. E.; Stenzel, M. H. *Macromolecular Rapid Communications* **2014**, *35*, 1128–1134.
- (31) Reinicke, S.; Espeel, P.; Stamenović, M. M.; Du Prez, F. E. *Polymer Chemistry* **2014**, *5*, 5461–5470.
- (32) Yan, J.-J.; Wang, D.; Wu, D.-C.; You, Y.-Z. *Chemical Communications* **2013**, *49*, 6057–6059.
- (33) Jia, Z.; Bobrin, V. A.; Truong, N. P.; Gillard, M.; Monteiro, M. J. *Journal of the American Chemical Society* **2014**, *136*, 5824–5827.
- (34) Garbiras, B. J.; Marburg, S. *Synthesis* **1999**, *2*, 270–274.

Chapter 6

An Epoxy Thiolactone on Stage

Part I: Multicomponent Reactions, Poly(thioether urethane)s and Respective Hydrogels

6.1 Introduction

The hunt for pioneering concepts regarding the preparation of new polymers and materials is an ongoing chapter in the yet unfinished book of every material scientist. Syntheses of such polymeric materials are achieved by living/controlled polymerization techniques which take advantage of

radical, cationic or anionic chain-growth reaction mechanisms. By these techniques - vinyl and ring-opening polymerization - polymers with high molecular weights, predetermined end group functionality and low dispersity are obtained; a broad product portfolio from poly(meth)acrylates and polystyrenes, to polyethers and polyesters can be designed. However, when it comes to multifunctional polymers (i) specific chemical functionalities - acidic, basic and other interacting functional groups - in the building blocks (the monomers) (ii) as well as easy handling under mild reaction conditions these polymerization techniques stand in their own way. This is a result of the typically higher complexity of these techniques with specific catalysts, ligands, the need of oxygen- and water-free conditions, and in some cases relatively high temperatures. As a consequence, these techniques often limit their use for industrial processes, forcing them into the corner of traditional academic research. Meanwhile, many scientists have gradually discovered the high potential of orthogonal ligation strategies and multicomponent reactions for the synthesis of polymers.^{1,2} Both concepts are often presented separately, however they are per definition connected to each other. Orthogonal chemistry includes what we know to be described as “click” chemistry but also i.e. ligation chemistries.³⁻⁵ The definitions of such chemical reactions need no explanations, since Sharpless’ concept of “click” chemistry has captured a very prominent position in the field of organic chemistry. With the use of such orthogonal chemistry, functional building blocks are selectively combined not only in a low-molecular but also in a high-molecular weight fashion. This brings it to multicomponent reactions, whose merits are primarily the versatility of the used building blocks and the broad range of possible architectural microstructures (linear polymers, branched structures, gels of any kind) but also the ease of handling, gentle reaction conditions and many more.⁶⁻¹¹ All these kind of polymerizations proceed in a step-growth manner and therefore become part of polycondensation/polyaddition processes. When it comes to step-growth polymerization processes, polyesters, polyamides and polyurethanes are the main and most important polymer classes. Al-

though molecular weights of these polymer classes are limited to a several 10 to 100 kDa they exhibit good mechanical properties thanks to the excellent inter- as well as intramolecular interactions of polymer chains. The cumulative effect of these chain interactions - dipole-dipole interaction, van der Waals forces, hydrophobic interaction - convert these single weak forces into strong interactions. A main disadvantage of polymers obtained by polycondensation or polyaddition is that for synthetic processes with mild reaction conditions the use of toxic reagents such as acid chlorides or isocyanates is needed. To prepare polyurethanes or polyamides without use of isocyanates and acid chlorides our group did fundamental research and developed monomers based on cyclic carbonates, phenyl carbonates in order to avoid isocyanates/acid chlorides of any kind.¹²⁻¹⁶

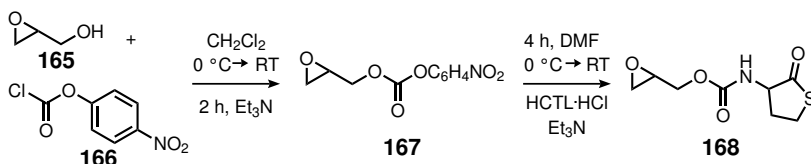
In this chapter, we combine all these concerns and deficiencies and present a bicyclic monomer suitable for polyaddition reaction and preparation of multifunctional polymers (rendering solutions for the synthesis of multifunctional polyurethanes). As a consequence, a large platform for any kind of polymeric architecture is created, using click- and thiolactone chemistry, the latter also picked up by our group^{13,16,17} and others.¹⁸⁻²⁷ In this consent, we synthesized a new bicyclic monomer containing an epoxide and a thiolactone ring, which is used in an approach of orthogonal chemistry to combine different building blocks. This happens by conversion of the thiolactone ring by an amine, thiol-ene Michael addition with an electron deficient double bond and ring-opening of the oxirane ring by a dialkylamine. If only the thiolactone ring is opened by an amine the in situ spawned thiol plays a vital role for the formation of polymers. The thiol is converted in a thiol-epoxy click-reaction to form a poly(thioether urethane). The polarity of aliphatic thioethers is similar to those of pure aliphatic segments. The resulting poly(TEU)s can therefore be contemplated as polyurethanes, just that in our approach no urethane bond is formed during synthesis, rather urethane groups are connected to polymer chains or networks via a thiol-epoxy reaction. Following up, the produc-

tion of networks is promising if polyacrylates and diamines are engaged. This way, hydrogels containing reactive groups are accessible. Part I of this chapter is subdivided in four sections. The first describes a terse synthetic path to the new epoxy thiolactone monomer. The second deals with the elaboration of model reactions, where this new monomer is subjected to a four component reaction. The third and main section of part I addresses the use of the epoxy thiolactone as precursor for poly(thioether urethane)s. The polymerization is extensively studied regarding the influence of catalyst, solvent, substrate concentration, in the formation of linear poly(thioether urethane)s and (cyclic) oligomers in a side reaction. Finally the last section shows the use of the epoxy thiolactone monomer as building block for reactive hydrogels bearing epoxy units in the network.

6.2 Results & Discussion

6.2.1 Synthesis of the Epoxy Thiolactone

The epoxy thiolactone was synthesized in a concise two-step synthesis route, renouncing on water- and oxygen-free conditions (Scheme 6.1). In the first step, addition-elimination of glycidol (**165**) to *para*-nitrophenyl



Scheme 6.1: Synthesis of epoxy thiolactone **168**.

chloroformate **166** according to Morisseau et al. should deliver glycidyl *p*-nitrophenyl carbonate **167**.²⁸ Thus, if **165** is reacted with **166** in CH_2Cl_2 from $0\text{ }^\circ\text{C}$ to room temperature using TEA as acid scavenger, the reaction

is completed after 2 h. The chloride group is a much better leaving group than the *p*-nitrophenolate and thus only one major product is formed. After an acidic work-up to remove residual base and washing with $\text{NaOH}_{(aq)}$ to reduce eventually formed *p*-nitrophenolate the product carbonate **167** is afforded in 87% yield. This crude glycidyl *p*-nitrophenyl carbonate **167** is used without further purification for the next reaction step. In a substitution reaction, the activated carbonate **167** reacts easily with homocysteine thiolactone hydrochloride (HCTL·HCl) under basic conditions with 10 mol% of DMAP as catalyst, by elimination of *p*-nitrophenolate as leaving group. Pure epoxy thiolactone **168** is obtained either by flash column chromatography or – as preferred for a large-scale synthesis – after thorough washing with aqueous potassium carbonate to remove the *p*-nitrophenolate from the reaction product. Using the aqueous work-up the epoxy thiolactone **168** is obtained as a slightly yellow solid in 60% yield. Structural data of both compounds were confirmed by NMR, MS, and IR spectroscopy (Section 6.4 and A.3.2).

Single crystal X-ray diffraction experiments confirmed the general structure of compound **168**. The crystal structure represents a solid solution of diastereomers of the organic molecule. The asymmetric unit contains only one molecule which reveals to be disordered. The disorder has been found around the stereocentre of the epoxide group. The main structure revealed the (*SS*)-isomer with approximately 56.6(6) percentage; whereas a minor percentage (43.4(6) percent) revealed the (*RS*)-epimer (Figure 6.1a). The other enantiomers are generated by a crystallographic inversion centre resulting in a 1-to-1-ratio of (*RR/SS*) and (*RS/SR*), respectively. The molecules are connected by hydrogen bonds formed between the NH-group and the epoxide oxygen building a centrosymmetric dimeric structure (Figure 6.1b). Information on data collection and refinement of the crystal structure are given as annex (CCDC 1447028, Section A.3.1).

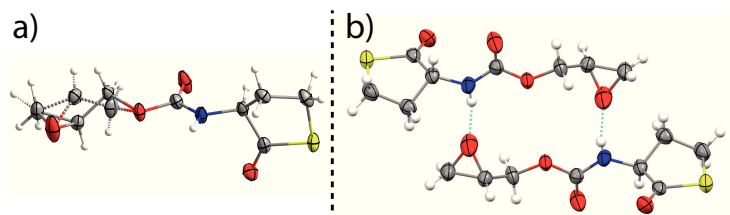
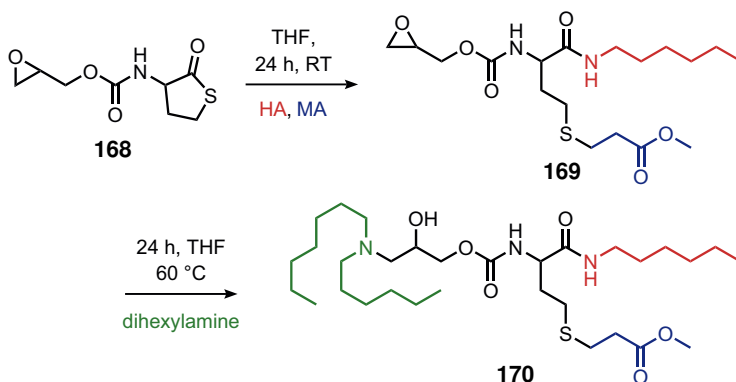


Figure 6.1: Displacement ellipsoid plot of a) the asymmetric unit of **168** showing the major structure of the (*SS*)-isomer (solid line) and the disordered, minor structure of the (*RS*)-epimer (dotted line) and b) two asymmetric units of the (*RR/SS*) enantiomers forming a dimer. Structure drawn at 70% probability, colour code: C - grey, H - white, N - blue, O - red, S - yellow.

6.2.2 Three and Four Component Reactions

To evaluate the selective conversion of the oxirane and the thiolactone ring in the bicyclic monomer **168** towards amines, model reactions were carried out. As it has been already shown in previous works,^{16,17,24,25,29–31} the thiolactone is able to react in a three component reaction first with an amine followed by an acrylate at room temperature. Upon full conversion, a new amide bond and a thioether are formed (compound **169**, Scheme 6.2).



Scheme 6.2: Model reactions performed with epoxy thiolactone **168**.

With a temperature jump of only 35 °C the epoxide is converted using a dialkylamine. If using sub-stoichiometric amounts of monoalkylamine (instead of dialkylamine), a bisalkylation occurs opening two epoxides (Figure A.30, Figure A.31). In our model reactions, we convert epoxy thiolactone **168** with hexylamine and methyl acrylate to the corresponding epoxy thioether **169** in one-pot at room temperature without any need of purification. In a second step, the crude epoxy thioether is subjected to ring-opening using dihexylamine (DHA) at 60 °C. The resulting product **170** is obtained quantitatively in high purity (analysis of the crude product shows no side products). In a four component reaction at 60 °C, compound **170** is generated using hexylamine, methyl acrylate, dihexylamine and epoxy thiolactone **168** in one-pot. The microstructures of the model compounds were confirmed by ¹H NMR spectroscopy (Figure 6.2). Regarding compound **168**, the NH proton 5 of the urethane group is found at $\delta = 7.72$ ppm. Multiplets 3 ($\delta = 4.44 - 4.27$ ppm, overlapping with thiolactone proton 6), 3' ($\delta = 3.76$ ppm) and 1 ($\delta = 2.77$ ppm and 2.61 ppm) show epoxy protons of the methylene groups as they generally split up due to the diastereomeric mixture. Methine proton 2 of the epoxy group and 6 of the thiolactone ring allow to monitor the reaction trajectory. Upon ring-opening and Michael addition in a three component reaction (product **169**) a new signal is generated for the amide proton at $\delta = 7.84$ ppm (★). The methylene group adjacent to the amide appears as a multiplet at $\delta = 3.04$ ppm (■). The multiplet of methine proton 6 shifts to lower field ($\delta = 3.97$ ppm). Methylene groups of the former acrylate exhibit two multiplets at $\delta = 2.68$ and 2.59 ppm (□). Upon addition of the dihexylamine to the epoxide to form compound **170**, signal 2 shifts from $\delta = 3.15$ to 3.68 ppm (detailed NMR analysis comprising ¹³C, COSY, HSQC, see section A.3.2). An intermediate epoxy thiol could not be isolated, since the thiol group, which is released after aminolysis of the thiolactone is able to react in situ in dry state (while removing the solvent and applying high vacuum) with the epoxide forming poly(TEU)s. This polymerization is further investigated.

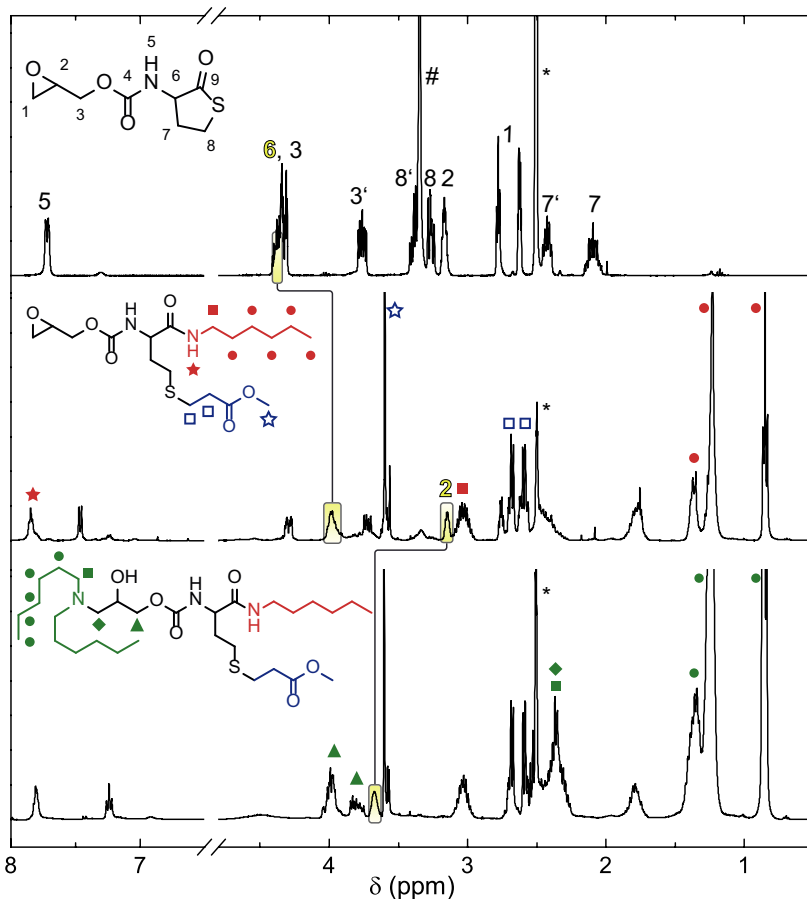
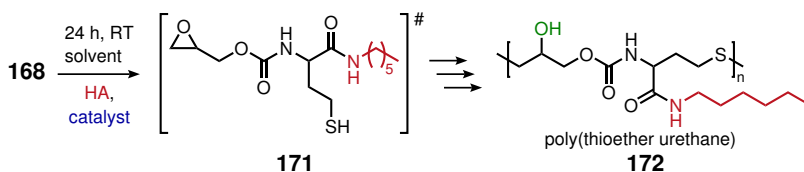


Figure 6.2: ^1H NMR spectra of educt **168** (top) and model compounds **169** (mid) and **170** (bottom).

6.2.3 Synthesis of Poly(thioether urethane)s

Reaction of the bicyclic monomer **168** with one equivalent of amine (in the absence of an acrylate) leads to selective conversion of the thiolactone by ring-opening and formation of an amide and a thiol. The resulting

epoxy thiol **171** is able to react in a polyaddition process as an AB-type monomer under basic conditions. Beside the introduction of a new functionality – the organic residue – by the amine used for ring-opening of the thiolactone, the obtained polymer **172** backbone exhibits a further functionality – a hydroxyl group. The latter increases the hydrophilicity of the polymer backbone and leaves open space for an additional functionalization, i.e. by conversion with an isocyanate. Thus, this epoxy thiolactone, which is a precursor for an active AB-monomer, offers a compelling instrument for the synthesis of poly(TEU)s **172** with various functionalities and properties (Scheme 6.3).



Scheme 6.3: Two-step cascade reaction of **168** delivering poly(thioether urethane)s **172** via an epoxy thiol intermediate **171**.

Kinetic investigations. By performing this reaction with a base as catalyst, a consecutive conversion of functional groups is induced. This means, that if **168** is converted to an epoxy thiol (k_1), this intermediate is subsequently converted to the poly(thioether urethane) (k_2). Since the rate constants k_1 and k_2 determine the overall reaction kinetics of this cascade reaction, it is important for the final molecular weight and dispersity to gather information on the impact of different catalysts. In our kinetic investigations, we used different catalysts: LiOH, DBU and DMAP. LiOH should act as an efficient catalyst for the thiol-epoxy reaction as experienced by Khan et al.^{32–34} DBU and DMAP should first catalyze the aminolysis of the thiolactone and per chance also the thiol-epoxy polyaddition. For the standard reaction conditions, the epoxy thiolactone **168** is converted with hexylamine in THF- d_8 ($c(\mathbf{168}) = 0.25 \text{ M}$) at room temperature using one of the proposed catalysts. Only for LiOH catalysis a mixture of THF- d_8 /D₂O

(9:1) was used for the sake of solubility. The resulting data were fitted to the first order kinetic law to get a qualitative comparison between the catalysts used. The microstructure of the resulting polymer was confirmed by ^1H - and ^{13}C NMR data (Figure A.32 and Figure A.33). Corresponding rate constants and kinetic plots are presented (Table 6.1, Figure 6.3).

Table 6.1: Rate constants of the one-pot polyaddition using different catalysts.

Catalyst	catalyst loading [mol%]	k_1^a	R^2^b	k_2^a	R^2^b	$\text{p}K_a$
none	-	0.320	0.992	0	-	-
DMAP	6	0.272	0.962	2.13E-3	0.898	9.2
LiOH	3	0.670	0.963	0.426	0.978	0.18 ^c
DBU	6	0.214	0.985	0.214	0.985	13.5

^a k_1 and k_2 represent the fitted rate constants of the first order kinetic fit (Section A.3.3). ^b R^2 depicts the coefficient of determination of the non-linear fit. ^c For LiOH, the $\text{p}K_b$ value was given.

If no catalyst is used, only the thiolactone ring-opening proceeds under these reaction conditions ($k_1 = 0.320$). However, after 24 h still no poly(TEU) has formed. As DMAP is a prominent catalyst for substitution reactions,³⁵ we used it with the aim to accelerate the thiolactone ring-opening simultaneously catalyzing the thiol-epoxy reaction. However, the kinetic data show that in the presence of 6 mol% DMAP as catalyst, the rate constant for the thiolactone ring-opening is lower than without a catalyst. The formation of poly(TEU) is slightly faster than without catalyst; still, after 50 h only 14% of the epoxy thiol is converted. This is probably a result of the low $\text{p}K_a$ value of DMAP; for the conversion of thiols to thiolates (estimated $\text{p}K_a = 9$) higher $\text{p}K_a$ values are needed. When LiOH (3 mol%) is used as catalyst, both, the thiolactone ring-opening as well as the polyaddition reaction is catalyzed. Though, k_1 is higher than k_2 (Table 6.1). DBU comes with a $\text{p}K_a$ of 13.5 and should be able to catalyze the thiol-epoxy addition. Besides, amidines are known to be efficient catalysts for the ring-opening polymerization of lactones.³⁶ The related ki-

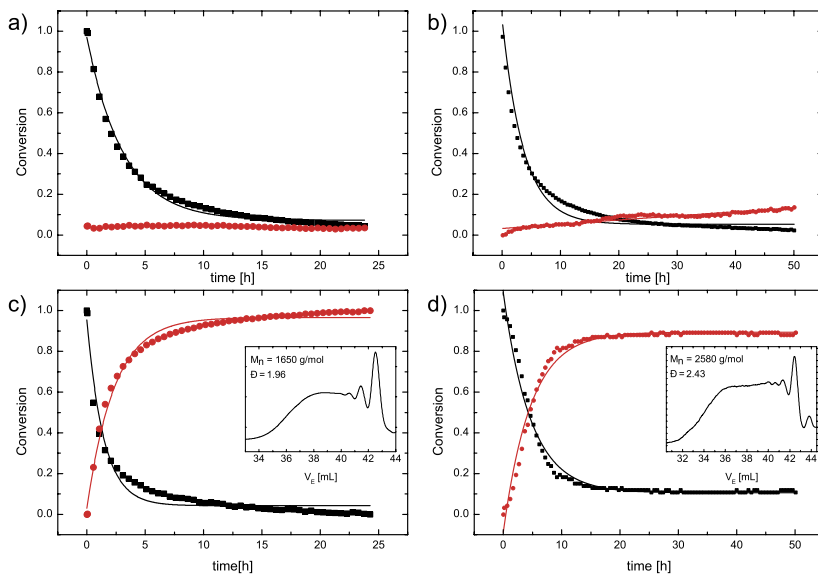


Figure 6.3: Online ^1H NMR kinetic data of the one-pot polyaddition of epoxy thiolactone **168** showing the consumption of the thiolactone ring by hexylamine (■) and the formation of poly(TEU)s by thiol-epoxy addition (●) with the use of a) no catalyst, b) DMAP (6 mol%), c) LiOH (3 mol%) and d) DBU (6 mol%). The overlaying solid lines represent respective fits. Inset graphs show the SEC elution curve of the corresponding polymer products with number average molecular weights and dispersity indices (M_w/M_n or \bar{D}).

netic experiment demonstrates that both the thiolactone consumption and the thiol-epoxy reaction exhibit the same reaction rates. By analyzing the reaction product obtained in DBU and LiOH catalysis by size exclusion chromatography (SEC) both products show beside a polymer, oligomer fractions. DBU gives higher molecular weights than LiOH, though the dispersity value of the LiOH-catalyzed polymerization is closer to two, being $\bar{D} = 1.96$ (Figure 6.3). In a step-wise reaction setting the influence of several catalysts on the thiol-epoxy addition was tested. LiOH and KO^tBu showed the highest activity (Figure A.35). Additionally, various inorganic bases were employed to see the impact on the molecular weight and dispersity of the poly(TEU)s. Yet, NaHCO_3 , CsOH and NaOH behave sim-

ilar to LiOH (Figure A.36). Upon increase of the catalyst loading to one equivalent, for LiOH, no polymer is obtained. Several other bases have been tested in the same manner, but did not show any crucial effect (Figure A.37).

Next, the influence of the catalyst concentration, the monomer concentration and the solvent polarity was studied. For this attempt, only LiOH and DBU were taken into consideration, since they show equally high conversion of functional groups and good dispersity (Figure 6.4).

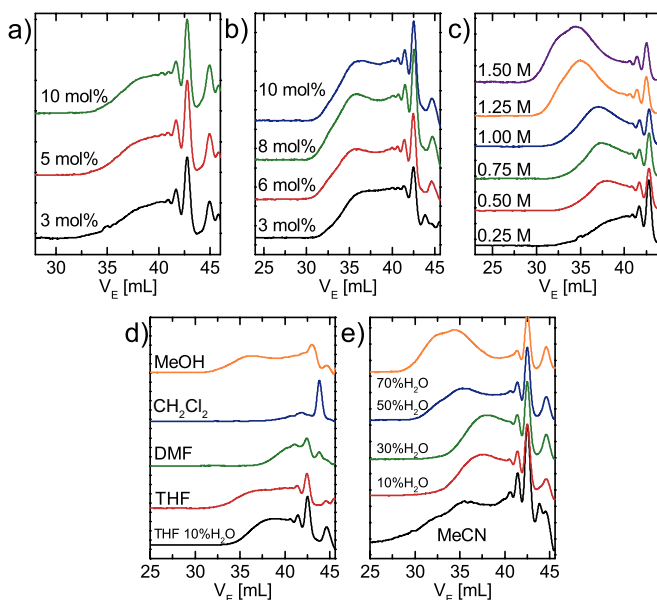


Figure 6.4: SEC elugrams of poly(TEU)s examining the influence of a) LiOH concentration, b) DBU concentration, c) monomer concentration, d) solvent polarity and e) acetonitrile-water mixtures.

Influence of the catalyst concentration. Using 3, 5 or 10 mol% of LiOH showed no difference regarding the SEC profiles (Figure 6.4a). The corresponding number average molecular weights are all in the same range

with dispersity values $\mathcal{D} = 2.0 - 2.1$. Using DBU as catalyst, molecular weights up to $M_n = 2690$ g/mol are obtained. However, the dispersity values are higher indicating a broad distribution (Table 6.2). It is assumed, that this is a result of oligomers formed, which are not able to further participate in polyaddition reactions. This hypothesis is also supported by the corresponding SEC profiles (Figure 6.4b). With increasing catalyst concentration, these show first a flattening at elution volumes below $V_E = 40$ mL. Later on, a maximum is observed at $V_E \sim 35$ mL.

Table 6.2: Reaction of epoxy thiolactone **168** with hexylamine using LiOH or DBU as catalyst in different concentration: SEC data.

Entry No.	catalyst		M_n [g/mol]	\mathcal{D}
		eq		
1	LiOH	0.03	1660	2.1
2	LiOH	0.05	1650	2.1
3	LiOH	0.10	1640	2.0
4	DBU	0.03	2530	2.5
5	DBU	0.06	2690	2.9
6	DBU	0.08	2670	3.0
7	DBU	0.10	2530	2.8

Dispersity values higher than two are an indication of a product mixture formed by different reaction routes. With regard to the expected dispersity values, we focused further investigations on the LiOH-catalyzed system.

Influence of the monomer concentration. In many step-growth processes the formation of oligomers or cycles is a reversible process. Existing cycles are accessible by active polymer chains and can thereby be retransformed into linear chains. In the same manner, linear chains are transformed via backbiting into cyclic oligomers. However, in the present thiol-epoxy polymerization this reversibility is not given, since ether bonds are formed, which under the reaction conditions are stable. Once cycles have formed they are excluded from further propagation. Thus, an inactive species has formed, which has to be removed to get pure polymer

with desired number average molecular weight and dispersity. A first evidence for the formation of cycles is investigated through variation of the monomer concentration. As explained by the Ruggli-Ziegler dilution principle (RZDP), the cyclization is suppressed when higher monomer concentrations are applied.³⁷ In contrast, working with diluted reaction mixtures the intramolecular reaction is favored. Consequently, epoxy thiolactone **168** was reacted with hexylamine using 3 mol% LiOH as catalyst and varying monomer concentrations of $c(\mathbf{168}) = 0.25 - 1.5$ M. Analyzing the SEC profiles (Figure 6.4c), it was concluded that with increasing concentration the intensity ratio of the first oligomeric peak to the main polymer peak decreases from $o/p = 2.52$ to 0.56. Furthermore, with increasing monomer concentration higher number average molecular weights are obtained. With increasing M_n the distribution also gets broader (as present oligomers are not yet removed). This implicates dispersity values up to $\mathcal{D} = 3.5$ (Table 6.3). Upon increase of the monomer concentration up to $c(\mathbf{168}) = 3$ M, no higher molecular weights were reached, only the oligomers were suppressed a little more (not shown). It is assumed, that there the reactivity of the system becomes limiting and concentration effects do not influence the reaction rate anymore.

Table 6.3: SEC data for the LiOH-catalyzed conversion of epoxy thiolactone **168** with hexylamine employing different monomer concentrations $c(\mathbf{168})$.

Entry No.	$c(\mathbf{168})$ [M]	M_n [g/mol]	\mathcal{D}	o/p^a
1	0.25	1660	2.1	2.52
2	0.50	2070	2.1	1.42
3	0.75	2230	2.2	1.28
4	1.00	2630	2.4	0.94
5	1.25	4210	3.0	0.72
6	1.50	4640	3.5	0.56

^a The o/p ratio was simply calculated by dividing the intensities of the first and most intensive oligomer peak by the main polymer peak.

By precipitation of the crude product (Entry 6, Table 6.3) from DMF in MeCN the pure polymer is obtained. The molecular weight increases to $M_n = 8520$ g/mol with a dispersity of $\mathcal{D} = 2.1$ (Figure A.38). Separation of the oligomers from the polymeric material is only feasible for the higher MW polymers (entry 5 and 6), since here the o/p ratio is less than one and the polymeric peak is sufficiently baseline-separated from the oligomers.

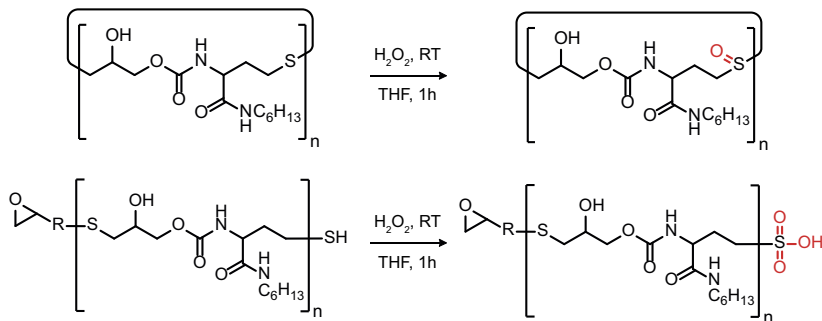
Influence of the solvent. Finally, the influence of the used solvent polarity was explored. The following organic solvents or solvent mixtures were used: THF, THF/10% water, DMF, CH_2Cl_2 , MeOH, MeCN and MeCN-water mixtures of 10%, 30%, 50% and 70% water. Therefore epoxy thiolactone **168** was reacted with one equivalent hexylamine at room temperature using 3 mol% LiOH as catalyst in the appropriate solvent ($c(\mathbf{168}) = 0.25$ M). SEC profiles (Figure 6.4d-e) show, that for pure THF as solvent, M_n is higher than using a THF-water mixture (9:1) (Table 6.4). In DMF, molecular weights of about $M_n = 1120$ g/mol are obtained. Using CH_2Cl_2 , no polymer is formed. MeOH and MeCN show broad dispersities, $\mathcal{D} = 3.0$ and 8.2 , respectively (Figure 6.4d-e). When it comes to MeCN-water mixtures, a clear trend is observed. A higher water content implies an increase of molecular weight ($2300 \sim 2400 < 2640 < 4320$) (Table 6.4, Figure 6.4e). To obtain high molecular weights it is advisable to use a high water fraction in the polyaddition reaction. Again pure polymer is obtained after precipitation from DMF in MeCN (Entry 10, Table 6.4). Looking at entry 10, a poly(TEU) of $M_n = 11100$ g/mol and a dispersity value of $\mathcal{D} = 1.9$ is obtained (Figure A.38).

Oligomer assessment. As it is shown in the previous SEC profiles of the poly(TEU) syntheses, the formation of oligomers seems inevitable. Although long reaction times are applied there is no indication for a disappearance of the oligomers. This raises the question of the nature of the oligomers: are they linear with α -thiol and ω -epoxy groups still present, or are cyclic oligomers formed. The formation of cycles would mean,

Table 6.4: SEC data for the LiOH-catalyzed conversion of epoxy thiolactone **168** with hexylamine employing different organic solvents and solvent mixtures ($c(\mathbf{168}) = 0.25 \text{ M}$).

Entry No.	Solvent	M_n [g/mol]	\bar{D}
1	THF	2250	2.4
2	THF / 10% H ₂ O	1660	2.0
3	DMF	1120	1.6
4	CH ₂ Cl ₂	-	-
5	MeOH	2340	3.0
6	MeCN	2630	8.2
7	MeCN / 10% H ₂ O	2400	2.5
8	MeCN / 30% H ₂ O	2300	2.2
9	MeCN / 50% H ₂ O	2640	3.4
10	MeCN / 70% H ₂ O	4320	4.5

that dead chains are produced, which lastly comes at cost of the degree of polymerization of the linear polymer chains and thus the molecular weight of the polymer. The assessment of the microstructure of the formed oligomers was verified via MALDI-TOF analysis after oxidation of the product (this was necessary since in this case linear and cyclic oligomers have the same molecular formula). For this, the different reactivity of thiols and thioether with H₂O₂ was used. Upon reaction with small amounts of H₂O₂ at room temperature, thiols are oxidized to sulfonic acids (mass increment = 48), whereas thioethers to sulfoxides or sulfones (mass increment = 16/32) (Scheme 6.4). MALDI-TOF results depict the reaction product obtained by conversion of epoxy thiolactone **168** with hexylamine (starting material) and its oxidation product with hydrogen peroxide (Figure 6.5). The starting material shows oligomers with masses for 2 to 7 repeating units. In between the oligomer peaks a mass increment of 318.1 g/mol is observed which fits to the exact mass of one repeating unit. Upon reaction with H₂O₂, a different oligomer pattern appears. Here, the mass increment between oligomers increases to 334.1 g/mol. This fits exactly to the mass of a repeating unit which was oxidized from the thioether to



Scheme 6.4: Reaction of linear or cyclic poly(TEU)s with H₂O₂.

the sulfoxide. Cyclic oligomers of 2 to 6 repeating units are perceived. Additionally to the main oligomer peaks, small satellite peaks appear with a mass increment of ± 16 g/mol. If we consider a cyclic dimer, this points to the existence of either a thioether/sulfoxide dimer (main peak -16) or a sulfoxide/sulfone dimer (main peak +16). In summary, the obtained masses and increments prove the suggested formation of cyclic oligomers in the reaction. Detailed data is found in the annex (Section A.3.5).

This result shows once more, that with regard to the Ruggli-Ziegler dilution principle, cyclization is suppressed to obtain the highest polymer fraction possible. Hence, the optimum conditions for polyadditions using epoxy thiolactone **168** are (i) using the highest applicable monomer concentration, (ii) the highest possible water fraction in the solvent mixture or (iii) both approaches combined if allowed by the solubility of the different components used in this polyaddition.

6.2.4 Hydrogel Synthesis

In the first part of this work the epoxy thiolactone **168** was used in multi-component reactions, whereas in the second part polymerization of **168** –

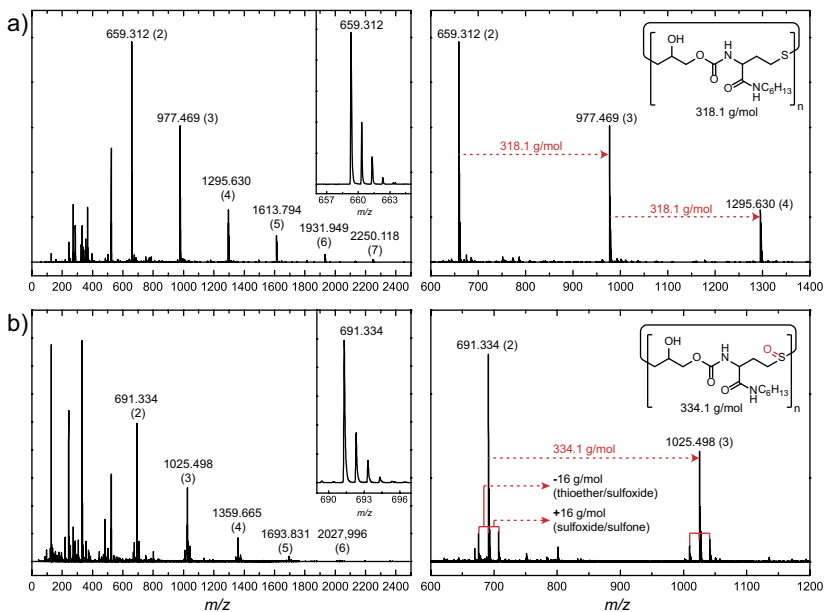
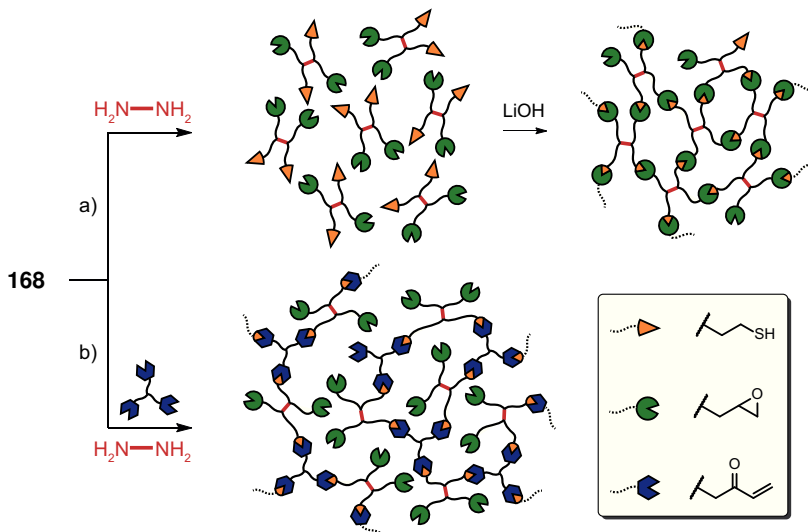


Figure 6.5: MALDI-TOF spectra of the cyclic oligomer assessment test. a) shows the full spectrum (left); a single peak (inset) and a magnification with selected mass increments of the poly(TEU). b) shows the MALDI-TOF data of the resulting oxidized product obtained from the reaction with H_2O_2 . Again a full spectrum (left), a single peak (inset) and a magnification with selected mass increments of the oxidized product (right) is presented.

induced by equimolar amounts of an amine – is presented leading to linear and cyclic thioether urethane oligomers and polymers with defined side chain functionalities (R-NH-CO). If both strategies are combined, it should be possible to build up networks or gels. This is achieved by two different strategies: (i) **168** is converted with 0.5 equivalents of a diamine to give a bis(thiol) bis(epoxide) which now functions as an A_2B_2 -type monomer. In the presence of lithium hydroxide this A_2B_2 -type monomer undergoes thiol-epoxy polymerization in one-pot, this time, forming a gel instead of linear poly(TEU)s (Scheme 6.5a.). (ii) **168** is again converted with half amount of diamine. Instead of LiOH, a triacrylate is present. In this mul-

ticomponent reaction, cross-linked gels are prepared, which host reactive epoxide groups inside (Scheme 6.5b). By means of the thiol-epoxy poly-



Scheme 6.5: Synthesis of hydrogels via a) the thiol-epoxy polymerization or b) multicomponent reaction using **168**.

merization strategy, one equivalent of **168** was stirred with 0.5 equivalents of a PEG(7) diamine under basic conditions (3 mol% LiOH) over night at room temperature in MeCN with a maximum water content. Upon gelation, a yellowish bulk hydrogel was formed (Figure 6.6a). For the second strategy – gelation through multicomponent reaction – **168** was converted in a three component reaction with 0.5 equivalents of PEG(X) diamine (X = 2 or 7) and 0.33 equivalents of trimethylolpropane triacrylate (TMPT). Here, gelation occurred much faster (attributed to the high reaction rate of the thiol-ene Michael addition). Stirring 5 min at room temperature in a water-MeCN mixture delivered a yellowish bulk hydrogel (Figure 6.6b-c). Subsequent to the gel formation, samples were dried and Raman spectra were recorded to detect eventually remaining epoxy groups. In contrast to our expectations, the sample gelled by thiol-epoxy polymerization still

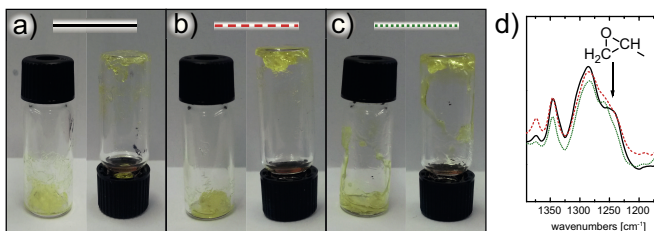


Figure 6.6: Yellow bulk hydrogel obtained by thiol-epoxy polymerization (a) and multicomponent reaction with TMPT and a PEG(X) diamine, b) X = 2, c) X = 7. d) shows a magnification of the corresponding Raman spectra (a,b,c). The ring stretch band of mono-substituted epoxy group appears as a shoulder.

contains epoxy groups (Figure 6.6a+d). This is probably due to the gel point which arises at an early stage of the reaction and thus immobilizes residual reactive groups in the gel network. For both essays obtained by multicomponent reaction, the shoulder at $\nu = 1243 \text{ cm}^{-1}$ indicates the presence of epoxy groups (Figure 6.6b-d). Full Raman spectra are found in the annex (Figure A.34).

6.3 Conclusion

In this part, a new epoxy thiolactone was synthesized. This coupling molecule was demonstrated to act in several concepts as a versatile toolbox for polymeric materials. In a model reaction, up to four different building blocks are combined in a multicomponent reaction to a single molecule. Selectivity of the different reaction sites was given and delivered the desired product. In a second approach, the epoxy thiolactone is converted with an amine and catalytic amounts of base to form functional poly(thioether urethane)s. Although DBU showed good catalytic properties, LiOH was even more efficient in catalyzing both, the aminolysis of the thiolactone ring and the thiol-epoxy polyaddition. Different param-

ters, such as catalyst loading, monomer concentration and solvent polarity were investigated. To obtain high molecular weight products exhibiting lowest dispersity, it is most advisable to use high concentrated solutions or MeCN-water mixtures with the highest possible water fraction. This way, it is possible to suppress cyclisation, which is an irreversible and thus terminating process for the thiol-epoxy polymerization. Residual cyclic oligomers are removed by precipitation. In the last section, two strategies for the generation of functional gels were elaborated. Using a diamine, gelation either occurs i) through thiol-epoxy polymerization under basic conditions or ii) in a multicomponent reaction involving a triacrylate. All these processes are feasible in one-pot and pose therefore an interesting platform for a variety of polymer architectures hosting functionalities.

6.4 Experimental Data

6.4.1 Materials

Triethylamine ($\geq 99\%$, Sigma Aldrich), *para*-nitrophenyl chloroformate ($>98\%$, TCI Chemicals), glycidol (techn, Acros Organics), homocysteine thiolactone hydrochloride (HCTL-HCl, 99%, ABCR), 4-dimethylaminopyridine ($\geq 99\%$, Fluka), *n*-hexylamine ($>99\%$, TCI Chemicals), methyl acrylate ($>99\%$, Sigma Aldrich), dihexylamine (97%, Sigma Aldrich), LiOH·H₂O (99%, Sigma Aldrich), 1,8-Diazabicyclo[5.4.0]undec-7-ene ($>99\%$, Fluka), α,ω -bis-amino octa(ethylene glycol) (PEG(7) diamine, Iris Biotech), 2,2'-(ethylenedioxy)bis(ethylamine) (PEG(2) diamine, $>97\%$, Alfa Aesar), trimethylolpropane triacrylate (Alfa Aesar) were used without further purification. Unless otherwise indicated, all solvents were purchased from commercial sources and were used without further purification.

6.4.2 Measurements

^1H and ^{13}C NMR spectra were recorded on a Bruker DPX-400 FT NMR spectrometer (400 MHz and 100 MHz, respectively) and are reported as follows: chemical shift δ (ppm) (multiplicity, coupling constant J (Hz), number of protons, assignment). CDCl_3 ($\delta_H = 7.26$ ppm, $\delta_C = 77.0$ ppm), THF-d_8 ($\delta_H = 1.73$ ppm, $\delta_C = 25.4$ ppm) and dimethylsulfoxide (DMSO, $\delta_H = 2.50$ ppm, $\delta_C = 39.5$ ppm) were used as an internal standard. Chemical shifts are reported in ppm to the nearest 0.01 ppm for ^1H and the nearest 0.1 ppm for ^{13}C .

Molecular weights (M_n and M_w) and dispersity values (M_w/M_n or \mathcal{D}) were determined by size exclusion chromatography (SEC). SEC analyses were carried out with dimethylformamide (DMF) as eluent. SEC with DMF (HPLC grade, VWR) as eluent was performed using an Agilent 1100 system equipped with a dual RI-/Visco detector (ETA-2020, WGE). The eluent contained $1 \text{ g}\cdot\text{L}^{-1}$ LiBr ($\geq 99\%$, Sigma Aldrich). The sample solvent contained traces of distilled water as internal standard. One pre-column (8x50 mm) and four PSS GRAM gel columns (8x300 mm) were applied at a flow rate of $1.0 \text{ mL}\cdot\text{min}^{-1}$ at 40°C . The diameter of the gel particles measured $10 \mu\text{m}$, the nominal pore widths were 30, 10^2 , 10^3 and 3000 \AA . Calibration was achieved using narrowly distributed poly(methyl methacrylate) standards (PSS Std. Mainz). Results were evaluated using the PSS WinGPC UniChrom software (Version 8.1).

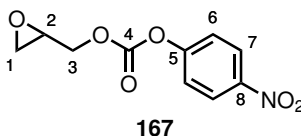
Raman spectroscopy was carried out on a Bruker FT-Raman-Spectrometer RFS 100/S with a Nd:YAG laser. The power of the laser was 200 mW at 1064 nm with a spectral resolution of 4 cm^{-1} . For each spectrum 500 scans were recorded. Raman intensity maxima are reported in wavenumbers (cm^{-1}). Infrared spectra were carried out on a ThermoNicolet FT-IR Nexus spectrometer and are recorded between KBr disks or using an ATR unit (ThermoNicolet, Smart SplitPEA). Transmission maxima are reported in wavenumbers (cm^{-1}) and only selected intensities are reported.

Differential scanning calorimetry (DSC) analysis was performed on a PerkinElmer DSC 8000 (PerkinElmer LAS, Rodgau, Germany) under nitrogen atmosphere using a scan rate of $10 \text{ K}\cdot\text{min}^{-1}$. For M_p the local maximum was selected.

ESI mass spectra were recorded on a Finnigan SSQ 7000 spectrometer and HRMS spectra on a Thermo Scientific LTQ Orbitrap XL spectrometer. MALDI-TOF and NALDI-TOF mass spectrometry were performed on a Bruker ultrafleXtreme equipped with a 337 nm smartbeam laser in the reflective mode. For NALDI-TOF, THF solutions of sodium trifluoroacetate ($2 \mu\text{L}$ of $10 \text{ mg}\cdot\text{mL}^{-1}$), and analyte ($20 \mu\text{L}$ of $10 \text{ mg}\cdot\text{mL}^{-1}$) were mixed and $2 \mu\text{L}$ thereof were applied on the sample plate. For MALDI-TOF, THF solutions of sodium trifluoroacetate ($0.5 \mu\text{L}$ of $10 \text{ mg}\cdot\text{mL}^{-1}$), analyte ($5 \mu\text{L}$ of $10 \text{ mg}\cdot\text{mL}^{-1}$) and DCTB matrix ($20 \mu\text{L}$ of $20 \text{ mg}\cdot\text{mL}^{-1}$) were mixed and $2 \mu\text{L}$ thereof were applied on the sample plate. CsI_3 was used as standard for internal calibration. Laser shots (6000) with 24% up to 60% laser power were collected. The laser repetition rate was 1000 Hz.

6.4.3 Syntheses

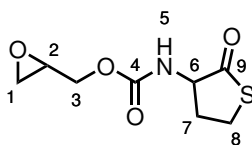
Synthesis of Glycidyl *p*-Nitrophenyl Carbonate **167**



Triethylamine (18.9 mL, 136.7 mmol) was added slowly (18.9 mL/h) to a stirred solution of *p*-nitrophenyl chloroformate **166** (25.0 g, 124.2 mmol) and glycidol **165** (8.67 mL, 130.4 mmol) in CH_2Cl_2 (124 mL, 1 M) at 0°C . The reaction mixture was allowed to warm to room temperature and

stirred for 2 h. Then, the reaction mixture was filtered. Next, the mixture was washed with $\text{HCl}_{(aq)}$ (100 mL, 1 M), $\text{NaOH}_{(aq)}$ (2 x 100 mL, 1 M) and $\text{HCl}_{(aq)}$ (100 mL, 1 M). The organic layer was dried (MgSO_4) and evaporated under reduced pressure to give the crude glycidyl *p*-nitrophenyl carbonate **167** (25.8 g, 87%) as a white solid. Spectroscopic data was consistent with those reported in literature.²⁸ Mp. 57.5 °C (determined by DSC). ^1H NMR (400 MHz, Chloroform-*d*) δ 8.28 (d, J = 9.1 Hz, 1H, H7), 7.39 (d, J = 9.1 Hz, 1H, H6), 4.60 (dd, J = 12.1, 2.9 Hz, 1H, H3), 4.16 (dd, J = 12.1, 6.3 Hz, 1H, H3), 3.33 (tt, J = 6.5, 2.8 Hz, 1H, H2), 2.92 (t, J = 4.4 Hz, 1H, H1), 2.74 (dd, J = 4.7, 2.6 Hz, 1H, H1). ^{13}C NMR (101 MHz, CDCl_3) δ 155.5 (C5), 152.5 (C4), 145.6 (C8), 125.5 (C7), 121.9 (C6), 69.6 (C3), 48.9 (C2), 44.7 (C1). IR (KBr) 3490, 3079, 1754 ($\text{O}_2\text{C}=\text{O}$), 1618, 1595, 1524 (NO_2) 1494, 1461, 1347, 1275, 1262 (C-O Epoxide), 1227 (Ph-O), 1052, 911, 867 (Epoxide), 723. HRMS (ESI) m/z for $\text{C}_{10}\text{H}_9\text{NO}_6$ ($\text{M} + \text{H}$)⁺ 240.04976.

Synthesis of Epoxy Thiolactone 168



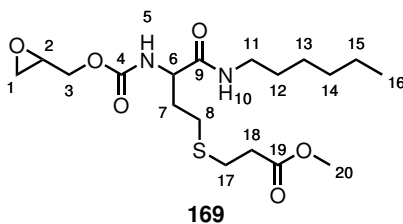
168

Triethylamine (2.79 mL, 20.1 mmol) was added slowly (2.79 mL/h) to a stirred solution of **167** (1.93 g, 8.06 mmol), HCTL-HCl (1.24 g, 8.06 mmol) and dimethylaminopyridine (98.4 mg, 8.06E-1 mmol) in DMF (40 mL, 0.2 M) at 0 °C. The reaction mixture was allowed to warm to room temperature and stirred for 4 h. Then, the reaction mixture was filtered and evaporated under reduced pressure. Next, CH_2Cl_2 (20 mL) was added and the mixture was washed with $\text{HCl}_{(aq)}$ (2 x 20 mL, 1 M). The organic layer was

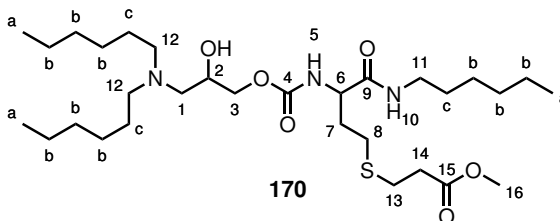
dried (MgSO_4) and evaporated under reduced pressure to give the crude epoxy thiolactone. Purification by flash column chromatography on alumina gel using $\text{CH}_2\text{Cl}_2/1\%$ MeOH as eluent gave epoxy thiolactone **168** (1.15 g, 65%) as a white crystalline solid. Mp. 75.8 °C (determined by DSC). R_F (9.9:0.1 CH_2Cl_2 -MeOH) 0.29. ^1H NMR (400 MHz, DMSO) δ 7.72 (dd, $J = 8.5, 2.8$ Hz, 1H, H5), 4.44 - 4.27 (m, 2H, H3 and H6), 3.76 (ddd, $J = 12.0, 6.6, 4.3$ Hz, 1H, H3), 3.40 (dd, $J = 11.6, 5.3$ Hz, H8), 3.30 - 3.23 (m, 1H, H8), 3.17 (tt, $J = 6.5, 2.8$ Hz, 1H, H2), 2.78 (t, $J = 4.6$ Hz, 1H, H1), 2.65 - 2.59 (m, 1H, H1), 2.43 (dt, $J = 12.0, 5.9$ Hz, 1H, H7), 2.09 (qdd, $J = 12.1, 7.0, 4.7$ Hz, 1H, H7). ^{13}C NMR (101 MHz, DMSO) δ 205.6, 205.7 (C9), 155.7, 155.8 (C4), 65.3, 65.2 (C3), 59.9 (C6), 49.3 (C2), 43.8 (C1), 29.8 (C7), 26.4 (C8). IR (KBr) 3349 (NH), 2922, 1717 (CONH), 1698 (COS), 1543 (NH bend), 1244 (CO epoxide), 1053, 907. HRMS (ESI) m/z for $\text{C}_8\text{H}_{11}\text{NO}_4\text{S}$ ($\text{M} + \text{H}$) $^+$ 218.04758, ($\text{M} + \text{Na}$) $^+$ 240.02962.

For large-scale synthesis, the following procedure was used: Triethylamine (15.1 mL, 109.2 mmol) was added slowly (15.1 mL/h) to a stirred solution of **167** (10.5 g, 43.7 mmol), HCTL-HCl (6.71 g, 43.7 mmol) and dimethylaminopyridine (534 mg, 4.37 mmol) in DMF (109 mL, 0.4 M) at 0 °C. The reaction mixture was allowed to warm to room temperature and stirred for 4 h. Then, the reaction mixture was filtered and evaporated under reduced pressure. Next, CH_2Cl_2 (100 mL) was added and the mixture was washed with $\text{HCl}_{(aq)}$ (100 mL, 0.1 M), $\text{K}_2\text{CO}_3_{(aq)}$ (6 x 100 mL, 0.1 M) and again $\text{HCl}_{(aq)}$ (100 mL, 0.1 M). The organic layer was dried (MgSO_4) and evaporated under reduced pressure to give the crude epoxy thiolactone **168** (5.7 g, 60%) as a white solid.

Synthesis of Epoxy Thioether **169** - Three Component Reaction



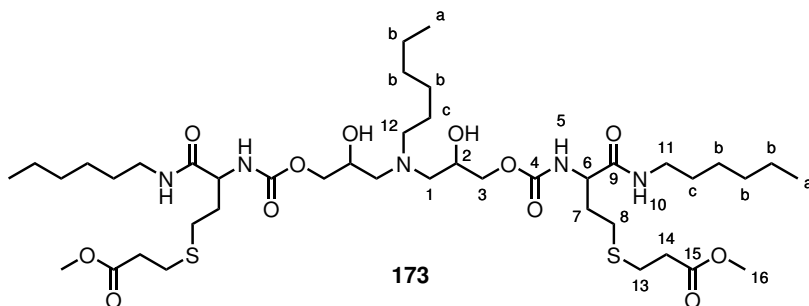
Hexylamine (24.6 μL , 0.178 mmol) and methyl acrylate (16.1 μL , 0.178 mmol) were added to a stirred solution of epoxy thiolactone **168** (38.6 mg, 0.178 mmol) in THF (0.888 mL, 0.2 M) at room temperature. The reaction mixture was stirred at room temperature for 24 h. Then, the solvent was evaporated under reduced pressure to give the crude epoxy thioether **169** (quant.) as a slightly yellow waxy solid. ^1H NMR (400 MHz, DMSO) δ 7.91 (t, $J = 5.0$ Hz, 1H, H10), 7.53 (d, $J = 8.1$ Hz, 1H, H5), 4.36 (ddd, $J = 12.2$, 4.9, 2.7 Hz, 1H, H3), 4.03 (dq, $J = 15.4$, 7.8, 7.4 Hz, 1H, H6), 3.79 (dd, $J = 12.2$, 6.6 Hz, 1H, H3), 3.66 (s, 3H, H20), 3.26 - 3.18 (m, 1H, H2), 3.18 - 3.00 (m, 2H, H11), 2.82 (q, $J = 4.2$ Hz, 1H, H1), 2.80 - 2.71 (m, 2H, H18), 2.71 - 2.62 (m, 3H, H1 and H17), 2.60 - 2.35 (m, 2H, H8), 1.96 - 1.74 (m, 2H, H7), 1.50 - 1.37 (m, 2H, H12), 1.31 (d, $J = 14.8$ Hz, 6H, H13-15), 0.92 (t, $J = 6.7$ Hz, 3H, H16). ^{13}C NMR (101 MHz, DMSO) δ 171.9 (C19), 171.0 (C9), 155.7 (C4), 54.0 (C6), 51.4 (C20), 49.4 (C2), 43.7 (C1), 38.5 (C11), 34.1 (C17), 32.2 (C7), 31.0 (C13), 29.0 (C12), 27.5 (C8), 26.0 (C14 and C18), 22.1 (C15), 13.9 (C16). IR (KBr) 3293 (NH), 2953, 2929, 2858, 1731 (COOMe), 1689 (OCONH), 1643 (CONH), 1538 (NH), 1437, 1351, 1280, 1241 (COC Epoxide, OCONH 2), 1195, 1172, 1051, 687. HRMS (NALDI) m/z for $\text{C}_{18}\text{H}_{32}\text{N}_2\text{O}_6\text{S}$ ($\text{M} + \text{Na}$) $^+$ 427.242.

Synthesis of Trialkylamino Thioether **170**

Hexylamine (16.6 μL , 0.127 mmol) and methyl acrylate (11.5 μL , 0.127 mmol) were added to a stirred solution of epoxy thiolactone **168** (27.5 mg, 0.127 mmol) in THF- d_8 (0.633 mL, 0.2 M) at room temperature. The reaction mixture was stirred at room temperature for 24 h. Full conversion to the crude epoxy thioether intermediate (**169**) was verified by ^1H NMR spectroscopy. Next, dihexylamine (29.5 μL , 0.127 mmol) was added and the reaction mixture was stirred at 60 $^\circ\text{C}$ for 6 days. Then, the solvent was evaporated under reduced pressure and the crude product was separated between CH_2Cl_2 (1.50 mL) and $\text{NH}_4\text{HCO}_3(aq)$ (1.50 mL, 0.05 M). The organic layer was evaporated under reduced pressure to give the trialkylamino thioether **170** (quant.) as a slightly yellow viscous oil. ^1H NMR (400 MHz, DMSO) δ 7.86 - 7.76 (m, 1H, H10), 7.24 (t, J = 8.3 Hz, 1H, H5), 4.06 - 3.89 (m, 2H, H6 and H3'), 3.87 - 3.73 (m, 1H, H3), 3.72 - 3.63 (m, 1H, H2), 3.60 (s, 3H, H16), 3.13 - 2.91 (m, 2H, H11), 2.75 - 2.63 (m, 2H, H14), 2.63 - 2.55 (m, 2H, H13), 2.55 - 2.22 (m, 8H, H1/H8 and H12), 1.90 - 1.66 (m, 2H, H7), 1.50 - 1.14 (m, 24H, $\text{H}^{b/c}$), 0.96 - 0.73 (m, 9H, H^a). ^{13}C NMR (101 MHz, DMSO) δ 171.9 (C15), 171.2 (C9), 156.2 (C4), 67.0 (C2 and C3), 57.4, 57.2 (C1), 54.3 (C12), 53.9 (C6), 51.4 (C16), 38.5 (C11), 34.1 (C13), 32.3 (C7), 31.3, 31.2, 31.0 (C^b), 29.0, 28.7 (C^c), 27.5 (C8), 26.7 (C^b), 26.5, 26.4 (C^c), 26.0 (C14), 22.2, 22.1 (C^b), 13.9 (C^a). IR (KBr) 3313 (NH), 2955, 2929, 2857, 1739 (OCONH/COOMe), 1658 (CONH), 1537 (NH), 1459, 1438, 1357, 1246, 1170, 1052. HRMS (MALDI) m/z for $\text{C}_{30}\text{H}_{59}\text{N}_3\text{O}_6\text{S}$ ($\text{M} + \text{Na}$) $^+$ 612.344.

For the one-pot four component reaction, the following procedure was used: Hexylamine (15.5 μL , 0.118 mmol), methyl acrylate (10.7 μL , 0.118 mmol) and dihexylamine (27.6 μL , 0.118 mmol) were added to a stirred solution of epoxy thiolactone **168** (25.7 mg, 0.118 mmol) in THF (0.592 mL, 0.2 M) at room temperature. The reaction mixture was stirred at 60 $^{\circ}\text{C}$ for 260 h. Then, the solvent was evaporated under reduced pressure and the crude product was separated between CH_2Cl_2 (1.50 mL) and $\text{NH}_4\text{HCO}_3(aq)$ (1.50 mL, 0.05 M). The organic layer was evaporated under reduced pressure to give the trialkylamino thioether **170** (quant.) as a slightly yellow viscous oil.

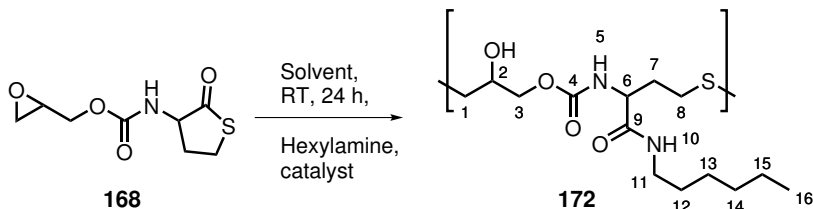
Synthesis of Trialkylamino Bis(thioether) **173**



Hexylamine (25.0 μL , 0.190 mmol) and methyl acrylate (11.5 μL , 0.127 mmol) were added to a stirred solution of epoxy thiolactone **168** (27.5 mg, 0.127 mmol) in THF- d_8 (0.633 mL, 0.2 M) at room temperature. The reaction mixture was stirred at 60 $^{\circ}\text{C}$ for 260 h. Then, the solvent was evaporated under reduced pressure and the crude product was separated between CH_2Cl_2 (1.50 mL) and $\text{NH}_4\text{HCO}_3(aq)$ (1.50 mL, 0.05 M). The organic layer was evaporated under reduced pressure to give the crude trialkylamino bis(thioether) **173** (quant.) as a slightly yellow viscous oil. ^1H NMR (400 MHz, DMSO) δ 7.82 (t, 2H, H10), 7.31 - 7.19 (m, 2H, H5),

4.69 (s, 2H, OH), 4.04 - 3.90 (m, 4H, H6 and H3'), 3.90 - 3.77 (m, 2H, H3), 3.74 - 3.64 (m, 2H, H2), 3.60 (s, 6H, H16), 3.13 - 2.95 (m, 4H, H11), 2.73 - 2.65 (m, 4H, H14), 2.63 - 2.55 (m, 4H, H13), 2.54 - 2.28 (m, 10H, H1 and H8 and H12), 1.88 - 1.69 (m, 4H, H7), 1.44 - 1.32 (m, 6H, H^c), 1.32 - 1.17 (m, 18H, H^b), 0.86 (s, 9H, H^a). ¹³C NMR (101 MHz, DMSO) δ 171.9 (C15), 171.2 (C9), 156.1 (C4), 66.9 (C3 and C2), 57.9 (C1), 53.9 (C12 and C6), 51.4 (C16), 38.5 (C11), 34.1 (C13), 32.3 (C7), 31.3 (C^b), 31.0 (C^b), 29.0 (C^c), 27.5 (C8), 26.5, 26.4 (C^c), 26.0 (C14 and C^b), 22.2, 22.1 (C^b), 14.0, 13.9 (C^a). IR (KBr) 3310 (NH), 2954, 2929, 2857, 1737 (OCONH/COOMe), 1657 (CONH), 1537 (NH), 1438, 1357, 1246, 1149, 1051. HRMS (MALDI) m/z for C₄₂H₇₉N₅O₁₂S₂ (M + Na)⁺ 932.471.

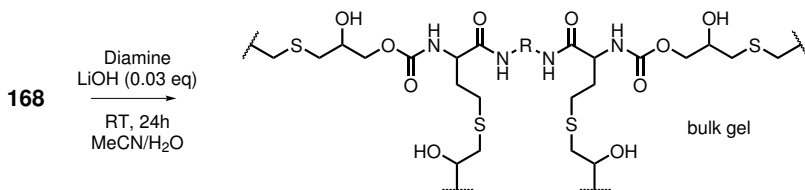
Polymer Synthesis - Typical Procedure



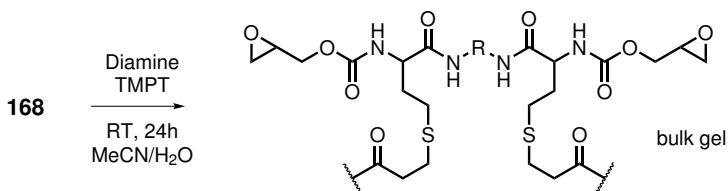
LiOH (6.20 μ L, 2.60E-3 mmol, 10 mg/mL solution) and water (28.4 μ L) were added to a stirred solution of epoxy thiolactone **168** (18.8 mg, 8.65E-2 mmol) in THF (311 μ L, $c(\mathbf{168})_{total} = 0.25$ M and THF/water 9:1) at room temperature. Next, hexylamine (11.4 μ L, 8.65E-2 mmol) was added and the reaction mixture was stirred at room temperature for 24 h. Then, the solvent was evaporated under reduced pressure to give the crude poly(thioether urethane) (quant.) as a slightly yellow solid. $M_n = 1850$ g/mol, $D = 2.1$. ¹H NMR (400 MHz, DMSO) δ 7.82 (t, $J = 5.5$ Hz, 1H, H10), 7.27 (d, $J = 8.1$ Hz, 1H, H5), 5.12 - 5.01 (m, 1H, OH), 4.05 - 3.80 (m, 3H, H3 and H6), 3.80 - 3.63 (m, 1H, H2), 3.13 - 2.93 (m, 2H, H11), 2.64 - 2.39

(m, 4H, H1 and H8), 1.90 - 1.68 (m, 2H, H7), 1.44 - 1.31 (m, 2H, H12), 1.31 - 1.13 (m, 6H, H13-15), 0.85 (t, $J = 6.6$ Hz, 3H, H16). ^{13}C NMR (101 MHz, DMSO) δ 171.2 (C9), 156.0 (C4), 68.5 (C2), 66.9 (C3), 54.0 (C6), 38.5 (C11), 35.0 (C1), 32.4 (C7), 31.0 (C13), 29.0 (C12), 28.6 (C8), 26.0 (C14), 22.1 (C15), 13.9 (C16). For every catalyst a 10 mg/mL stock solution was prepared, LiOH in water or D_2O , TBD/DMAP in THF or THF-d_8 . Unless otherwise noted, the temperature was always maintained at 25°C , one eq of hexylamine was used and $t = 24$ h. All polymerizations of **168** with hexylamine were conducted in an analogue manner (Table 6.5).

Gelation via Thiol-Epoxy Polymerization (G1)



LiOH ($6.59 \mu\text{L}$, $2.80\text{E-}3$ mmol, 10 mg/mL solution in H_2O) and water ($12.5 \mu\text{L}$) were added to a stirred solution of epoxy thiolactone **168** (19.9 mg, $9.17\text{E-}2$ mmol) and PEG(7) diamine (16.9 mg, $4.59\text{E-}2$ mmol) in MeCN ($26.6 \mu\text{L}$, $c(\mathbf{168})_{\text{total}} = 2$ M or 50 wt%) at room temperature. The reaction mixture was stirred at room temperature for 24 h. After 24 h a slightly yellow bulk hydrogel was formed.

Gelation via Thiol-Ene Michael Addition - Typical Procedure

PEG(2) diamine (7.77 μL , 5.29E-2 mmol) and trimethylolpropane triacrylate (9.51 μL , 3.53E-2 mmol) were added to a stirred solution of epoxy thiolactone **168** (23.0 mg, 0.106 mmol) in an MeCN/water mixture (30.5/22.0 μL , $c(\mathbf{168})_{\text{total}} = 2 \text{ M}$ or 50 wt%) at room temperature. The reaction mixture was stirred at room temperature for 5 min. After 5 min a slightly yellow bulk hydrogel was formed. Hydrogel preparations via multicomponent reaction of **168** were conducted in an analogue manner (Table 6.6).

Table 6.5: One-pot polymerization of epoxy thiolactone **168** with hexylamine.

Exp.	168		M	V_{total} μL	catalyst		solvent	μL	hexylamine μL
	mg, (mmol)	mg, (mmol)			eq	μL , (mmol)			
1	36.2, (0.167)	-	0.25	667	-	-	THF-d ₈ ^a	667	21.9
2	36.9, (0.170)	DMAP	0.06	679	125, (1.02E-3)	-	THF-d ₈ ^b	554	22.3
3	35.3, (0.163)	LiOH ^c	0.03	650	11.7, (4.88E-3)	-	THF-d ₈ /D ₂ O (9:1) ^a	585/53.3	21.4
4	36.7, (0.169)	DBU ^d	0.06	676	1.51, (1.01E-3)	-	THF-d ₈ ^b	676	22.2
5	91.5, (0.421)	LiOH	0.03	1.685	30.3, (1.26E-2)	-	THF	1.685	55.4
6	92.2, (0.424)	TBD	0.03	1.698	177, (1.27E-2)	-	THF	1.698	55.8
7	90.5, (0.417)	NaOEt	0.03	1.666	85.0, (1.25E-2)	-	THF	1.666	54.7
8	92.6, (0.426)	DBU ^d	0.03	1.705	1.91 (1.28E-2)	-	THF	1.705	56.0
9	96.0, (0.442)	KO ^t Bu	0.03	1.768	12.1, (1.33E-2)	-	THF	1.768	58.1
10	18.8, (8.65E-2)	LiOH	0.03	346	6.22, (2.60E-3)	-	THF/H ₂ O (9:1)	311/28.4	11.4
11	19.5, (8.98E-2)	NaOH	0.03	359	10.8, (2.69E-3)	-	THF/H ₂ O (9:1)	323/25.1	11.8
12	21.7, (9.99E-2)	CSOH ^e	0.03	400	22.4, (3.00E-3)	-	THF/H ₂ O (9:1)	360/17.6	13.1
13	19.5, (8.98E-2)	NaHCO ₃	0.03	359	22.6, (2.69E-3)	-	THF/H ₂ O (9:1)	323/13.3	11.8
14	18.8, (8.65E-2)	LiOH	1.00	346	2.1 mg, ^f (8.65E-2)	-	THF/H ₂ O (9:1)	311/34.6	11.4
15	20.2, (9.30E-2)	CSOH	1.00	372	13.9 mg, ^f (8.65E-2)	-	THF/H ₂ O (9:1)	335/37.2	12.2
16	14.4, (6.63E-2)	NaOAc	0.03	265	16.3 (1.99E-3)	-	THF/H ₂ O (9:1)	239/10.2	8.71
17	15.1, (6.95E-2)	NaOAc	1.00	278	5.7 mg, ^f (6.95E-2)	-	THF/H ₂ O (9:1)	250/27.8	9.13
18	18.2, (8.38E-2)	NaOTfAc	0.03	335	34.2, (2.51E-3)	-	THF/H ₂ O (9:1)	302/0.7	11.0
19	14.9, (6.86E-2)	NaOTfAc	1.00	274	9.33 mg, ^f (6.86E-2)	-	THF/H ₂ O (9:1)	247/27.4	9.01
20	15.0, (6.90E-2)	Et ₃ N	0.03	276	21.0, (2.07E-3)	-	THF/H ₂ O (9:1)	248/6.6	9.07

Table 6.5: (continued ...)

Exp.	168		V_{total} μL	catalyst	solvent	hexylamine	
	mg, (mmol)	M				eq	μL , (mmol)
21	15.9, (7.32E-2)	0.25	293	Et_3N 1.00	THF/H ₂ O (9:1)	264/29.3	9.62
22	16.2, (7.46E-2)	0.25	298	Pyridine 0.03	THF/H ₂ O (9:1)	268/12.1	9.80
23	14.3, (6.58E-2)	0.25	263	Pyridine 1.00	THF/H ₂ O (9:1)	237/26.3	8.65
24	39.9, (0.184)	0.25	736	LiOH 0.03	THF/H ₂ O (9:1)	662/60.4	24.1
25	41.6, (0.192)	0.25	768	LiOH 0.05	THF/H ₂ O (9:1)	691/53.9	25.2
26	45.0, (0.207)	0.25	828	LiOH 0.10	THF/H ₂ O (9:1)	745/33.2	27.2
27	7.9, (3.64E-2)	0.25	145	DBU 0.03	THF	129	4.78
28	8.8, (4.05E-2)	0.25	162	DBU 0.06	THF	125	5.32
29	11.0, (5.06E-2)	0.25	203	DBU 0.08	THF	141	6.65
30	9.8, (4.51E-2)	0.25	180	DBU 0.10	THF	112	5.93
31	38.1, (0.175)	0.50	351	LiOH 0.03	THF/H ₂ O (9:1)	316/22.5	23.0
32	36.7, (0.169)	0.75	225	LiOH 0.03	THF/H ₂ O (9:1)	203/10.4	22.2
33	38.1, (0.175)	1.00	175	LiOH 0.03	THF/H ₂ O (9:1)	158/4.9	23.0
34	16.2, (7.46E-2)	1.25	60.0	LiOH 0.03	THF/H ₂ O (9:1)	54/0.64	9.80
35	40.2, (0.185)	1.50	123	LiOH 0.03	THF/H ₂ O (9:1)	111/0	24.3
36	9.6, (4.42E-2)	0.25	177	LiOH 0.03	DMF	174	5.81
37	11.2, (5.16E-2)	0.25	206	LiOH 0.03	CH ₂ Cl ₂	203	6.78
38	8.8, (4.05E-2)	0.25	162	LiOH 0.03	MeOH	159	5.32
39	9.9, (4.56E-2)	0.25	182	LiOH 0.03	MeCN	179	5.99
40	8.4, (3.87E-2)	0.25	155	LiOH 0.03	MeCN/H ₂ O (9:1)	139/12.7	5.08

Table 6.5: (continued...)

Exp.	168		V_{total}		catalyst	solvent		hexylamine μL
	mg, (mmol)	M	μL	M		eq	μL , (mmol)	
41	11.5, (5.29E-2)	0.25	212	LiOH	0.03	3.80, (1.59E-3)	MeCN/H ₂ O (7:3)	148/59.7
42	8.3, (3.82E-2)	0.25	153	LiOH	0.03	2.75, (1.15E-3)	MeCN/H ₂ O (5:5)	76.4/73.7
43	9.8, (4.51E-2)	0.25	180	LiOH	0.03	3.24, (1.35E-3)	MeCN/H ₂ O (3:7)	54.1/123

^a Benzene (1.00 eq) was added as constant reference for integration purposes.

^b idem to a), just CH₂Cl₂ was used as reference. ^c LiOH was prepared as a 10 mg/mL stock solution. Thereoff the amounts needed (μL) was taken and subtracted from the residual water which had to be added. ^d Here, DBU was added in bulk ($d = 1.018 \text{ g/mL}$).

^e For CsOH, a 20 mg/mL solution in water was used. ^f Base was added as solid to the reaction mixture.

^g Here, Et₃N was added in bulk ($d = 0.73 \text{ g/mL}$). ^h Here, pyridine was added in bulk ($d = 0.98 \text{ g/mL}$).

Table 6.6: Gelation experiments for the hydrogel formation of 168 with selected acrylates and diamines via thiol-ene Michael addition.

Exp.	168		diamine		acrylate		wt%		V(H ₂ O)		gelation time	
	mg, (mmol)		mg, (mmol)		mg, (mmol)		wt%	μL	μL	μL	min	
G2	23.0, (0.106)	PEG(2) diamine	7.85, (0.0529)	TMPT	10.5, (0.0353)		50	22.0	30.5	30.5	5 min	
G3	21.8, (0.100)	PEG(7) diamine	18.5, (0.0502)	TMPT	9.91, (0.0334)		50	20.9	29.1	29.1	5 min	

Part II: Amino Acid-based Polyelectrolytes for Nanoparticle Synthesis

6.5 Introduction

Through the growing awareness of synthetic chemists, that the activity and function of existing biomolecules can be modified by chemical means, the synthesis of bio-mimicking polymers or biohybrid materials has experienced a tremendous progress over the past decades.^{38–40} While the use of polymer biohybrids as therapeutics and for medications has been continuously developed,⁴¹ the necessity for synthetic strategies of such biopolymers has still been an unceasing object of research at the present time.⁴² Whether it be a simple PEGylation of an existing biomolecule or the synthesis of biopolymers itself, valuable concepts have been developed. The former term defines the modification of existing biomolecules or drug agents through conjugation with a PEG residue, which is non-toxic and non-immunogenic.⁴³ Through such conjugations, decreased immunogenicity of the drug as well as enhanced pharmacokinetic behavior is observed.⁴⁴ If we focus on the chemical synthesis of biomacromolecules such as polypeptides, controlled living polymerizations are among the most established procedures to synthesize such poly(amino acids). One of the major routes to obtain polypeptides with controlled dispersities and molecular weights is via the ring-opening polymerization of Leuchs anhydrides or N-carboxyanhydrides (NCA).⁴⁵ These NCAs are synthesized from a broad range of different amino acids⁴⁶ and were first studied by Hermann Leuchs in 1906.⁴⁷ Next to this synthetic method, which has made the large scale production of polypeptides readily accessible, substrates such as ϵ -caprolactone for the synthesis of polycaprolactone (PCL)^{48,49} or lactide for the synthesis of poly(lactic acid) (PLA)^{50,51} are of good use for biological applications. This is mainly due to their in-

trinsic properties, non-toxicity and biodegradability.⁴⁹ All these polymers consist of amino acids or other biocompatible building blocks in the polymer backbone and with this are able to mimic molecules found in nature. However, as to our knowledge there has been only little effort done to incorporate amino acid in the side chain of polymers and this way retain the functional groups of the specific amino acids. By the above mentioned methods, polymers with charged side groups are only obtained by using the anhydrides of alkaline or acidic amino acids (glutamic acid, aspartic acid, lysine or ornithine and others).^{52–54} Furthermore the present amino or acid groups have to be protected to bring anionic polymerization procedures to work. Other methods involve the functionalization of polymers by peptide couplings or the synthesis of specific amino acid-functional acrylate monomers.^{55–58} In part I of this chapter, we presented a new approach to synthesize poly(thioether urethane)s using a bicyclic monomer via thiol-epoxy polymerization.⁵⁹ We made use of homocysteine thiolactone, being investigated in a lot of procedures mainly by us^{13,16,17} and others.^{19,26,31,60,61} This homocysteine served as a motif for double-modification using an amine and a Michael acceptor in a click-like reaction sequence or in multicomponent reactions to synthesize functional polymers.^{24,29,62,63} While others made use of this structural motif to functionalize existing polymers via this double-modification, we used the thiol released upon thiolactone ring-opening to start a base-catalyzed thiol-epoxy polyaddition. In the present part II and with this synthetic tool at hand, we intend to use this thiolactone to incorporate a variety of amino acids or amino acid derivatives into the side chain of the resulting poly(thioether urethane)s. The results show, that in a one-pot procedure, renouncing on water- and oxygen-free conditions, the reaction runs smoothly, producing anionic, cationic or even zwitterionic polymers as building blocks. The range of chosen amino acids, shows the ease of this procedure and with this the high potential for the synthesis of amino acid-functional poly(TEU)s. The first section is concerned about the poly(thioether urethane) synthesis using different amino acids and derivatives. Polymers are

analyzed according to their microstructure, molecular weight, dispersity and overall charge (via NMR spectroscopy, SEC and pH measurements). In a second section, we were able to use oppositely charged polymers to generate particles, which formed under self-complexation of the respective polyelectrolytes. FESEM micrographs are presented and analyzed.

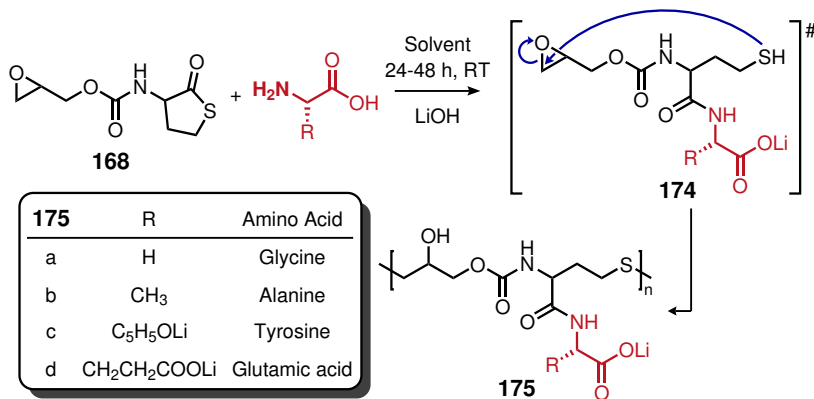
6.6 Results & Discussion

As in earlier publications, the concept of the present section relies on the one-pot reaction and orthogonal behavior of the epoxy thiolactone monomer (Scheme 6.6). The thiolactone ring is an active ester due to (i) the ring strain and (ii) the fact that it is a thioester. Hence, at room temperature the thiolactone of **168** is easily converted with an amino acid to form a stable amide while simultaneously a thiol moiety is released from the ring (compound **174**). This thiolactone is able to react in situ with a Michael acceptor or other radical thiol-ene acceptors.^{23,60} However in absence of such and in making use of the base-catalyzed thiol-epoxy reaction, the intermediate epoxy thiol **174** is able to build up polymers with this same intermediate AB-type monomer as repeating unit. The result of this thiol-epoxy polyaddition is the formation of poly(thioether urethane)s with free pendant hydroxyl groups (left for potential functionalization) and the incorporated amino acid residue (**175**).

6.6.1 Synthesis of Amino Acid Functional Poly(TEU)s

Firstly, the reactivity of simple amino acids was investigated. It is known from the first part of this chapter, that highest molecular weights and suppression of oligomer formation occurs under conditions using high concentrations of monomer and polar solvents like water or alike. However, as

amino acids in their neutral form are present as zwitterionic species, and for solubility reasons, it is necessary to deprotonate any acidic residues of the present substrates to form the corresponding lithium salts with active amino groups. These free amines are now able to react and open the thiolactone ring at room temperature. Consequently, in a one-pot reaction, epoxy thiolactone **168**, the amino acid and LiOH are mixed in a solvent mixture at ambient temperature (Scheme 6.6). After only few minutes, the amino acid substrate is brought to its neutral Li-salt state and with this is fully solubilized. As the polyaddition proceeds, solutions turn viscous and after full conversion are directly dried in vacuo or purified by precipitation (not always necessary). As an example, glycine was reacted with



Scheme 6.6: Synthesis of poly(thioether urethane)s using epoxy thiolactone **168** and various amino acids.

equimolar amounts of epoxy thiolactone **168** and LiOH as base (1.03 eq) in a MeCN/65% water mixture ($c(\mathbf{168}) = 3.0$ M) at room temperature in a glass vial. The reaction was carried out at aerial conditions for 24 h. After the polyaddition was complete, product polymer **175a** was concentrated in vacuo and oligomers were removed through precipitation in EtOH. The ¹H NMR spectrum confirms the desired microstructure (Figure 6.7); **168** was recorded in a 1:1 mixture of DMSO-d₆/D₂O for reasons of compara-

bility. The methine proton 6 shifts from $\delta = 4.60$ ppm to $\delta = 4.31$ ppm. Signals of thiolactone ring protons 7 and 8 both shift to higher field ($\delta = 2.68$ ppm and $\delta = 2.13/1.97$ ppm, respectively). Upon thiol-epoxy addition, protons 3 overlap with multiplet from proton 2 in the region $\delta = 4.24 - 3.97$ ppm. Adjacent methylene group 1, which splits up before the oxirane ring is opened, shifts to higher field too, giving one multiplet at $\delta = 2.74$ ppm. The lately introduced methylene group of amino acid glycine (11) shows a sharp signal at $\delta = 3.75$ ppm. Protons from the urethane, amide, acid and hydroxyl groups are not detected since the proton exchange with D_2O is too fast. The spectra for **175b-d** show similar shifts and signals (Section A.3.6). In converting the specific amino acids with the epoxy thiolactone,

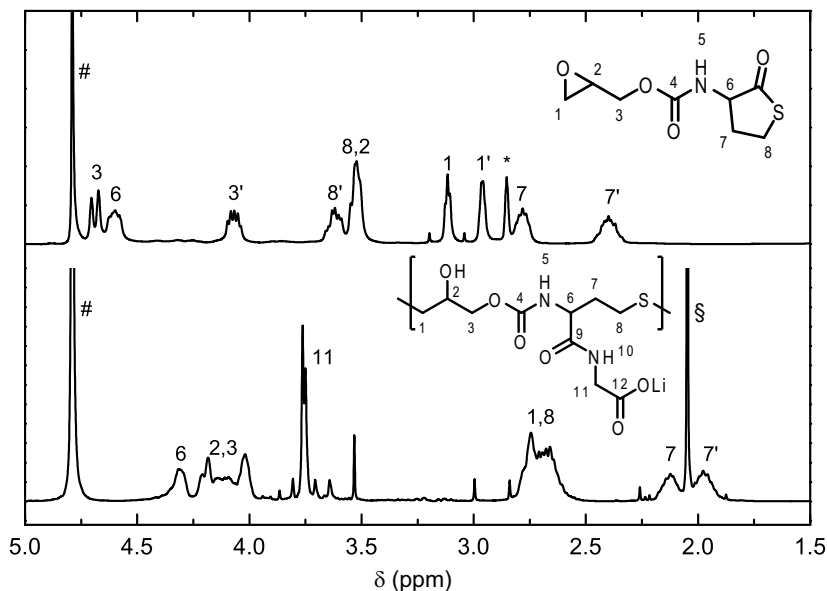


Figure 6.7: 1H NMR spectra of educt **168** and glycine-functional poly(TEU) **175a**. Recorded in D_2O (#), residual solvent peaks: * DMSO, § acetone.

different molecular weights are obtained. Only optimized conditions are given (Table 6.7). Regarding to the solubility of the reagents and the maximum possible water content, the chosen concentration are the highest

possible for each substrate. If we look at polyTEUs **175a-d**, it becomes noticeable that the steric hindrance of the active amino group correlates strongly with the molecular weights obtained for the thiol-epoxy polyaddition. Glycine reacts easily with **168**, since no side group in α -position to the carbonyl group is present. Amino groups of substrates, which have no higher substitutions at the adjacent carbon atom, are of higher nucleophilicity and thus reach higher molecular weights, while at the same time the formation of cyclic oligomers is enhanced, too (Figure 6.8a). There-

Table 6.7: SEC data of obtained poly(thioether urethane)s using **168**.

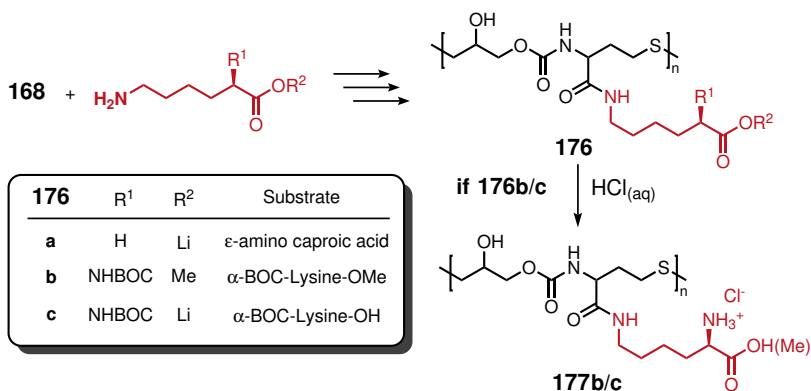
Polymer	Substrate	Solvent ^a	c(168) [M]	t [h]	M_n [g/mol]	\bar{D}
175a	Gly	MeCN/H ₂ O	3.0	24	6230 ^b	1.9
175b	Ala	MeCN/H ₂ O	3.5	48	5200	1.8
175c	Tyr	MeCN/H ₂ O	3.0	48	2130	1.7
175d	Glu	MeCN/H ₂ O	2.0	72	5570	1.3
176a	EACA	MeCN/H ₂ O	3.0	72	9590	1.8
176b	N-BOC-Lys-OMe	MeOH	3.0	24	3550 ^c	2.0
176c	N-BOC-Lys-OH	MeCN/H ₂ O	3.0	24	3900	2.1
177b	Lys-OMe	-	-	-	1830 ^c	1.9
177c	Lys-OH	-	-	-	3170	2.2
178	Carnosine	MeCN/H ₂ O	3.0	24	3500 ^b	1.9

^a The solvent mixture consisted of MeCN with 65% water content.

^b Precipitated in ethanol. ^c SEC data measured in DMF as eluent.

fore, after precipitation in pure ethanol, polymer **175a** reaches a number average molecular weight of $M_n = 6230$ g/mol. The elution maximum is located at $V_E = 25.4$ mL (Figure 6.8a). Sterically more loaded substrates reached lower conversion and molecular weights in the double amount of time, but were mostly free of oligomers. Consequently, the reaction of **168** with alanine and tyrosine gives polymers **175b** and **175c** with number average molecular weights of $M_n = 5200$ and 2130 g/mol, respectively. The former shows an elution maximum at $V_E = 25.9$ mL (with a minor oligomer peak at $V_E = 29.3$ mL; Figure 6.8b), the latter at $V_E = 26.7$ mL (Figure 6.8c). For polymer **175d**, a dicarboxylic acid is introduced using

glutamic acid. Here the amount of LiOH added up to 2.03 eq giving a dicarboxylic acid salt; a number average molecular weight of $M_n = 5570$ g/mol was obtained ($V_E = 26.1$ mL, Figure 6.8d). For the above mentioned polymers, the dispersity values are all in agreement with step-growth reactions. In another synthetic approach, the reactivity of lysine surrogate ϵ -aminocaproic acid (EACA) is tested (Scheme 6.7). Using EACA in a polyaddition with **168**, the poly(TEU) **176a** is obtained. Polymer **176a** shows a number average molecular weight of $M_n = 9590$ g/mol and a dispersity of $\mathcal{D} = 1.8$. The SEC profile shows a single peak with an elu-



Scheme 6.7: Synthesis of poly(thioether urethane)s using epoxy thiolactone **168** and lysine derivatives and subsequent deprotection of the BOC group to obtain polyelectrolytes.

tion maximum of $V_E = 25.2$ mL (Figure 6.8e). The overall good reactivity of EACA is thus ascribed to the spacial flexibility of the amino group in ϵ -position. For the same reaction protocol applied to lysine, two different derivatives are taken into consideration. The first one is the α -N-BOC protected lysine methyl ester, whereas the second one is represented by the α -N-BOC lysine with the free carboxylic acid group. The subsequent BOC deprotection would allow us to gather an alkaline polymer with an amine/ammonium group (polymer **177b**) or a zwitterionic polyampholyte at the isoelectric point (**177c**). After reacting **168** with the N-BOC lysine

methyl ester in methanol, polymer **176b** with a number average molecular weight of $M_n = 3550$ g/mol is obtained ($V_E = 37.3$ mL, measured with DMF SEC, Figure 6.8f). Using N-BOC lysine acid, for poly(TEU) **176c** higher molecular weights are achieved ($M_n = 3900$ g/mol, $V_E = 25.5$ mL, Figure 6.8g). For both protected lysine-functional poly(thioether urethane)s, the dispersities are between $\bar{D} = 2.0 - 2.1$. The microstructure of all three polymers was confirmed by ^1H NMR spectroscopy (Section A.3.6). In the second reaction step, both lysine-functional poly(thioether urethane)s **176b/c** are deprotected using aqueous HCl. For **176b** this reaction proceeds in methanol as solvent to maintain the methoxy ester, while for **176c** this reaction is carried out in pure water. Upon deprotection, the acidified lysine-functional poly(TEU) (**177b/c**) are obtained in quantitative yield, no purification is necessary. The molecular weight of **177b** is $M_n = 1830$ g/mol ($\bar{D} = 1.9$). Looking at the SEC traces, the elution maximum shifts from $V_E = 37.3$ mL to $V_E = 39.9$ mL (Figure 6.8f). The synthesized **177c** shows a molecular weight of $M_n = 3170$ g/mol and a dispersity value of $\bar{D} = 2.2$, which was determined using a multiangle laser light scattering (MALLS) detector. The elution maximum shifts from $V_E = 25.5$ mL to $V_E = 27.9$ mL (Figure 6.8g). The strong tailing is probably due to the change of the electronic structure of the polymers from a neutral state to a charged one. Further general decrease of the molecular weight is expected due to the cleavage of the BOC group and release of CO_2 . Furthermore, the elution curve of **177c** shows two salt peaks at $V_E = 30.7$ and 30.1 mL. These peaks are related to a neutralization reaction of the the acidic polymer **177c** and the eluent, which contains small amounts of NaNO_3 and NaN_3 (sodium salts as additives reduce the interactions of the sample with the stationary phase). As a result of this neutralization, two salt peaks occur being no less than NaCl (Figure A.48). Refractive index measurements for poly(TEU) **177b** delivered the dn/dc value for the MALLS SEC evaluation (Figure A.49). With the aforementioned two-step sequence, zwitterionic polymers like **177c** are readily accessible. However, to exclude the use of acid, one could think of amino acids like histidine or tryptophan as precur-

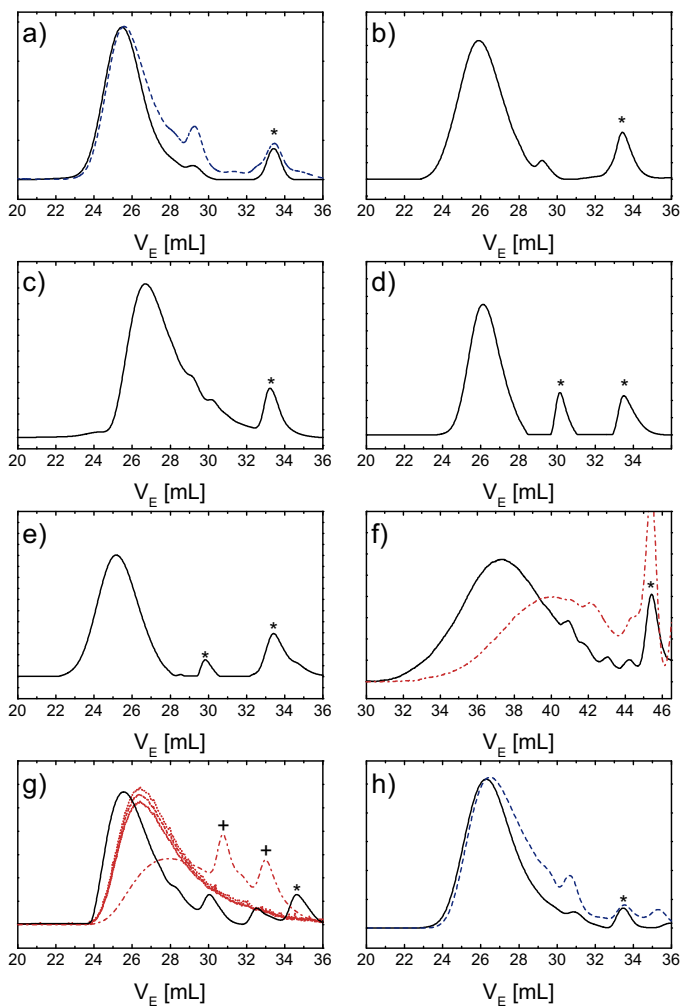
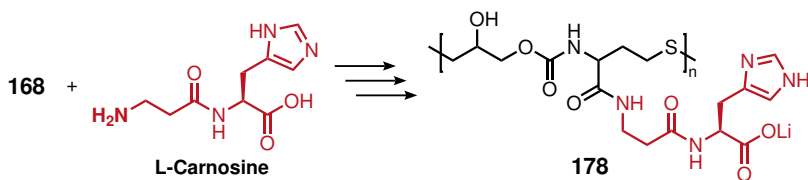


Figure 6.8: SEC profiles of functional poly(TEU)s: a) **175a** (glycine) showing the crude product (dashed blue) and the purified polymer (solid black), b) **175b** (alanine), c) **175c** (tyrosine), d) **175d** (glutamic acid), e) **176a** (EACA), f) **176b** (solid black) and BOC deprotected **177b** (red dash dot), g) **176c** (solid black) and BOC deprotected **177c** (RI signal: red dash dot; MALLS signal: red dot) and h) **178** (L-carnosine) as crude (dashed blue) and purified product (solid black).

sors for zwitterionic polymers. As experiments have shown, these are sterically too challenging and only oligomers are afforded in reaction with **168** (not shown). Carnosine also known as β -alanyl-L-histidine is a commercially available dipeptide. It is known for its antioxidant properties which rely on the chelating effect of the imidazole group for ions like iron, copper, zinc or calcium. Besides, it is able to interact with hydroxyl radicals as a radical scavenger or even singlet oxygen.^{64,65} Because of this and other properties it is often considered as a protective and anti-ageing peptide.⁶⁶ Finally, bearing a carboxylic acid and the imidazole side group, carnosine shows good pH-buffering capacity and is used as direct precursor for zwitterionic poly(thioether urethane)s. With the β -alanyl group comprising a sterically unhindered amino group, carnosine was reacted with **168** at room temperature using 1.03 eq of LiOH as base (Scheme 6.8). After 24 h the reaction was complete, precipitation in ethanol gave the pure polymer **178** (for ¹H NMR spectroscopy see Figure A.47). A number average molecular weight of $M_n = 3500$ g/mol is obtained ($D = 1.9$, Table 6.7). The SEC trace shows a single peak with $V_E = 26.3$ mL (Figure 6.8h).



Scheme 6.8: One-pot synthesis of zwitterionic poly(TEU) **178** using carnosine as substrate.

Due to the ionic groups, all polymers show pH-responsive or pH-buffering behavior. This behavior was checked by autotitration (Figure A.50). Polymers obtained as lithium salts were titrated with $\text{HCl}_{(aq)}$ (0.1 N) the pK_b value was determined from the corresponding conductivity traces and converted to values for pK_a . Polymers **177b** and **c**, which were in acidic state due to the acidic deprotection step, were titrated with $\text{NaOH}_{(aq)}$ (0.1 N). Polymer **175a** shows a single pH transition starting from $\text{pH} = 11.10$ to

4.50. The transition is quite broad and the $pK_a = 2.32$, which corresponds well to the pK_a of glycine (Table 6.8). Conductivity measurements show, that the polyelectrolyte rather behaves like a weak acid (Figure A.50a). For polymer **175b**, the pK_a value is slightly higher than the literature value for alanine ($pK_a = 3.38$, Table 6.8). Tyrosine-functional polymer **175c** represents a rather non-polar poly(TEU), due to the aromatic phenyl content. This is also reflected by the measured conductivity, which increases continuously with added amount of $HCl_{(aq)}$ (Figure A.50c). The pH trace shows a pK_a of approximately 4.02 ($pK_{a,lit} = 2.20$, Table 6.8). Poly(TEU) **175d** having glutamic acid as functional side group should exhibit two different pH transitions according to the different carboxylic acid groups. However, according to pH trace, only one transition with $pK_a = 3.58$ is observed (Figure A.50d). Comparing this value with literature data for these acid groups, it is anticipated that only a mean pK_a appears between both literature values (Table 6.8). The carboxylic acid of lysine surrogate EACA shows a $pK_a = 4.43$. The pK_a value obtained from the pH profile is slightly lower ($pK_a = 3.38$). Upon addition of an excess of $HCl_{(aq)}$ the pH value further decreases which misleadingly appears as a second pH transition (Figure A.50e). Polymer **177b** comprises ammonium groups and represents an alkaline poly(TEU) or polyelectrolyte. Starting from an acidic pH, **177b** shows a $pK_a = 6.39$ corresponding to deprotonation of the ammonium group. The obtained constant is again lower than the value proposed by literature. Looking at **177c**, two transition points in the pH measurement appear (Figure A.50g). The first transition corresponds to the dissociation of the acidic ammonium in α -position ($pK_a = 9.15$). After the ammonium group is fully deprotonated, the carboxylic acid is neutralized by further added $NaOH_{(aq)}$ ($pK_a = 4.60$). Finally, the pH profile of polymer **178** proves the pH-responsive behavior expected for this one-pot polyampholyte. Starting from acidic pH values, the free carboxylic acid shows a $pK_a = 4.71$. With increasing amount of added acid, a second transition is perceived at $pK_a = 9.39$. The latter is ascribed to the transformation of the imidazole- into an imidazolium group. To sum up, it can be stated that

beside the expected microstructure, which was proven by ^1H NMR spectroscopy and SEC measurements, the pH-responsive behavior has been successfully demonstrated by potentiometric titrations of all poly(TEU)s.

Table 6.8: Autotitration data of poly(TEU)s with amino acids or derivatives in the side chain.

Polymer	Substrate	pK_a		
		COOH	ammonium	literature
175a	Gly	2.32	-	2.35
175b	Ala	3.38	-	2.30
175c	Tyr	4.02	-	2.20
175d	Glu	3.58	-	2.2/4.2
176a	EACA	3.38	-	4.43
177b	Lys-OMe ^a	-	6.39	7.2
177c	Lys-OH ^a	4.60	9.15	2.2/9.0
178	Carnosine	4.13	10.70	2.65/6.88

^a Samples were titrated from acidic to basic pH using 0.1 N NaOH_(aq).

6.6.2 Nanoparticles through Polyelectrolyte Complexation

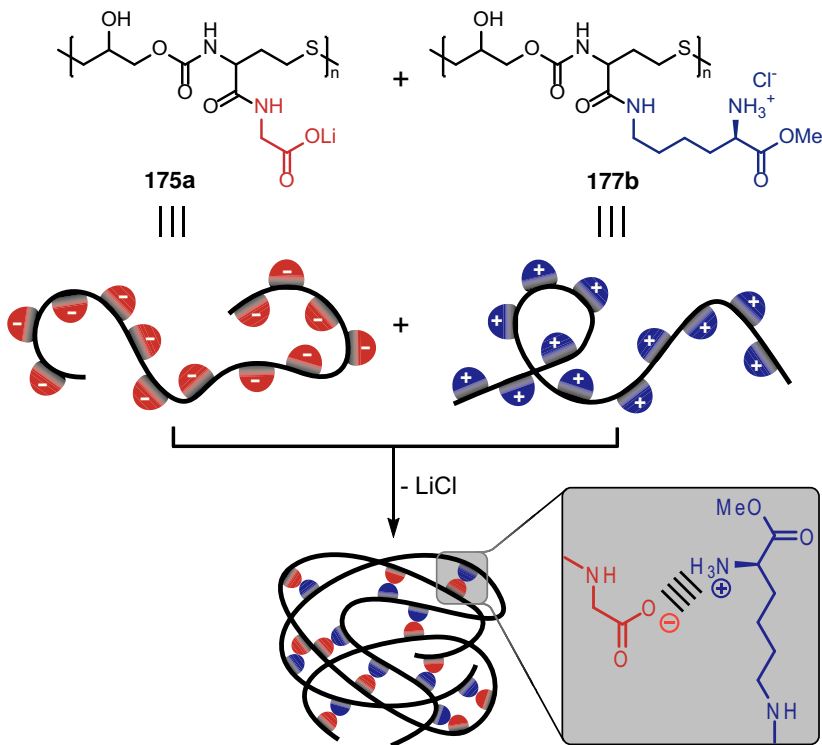
In contrast to conventional methods, nanoparticle syntheses through complexation processes are only achieved using charged polymers. If a polymer with cationic groups is mixed with an anionic polyelectrolyte, the opposite charges result in a strong electrostatic interaction between the chains. Macromolecular salts or polyelectrolyte complexes (PEC) are formed.⁶⁷ Polymers which combine positive and negative charges in the chain are known as polyampholytes. Either two oppositely charged polyelectrolytes or one single polypolyampholytes are able to form submicrometer-sized particles without covalent cross-linking. The electrostatic interactions are the main driving force for aggregation of the polymer chains and lead

to physical cross-links between such. This way, stable biodegradable nanoparticles are obtained by simply mixing/dispersing two oppositely charged polyelectrolytes^{68–71} or a single polyampholyte in solution.^{55,56,72} Due to their unique properties and bio-mimicking microstructure, many are able to encapsulate drug agents, DNA or other biomacromolecules as nanocarriers. Within this section, we synthesized different polyelectrolytes, which should be able to form PECs due to the amino acids in the side chain. Hence, for the preparation of PECs, we chose the acidic polymer **175a** and alkaline polymer **177b**. In a typical reaction set-up, stock solutions of both poly(TEU)s were prepared. A specific amount of **175a** was dissolved in water prior to addition of **177b** (Scheme 6.9). Depending on the concentration, solutions turned opaque or if too concentrated a solid white powder precipitated (not shown). Prior to dynamic light scattering (DLS) measurements, every aggregate solution was dialysed against water to remove residual LiCl, which was formed during the complexation. A range of different concentrations was chosen to investigate an eventual impact of the concentration on the size of the built aggregates (Table 6.9). Corresponding radii distributions are found in the annex (Figure A.51).

Table 6.9: Influence of polymer concentration on the size of the prepared PEC's.

No.	c(Polymer) [mM]	radius [nm]	std. deviation [nm]	Đ
1	5	368.39	9.87	0.240
2	1	260.61	5.84	0.344
3	0.5	138.72	5.34	0.091
4	0.1	63.490	1.77	0.352
5	0.05	337.79	4.77	0.418

From the DLS measurements, it can be stated, that with decreasing concentration of polymer solutions, PEC radii decrease. The smallest particle size is obtained for a concentration of $c = 0.1$ mM ($r = 63.490$ nm). Although the particle size of experiment 4 is the lowest, the dispersity of the particles is among the highest of the measured samples. Sample 3



Scheme 6.9: Synthesis of PEC by complexation of **175a** and **177b**.

with a concentration of $c = 0.5$ mM comes with the lowest dispersity of $\mathcal{D} = 0.091$. However, sample 4 was further investigated via imaging methods like field emission scanning electron microscopy (FESEM). To eliminate artifacts from the product PEC, first the starting material was analysed via FESEM. Polymer **175a** shows strong tendency to crystallize on the wafer. Upon drying of the sample, enough time is given to promote crystallization. The crystallites come in a dendritic shape (Figure 6.9a-b). Although polymer **177b** is also present as salt (ammonium chloride) similar patterns as for **175a** are not observed (Figure 6.9c). Instead, the polymer is detected as small white spots with a diameter around $d = 1 \mu\text{m}$ (Figure 6.9d). The overall wafer of the sample with the PEC nanoparticles shows structural

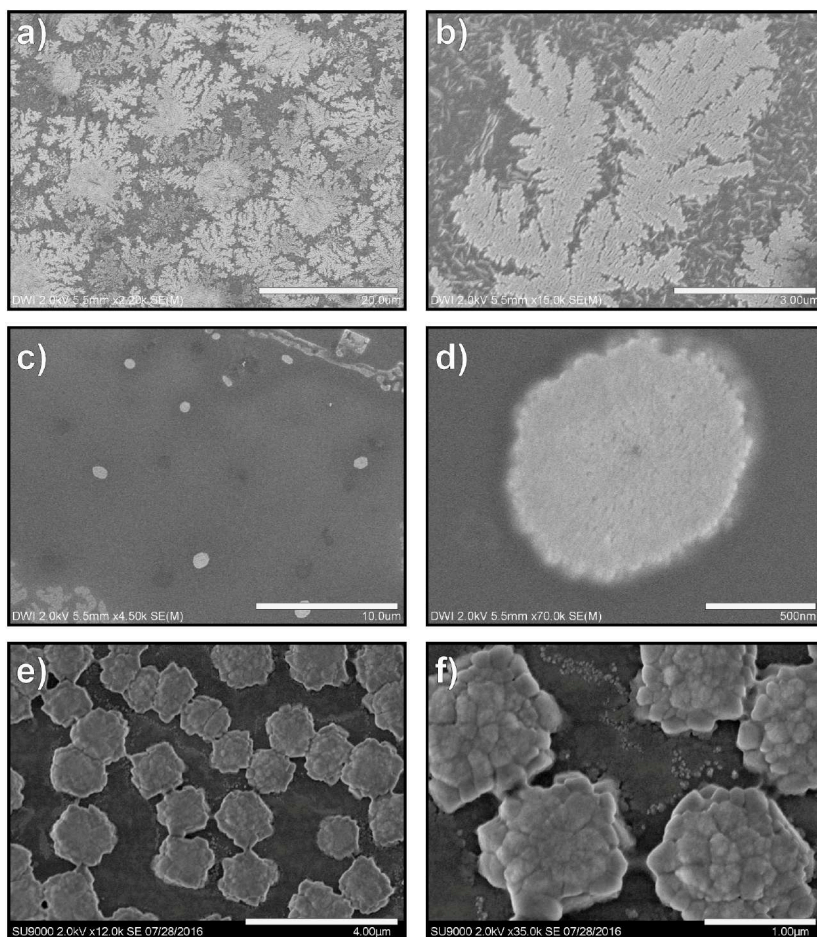


Figure 6.9: FESEM micrographs of polymer a) **175a** (scale bar 20 μm) and b) a magnification of the crystalline structure (scale bar 3 μm). Micrographs c) and magnification d) show polymer **177b** as white spots (scale bar 10 μm and 500 nm, respectively). Micrographs e) and magnification f) show a possible clusters of PEC particles (scale bar 4 μm and 1 μm, respectively.)

features of a polymer film. Upon magnification (Figure 6.9e), several spots are detected, where particles with rough surfaces and diameters around $1.5 \mu\text{m}$ are located. On a closer look, it becomes clear, that these particles seem to be whole clusters of smaller particles (Figure 6.9f). The investigated sample indicates, that the particles of sample 4 ($r = 63.49 \text{ nm}$) are not stable in the dry state; instead they aggregate to bigger clusters, ultimately resulting in a polymer film. However, the assignment of these polymeric structures cannot be specified with certainty. What can be confirmed with high probability is, that the particles in solution from sample 4 ($r = 63.49 \text{ nm}$), are not stable upon drying, since no spherical nanoparticles are detected on the corresponding micrographs. Further imaging experiments involving in solution cryo-TEM or cryo-FESEM have to be done to consolidate the comprehension of the resulting structures on the micrographs.

6.7 Conclusion

In this section, poly(thioether urethane)s are synthesized in aqueous solvent mixtures. The epoxy thiolactone is converted with different amino acids and amino acid derivatives. Chosen substrates are glycine, alanine, tyrosine, glutamic acid, ϵ -aminocaproic acid, BOC protected lysine derivatives and the dipeptide carnosine. The molecular weights obtained by such thiol-epoxy polyadditions range from $2130 < M_n < 9590 \text{ g/mol}$. Regarding the overall reactivity of the substrates, less sterically hindered amino groups are of higher nucleophilicity than sterically hindered ones. The dispersities of the obtained poly(TEU)s are between $1.3 < \text{Đ} < 2.2$, which is expected for step-growth polymerizations. By using a protocol involving BOC protected lysines, this multicomponent reaction system offers the possibility to synthesize cationic and zwitterionic lysine polymers in a simple manner. Using carnosine as a substrate, zwitterionic polymers

are obtained in a one-pot procedure at benign reaction conditions. The polyelectrolytes are studied with regards to their pH-buffering behaviour. Lastly polyelectrolyte complexes are synthesized using a positively and a negatively charged polymer by self-complexation. The resulting nanoparticles show sizes from $63.490 < r < 368.39$ nm. The sample exhibiting the lowest radii is investigated in FESEM images.

6.8 Experimental Data

6.8.1 Materials

Ultrapure MilliQ water with a resistivity of $18.2 \text{ M}\Omega/\text{cm}$ was used for all experiments. $\text{LiOH}\cdot\text{H}_2\text{O}$ (99%, Sigma Aldrich), glycine (p.A, Merck), L-alanine (Degussa), L-tyrosine (>99%, Merck), L-glutamic acid ($\geq 99\%$, Merck), BOC-L-Lysine-OMe acetate salt (Bachem), N^α -(tert-Butoxycarbonyl)-L-lysine (>98.0%, TCI Chemicals) and L-carnosine (fluorochem) were used without further purification. Unless otherwise indicated, all solvents were purchased from commercial sources and were used without further purification.

6.8.2 Measurements

^1H spectra were recorded on a Bruker DPX-400 FT NMR spectrometer (400 MHz) and are reported as follows: chemical shift δ (ppm) (multiplicity, coupling constant J (Hz), number of protons, assignment). D_2O ($\delta_{\text{H}} = 4.79$ ppm) and dimethylsulfoxide (DMSO, $\delta_{\text{H}} = 2.50$ ppm) were used as an internal standard. Chemical shifts are reported in ppm to the nearest 0.01 ppm for ^1H .

Molecular weights (M_n and M_w) and dispersity values (M_w/M_n or \bar{D}) were determined by size exclusion chromatography (SEC). SEC analyses were carried out with dimethylformamide (DMF) or water as eluent. SEC with DMF (HPLC grade, VWR) as eluent was performed using an Agilent 1100 system equipped with a dual RI/Visco detector (ETA-2020, WGE). The eluent contained $1 \text{ g}\cdot\text{L}^{-1}$ LiBr ($\geq 99\%$, Sigma Aldrich). The sample solvent contained traces of distilled water as internal standard. One pre-column (8x50 mm) and four PSS GRAM gel columns (8x300 mm) were applied at a flow rate of $1.0 \text{ mL}\cdot\text{min}^{-1}$ at $40 \text{ }^\circ\text{C}$. The diameter of the gel particles measured $10 \text{ }\mu\text{m}$, the nominal pore widths were 30, 10^2 , 10^3 and 3000 \AA . Calibration was achieved using narrowly distributed poly(methyl methacrylate) standards (PSS Std. Mainz). SEC with H_2O (HPLC grade, Carl Roth) as eluent was performed using an Agilent 1200 system equipped with a refractive index detector and a multiple-angle laser light scattering (MALLS) detector (DawnEOS, Wyatt Technology). The eluent contained 0.1 M sodium nitrate (NaNO_3 , p.A, Merck KGaA) and 0.01 wt% sodium azide (NaN_3 , extra pure, Merck KGaA). As internal standard $50 \text{ }\mu\text{L}$ ethylene glycol (99.5%, Fluka) was used. One pre-column (8x50 mm) and three Suprema-Lux gel columns (8x300 mm) were applied at a flow rate of $1.0 \text{ mL}\cdot\text{min}^{-1}$ at $40 \text{ }^\circ\text{C}$. The diameter of the gel particles measured $5 \text{ }\mu\text{m}$, the nominal pore widths were 30, 1000 and 3000 \AA . Calibration was achieved using narrow distributed poly(ethylene glycol) standards (Polymer Standards Service). Results were evaluated using the PSS WinGPC UniChrom software (Version 8.1).

The potentiometric and conductivity titration of the poly(thioether urethane)s was conducted by titration of an acidified or basic polymer solution (0.15 wt%, 30 mg in 20 mL water) using 0.1 N $\text{NaOH}_{(aq)}$ or 0.1 N $\text{HCl}_{(aq)}$ solutions at $25 \text{ }^\circ\text{C}$, respectively.

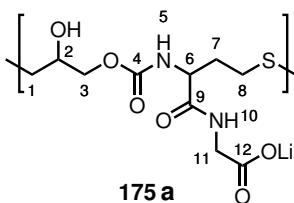
Dynamic light scattering, the particle sizes and size distribution were measured by a laser light scattering instrument (ALV/DLS/SLS-5000) equipped with an ALV-5000/EPP multiple digital time correlator and laser goniometry system ALV/CGS-8F S/N 025 with a helium neon laser (Uniphase 1145P,

output power of 22 mW and wavelength of 632.8 nm) as a light source, at a fixed scattering angle of 90 °.

Field emission scanning electron microscopy (FESEM) images were acquired using a Hitachi S4800 FE-SEM and a Hitachi SU9000 FE-SEM. For sample preparation one droplet of the particle solution was placed on a silicon wafer and dried at room temperature. The samples were sputtered with gold prior to the measurement.

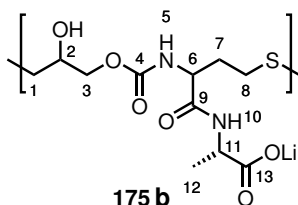
6.8.3 Syntheses

Glycine-functional Poly(TEU) **175a**



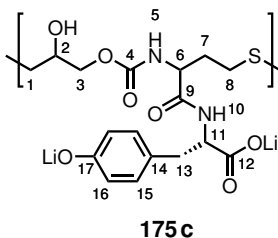
Epoxy thiolactone **168** (75.0 mg, 0.345 mmol), glycine (25.9 mg, 0.345 mmol) and LiOH (14.9 mg, 0.356 mmol) were dissolved in a stirred mixture of MeCN/65% H_2O (40.3/74.8 μL , $c(\mathbf{168})_{total} = 3.0 \text{ M}$) at room temperature. The reaction mixture was stirred at room temperature for 24 h. Then, the solvent was evaporated under reduced pressure to give the crude poly(thioether urethane). Purification by precipitation from H_2O (200 μL) in ethanol (10 mL) gave product **175a** (95.0 mg, 61%) as a slightly yellow solid. $M_n = 6230 \text{ g/mol}$, $\overline{D} = 1.9$. $^1\text{H NMR}$ (400 MHz, D_2O) δ 4.37 - 4.25 (m, 1H, H6), 4.25 - 3.98 (m, 3H, H2/3), 3.80 - 3.73 (m, 2H, H11), 2.83 - 2.58 (m, 4H, H1/H8), 2.21 - 1.89 (m, 2H, H7).

Synthesis of Alanine-functional Poly(TEU) **175b**



Epoxy thiolactone **168** (57.3 mg, 0.264 mmol), L-alanine (23.5 mg, 0.264 mmol) and LiOH (11.4 mg, 0.272 mmol) were dissolved in a stirred mixture of MeCN/65% H_2O (26.4/49.0 μL , $c(\mathbf{168})_{total} = 3.5 \text{ M}$) at room temperature. The reaction mixture was stirred at room temperature for 48 h. Then, the solvent was evaporated under reduced pressure to give the crude product **175b** (quant.) as a slightly yellow solid. $M_n = 5200 \text{ g/mol}$, $\bar{D} = 1.8$. $^1\text{H NMR}$ (400 MHz, D_2O) δ 4.34 - 3.95 (m, 6H, H2/3/6/11), 2.84 - 2.55 (m, 4H, H1/8), 2.16 - 1.87 (m, 2H, H7), 1.50 - 1.41, 1.36 - 1.26 (m, 3H, H12).

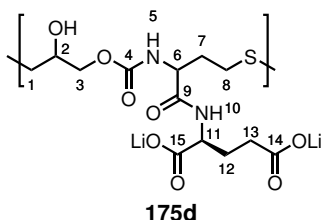
Synthesis of Tyrosine-functional Poly(TEU) **175c**



Epoxy thiolactone **168** (25.4 mg, 0.117 mmol), L-tyrosine (21.2 mg, 0.117 mmol) and LiOH (10.0 mg, 0.237 mmol) were dissolved in a stirred mix-

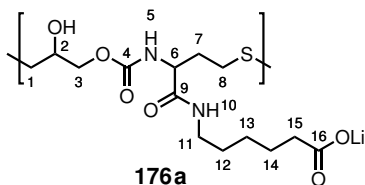
ture of MeCN/65% H_2O (13.6/25.3 μL , $c(168)_{total} = 3.0 \text{ M}$) at room temperature. The reaction mixture was stirred at room temperature for 48 h. Then, the solvent was evaporated under reduced pressure to give the crude product **175c** (quant.) as a slightly yellow solid. $M_n = 2130 \text{ g/mol}$, $\overline{D} = 1.7$. $^1\text{H NMR}$ (400 MHz, D_2O) δ 7.09 - 6.93 (m, 2H, H15), 6.77 - 6.57 (m, 2H, H16), 4.49 - 4.30 (m, 1H, H11), 4.27 - 3.85 (m, 4H, H2-3 and H6), 2.89 - 2.38 (m, 6H, H1/8/13), 2.13 - 1.83 (m, 2H, H7).

Synthesis of Glutamic Acid-functional Poly(TEU) **175d**



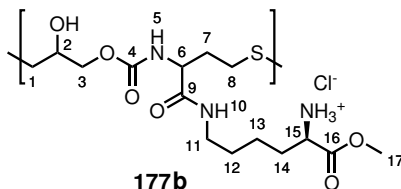
Epoxy thiolactone **168** (100 mg, 0.460 mmol), L-glutamic acid (67.7 mg, 0.460 mmol) and LiOH (39.2 mg, 0.935 mmol) were dissolved in a mixture of MeCN/65% H_2O (81/150 μL , $c(168)_{total} = 2.0 \text{ M}$) at room temperature. The reaction mixture was stirred at room temperature for 48 h. Then, the solvent was evaporated under reduced pressure to give the crude product **175d** (quant.) as a slightly yellow solid. $M_n = 5570 \text{ g/mol}$, $\overline{D} = 1.3$. $^1\text{H NMR}$ (400 MHz, D_2O) δ 4.35 - 3.97 (m, 5H, H2/3/6/11), 2.83 - 2.58 (m, 4H, H1/8), 2.25 - 2.15 (m, 2H, H13), 2.15 - 1.82 (m, 4H, H7 and H12).

Synthesis of ϵ -Aminocaproic Acid-functional Poly(TEU) **176a**



Epoxy thiolactone **168** (100 mg, 0.460 mmol), EACA (60.4 mg, 0.460 mmol) and LiOH (19.9 mg, 0.474 mmol) were dissolved in a stirred mixture of MeCN/65% H_2O (53.7/99.7 μL , $c(168)_{total} = 3.0 \text{ M}$) at room temperature. The reaction mixture was stirred at room temperature for 24 h. Then, the solvent was evaporated under reduced pressure to give the crude product **176a** (quant.) as a slightly yellow solid. $M_n = 9590 \text{ g/mol}$, $\text{Đ} = 1.8$. $^1\text{H NMR}$ (400 MHz, D_2O) δ 4.27 - 3.94 (m, 4H, H2/3/6), 3.26 - 3.13 (m, 2H, H11), 2.80 - 2.53 (m, 4H, H1/8), 2.16 (t, $J = 7.8 \text{ Hz}$, 2H, H15), 2.11 - 1.89 (m, 2H, H7), 1.62 - 1.43 (m, 4H, H12 and H14), 1.36 - 1.22 (m, 2H, H13).

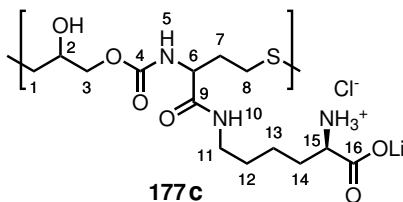
Synthesis of Lysine Methyl Ester-functional Poly(TEU) **177b**



Epoxy thiolactone **168** (150 mg, 0.691 mmol), N-BOC-L-Lysine-OMe (221 mg, 0.691 mmol) and LiOH (29.8 mg, 0.711 mmol) were dissolved in

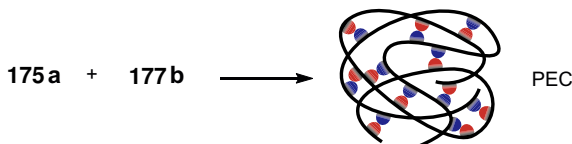
methanol (230 μL , $c(168)_{total} = 3.0 \text{ M}$) at room temperature. The reaction mixture was stirred at room temperature for 24 h. Then, the solvent was evaporated under reduced pressure to give the crude poly(thioether urethane) **176b**. The crude product (330 mg, 0.691 mmol) was dissolved in MeOH (6.91 mL, 0.1 M) at room temperature. Then, $\text{HCl}_{(aq)}$ (1.10 mL, 13.8 mmol) was added and the reaction mixture was stirred at room temperature for 24 h. Next, the solution was filtered and evaporated under reduced pressure to give product **177b** (quant.) as a white hygroscopic solid. $M_n = 1830 \text{ g/mol}$, $D = 1.9$. $^1\text{H NMR}$ (400 MHz, D_2O) δ 4.32 - 4.07 (m, 4H, H3/6/15), 4.06 - 3.98 (m, 1H, H2), 3.85 (s, 3H, H17), 3.28 - 3.18 (m, 2H, H11), 2.83 - 2.57 (m, 4H, H1 and H8), 2.10 - 1.86 (m, 4H, H7 and H14), 1.62 - 1.32 (m, 4H, H12 and H13).

Synthesis of Lysine-functional Poly(TEU) **177c**



Epoxy thiolactone **168** (150 mg, 0.691 mmol), N-BOC-L-Lysine-OH (170 mg, 0.691 mmol) and LiOH (29.8 mg, 0.711 mmol) were dissolved in a stirred mixture of MeCN/65% H_2O (80.6/150 μL , $c(168)_{total} = 3.0 \text{ M}$) at room temperature. The reaction mixture was stirred at room temperature for 24 h. Then, the solvent was evaporated under reduced pressure to give the crude poly(thioether urethane) **176c**. The crude product (324 mg, 0.691 mmol) was dissolved in H_2O (6.91 mL, 0.1 M) at room temperature. Then, $\text{HCl}_{(aq)}$ (2.20 mL, 27.6 mmol) was added and the reaction mixture was stirred at room temperature for 24 h. Next, the solution was filtered

Synthesis of PEC Nanoparticles



For the synthesis of PEC nanoparticles, two different stock solutions were prepared: Solution A comprised **175a** (10 mg/mL in H₂O) and solution B contained **177b** (13.88 mg/mL in H₂O). The total volume of the samples was $V_{total} = 6.7$ mL. For the synthesis of PEC nanoparticles, water (4.7 mL) was provided in a glass vial. The required amounts of polymer from solutions A and B were each and separately diluted to 1 mL. In the next step, first **175a** (diluted 1 mL solution) was added, then under vigorous stirring, **177b** (diluted 1 mL solution) was added to the reaction mixture. After stirring the sample for 20 min at room temperature, LiCl was removed by dialysis using Spectra/Por dialysis membranes (Spectrumlabs.com, RC, MWCO = 100-500 Da) in water (2 L) over night prior to DLS measurements.

References

- (1) Kakuchi, R. *Angewandte Chemie International Edition* **2014**, *53*, 46–48.
- (2) Barner-Kowollik, C.; DuPrez, F. E.; Espeel, P.; Hawker, C. J.; Junkers, T.; Schlaad, H.; VanCamp, W. *Angewandte Chemie International Edition* **2011**, *50*, 60–62.
- (3) Gruending, T.; Oehlenschlaeger, K. K.; Frick, E.; Glassner, M.; Schmid, C.; Barner-Kowollik, C. *Macromolecular Rapid Communications* **2011**, *32*, 807–812.
- (4) Duerr, C. J.; Lederhose, P.; Hlalele, L.; Abt, D.; Kaiser, A.; Brandau, S.; Barner-Kowollik, C. *Macromolecules* **2013**, *46*, 5915–5923.
- (5) Hildebrandt, K.; Pauloehrl, T.; Blinco, J. P.; Linkert, K.; Baerner, H. G.; Barner-Kowollik, C. *Angewandte Chemie International Edition* **2015**, *54*, 2838–2843.

- (6) Kreye, O.; Toth, T.; Meier, M. A. R. *Journal of the American Chemical Society* **2011**, *133*, 1790–1792.
- (7) Kreye, O.; Turunc, O.; Sehlinger, A.; Rackwitz, J.; Meier, M. A. R. *Chemistry - A European Journal* **2012**, *18*, 5767–5776.
- (8) Kakuchi, R.; Theato, P. *ACS Macro Letters* **2013**, *2*, 419–422.
- (9) Lee, I.-H.; Kim, H.; Choi, T.-L. *Journal of the American Chemical Society* **2013**, *135*, 3760–3763.
- (10) Wang, Y.-Z.; Deng, X.-X.; Li, L.; Li, Z.-L.; Du, F.-S.; Li, Z.-C. *Polymer Chemistry* **2013**, *4*, 444–448.
- (11) Zhu, C.; Yang, B.; Zhao, Y.; Fu, C.; Tao, L.; Wei, Y. *Polymer Chemistry* **2013**, *4*, 5395–5400.
- (12) Ubaghs, L.; Fricke, N.; Keul, H.; Höcker, H. *Macromolecular Rapid Communications* **2004**, *25*, 517–521.
- (13) Keul, H.; Mommer, S.; Möller, M. *European Polymer Journal* **2013**, *49*, 853–864.
- (14) Anders, T.; Keul, H.; Möller, M. *Designed Monomers and Polymers* **2011**, *14*, 593–608.
- (15) Anders, T.; Keul, H.; Möller, M. *e-Polymers* **2013**, *11*, 832–850.
- (16) Mommer, S.; Keul, H.; Möller, M. *Macromolecular Rapid Communications* **2014**, *35*, 1986–1993.
- (17) Mommer, S.; Lamberts, K.; Keul, H.; Möller, M. *Chemical Communications* **2013**, *49*, 3288–3290.
- (18) Espeel, P.; Goethals, F.; Du Prez, F. E. *Journal of the American Chemical Society* **2011**, *133*, 1678–1681.
- (19) Espeel, P.; Carrette, L. L. G.; Bury, K.; Capenberghs, S.; Martins, J. C.; Prez, F. D.; Madder, A. *Angewandte Chemie International Edition* **2013**, *52*, 13261–13264.
- (20) Espeel, P.; Goethals, F.; Driessen, F.; Nguyen, L.-T. T.; Du Prez, F. E. *Polymer Chemistry* **2013**, *4*, 2449–2456.
- (21) Goethals, F.; Martens, S.; Espeel, P.; van den Berg, O.; Du Prez, F. E. *Macromolecules* **2013**, *47*, 61–69.
- (22) Espeel, P.; Du Prez, F. E. *European Polymer Journal* **2014**, *62*, 247–272.
- (23) Driessen, F.; Du Prez, F. E.; Espeel, P. *ACS Macro Letters* **2015**, *4*, 616–619.
- (24) Zhang, Z.; You, Y.-Z.; Wu, D.-C.; Hong, C.-Y. *Polymer* **2014**, *64*, 221–226.
- (25) Yan, J.-J.; Wang, D.; Wu, D.-C.; You, Y.-Z. *Chemical Communications* **2013**, *49*, 6057–6059.

- (26) Zhao, Y.; Yang, B.; Zhang, Y.; Wang, S.; Fu, C.; Wei, Y.; Tao, L. *Polymer Chemistry* **2014**, *5*, 6656–6661.
- (27) Yu, L.; Wang, L.-H.; Hu, Z.-T.; You, Y.-Z.; Wu, D.-C.; Hong, C.-Y. *Polymer Chemistry* **2015**, *6*, 1527–1532.
- (28) Morisseau, C.; Bernay, M.; Escaich, A.; Sanborn, J. R.; Lango, J.; Hammock, B. D. *Analytical Biochemistry* **2011**, *414*, 154–162.
- (29) Espeel, P.; Goethals, F.; Stamenović, M. M.; Petton, L.; Du Prez, F. E. *Polymer Chemistry* **2012**, *3*, 1007–1015.
- (30) Reinicke, S.; Espeel, P.; Stamenović, M. M.; Du Prez, F. E. *ACS Macro Letters* **2013**, *2*, 539–543.
- (31) Reinicke, S.; Espeel, P.; Stamenović, M. M.; Du Prez, F. E. *Polymer Chemistry* **2014**, *5*, 5461–5470.
- (32) Gadwal, I.; Binder, S.; Stuparu, M. C.; Khan, A. *Macromolecules* **2014**, *47*, 5070–5080.
- (33) Gadwal, I.; Rao, J.; Baettig, J.; Khan, A. *Macromolecules* **2013**, *47*, 35–40.
- (34) Gadwal, I.; Stuparu, M. C.; Khan, A. *Polymer Chemistry* **2015**, *6*, 1393–1404.
- (35) Ragnarsson, U.; Grehn, L. *Accounts of Chemical Research* **1998**, *31*, 494–501.
- (36) Lohmeijer, B. G. G.; Pratt, R. C.; Leibfarth, F.; Logan, J. W.; Long, D. A.; Dove, A. P.; Nederberg, F.; Choi, J.; Wade, C.; Waymouth, R. M.; Hedrick, J. L. *Macromolecules* **2006**, *39*, 8574–8583.
- (37) Kricheldorf, H. In *Polycondensation*; Springer Berlin Heidelberg: 2014; Chapter 7, pp 95–116.
- (38) Dirks, A.; Cornelissen, J. J. L. M.; van Delft, F. L.; van Hest, J. C. M.; Nolte, R. J. M.; Rowan, A. E.; Rutjes, F. P. J. T. *QSAR & Combinatorial Science* **2007**, *26*, 1200–1210.
- (39) Sanchez, C.; Shea, K. J.; Kitagawa, S. *Chem. Soc. Rev.* **2011**, *40*, 471–472.
- (40) *Chemistry of Bioconjugates: Synthesis, Characterization, and Biomedical Applications*; Narain, R., Ed.; John Wiley & Sons, Inc.: 2014.
- (41) Haag, R.; Kratz, F. *Angewandte Chemie International Edition* **2006**, *45*, 1198–1215.
- (42) Scholz, C.; Vayaboury, W. *Polymer Preprints* **2008**, *49*, 486–487.
- (43) Harris, J. M.; Chess, R. B. *Nat Rev Drug Discov* **2003**, *2*, 214–221.
- (44) Veronese, F. M.; Mero, A. *BioDrugs* **2008**, *22*, 315–329.
- (45) Klok, H.-A. In *Encyclopedia of Polymer Science and Technology*; John Wiley & Sons, Inc.: 2002.

- (46) Kricheldorf, H. R. In *α -Aminoacid-N-Carboxy-Anhydrides and Related Heterocycles: Syntheses, Properties, Peptide Synthesis, Polymerization*; Springer Berlin Heidelberg: Berlin, Heidelberg, 1987, pp 3–58.
- (47) Leuchs, H. *Berichte der deutschen chemischen Gesellschaft* **1906**, *39*, 857–861.
- (48) Labet, M.; Thielemans, W. *Chemical Society Reviews* **2009**, *38*, 3484–3504.
- (49) Ulery, B. D.; Nair, L. S.; Laurencin, C. T. *Journal of Polymer Science Part B: Polymer Physics* **2011**, *49*, 832–864.
- (50) Kulkarni, R. K.; Moore, E. G.; Hegyeli, A. F.; Leonard, F. *Journal of Biomedical Materials Research* **1971**, *5*, 169–181.
- (51) Garlotta, D. *Journal of Polymers and the Environment* **2001**, *9*, 63–84.
- (52) Katchalski, E.; Sela, M. In, C.B. Anfinsen M.L. Anson, K. B., Edsall, J. T., Eds.; *Advances in Protein Chemistry*, Vol. 13; Academic Press: 1958, pp 243–492.
- (53) Debabov, V. G.; Davydov, V. D.; Morozkin, A. A. *Bulletin of the Academy of Sciences of the USSR, Division of chemical science* **1966**, *15*, 2083–2086.
- (54) Van Dijk-Wolthuis, W. N. E.; van de Water, L.; van de Wetering, P.; Van Steenberghe, M. J.; Kettenes-van den Bosch, J. J.; Schuyf, W. J. W.; Hennink, W. E. *Macromolecular Chemistry and Physics* **1997**, *198*, 3893–3906.
- (55) Shen, H.; Akagi, T.; Akashi, M. *Macromolecular Bioscience* **2012**, *12*, 1100–1105.
- (56) Piyapakorn, P.; Akagi, T.; Hachisuka, M.; Onishi, T.; Matsuoka, H.; Akashi, M. *Macromolecules* **2013**, *46*, 6187–6194.
- (57) Alswieleh, A. M.; Cheng, N.; Canton, I.; Ustbas, B.; Xue, X.; Ladmiral, V.; Xia, S.; Ducker, R. E.; Zubir, O. E.; Cartron, M. L.; Hunter, C. N.; Leggett, G. J.; Armes, S. P. *Journal of the American Chemical Society* **2014**, *136*, 9404–9413.
- (58) Ladmiral, V.; Charlot, A.; Semsarilar, M.; Armes, S. P. *Polym. Chem.* **2015**, *6*, 1805–1816.
- (59) Mommer, S.; Truong, K.-N.; Keul, H.; Möller, M. *Polymer Chemistry* **2016**, *7*, 2291–2298.
- (60) Rudolph, T.; Espeel, P.; Du Prez, F. E.; Schacher, F. H. *Polymer Chemistry* **2015**, *6*, 4240–4251.
- (61) Satti, A. J.; Espeel, P.; Martens, S.; Hoeylandt, T. V.; Prez, F. E. D.; Lynen, F. *Journal of Chromatography A* **2015**, *1426*, 126–132.
- (62) Zhang, Z.; You, Y.-Z.; Wu, D.-C.; Hong, C.-Y. *Macromolecules* **2015**, *48*, 3414–3421.
- (63) Yang, L.; Zhang, Z.; Cheng, B.; You, Y.; Wu, D.; Hong, C. *Science China Chemistry* **2015**, *58*, 1734–1740.
- (64) Boldyrev, A. A. *International Journal of Biochemistry* **1993**, *25*, 1101–1107.

-
- (65) Guiotto, A.; Calderan, A.; Ruzza, P.; Borin, G. *Current Medicinal Chemistry* **2005**, *12*, 2293–2315.
- (66) Hipkiss, A. R. *The International Journal of Biochemistry & Cell Biology* **1998**, *30*, 863–868.
- (67) Lankalapalli, S.; Kolapalli, V. R. M. *Indian J Pharm Sci* **2009**, *71*, 481–487.
- (68) Sæther, H. V.; Holme, H. K.; Maurstad, G.; Smidsrød, O.; Stokke, B. T. *Carbohydrate Polymers* **2008**, *74*, 813–821.
- (69) Shu, S.; Zhang, X.; Teng, D.; Wang, Z.; Li, C. *Carbohydrate Research* **2009**, *344*, 1197–1204.
- (70) Müller, M.; Kessler, B.; Fröhlich, J.; Poeschla, S.; Torger, B. *Polymers* **2011**, *3*, 762.
- (71) Birch, N. P.; Schiffman, J. D. *Langmuir* **2014**, *30*, 3441–3447.
- (72) Ahmed, S.; Hayashi, F.; Nagashima, T.; Matsumura, K. *Biomaterials* **2014**, *35*, 6508–6518.

Chapter 7

Summary

In this work, three different coupling agents have been synthesized. The synthesis for the ethylene carbonate thiolactone coupler has been optimized, starting from a chloroformate and HCTL. After this concise one-step route, model reactions were carried out. In using 2 different amines the more reactive thiolactone was opened by amidation prior to ring-opening of the ethylene carbonate by the second amine. Upon aminolysis of the rings, a thiol from the thiolactone ring and a hydroxyl from the ethylene carbonate ring were liberated. Next, these functionalities were converted with methyl acrylate as Michael acceptor and an acid bromide to obtain a fully functionalized coupling molecule. Every intermediate of the reaction sequence was isolated, the reactions proceeded at benign reaction conditions at the same time being highly selective. Finally, the four-step reaction strategy was carried out in one pot without purification of the intermediates. The telescoped yield of the fully functionalized coupler was 38%.

The second coupler was a bis(thiolactone) coupler, containing one γ -

thiobutylolactone with β -substitution and the HCTL, which has been used before. The synthesis of the first cycle, started from itaconic acid and was optimized, too. Having an acid chloride and HCTL at hand, the bis(thiolactone) coupler was synthesized in 97% yield. Again, model reactions were carried out, this time revealing, that there was no orthogonality between both thiolactone cycles. The bis(thiolactone) was therefore considered to be an AA-type monomer for polyaddition. Different polymers were synthesized using two diamines as BB-type comonomers with different thermal behaviour. In mixing the diamines in different ratios, the thermal properties of the resulting polyamides was successfully adjusted. The T_g varied in a range from $-50\text{ }^\circ\text{C}$ to $92\text{ }^\circ\text{C}$. The M_n of the obtained polyamides ranged from 980 to 2400 g/mol, indicating that the nucleophilicity of the chosen diamines plays a significant role in the polyaddition process. After formation of the polyamides, the free thiol groups (2 per repeating unit) were trapped by using methyl acrylate in a Michael-type addition. In another post-polymerization modification approach, first a hydrophobic polyamide was prepared having free reactive pendant thiol groups. In a second step, these thiol groups were converted with acrylate-functional PEG building blocks of different molecular weights. The outcome of this reaction strategy was an amphiphilic polymer with hydrophilic PEG side chains and a hydrophobic backbone. The amphiphilic polymers were fully water-soluble and exhibited molecular weights of $M_n = 3400$ and 11000 g/mol, respectively.

The last synthesized coupling molecule was structurally related to the first one. Again, the coupler comprised a HCTL, this time connected with an oxirane ring. The synthesis of the coupler was based on the use of a glycidyl nitrophenyl carbonate. Within two steps and optimized reaction conditions, the desired coupling agent was obtained 60% yield. This epoxy thiolactone coupler was investigated again regarding the chemoselectivity of the rings. Upon ring-opening of the thiolactone at room temperature in presence of both an amine and methyl acrylate the thiolactone was con-

verted in a three component reaction leaving the oxirane ring intact. In a second reaction, amination of the oxirane ring occurred at elevated temperatures using a dialkylamine. These reactions were highly selective so that the whole reaction sequence was carried out in one pot in a four component reaction set-up. When the aminolysis of the thiolactone did take place without the use of a present Michael acceptor, an epoxy thiol was obtained, which was able to undergo a thiol-epoxy polyaddition reaction. The reaction was studied according to the use of different catalysts. LiOH turned out to be most efficient in catalytic quantities of 3 mol%. Further, the impact of the monomer concentration, solvent polarity and formation of cyclic oligomers was investigated. The optimum reaction conditions to deliver high molecular weights, low dispersities and suppression of cyclization required the use of highly concentrated monomer solutions as well as highly polar solvents like water mixtures. Adhering to these reaction conditions gave poly(thioether urethane)s of molecular weights up to $M_n = 11100$ g/mol. In a third approach, the epoxy thiolactone coupler was used for the preparation of bulk hydrogels. Here the epoxy thiolactone was converted with a diamine, forming an AA, BB-type species which was able to cross-link (i) by use of catalytic amounts of LiOH leading to thio-epoxy driven gel formation and (ii) by multicomponent reaction in presence of a triacrylate.

In the second part of the epoxy thiolactone chapter, the latter was reacted with a variety of amino acids to obtain polyelectrolytes. The substitution pattern of the α -amino acids showed, that there are strong differences in reactivity, due to sterically challenging reaction sites. For the reaction of the coupler with amino acids, again the highest concentration was identified to get molecular weights from $M_n = 2130 - 9590$ g/mol. Glycine, alanine, tyrosine and glutamic acid were used as simple amino acids. ϵ -aminocaproic acid, was used as a lysine surrogate. Later the coupling agent was converted with α -BOC protected lysines to obtain charged polyelectrolytes after deprotection of the BOC protection group.

Through this reaction sequence, charged poly(thioether urethane)s were accessible within two reaction steps. By use of the dipeptide carnosine, which is also known to have strong anti-oxidant effects, a zwitterionic polymer was obtained by a simple one-pot reaction of the dipeptide and the epoxy thiolactone coupling agent. Furthermore, autotitration experiments gave information on pH transitions and corresponding pK_a values. Finally, by using two oppositely charged poly(thioether urethane)s, nanoparticles were obtained through complexation of the polyelectrolytes. The particle radii ranged from $63.49 < r < 368.39$ nm. Imaging methods like FESEM revealed, that the particles were most probably not stable upon the drying process on the wafer and instead formed a polymer film, which spread over the entire wafer.

Appendix A

Additional Information

A.1 Ethylene Carbonate Thiolactone Coupler

A.1.1 Crystallographic Data

Suitable crystals for single crystal X-ray diffraction (XRD) were obtained by recrystallization from 2-butanone as colorless prisms. Intensity data were collected at 100 K on a Bruker D8 goniometer with a Bruker SMART APEX CCD detector in ω -scan mode using Mo- K_{α} radiation ($\lambda = 0.71073 \text{ \AA}$) from an Incoatec microsource with multi layer optics. Temperature was controlled with an Oxford Cryostream 700. Data were processed with SAINT+¹ and multi scan absorption corrections were applied with SAD-ABS.² The structure was solved by direct methods using SHELXS97³ and refined on F_2 with SHELXL97.³ Non-H atoms were refined with anisotropic displacement parameters. The amino-H was found in difference fourier map and refined freely with $U_{iso}(\text{H}) = 1.2 U_{eq}(\text{N})$; all other hydrogen atoms

were placed in idealized positions with $U_{iso}(\text{H}) = 1.2 U_{eq}(\text{C})$. Supplementary crystallographic data can be obtained free of charge from the Cambridge Crystallographic Data Centre via http://www.ccdc.cam.ac.uk/data_request/cif (CCDC 919540).

Table A.1: Crystal data and refinement results of the *RR/SS* diastereomer of **148**.

Chemical formula	$\text{C}_9\text{H}_{11}\text{NO}_6\text{S}$
M_r	261.25
Crystal system, space group	Monoclinic, $P 2_1/c$
a, b, c (\AA)	8.6927(9), 15.1581(15), 8.4584(8)
β ($^\circ$)	95.606(2)
V (\AA^3)	1109.19(19)
Z	4
μ (mm^{-1})	0.309
Crystal size (mm)	0.27 x 0.21 x 0.18
Index ranges	$-11 \leq h \leq 11$, $-20 \leq k \leq 20$, $-11 \leq l \leq 11$
Reflections collected	15268
Independent reflections	2810 [$R_{int} = 0.0426$]
T_{min} , T_{max}	0.9212, 0.9465
Data / restraints / parameters	2810 / 0 / 157
Goodness-of-fit on F_2	1.038
Final R indices [$l > 2\sigma(l)$]	$R_1 = 0.0347$, $wR_2 = 0.0879$
R indices (all data)	$R_1 = 0.0441$, $wR_2 = 0.0944$
Largest diff. peak and hole	0.410 and $-0.192 e \cdot \text{\AA}^{-3}$

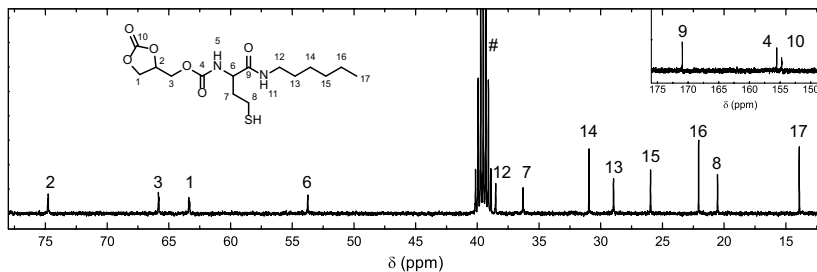
A.1.2 ^{13}C NMR Spectra of Model Compounds

Figure A.1: ^{13}C spectrum of thiol 149. Residual solvent peak: # DMSO.

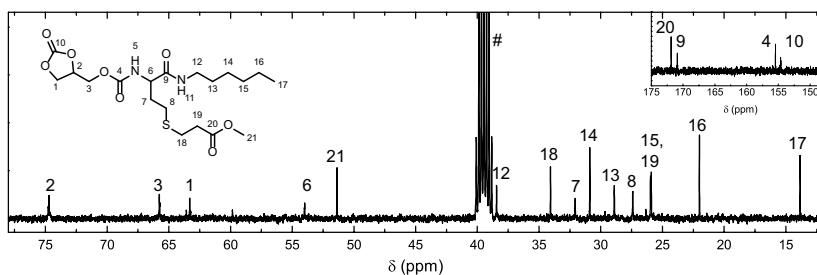


Figure A.2: ^{13}C spectrum of thiol 150. Residual solvent peak: # DMSO.

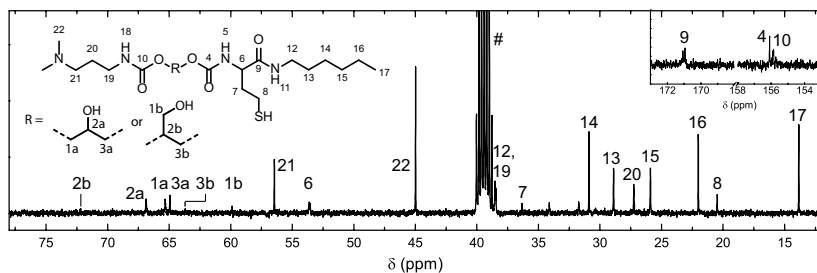


Figure A.3: ^{13}C spectrum of thiol 151. Residual solvent peak: # DMSO.

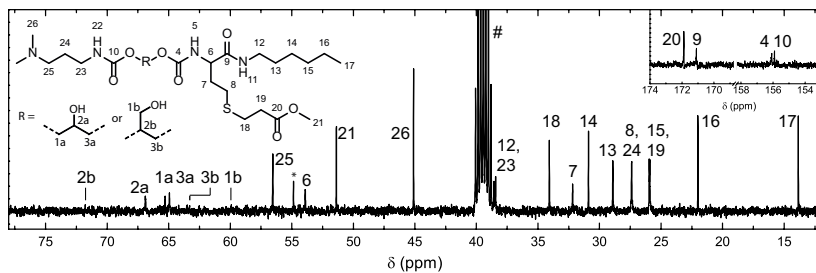


Figure A.4: ^{13}C spectrum of thiol **152**. Residual solvent peaks: # DMSO, * CH_2Cl_2 .

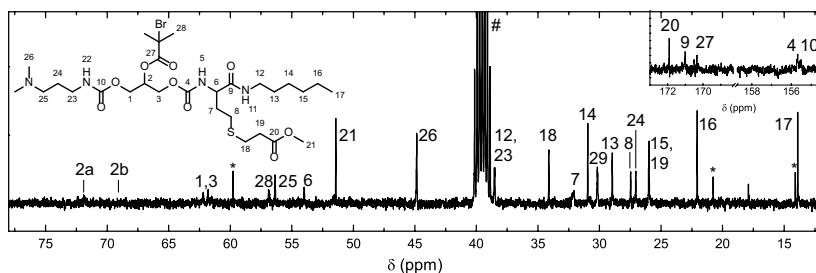
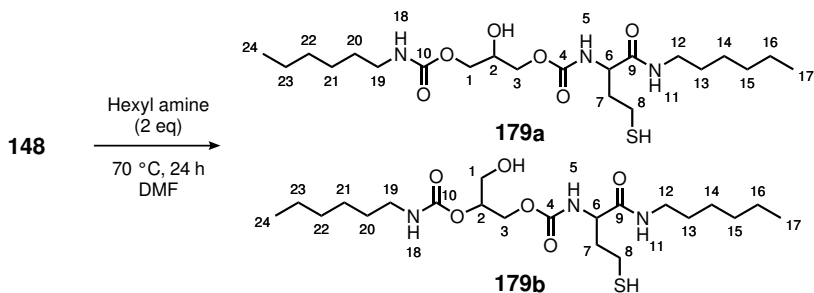


Figure A.5: ^{13}C spectrum of thiol **153**. Residual solvent peaks: # DMSO, * EtOAc.

A.1.3 NMR Analysis of the Isomers

To analyze the coupling patterns of the isomers formed by the reaction of the second amine and the ethylene carbonate ring, the coupler **148** was converted with 2.0 eq of hexyl amine at 70 °C (Scheme A.1).

The ^1H NMR data show that both isomers bear different chemical shifts for the protons 1, 2 and 3. To start with the alkyl chains, protons 17 and 24 are found as a triplet at $\delta = 0.85$ ppm. Methylene groups 14 to 16 and 21 to 23 appear at $\delta = 1.23$ ppm. Protons 13 and 20 show a broad singlet at $\delta = 1.38$ ppm. The multiplet at $\delta = 1.94 - 1.67$ ppm shows methylene



Scheme A.1: Reaction of the coupler with 2.0 equivalents of hexyl amine.

group 7, whereas the methylene group adjacent to the thiol (8) overlaps with the DMSO signal at $\delta = 2.54 - 2.37$ ppm. Both CH_2 groups next to the NH groups are observed as a multiplet at $\delta = 3.12 - 2.90$ ppm. The amide and urethane protons 11 and 18 are each assigned to a broad triplet at $\delta = 7.84$ and 7.13 ppm, respectively. Urethane proton 5 appears as a doublet at $\delta = 7.30$ ppm with a 3J coupling value of 7.1 Hz. The adjacent proton at the stereocenter (6) is shifted to $\delta = 4.07 - 3.96$ ppm. The alcohol group of isomer **179a** is found at $\delta = 5.11$ ppm, whereas OH^b is shifted to higher field ($\delta = 4.88$ ppm). Methine protons 2a and 2b are observed at $\delta = 3.79$ and 4.74 ppm, respectively. **1b** shows a broad triplet at $\delta = 3.48$ ppm. Methylene group 1a is overlapping with methylene group 3a at $\delta = 3.99 - 3.83$ ppm. The signal of 3b is splitting up and shows two multiplets. The first is located at $\delta = 4.25 - 4.07$ ppm, the second overlaps with protons 3a and 1a at $\delta = 3.99 - 3.83$ ppm. The complex coupling interactions between the nuclei of each isomer could be resolved by $^1\text{H}, ^1\text{H}$ -COSY measurements (Figure A.6).

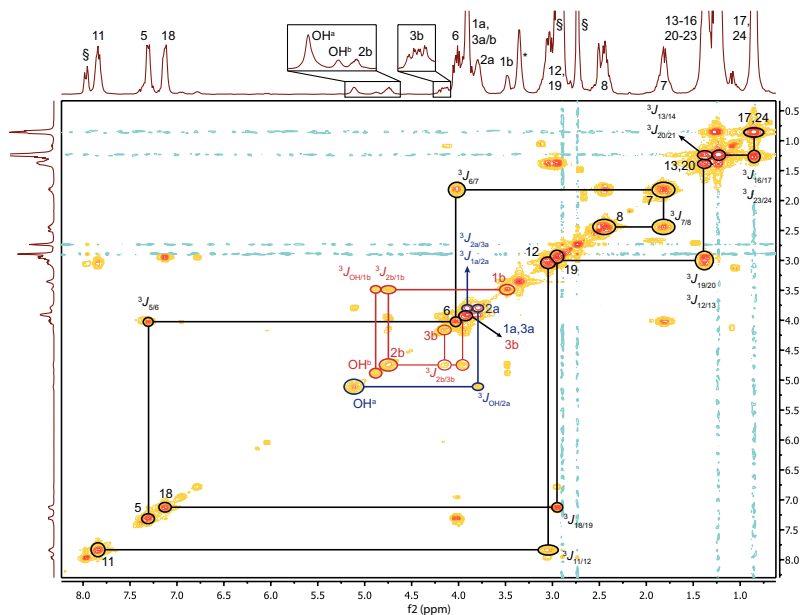


Figure A.6: $^1\text{H}, ^1\text{H}$ -COSY spectrum of isomeric thiol alcohols **179a** and **179b**. Residual solvent peaks: * H_2O , # DMSO, § DMF.

A.2 Bis(Thiolactone) Coupler

A.2.1 NMR Spectra

As found below, supporting spectra for the characterization of bis(thiolactone) **155** are shown. Amide proton **6** couples to methine proton **7** via a $^3J_{6/7}$ coupling. Signal **7** stands for the proton, which is adjacent to **8** according to the $^3J_{7/8}$ constant. Protons **8** show a $^3J_{8/9}$ coupling to protons **9**. The second thiolactone cycle shows similar coupling constants. Protons **2** couple to methine **3**, which is itself adjacent to methylene group **4**. Corresponding $^3J_{2/3}$ and $^3J_{3/4}$ constants are highlighted.

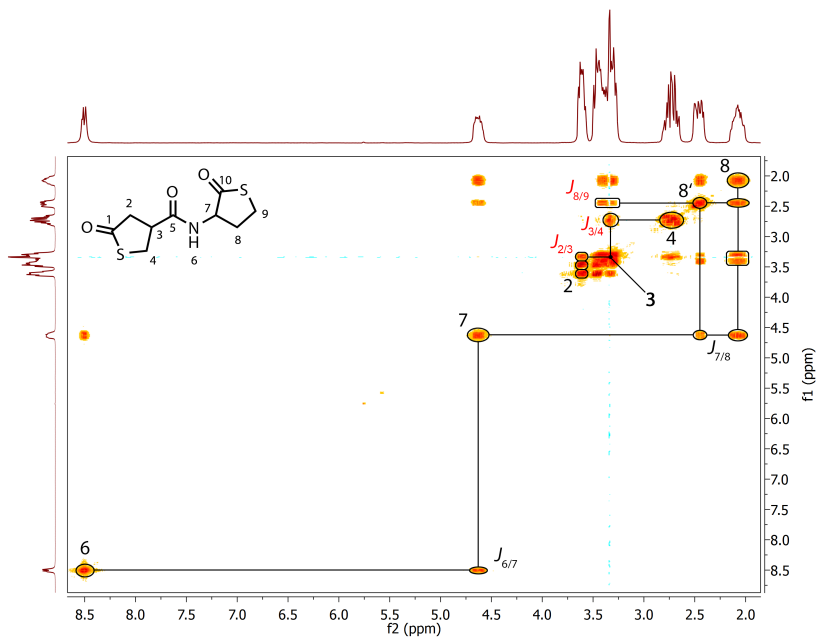


Figure A.7: $^1\text{H}, ^1\text{H}$ -COSY of the bis(thiolactone) **155**.

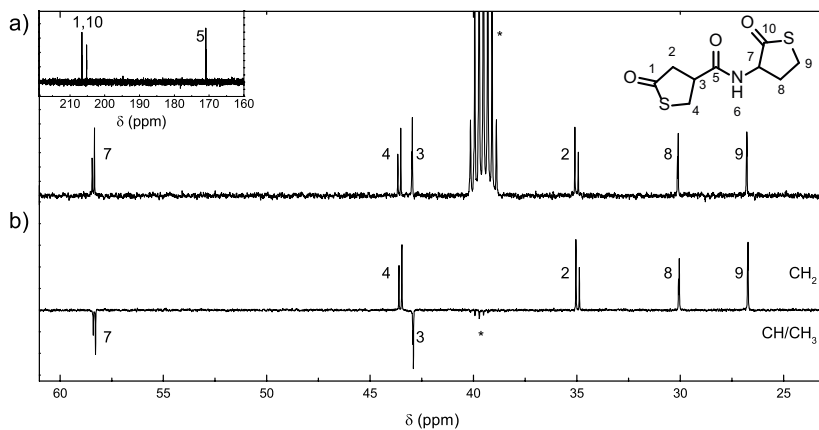


Figure A.8: a) ^{13}C NMR spectrum and b) DEPT135 spectrum of bis(thiolactone) **155**. Residual solvent peak: * DMSO.

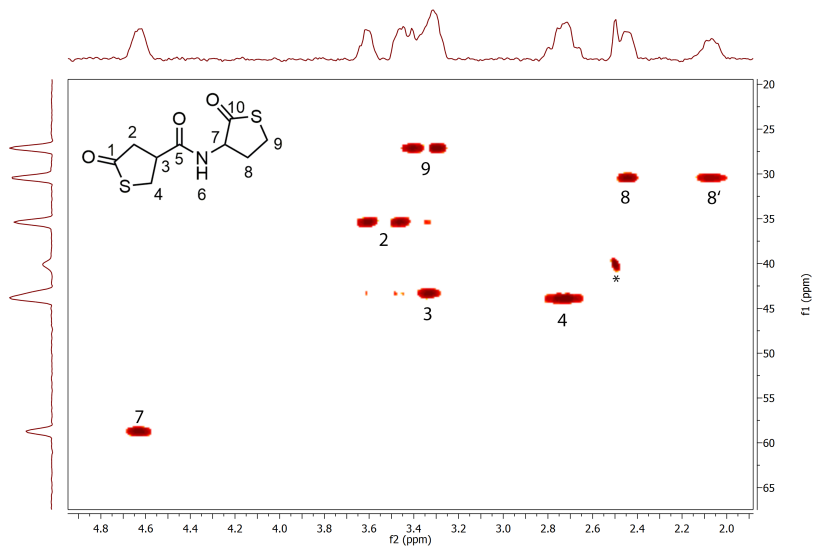


Figure A.9: HSQC of bis(thiolactone) **155**. Residual solvent peak: * DMSO.

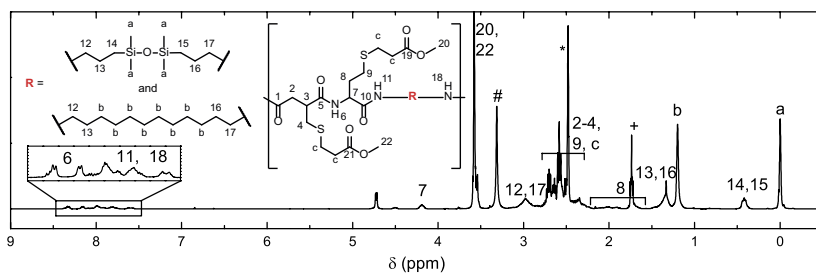


Figure A.10: ^1H NMR spectrum of polymer **P2** prepared from bis(thiolactone) **155** and BTD/DAD. Residual solvent peaks: * DMSO, # H_2O , + THF.

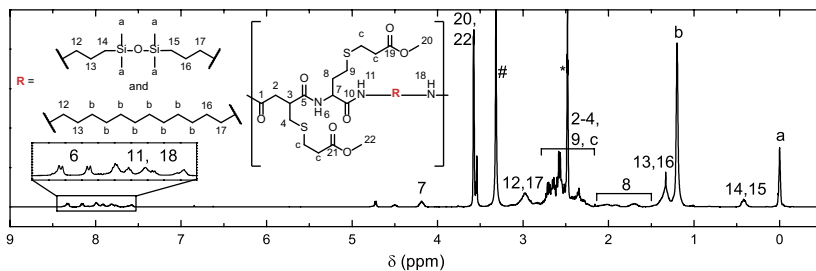


Figure A.11: ^1H NMR spectrum of polymer **P3** prepared from bis(thiolactone) **155** and BTD/DAD. Residual solvent peaks: * DMSO, # H_2O .

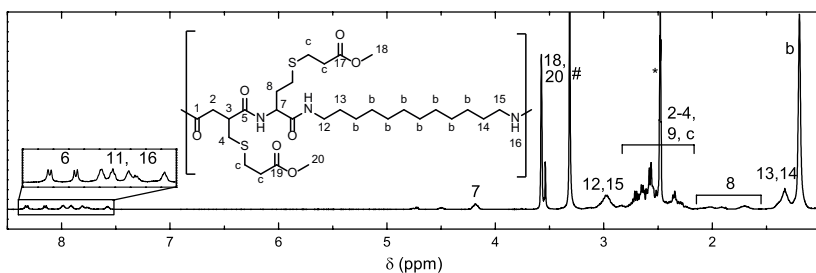


Figure A.12: ^1H NMR spectrum of polymer **P4** prepared from bis(thiolactone) **155** and DAD. Residual solvent peaks: * DMSO, # H_2O .

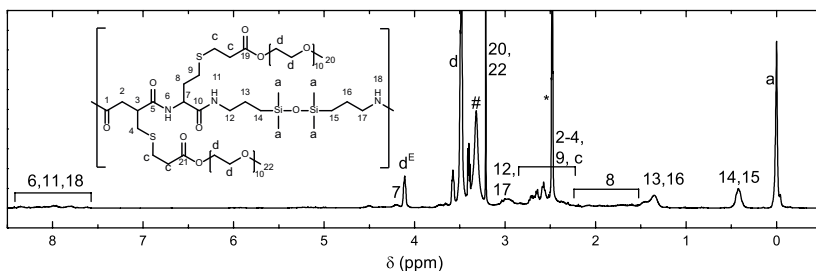


Figure A.13: ^1H NMR spectroscopy of the polymer **P5** obtained by post-polymerization modification of a thiol-functional polyamide. Residual solvent peaks: * DMSO, # H_2O . The ^1H NMR spectrum of **P6** is identical; only the intensity of the signal $\underline{d^E}$ is higher.

A.2.2 Other

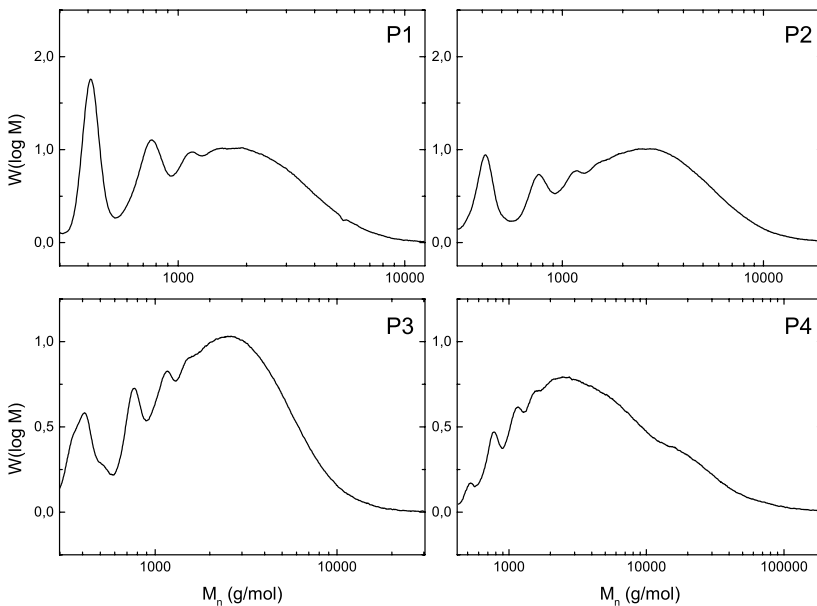


Figure A.14: SEC traces of methyl acrylate-functional polyamides with different ratios of BTD:DAD showing **P1** (1:0), **P2** (0.5:0.5), **P3** (0.25:0.75) and **P4** (0:1).

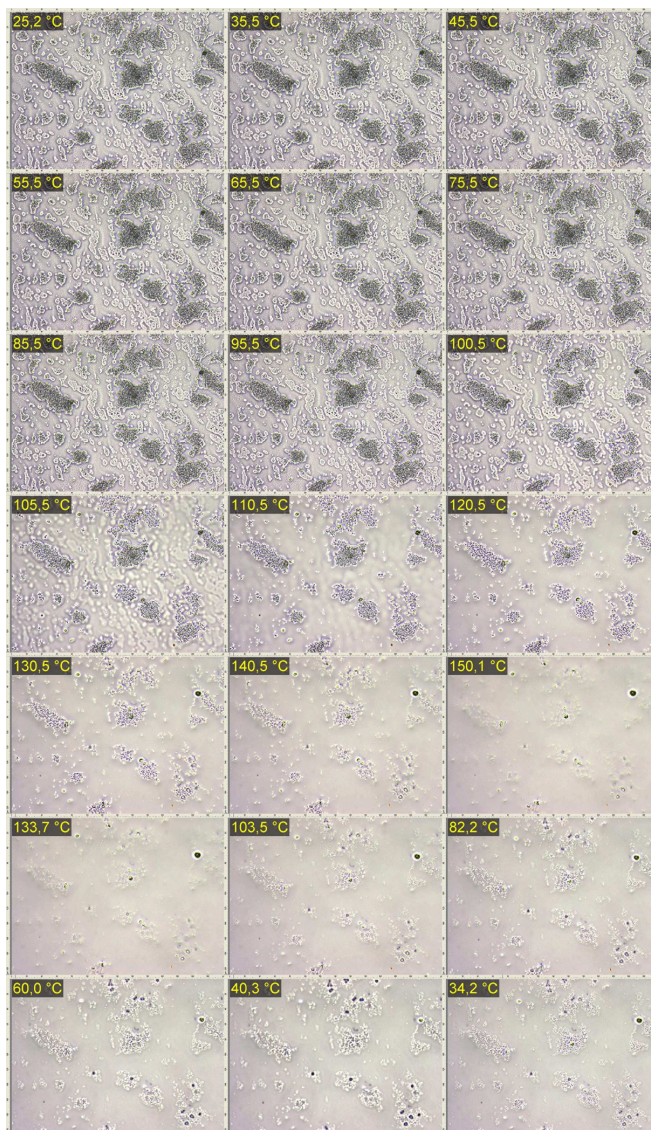


Figure A.15: Optical micrographs of **P4** (BTD:DAD, 0:1), heated to 150 °C with a heating rate of 3 K·min⁻¹. Subsequently, the sample temperature was held at 150 °C for 10 min prior to cooling the sample to room temperature by ambient air.

A.3 Epoxy Thiolactone Coupler

A.3.1 Crystallographic Data of 168

Suitable crystals for single crystal X-ray diffraction were obtained by recrystallization from CH_2Cl_2 as colourless blocks. Intensity data were collected on a Bruker D8 goniometer with a Bruker SMART APEX CCD area detector in ω -scan mode using Mo- K_α radiation ($\lambda = 0.71073 \text{ \AA}$) from an Incoatec microsource with multilayer optics at 100 K. Temperature was controlled with an Oxford Cryostream 700 instrument. Data were processed with SAINT⁴ and multi-scan absorption corrections were applied with SADABS.² The structure was solved by direct methods using SHELXS97³ and refined by full-matrix least-square procedures based on F_2 as implemented in SHELXL-2013.⁵ Non-hydrogen atoms were refined with anisotropic displacement parameters. The amino-H was found in difference fourier map; its coordinates were refined, and its U_{iso} was constrained to $U_{iso}(\text{H}) = 1.2 U_{eq}(\text{N})$; all other hydrogen atoms were placed in idealized positions with $U_{iso}(\text{H}) = 1.2 U_{eq}(\text{C})$. The asymmetric unit contains only one molecule which reveals to be disordered (Figure A.16). The disorder has been found around the stereocenter of the epoxide group, thus, representing a solid solution of diastereomers of the organic molecule. Within the epoxide end, carbon C8 and oxygen O4 are com-

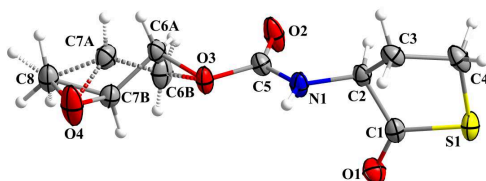


Figure A.16: Displacement ellipsoid plot of the asymmetric unit of **168** showing the majority (*SS*)-isomer (solid line) and the disordered, minority (*RS*)-epimer (dotted line) (drawn at 70% probability, labeled).

mon to both isomers, and their coordinates and displacement parameters were constrained to be equal in either isomer (SHELX commands EXYZ, EADP). In addition, restraints for the distances between C6A and C7A, and C6B and C7B were introduced. This similarity restraint (SADI) also restrains the distances between O3/C6A, O3/C6B, and O4/C7A, O4/C7B, and C8/C7A, C8/C7B (Figure A.16). Supplementary crystallographic data can be obtained free of charge from the Cambridge Crystallographic Data Centre via http://www.ccdc.cam.ac.uk/data_request/cif (CCDC 1447028).

Table A.2: Crystal data and refinement results of **168**.

Chemical formula	$C_8H_{11}NO_4S$
M_r	217.24
Crystal system, space group	Triclinic, $P\bar{1}$
T (K)	100(2)
a, b, c (\AA)	6.4922(13), 8.3800(17), 9.896(2)
α, β, γ ($^\circ$)	74.212(3), 73.241(3), 80.346(3)
V (\AA^3)	493.75(17)
Z	2
μ (mm^{-1})	0.316
Crystal shape, Crystal size (mm)	Colourless block, 0.29 x 0.21 x 0.15
Index ranges	$-7 \leq h \leq 7,$ $-10 \leq k \leq 10,$ $-11 \leq l \leq 11$
Reflections collected	5316
Independent reflections	1787 [$R_{int} = 0.0331$]
T_{min}, T_{max}	0.6612, 0.7452
Data / restraints / parameters	1787 / 4 / 150
Goodness-of-fit on F_2	1.044
Final R indices [$l > 2\sigma(l)$]	$R_1 = 0.0339, wR_2 = 0.0800$
R indices (all data)	$R_1 = 0.0397, wR_2 = 0.0832$
Largest diff. peak and hole	0.207 and $-0.191 e \cdot \text{\AA}^{-3}$

A.3.2 NMR and Raman Spectra

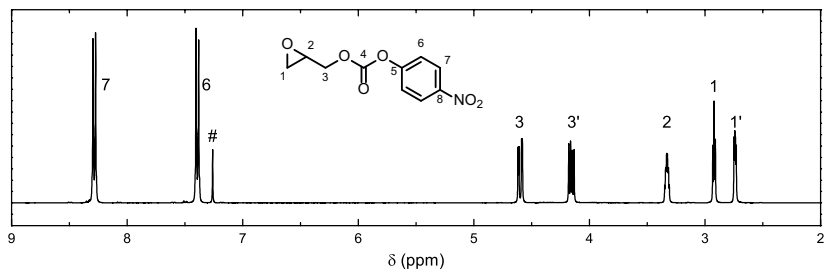


Figure A.17: ^1H NMR spectrum of *p*-nitrophenyl glycidyl carbonate **167**. Recorded in chloroform-*d* (#).

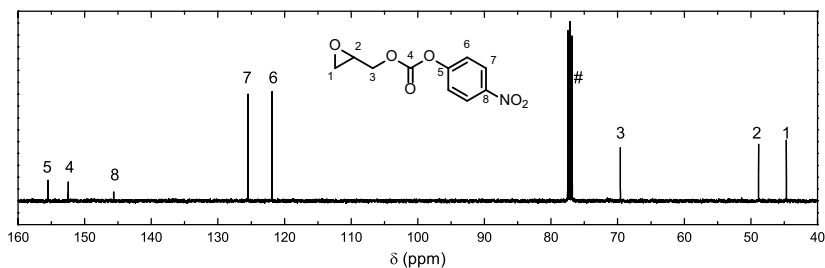


Figure A.18: ^{13}C NMR spectrum of *p*-nitrophenyl glycidyl carbonate **167**. Recorded in chloroform-*d* (#).

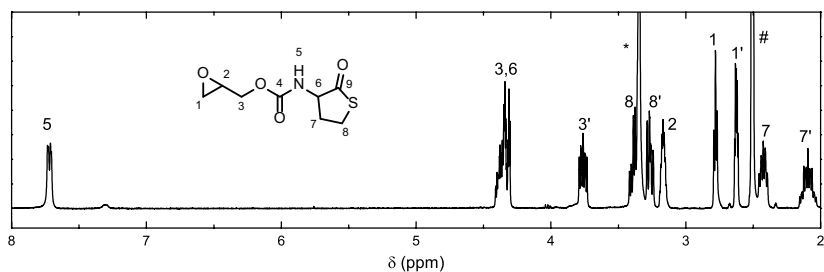


Figure A.19: ^1H NMR spectrum of epoxy thiolactone **168**. Recorded in DMSO-*d*₆ (#), residual solvent peaks: * H₂O and HDO.

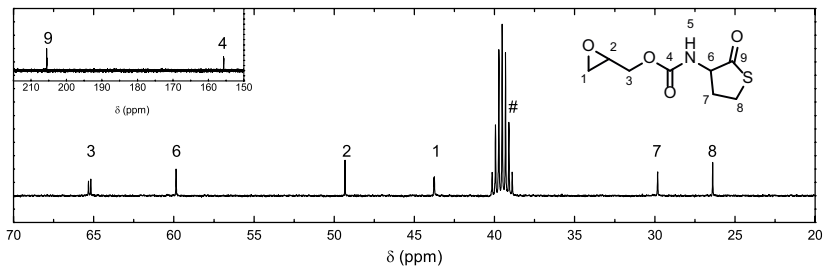


Figure A.20: ^{13}C NMR spectrum of epoxy thiolactone **168**. Recorded in DMSO- d_6 (#).

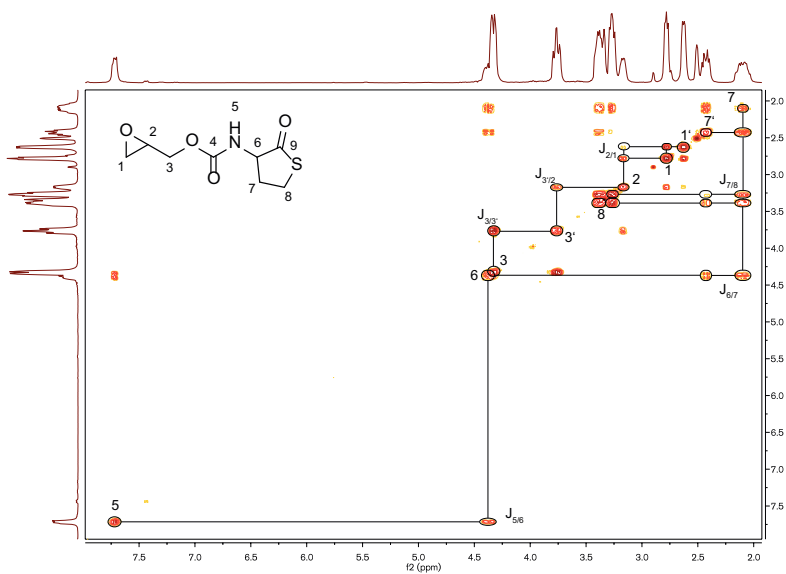


Figure A.21: $^1\text{H},^1\text{H}$ -COSY spectrum of epoxy thiolactone **168**. Recorded in DMSO- d_6 .

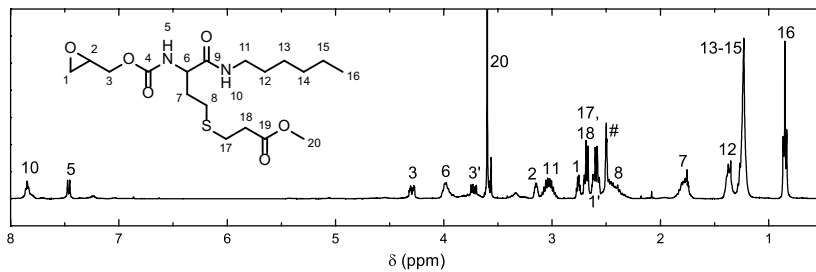


Figure A.22: ¹H NMR spectrum of epoxy thioether **169**. Recorded in DMSO-d₆ (#).

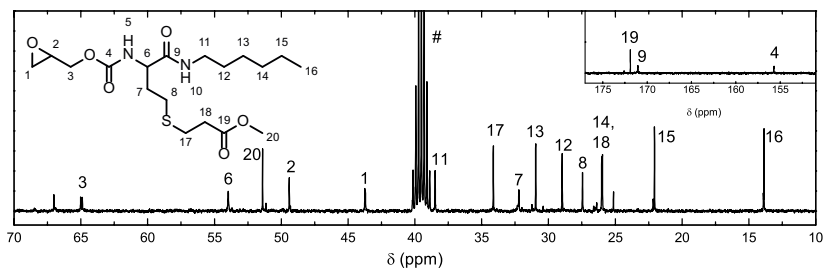


Figure A.23: ¹³C NMR spectrum of epoxy thioether **169**. Recorded in DMSO-d₆ (#).

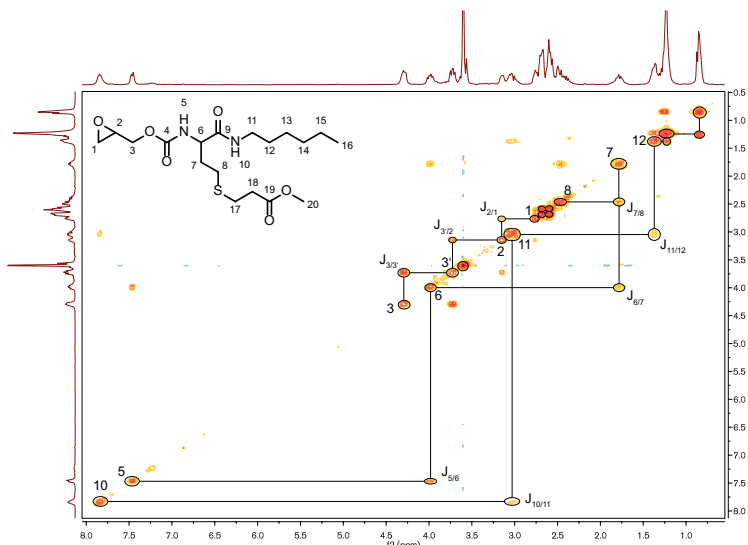


Figure A.24: $^1\text{H}, ^1\text{H}$ -COSY spectrum of epoxy thioether **169**. Recorded in DMSO-d_6 .

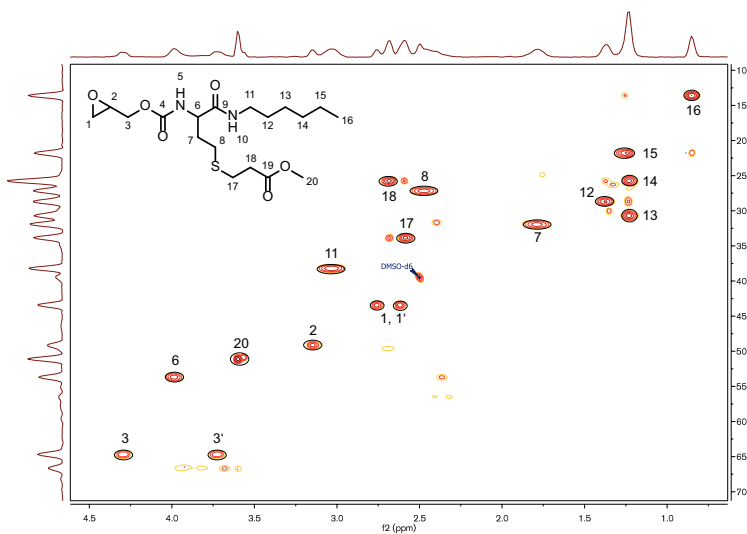


Figure A.25: HSQC spectrum of epoxy thioether **169**. Recorded in DMSO-d_6 .

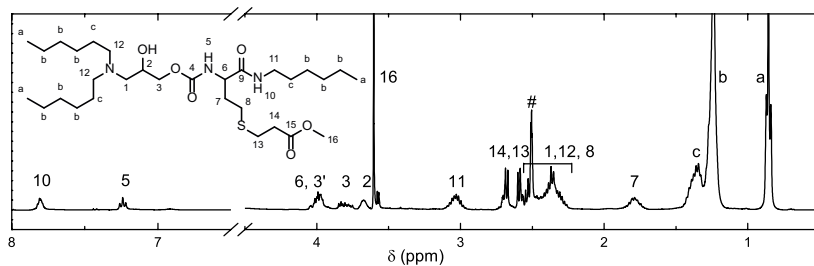


Figure A.26: ^1H NMR spectrum of trialkylamino thioether **170**. Recorded in DMSO-d_6 (#).

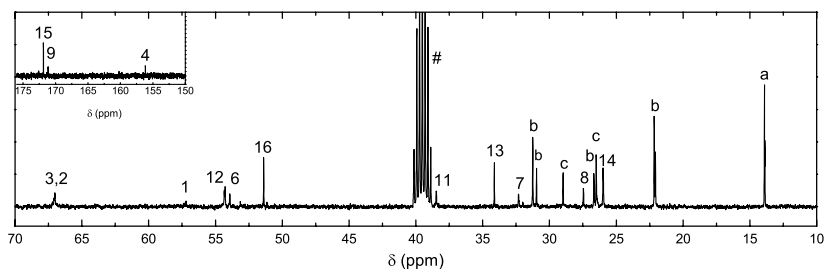


Figure A.27: ^{13}C NMR spectrum of trialkylamino thioether **170**. Recorded in DMSO-d_6 (#).

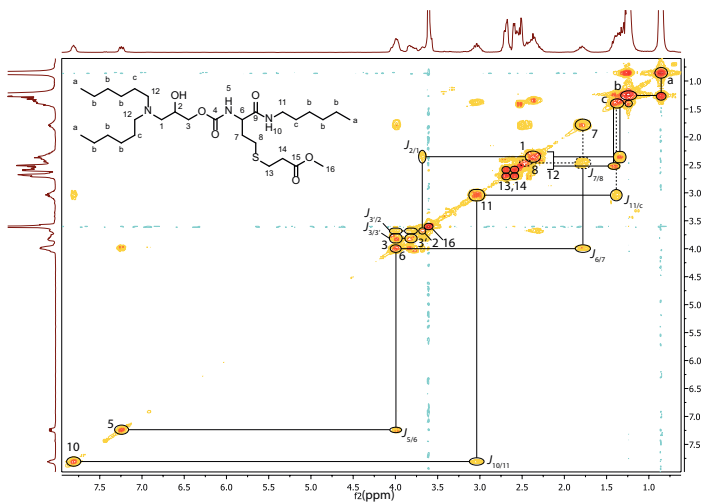


Figure A.28: ^1H , ^1H -COSY spectrum of trialkylamino thioether **170**. Recorded in DMSO-d_6 .

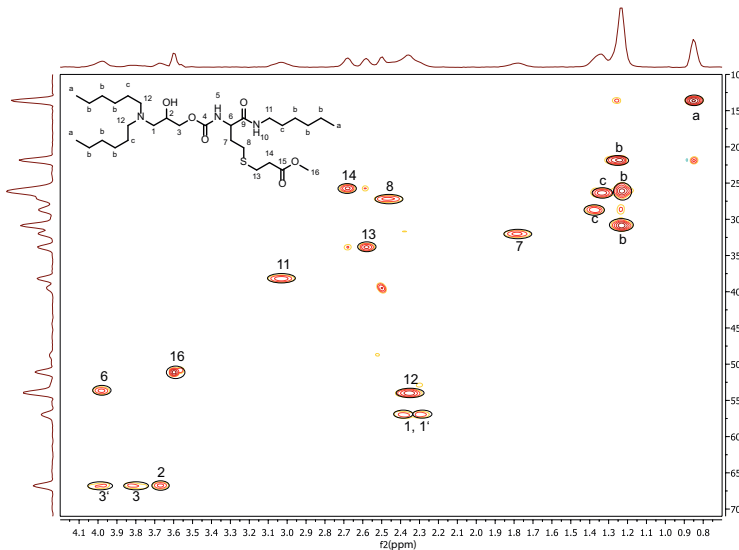


Figure A.29: HSQC spectrum of trialkylamino thioether **170**. Recorded in DMSO-d_6 .

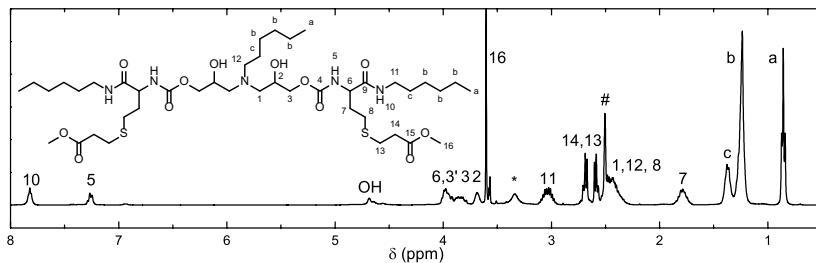


Figure A.30: ^1H NMR spectrum of trialkylamino bis(thioether) **173**. Recorded in DMSO-d_6 (#), residual solvent peaks: * H_2O and HDO .

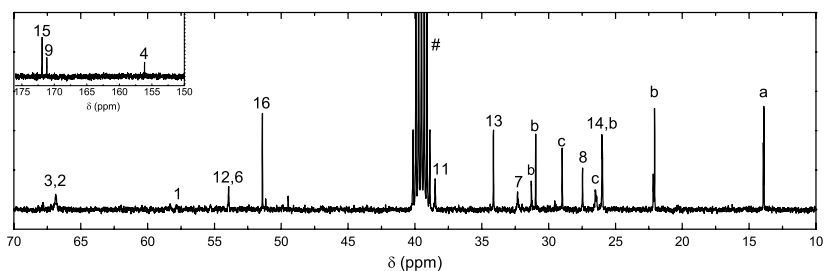


Figure A.31: ^{13}C NMR spectrum of trialkylamino bis(thioether) **173**. Recorded in DMSO-d_6 (#).

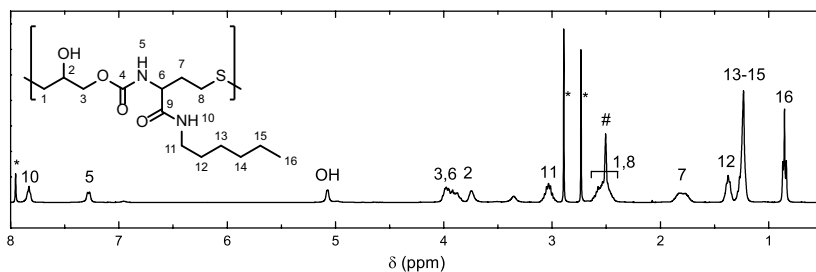


Figure A.32: ^1H NMR spectrum of poly(TEU) **172**. Recorded in DMSO-d_6 (#), residual solvent peaks: * DMF.

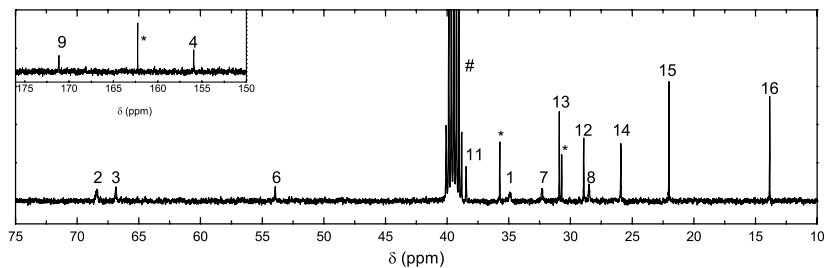


Figure A.33: ^{13}C NMR spectrum of poly(TU) 172. Recorded in DMSO- d_6 (#), residual solvent peaks: * DMF.

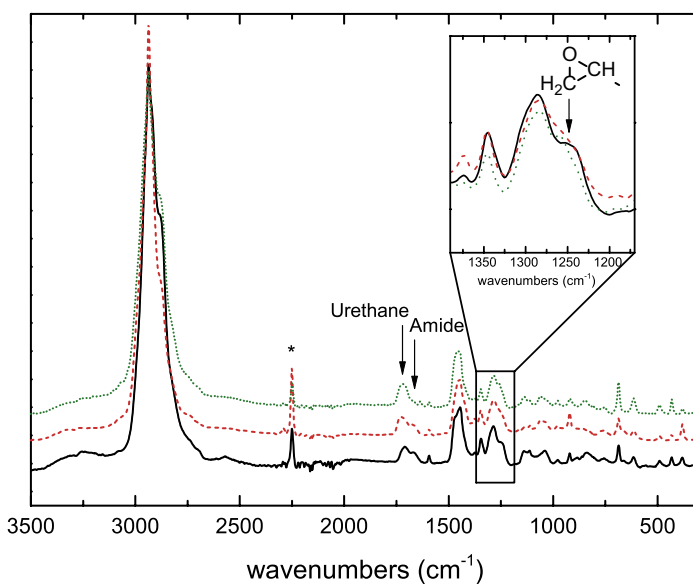


Figure A.34: Raman spectra of hydrogels obtained by thiol-epoxy polymerization (solid black line), and by multicomponent reaction using thiol-ene Michael addition with a PEG(X) diamine and TMPT (X = 2, dashed red line; X = 7, dotted green line). Inset graph shows the ring stretch band of the monosubstituted epoxide.

A.3.3 Kinetic Data

By online ^1H NMR spectroscopy the conversion of thiolactone ring (delivering k_1) and the disappearance of the epoxy signals (similar to the formation of polymer and rate constant k_2) was monitored. The samples were shimmed to the appropriate solvent without hexylamine at first. Then, hexylamine was added, the reaction started and the sample was reshimmed as fast as possible prior to the start of the kinetic measurement series. Once the first measurement of the reactive mixture was started, measurements (which lasted exactly 18 s) were conducted in a time interval of 30 minutes for a total time of 24 or 50 hours. Therefore, the final times used for the fitting of the kinetic data plots were corrected. The resulting data plots were fitted to the first order kinetic law. The fact,

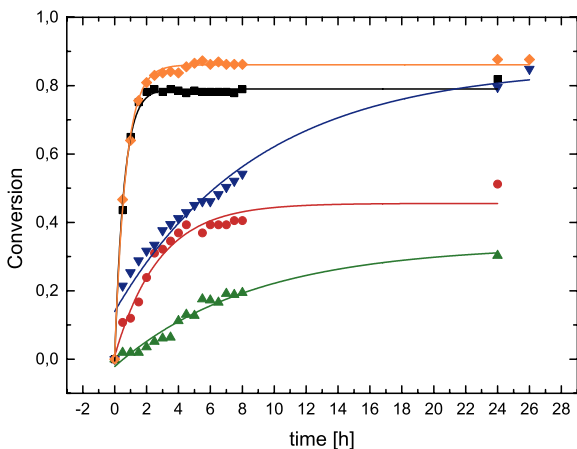


Figure A.35: Conversion Vs. time plot of the thiol-epoxy reaction using 3 mol% of LiOH (■), TBD (●), NaOEt (▲), DBU (▼) and KOtBu (◆) as base.

that without the use of the catalyst only the thiolactone ring is opened, makes a step wise reaction possible. Thus, the efficiency of the catalysts only in the thiol-epoxy reaction was evaluated first. To achieve this, the thiolactone was opened in absence of a base. After 20 to 24 h, a corre-

sponding base was added, and conversion vs. time plots were produced. This time DMAP was excluded as it turned out to be not effective for the polymerization. Instead and additionally to LiOH and DBU, TBD, NaOEt and KOtBu were used (each 3 mol%). The conversion vs. time plot shows that KOtBu ($pK_a = 17$) works equally fast as LiOH, both reaching a conversion plateau after only four to six hours. DBU ($pK_a = 13.5$) shows a slower start but reaches the same conversion ($\sim 85\%$) at 26 h as KOtBu. Yet from the progression of the data points it is assumed, that the reaction is not finished at 26 h, since no plateau is detected. With the use of TBD ($pK_a = 15.2$) and after 24 h, only 51% of the epoxy thiol is converted to the product polymer. And finally using NaOEt ($pK_a = 15.9$) as base, a very slow conversion is found. After 24 h only 30% of the epoxy thiol has reacted (Figure A.35).

A.3.4 Polymerization Parameters

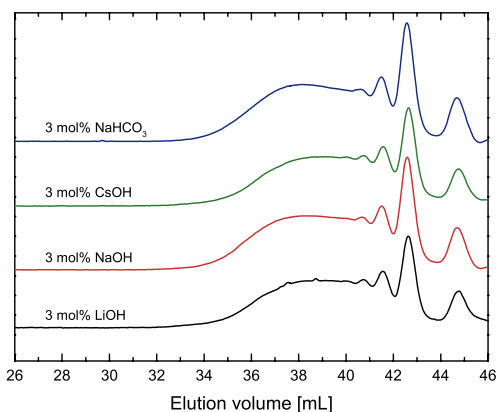


Figure A.36: Influence of the alkaline catalysts on the SEC elution curves of the resulting poly(thioether urethane)s.

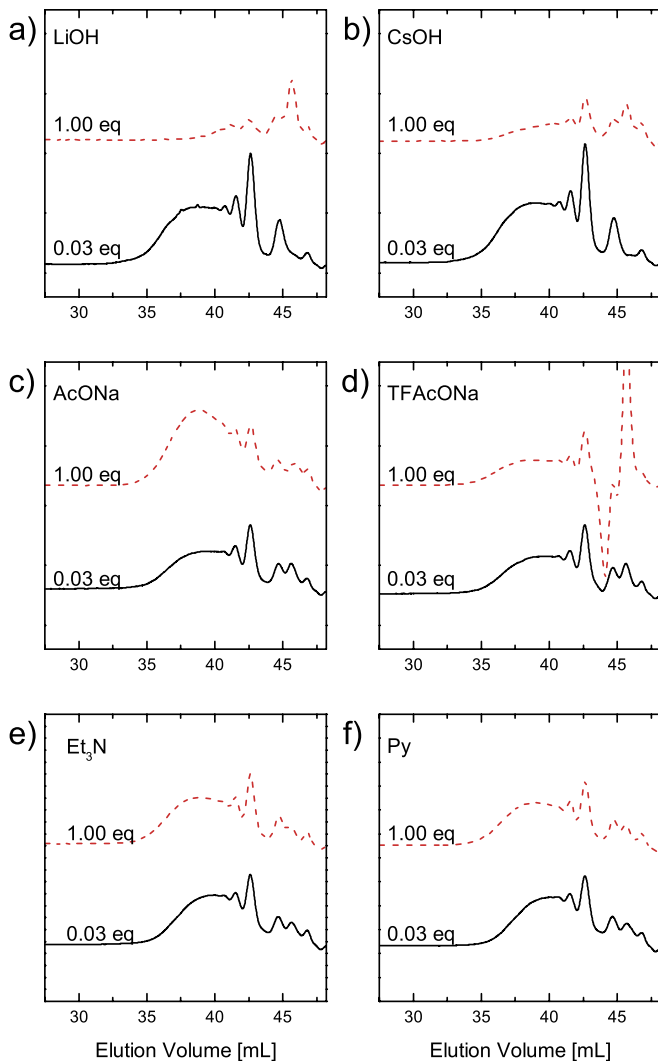


Figure A.37: SEC elution curves for poly(thioether urethane)s with 0.03 eq (solid black lines) or 1.00 eq (dashed red lines) of a) LiOH, b) CsOH, c) sodium acetate, d) sodium trifluoroacetate, e) triethylamine and f) pyridine.

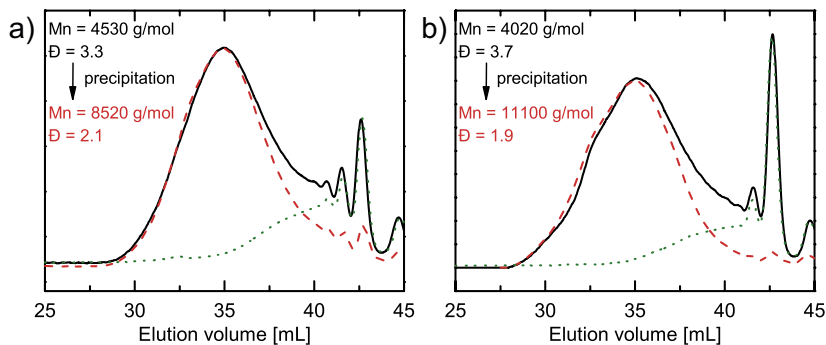


Figure A.38: Precipitation of poly(TEU) **172** from DMF in MeCN showing the elugram of the crude unpurified poly(TEU) (solid black line) the purified polymer (dashed red line) and the mother liquor (dotted green line). Synthesis conditions: a) $c(\mathbf{168}) = 1.50$ M, THF/H₂O (90:10), RT, 24 h, 3 mol% LiOH, 1 eq hexyl amine. b) $c(\mathbf{168}) = 0.25$ M, H₂O/MeCN (70:30), RT, 24 h, 3 mol% LiOH, 1 eq hexyl amine.

A.3.5 Cyclic Oligomer Assessment Test

To verify if in the lower molecular weight region cyclisation occurs, a cyclic oligomer assessment test was carried out. Selected samples were dissolved in THF (10 mg·mL⁻¹) and stirred with H₂O₂ for a maximum of 2 hours at room temperature. After 2 hours, 5 μ L of the reaction mixtures were mixed with solutions of sodium trifluoroacetate (0.5 μ L of 10 mg·mL⁻¹) and DCTB matrix (20 μ L of 20 mg·mL⁻¹) and directly spotted on the MALDI-TOF target.

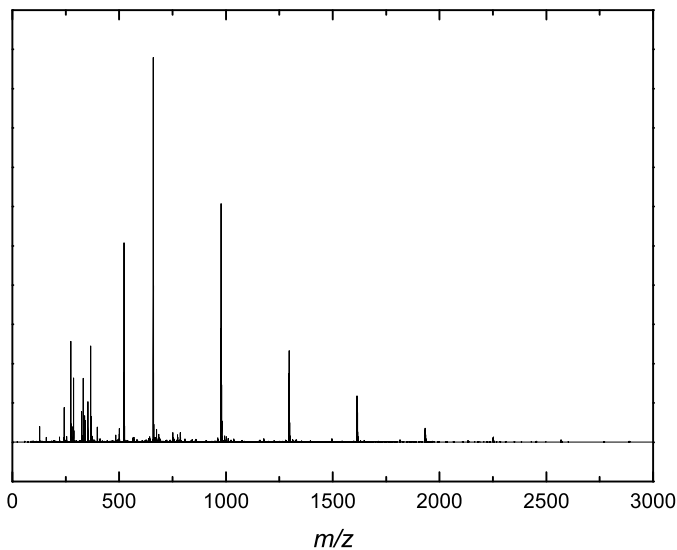


Figure A.39: MALDI-TOF MS spectrum of poly(thioether urethane) **172** prior oxidation by H_2O_2 .

Table A.3: MALDI-TOF MS data of poly(thioether urethane) **172** prior oxidation by H_2O_2 . Reported peaks describe masses of $[\text{M} + \text{Na}]^+$ ($\text{MW} = 22.99 \text{ g/mol}$).

N(Thioether Urethane)	m/z(calculated)	m/z(found)	Intensity (a.u.)
2	659.31	659.312	236966.94
3	977.47	977.469	143271.72
4	1295.63	1295.630	65216.42
5	1613.79	1613.794	28243.79
6	1931.95	1931.949	10005.37
7	2250.11	2250.118	2675.82
8	2568.27	2568.282	1037.08
9	2886.43	2886.444	383.80

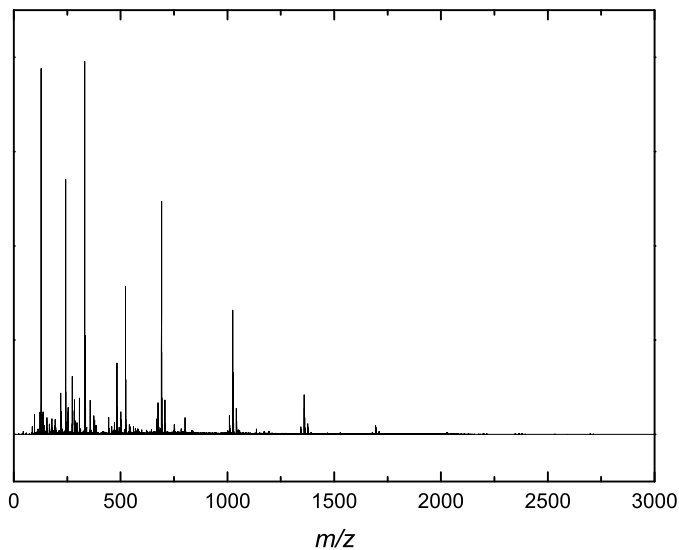


Figure A.40: MALDI-TOF MS spectrum of poly(sulfoxide urethane)s obtained through oxidation with H_2O_2 .

Table A.4: MALDI-TOF MS data of poly(sulfoxide urethane)s obtained through oxidation with H_2O_2 . Reported peaks describe masses of $[\text{M} + \text{Na}]^+$ (MW = 22.99 g/mol).

N(Thioether Urethane)	m/z(calculated)	m/z(found)	Intensity (a.u.)
2	691.31	691.334	207487.33
3	1025.47	1025.498	109529.30
4	1359.63	1359.665	34936.90
5	1693.79	1693.831	7591.84
6	2027.95	2027.996	1601.10

A.3.6 Amino Acid-based Poly(TEU)s: Spectra

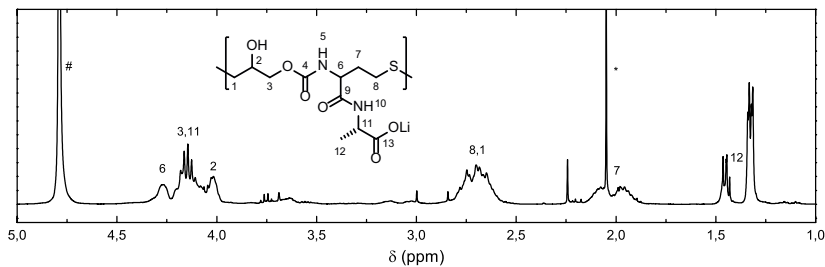


Figure A.41: ^1H NMR spectrum of poly(TEU) **175b**. Recorded in D_2O (#), residual solvent peaks: * Acetone.

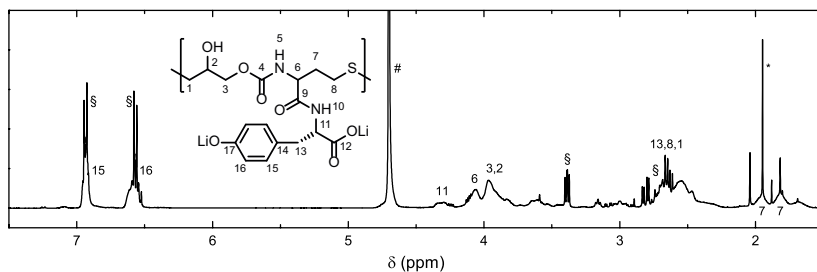


Figure A.42: ^1H NMR spectrum of poly(TEU) **175c**. Recorded in D_2O (#), residual solvent peaks: * Acetone. Remaining monomer traces are depicted by §.

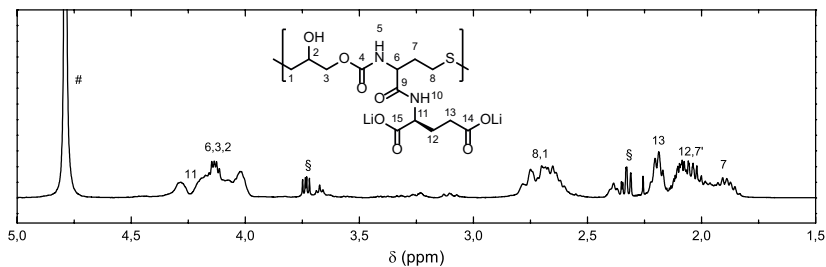


Figure A.43: ^1H NMR spectrum of poly(TEU) **175d**. Recorded in D_2O (#). Remaining monomer traces are depicted by §.

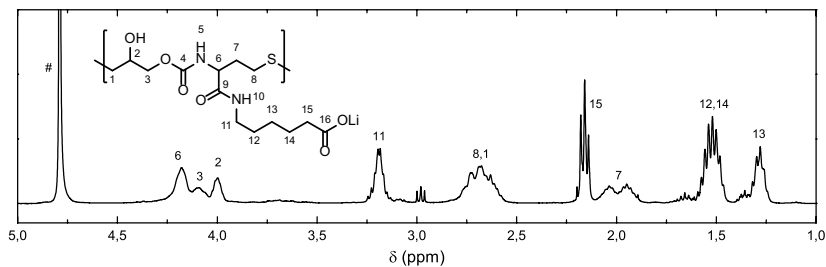


Figure A.44: ^1H NMR spectrum of poly(TEU) **176a**. Recorded in D_2O (#).

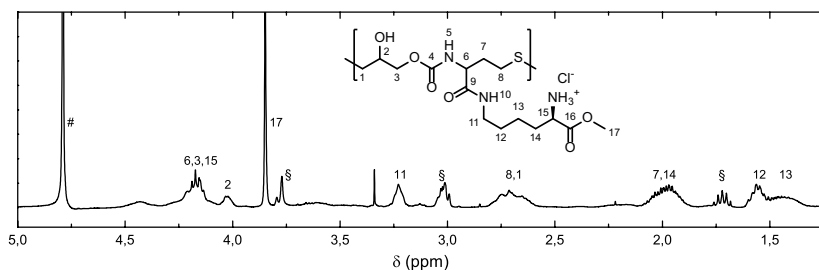


Figure A.45: ^1H NMR spectrum of poly(TEU) **177b**. Recorded in D_2O (#). Remaining monomer traces are depicted by §.

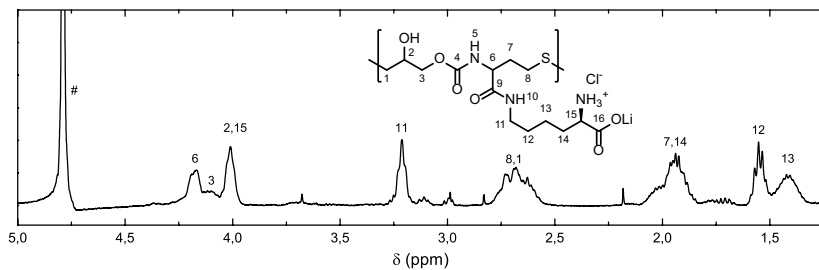


Figure A.46: ^1H NMR spectrum of poly(TEU) **177c**. Recorded in D_2O (#).

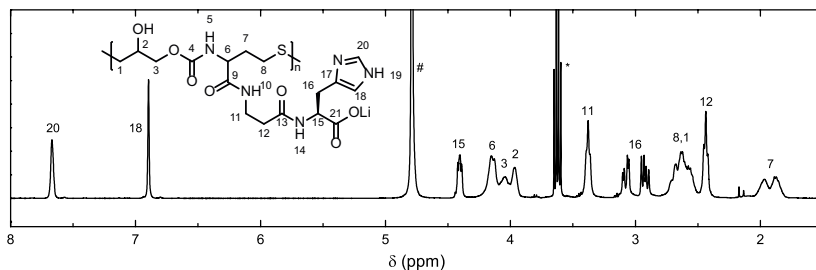


Figure A.47: ^1H NMR spectrum of poly(TEU) **178**. Recorded in D_2O (#), residual solvent peaks: * Ethanol.

A.3.7 Amino Acid-based Poly(TEU)s: Other

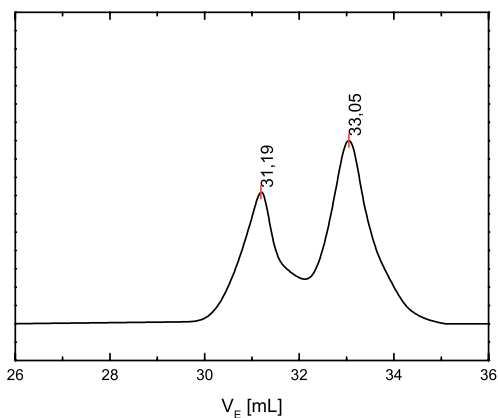


Figure A.48: SEC profile of NaCl salt peaks, which occur through neutralization of $\text{NaNO}_3/\text{NaN}_3$ with alkaline poly(TEU) **177c**.

Refractive index measurements: According to Bashkatov et al, the refractive index of water at $40\text{ }^\circ\text{C}$ with a wavelength of 361.05 nm is $n = 1.3454$.⁶ Thus the device wavelength was adjusted to 361.05 nm . First an aqueous $\text{NaNO}_3/\text{NaN}_3$ ($0.1\text{ M}/0.01\text{ wt}\%$) was measured against water. The difference in n was 0.049 . Now a corrected refractive index for the SEC

eluent is calculated ($n = 1.3454 + 0.049 = 1.3944$) which was taken for the future measurements of **177b** in the SEC eluent. The chosen polymer concentrations were $c = 0.1, 0.5, 1.0, 2.5, 5.0, 7.5, 10.0$ mg/mL.

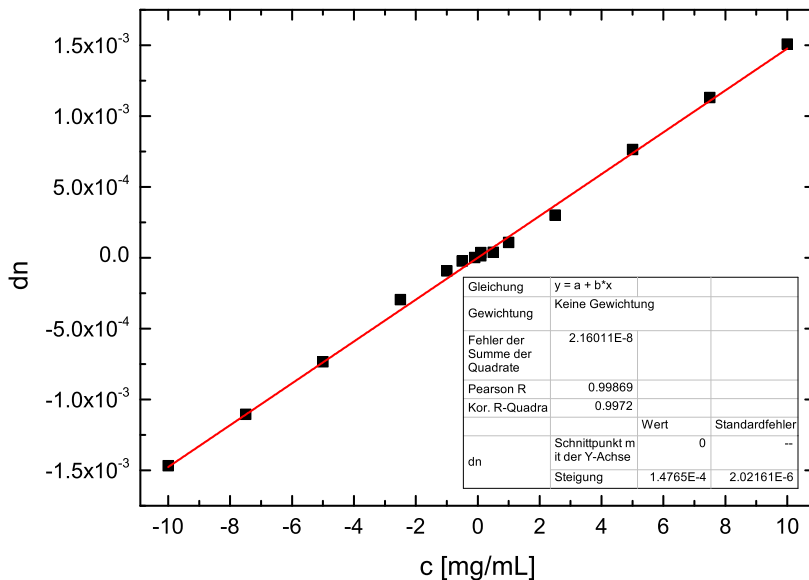


Figure A.49: dn/dc measurements for polymer **177b** with different concentrations (■) and respective linear fit (red line) to determine the dn/dc value.

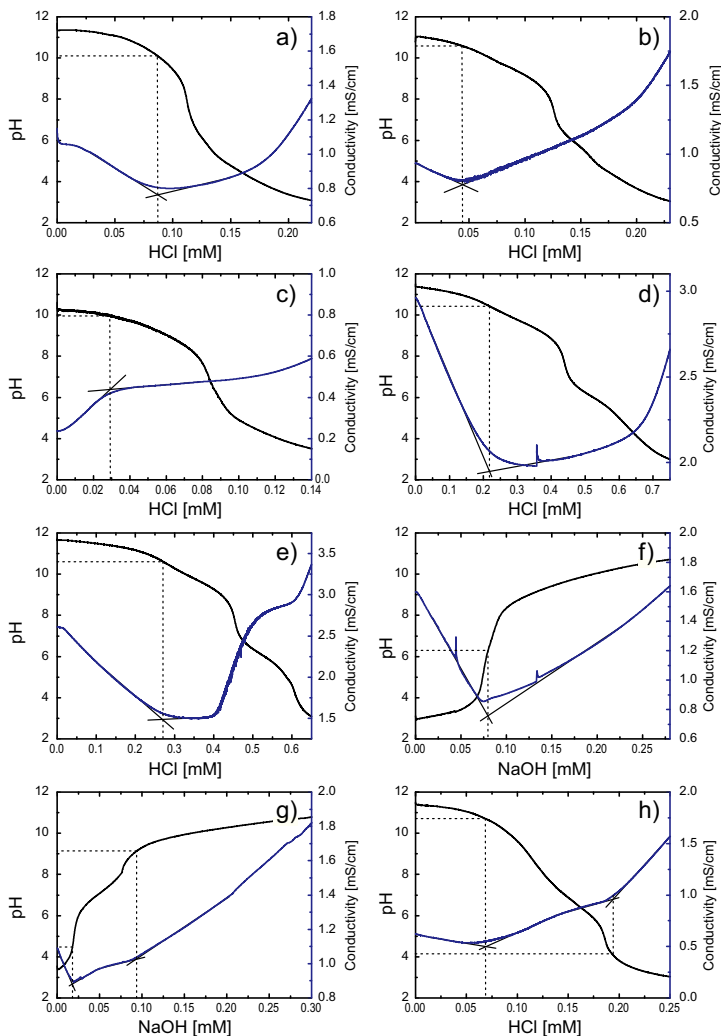


Figure A.50: Autotitration experiments showing the pH trace (black line) and the conductivity (blue line) of poly(TEU)s a) **175a** (glycine), b) **175b** (L-alanine), c) **175c** (L-tyrosine), d) **175d** (L-glutamic acid), e) **176a** (EACA), f) **177b** (L-lysine methyl ester), g) **177c** (L-lysine) and h) **178** (L-carnosine).

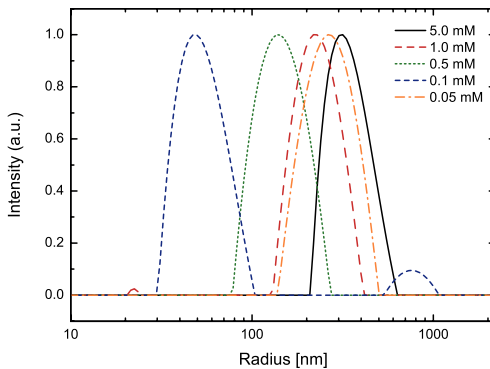


Figure A.51: DLS measurements of PEC with different concentrations of the starting polymers.

References

- (1) Bruker *SAINT+*, Version 6.02. Bruker AXS Inc. **1999**, Madison, Wisconsin, USA.
- (2) Sheldrick, G. M. *SADABS*, Version 2.03. **1996**, University of Göttingen, Germany.
- (3) Sheldrick, G. M. *Acta Crystallographica* **2008**, A64, 112–122.
- (4) Bruker *SAINT and SAINT#*, Program for Reduction of Data Collected on Bruker CCD Area Detector diffractometer, Version 7.68, Bruker AXS Inc. **2009**, Madison, Wisconsin, USA.
- (5) Sheldrick, G. M. *SHELXL13*, Program package for crystal structure determination for single crystal diffraction **2013**, University of Göttingen, Germany.
- (6) Bashkatov, A. N.; Genina, E. A. *Proc. SPIE* **2003**, 5068, 393–395.

List of Abbreviations

AGE	allyl glycidyl ether
ATRP	atom transfer radical polymerization
BOC	<i>tert</i> -butyloxycarbonyl
BSA	bovine serum albumin
BTD	bis(aminopropyl)tetramethyldisiloxane
COLBERT	Catalytic Opening of Lateral Benzoxazine Rings by Thiols
COSY	correlated spectroscopy
CTA	chain transfer agent
CuAAC	Copper-catalyzed azide-alkyne cycloaddition
\bar{D}	dispersity (M_w/M_n)
DA	Diels-Alder
DA_{inv}	inverse electron demand Diels-Alder
DABCO	1,4-diazabicyclo[2.2.2]octane
DAD	1,12-diaminododecane
DBU	1,8-Diazabicyclo[5.4.0]undec-7-en
DHA	dihexylamine
DIPEA	diisopropylethylamine
DLS	dynamic light scattering
DMAP	dimethylaminopyridine
DMF	dimethylformamid
DMPA	2,2-dimethoxy-2-phenylacetophenone

DMSO	dimethylsulfoxide
DSC	Differential Scanning Calorimetry
DTT	1,4-dithio-D-threitol
EACA	ε -aminocaproic acid
EEGE	ethoxy ethyl glycidyl ether
eq	equivalent(s)
ESI	Electrospray Ionization
FESEM	field emission scanning electron microscopy
HA	hexylamine
HCTL	homocysteine thiolactone
HFPO	hexafluoropropylene oxide
HOMO	highest occupied molecular orbital
HSQC	heteronuclear single quantum coherence
KPS	potassium peroxydisulfate
LUMO	lowest unoccupied molecular orbital
M_n	number average molecular weight
MA	methyl acrylate
MALDI-TOF		Matrix Assisted Laser Desorption Ionisation - Time Of Flight
MALLS	multiangle laser light scattering
MBS	<i>meta</i> -imidobenzoyl N-hydroxysuccinimide ester
Mp	melting point
NALDI-TOF		Nanocrystal Assisted Laser Desorption Ionisation - Time Of Flight
NCA	N-carboxyanhydrides
NIPAAm	N-isopropylacrylamide
NMR	Nuclear Magnetic Resonance
o/w	oil-in-water
PCL	poly(ε -caprolactone)
PDMS	poly(dimethyl siloxane)
PEC	polyelectrolyte complexes
PEG	poly(ethylene glycol)
PEI	poly(ethylene imine)

PLA	poly(lactic acid)
PMMA	poly(methyl methacrylate)
PPO	poly(propylene oxide)
PS	polystyrene
PTHF	polytetrahydrofuran
PU	polyurethane
quant.	quantitative
RAFT	Reversible Addition-Fragmentation chain Transfer
ROP	Ring-opening polymerization
RZDP	Ruggli-Ziegler dilution principle
SEC	Size Exclusion Chromatography
spAAC	strain-promoted azide-alkyne cycloaddition
sulfo-SMCC	sulfosuccinimidyl 4-(N-maleimidomethyl)cyclohexane-1-carboxylate
TBD	1,5,7-triazabicyclo[4.4.0]dec-5-ene
tBGE	<i>tert</i> -butyl glycidyl ether
TCEP	tris(2-carboxyethyl)phosphine
TEA	triethylamine
TEU	thioether urethane
TFA	trifluoroacetic acid
T_g	glass transition temperature
THF	tetrahydrofuran
TMPT	trimethylolpropane triacrylate
V_E	elution volume
XRD	X-ray Diffraction

List of Figures

- 1.1 Diversity and number of building blocks in relation to the complexity of the created systems and architectures, distinguishing organic chemistry (black bars) from nature (red bar). 2
- 1.2 Complex structures need advanced connection chemistries. Therefore, three major synthetic pathways are disclosed: Connection of building blocks, polymer functionalization and polymer synthesis. 3
- 1.3 General requirements for efficient reactions providing advanced connections between multiple molecules. 4
- 3.1 Compilation of thiol-X reactions. 37
- 4.1 Comparison of the ^{13}C NMR spectra of (*RR/SS*)-**148** (top) and the enriched *RS/SR* diastereomeric mixture (bottom). . . 77

- 4.2 Displacement ellipsoid plot of two asymmetric units of the *RR/SS* diastereomer forming a dimer (drawn at 80% probability, color code: C - black, H - white, O - red, N - blue, S - yellow). 78
- 4.3 Comparison of the ^1H NMR spectra of the multifunctional coupler (**148**), the thiol (**149**), thioether **150**, thiol-alcohol **151**, thioether alcohol **152** and the fully functionalized coupler **153**. Residual solvent peaks: * H_2O , # DMSO, § CH_2Cl_2 . 79
- 5.1 ^1H NMR spectra of bis(thiolactone) **155** and the corresponding products resulting from the model reactions with hexylamine and methyl acrylate to deliver **162** and **163**, respectively. Residual solvent peaks: * DMSO, + Acetone, # H_2O , § CH_2Cl_2 99
- 5.2 ^1H NMR spectrum of polymer **P1** prepared from bis(thiolactone) **155** and BTD. Residual solvent peaks: * DMSO, # H_2O , + THF. 101
- 5.3 DSC first heating curve for polyamides with different ratios of BTD:DAD showing **P1** (1:0, solid), **P2** (0.5:0.5, dash), **P3** (0.25:0.75, dot) and **P4** (0:1, dash dot). 103
- 5.4 X-ray diffraction pattern of polymer **P4** (BTB:DAD, 0:1) with baseline (red). Only minor crystalline peaks are observed (c). Two big diffusion halos (a) dominate the diffraction pattern and superimpose with the remaining crystalline signals. Therefore, only low crystallinity is estimated (crystallinity could not be calculated due to the high amorphous content of the polymer). * marks an artifact peak caused by the detector. 104

- 5.5 a) SEC elugrams of the thiol-functional precursor (black line) and product **P5** (red line). b) Overlapping elugrams showing the thiol-functional polymer precursor (black line), the acrylate-functional PEG with a $M_n = 1700$ g/mol (dashed red line) and the final product **P6** (solid red line). c) Raman spectra of the starting thiol-functional polymer (black line) and product **P5** (red line) obtained by post-polymerization modification. 105
- 6.1 Displacement ellipsoid plot of a) the asymmetric unit of **168** showing the major structure of the (*SS*)-isomer (solid line) and the disordered, minor structure of the (*RS*)-epimer (dotted line) and b) two asymmetric units of the (*RR/SS*) enantiomers forming a dimer. Structure drawn at 70% probability, colour code: C - grey, H - white, N - blue, O - red, S - yellow. 126
- 6.2 ^1H NMR spectra of educt **168** (top) and model compounds **169** (mid) and **170** (bottom). 128
- 6.3 Online ^1H NMR kinetic data of the one-pot polyaddition of epoxy thiolactone **168** showing the consumption of the thiolactone ring by hexylamine (■) and the formation of poly(TEU)s by thiol-epoxy addition (●) with the use of a) no catalyst, b) DMAP (6 mol%), c) LiOH (3 mol%) and d) DBU (6 mol%). The overlaying solid lines represent respective fits. Inset graphs show the SEC elution curve of the corresponding polymer products with number average molecular weights and dispersity indices (M_w/M_n or \mathcal{D}). 131

- 6.4 SEC elugrams of poly(TEU)s examining the influence of a) LiOH concentration, b) DBU concentration, c) monomer concentration, d) solvent polarity and e) acetonitrile-water mixtures. 132
- 6.5 MALDI-TOF spectra of the cyclic oligomer assessment test. a) shows the full spectrum (left); a single peak (inset) and a magnification with selected mass increments of the poly(TEU). b) shows the MALDI-TOF data of the resulting oxidized product obtained from the reaction with H₂O₂. Again a full spectrum (left), a single peak (inset) and a magnification with selected mass increments of the oxidized product (right) is presented. 138
- 6.6 Yellow bulk hydrogel obtained by thiol-epoxy polymerization (a) and multicomponent reaction with TMPT and a PEG(X) diamine, b) X = 2, c) X = 7. d) shows a magnification of the corresponding Raman spectra (a,b,c). The ring stretch band of mono-substituted epoxy group appears as a shoulder. 140
- 6.7 ¹H NMR spectra of educt **168** and glycine-functional poly(TEU) **175a**. Recorded in D₂O (#), residual solvent peaks: * DMSO, § acetone. 159
- 6.8 SEC profiles of functional poly(TEU)s: a) **175a** (glycine) showing the crude product (dashed blue) and the purified polymer (solid black), b) **175b** (alanine), c) **175c** (tyrosine), d) **175d** (glutamic acid), e) **176a** (EACA), f) **176b** (solid black) and BOC deprotected **177b** (red dash dot), g) **176c** (solid black) and BOC deprotected **177c** (RI signal: red dash dot; MALLS signal: red dot) and h) **178** (L-carnosine) as crude (dashed blue) and purified product (solid black). 163

- 6.9 FESEM micrographs of polymer a) **175a** (scale bar 20 μm) and b) a magnification of the crystalline structure (scale bar 3 μm). Micrographs c) and magnification d) show polymer **177b** as white spots (scale bar 10 μm and 500 nm, respectively). Micrographs e) and magnification f) show a possible clusters of PEC particles (scale bar 4 μm and 1 μm , respectively.) 169
- A.1 ^{13}C spectrum of thiol **149**. Residual solvent peak: # DMSO. 191
- A.2 ^{13}C spectrum of thiol **150**. Residual solvent peak: # DMSO. 191
- A.3 ^{13}C spectrum of thiol **151**. Residual solvent peak: # DMSO. 191
- A.4 ^{13}C spectrum of thiol **152**. Residual solvent peaks: # DMSO, * CH_2Cl_2 192
- A.5 ^{13}C spectrum of thiol **153**. Residual solvent peaks: # DMSO, * EtOAc. 192
- A.6 $^1\text{H},^1\text{H}$ -COSY spectrum of isomeric thiol alcohols **179a** and **179b**. Residual solvent peaks: * H_2O , # DMSO, § DMF. . . 194
- A.7 $^1\text{H},^1\text{H}$ -COSY of the bis(thiolactone) **155**. 195
- A.8 a) ^{13}C NMR spectrum and b) DEPT135 spectrum of bis(thiolactone) **155**. Residual solvent peak: * DMSO. . . . 195
- A.9 HSQC of bis(thiolactone) **155**. Residual solvent peak: * DMSO. 196

- A.10 ^1H NMR spectrum of polymer **P2** prepared from bis(thiolactone) **155** and BTD/DAD. Residual solvent peaks: * DMSO, # H_2O , + THF. 196
- A.11 ^1H NMR spectrum of polymer **P3** prepared from bis(thiolactone) **155** and BTD/DAD. Residual solvent peaks: * DMSO, # H_2O 197
- A.12 ^1H NMR spectrum of polymer **P4** prepared from bis(thiolactone) **155** and DAD. Residual solvent peaks: * DMSO, # H_2O 197
- A.13 ^1H NMR spectroscopy of the polymer **P5** obtained by post-polymerization modification of a thiol-functional polyamide. Residual solvent peaks: * DMSO, # H_2O . The ^1H NMR spectrum of **P6** is identical; only the intensity of the signal d^E is higher. 197
- A.14 SEC traces of methyl acrylate-functional polyamides with different ratios of BTD:DAD showing **P1** (1:0), **P2** (0.5:0.5), **P3** (0.25:0.75) and **P4** (0:1). 198
- A.15 Optical micrographs of **P4** (BTD:DAD, 0:1), heated to 150 °C with a heating rate of 3 K·min⁻¹. Subsequently, the sample temperature was hold at 150 °C for 10 min prior to cooling the sample to room temperature by ambient air. . 199
- A.16 Displacement ellipsoid plot of the asymmetric unit of **168** showing the majority (*SS*)-isomer (solid line) and the disordered, minority (*RS*)-epimer (dotted line) (drawn at 70% probability, labeled). 200

A.17 ^1H NMR spectrum of <i>p</i> -nitrophenyl glycidyl carbonate 167 . Recorded in chloroform-d (#).	202
A.18 ^{13}C NMR spectrum of <i>p</i> -nitrophenyl glycidyl carbonate 167 . Recorded in chloroform-d (#).	202
A.19 ^1H NMR spectrum of epoxy thiolactone 168 . Recorded in DMSO- d_6 (#), residual solvent peaks: * H_2O and HDO. . . .	202
A.20 ^{13}C NMR spectrum of epoxy thiolactone 168 . Recorded in DMSO- d_6 (#).	203
A.21 $^1\text{H}, ^1\text{H}$ -COSY spectrum of epoxy thiolactone 168 . Recorded in DMSO- d_6	203
A.22 ^1H NMR spectrum of epoxy thioether 169 . Recorded in DMSO- d_6 (#).	204
A.23 ^{13}C NMR spectrum of epoxy thioether 169 . Recorded in DMSO- d_6 (#).	204
A.24 $^1\text{H}, ^1\text{H}$ -COSY spectrum of epoxy thioether 169 . Recorded in DMSO- d_6	205
A.25 HSQC spectrum of epoxy thioether 169 . Recorded in DMSO- d_6	205
A.26 ^1H NMR spectrum of trialkylamino thioether 170 . Recorded in DMSO- d_6 (#).	206
A.27 ^{13}C NMR spectrum of trialkylamino thioether 170 . Recorded in DMSO- d_6 (#).	206

- A.28 $^1\text{H}, ^1\text{H}$ -COSY spectrum of trialkylamino thioether **170**.
Recorded in DMSO- d_6 207
- A.29 HSQC spectrum of trialkylamino thioether **170**. Recorded
in DMSO- d_6 207
- A.30 ^1H NMR spectrum of trialkylamino bis(thioether) **173**.
Recorded in DMSO- d_6 (#), residual solvent peaks: * H_2O
and HDO. 208
- A.31 ^{13}C NMR spectrum of trialkylamino bis(thioether) **173**.
Recorded in DMSO- d_6 (#). 208
- A.32 ^1H NMR spectrum of poly(TEU) **172**. Recorded in DMSO-
 d_6 (#), residual solvent peaks: * DMF. 208
- A.33 ^{13}C NMR spectrum of poly(TEU) **172**. Recorded in DMSO-
 d_6 (#), residual solvent peaks: * DMF. 209
- A.34 Raman spectra of hydrogels obtained by thiol-epoxy poly-
merization (solid black line), and by multicomponent reac-
tion using thiol-ene Michael addition with a PEG(X) diamine
and TMPT (X = 2, **dashed red line**; X = 7, **dotted green line**).
Inset graph shows the ring stretch band of the monosubstituted
epoxide. 209
- A.35 Conversion Vs. time plot of the thiol-epoxy reaction using
3 mol% of LiOH (■), TBD (●), NaOEt (▲), DBU (▼) and
KOtBu (◆) as base. 210
- A.36 Influence of the alkaline catalysts on the SEC elution curves
of the resulting poly(thioether urethane)s. 211

- A.37 SEC elution curves for poly(thioether urethane)s with 0.03 eq (solid black lines) or 1.00 eq (dashed red lines) of a) LiOH, b) CsOH, c) sodium acetate, d) sodium trifluoroacetate, e) triethylamine and f) pyridine. 212
- A.38 Precipitation of poly(TEU) **172** from DMF in MeCN showing the elugram of the crude unpurified poly(TEU) (solid black line) the purified polymer (dashed red line) and the mother liquor (dotted green line). Synthesis conditions: a) c(**168**) = 1.50 M, THF/H₂O (90:10), RT, 24 h, 3 mol% LiOH, 1 eq hexyl amine. b) c(**168**) = 0.25 M, H₂O/MeCN (70:30), RT, 24 h, 3 mol% LiOH, 1 eq hexyl amine. 213
- A.39 MALDI-TOF MS spectrum of poly(thioether urethane) **172** prior oxidation by H₂O₂. 214
- A.40 MALDI-TOF MS spectrum of poly(sulfoxide urethane)s obtained through oxidation with H₂O₂. 215
- A.41 ¹H NMR spectrum of poly(TEU) **175b**. Recorded in D₂O (#), residual solvent peaks: * Acetone. 216
- A.42 ¹H NMR spectrum of poly(TEU) **175c**. Recorded in D₂O (#), residual solvent peaks: * Acetone. Remaining monomer traces are depicted by §. 216
- A.43 ¹H NMR spectrum of poly(TEU) **175d**. Recorded in D₂O (#). Remaining monomer traces are depicted by §. 216
- A.44 ¹H NMR spectrum of poly(TEU) **176a**. Recorded in D₂O (#). 217
- A.45 ¹H NMR spectrum of poly(TEU) **177b**. Recorded in D₂O (#). Remaining monomer traces are depicted by §. 217

- A.46 ^1H NMR spectrum of poly(TEU) **177c**. Recorded in D_2O (#). 217
- A.47 ^1H NMR spectrum of poly(TEU) **178**. Recorded in D_2O (#), residual solvent peaks: * Ethanol. 218
- A.48 SEC profile of NaCl salt peaks, which occur through neutralization of $\text{NaNO}_3/\text{NaN}_3$ with alkaline poly(TEU) **177c**. . . 218
- A.49 dn/dc measurements for polymer **177b** with different concentrations (■) and respective linear fit (red line) to determine the dn/dc value. 219
- A.50 Autotitration experiments showing the pH trace (black line) and the conductivity (blue line) of poly(TEU)s a) **175a** (glycine), b) **175b** (L-alanine), c) **175c** (L-tyrosine), d) **175d** (L-glutamic acid), e) **176a** (EACA), f) **177b** (L-lysine methyl ester), g) **177c** (L-lysine) and h) **178** (L-carnosine). 220
- A.51 DLS measurements of PEC with different concentrations of the starting polymers. 221

List of Schemes

2.1	Heterobifunctional coupling agents based on a succinimide active ester and a maleimide moiety.	10
2.2	Silane coupling agent and homobifunctional coupling agents based on heterocycles used as chain extenders for polycondensates.	12
2.3	Hexafluoropropylene oxide coupling agent, coupling three active polymer chains of the same type.	13
2.4	Heterobi- and -trifunctional coupling agents, based on benzoxazinones and oxazolines, showing the selective conversion of each reactive cycle and the preparation of poly(ester amides).	14
2.5	Coupling agents based on acyl lactams and benzoxazinones.	15
2.6	Biscarbonate and bislactone couplers for the synthesis of hydroxy-functional PU/PA.	16
2.7	Carbonate coupler 26 as monomer for hydroxy-functional PU and building block for multifunctional polymers.	17
2.8	Alternative carbonate couplers with different carbonate bound leaving groups.	18
2.9	Biscyclic heterobifunctional couplers linked by different spacers.	19

2.10 Heterobifunctional azetidinium coupler based on piperazine and epichlorhydrin and its reactivity towards functional amines.	20
2.11 Reaction of azides with alkynes via the copper-catalyzed 1,3-dipolar azide-alkyne cycloaddition or the strain-promoted azide-alkyne cycloaddition.	22
2.12 Reaction of functional maleimides with anthracenes in an irreversible process and the reversible DA reaction of 48 using furan derivatives.	24
2.13 HeteroDA reaction of classic RAFT agents like model dithioester 53 with a dienophile to give a dihydrothiopyran adduct.	25
2.14 Inverse electron demand Diels-Alder reaction of functional 1,2,4,5-tetrazines with <i>trans</i> -cyclooctene.	26
2.15 Reaction of triazolinediones with random hexadienyl-equipped residues.	27
3.1 Series of thiol compounds showing the trends of acidity and nucleophilicity.	38
3.2 Reactivity of a series of alkylhalides.	38
3.3 Proposed mechanism of the COLBERT process.	41
3.4 Base-catalyzed azlactone ring-opening using thiols.	42
3.5 Base-catalyzed Michael-type thiol-ene addition of a thiol to an acryl species (X = O, NH).	43
3.6 Nucleophile-catalyzed Michael-type thiol-ene addition of a thiol to an acryl species (X = O, NH).	44
3.7 Selection of bases catalyzing the thiol-ene Michael addition. Bases are separated in non-nucleophilic, N-centered and P-centered bases.	45
3.8 Catalytic activity of heterocyclic azo-catalysts for the thiol-vinylsulfone Michael addition.	45

3.9 Overall reactivity of Michael acceptors towards thiols. N and P depict either azo- or phospho-based catalysis.	47
3.10 Radical thiol-ene addition of thiols to alkenes using – exemplary – the photoinitiator DMPA (95).	47
3.11 Overall reactivity of alkenes towards thiols for the radical thiol-ene addition.	49
3.12 Reaction of alkynes to mono- and dithioethers via radical-mediated thiol-yne reaction and selective Rhodium-catalyzed addition.	50
3.13 Thiol-disulfide exchange reaction as found in nature and the chemical approach via pyridyl disulfides.	51
3.14 Metabolism and chemical transformations of homocysteine.	53
3.15 Reaction of a thiolactone derivative with a functional amines and subsequent thiol-X reaction.	54
3.16 Auto-amidation of the neutral thiolactone forming a diketopiperazine.	54
3.17 Stepwise mechanism of the nucleophilic addition of ethylamine via the amine-assisted and the thiol-assisted path.	56
3.18 Thiolactones and poly(thioester) obtained through ring-opening polymerization.	57
3.19 Thiolactone 117 as a key element in macromolecular design of functional polymers.	57
3.20 Random thiolactone 119 as reagent for multicomponent reactions.	60
3.21 Reaction of a bis(thiolactone) in a multicomponent cascade.	62
4.1 Combination of four building blocks A-D within one molecule.	75
4.2 One-step synthesis of the multifunctional coupler from glycerol carbonate chloroformate and homocysteine thiolactone hydrochloride.	76

5.1	Concept for the preparation of thiol-functional polyamides with subsequent modification of the pendant thiol groups to obtain a polyamide with functionalized side groups.	96
5.2	Synthesis route for the preparation of bis(thiolactone) 155	97
5.3	Conversion of bis(thiolactone) 155 with hexylamine and subsequent Michael addition with methyl acrylate.	98
5.4	Preparation of polyamides using bis(thiolactone) 155 and different diamines (BTD and DAD). DTT was used to prevent cross-linking of P1-P4 . Post-polymerization modification of a thiol-functional polyamide P1 using acrylate-functional mPEG to give the water-soluble polymers P5 and P6	101
6.1	Synthesis of epoxy thiolactone 168	124
6.2	Model reactions performed with epoxy thiolactone 168	126
6.3	Two-step cascade reaction of 168 delivering poly(thioether urethane)s 172 via an epoxy thiol intermediate 171	129
6.4	Reaction of linear or cyclic poly(TEU)s with H ₂ O ₂	137
6.5	Synthesis of hydrogels via a) the thiol-epoxy polymerization or b) multicomponent reaction using 168	139
6.6	Synthesis of poly(thioether urethane)s using epoxy thiolactone 168 and various amino acids.	158
6.7	Synthesis of poly(thioether urethane)s using epoxy thiolactone 168 and lysine derivatives and subsequent deprotection of the BOC group to obtain polyelectrolytes.	161
6.8	One-pot synthesis of zwitterionic poly(TEU) 178 using carnosine as substrate.	164
6.9	Synthesis of PEC by complexation of 175a and 177b	168
A.1	Reaction of the coupler with 2.0 equivalents of hexyl amine.	193

List of Tables

- 5.1 Experimental data of the prepared polyamides. 102
- 5.2 Polyaddition of bis(thiolactone) **155** using different compositions of the selected diamines. 117
- 6.1 Rate constants of the one-pot polyaddition using different catalysts. 130
- 6.2 Reaction of epoxy thiolactone **168** with hexylamine using LiOH or DBU as catalyst in different concentration: SEC data. 133
- 6.3 SEC data for the LiOH-catalyzed conversion of epoxy thiolactone **168** with hexylamine employing different monomer concentrations $c(\mathbf{168})$ 134
- 6.4 SEC data for the LiOH-catalyzed conversion of epoxy thiolactone **168** with hexylamine employing different organic solvents and solvent mixtures ($c(\mathbf{168}) = 0.25 \text{ M}$). 136
- 6.5 One-pot polymerization of epoxy thiolactone **168** with hexylamine. 152

6.5 (continued...)	153
6.5 (continued...)	154
6.6 Gelation experiments for the hydrogel formation of 168 with selected acrylates and diamines via thiol-ene Michael addition.	154
6.7 SEC data of obtained poly(thioether urethane)s using 168 .	160
6.8 Autotitration data of poly(TEU)s with amino acids or derivatives in the side chain.	166
6.9 Influence of polymer concentration on the size of the prepared PEC's.	167
A.1 Crystal data and refinement results of the <i>RR/SS</i> diastereomer of 148 .	190
A.2 Crystal data and refinement results of 168 .	201
A.3 MALDI-TOF MS data of poly(thioether urethane) 172 prior oxidation by H ₂ O ₂ . Reported peaks describe masses of [M + Na] ⁺ (MW = 22.99 g/mol).	214
A.4 MALDI-TOF MS data of poly(sulfoxide urethane)s obtained through oxidation with H ₂ O ₂ . Reported peaks describe masses of [M + Na] ⁺ (MW = 22.99 g/mol).	215

Curriculum Vitae

Personal details

Name	Stefan Mommer
Date of birth	August 4 th , 1989
Place of birth	Eupen, Belgium
Citizenship	Belgian

Education

Apr 2013 - May 2017	PhD in Polymer Chemistry with Prof. Dr. M. Möller, DWI - Leibniz Institute for Interactive Materials, Rheinisch-Westfälische Technische Hochschule, Aachen (Germany)
Sep 2016 - Dec 2016	GARG Scholarship, Osaka University, Osaka (Japan). Research stay with Prof. Dr. M. Akashi.
Dec 2012	Master of Science RWTH Aachen (1.2, excellent), Rheinisch-Westfälische Technische Hochschule, Aachen (Germany)
Oct 2011 - Jan 2012	Erasmus Scholarship, University of York, York (United Kingdom). Research course with Prof. Dr. P. O'Brien, studies towards the total synthesis of samaderine C.
July 2010	Bachelor of Science RWTH Aachen (2.2, good), Rheinisch-Westfälische Technische Hochschule, Aachen (Germany)
June 2007	High School Diploma (1.3), Pater-Damian Sekundarschule, Eupen (Belgium)

